

UNIVERSITY OF BELGRADE  
FACULTY OF MECHANICAL ENGINEERING

Marta R. Trinić

**MODELING AND OPTIMISATION OF CORN COB  
PYROLYSIS**

Doctoral Dissertation

Belgrade, 2015

УНИВЕРЗИТЕТ У БЕОГРАДУ

МАШИНСКИ ФАКУЛТЕТ

Марта Р. Трнинић

**МОДЕЛИРАЊЕ И ОПТИМИЗАЦИЈА ПРОЦЕСА  
ПИРОЛИЗЕ КУКУРУЗНОГ ОКЛАСКА**

докторска дисертација

Београд, 2015

## **КОМИСИЈА ЗА ПРЕГЛЕД И ОДБРАНУ**

**Ментор:**

Проф. др Александар Јововић  
Универзитет у Београду Машински  
факултет

**Чланови комисије**

Проф. др Драгослава Стојиљковић  
Универзитет у Београду Машински  
факултет

Проф. др Мирослав Станојевић  
Универзитет у Београду Машински  
факултет

Проф. др Дејан Радић  
Универзитет у Београду Машински  
факултет

Проф. др Нико Самец  
Машински факултет Универзитета у  
Марибору  
(Fakulteta za strojnštvo v Mariboru,  
Slovenia)

**Датум одбране:**

*To my mother Radmila*

*“All that I am or ever hope to be, I owe to my mother.” —Abraham Lincoln*

## ACKNOWLEDGEMENT

*"If you want to go quickly, go alone. If you want to go far, go together."*

Very rarely do we acknowledge the role of people who shape us and help us to find ourselves not only in personal life but also in scientific world.

Fulfilling a PhD degree is a quite challenging and almost impossible without the guidance of the people who were directly involved in the completion of this work and others who simply exist in my life. This is like a window to show the human side of all this work, and a fair opportunity to say everybody involved in this process thank you.

I express my profound sense of reverence to my former supervisor Professor Goran Jankeš for allowing me to start this research under his auspices. Even after his retirement, he remained a supporter and provided insight and direction-right up to the end.

With a deep sense of reverence and gratitude I express my indebtedness to my mentor Professor Aleksandar Jovović. Professor Aleksandar Jovović supported me in all stages of this work. He always gave me constant encouragement, advice and untiring help, despite his busy agenda. I am especially grateful for his constant guidance and the freedom he gave me to do this work. Without a coherent and illuminating instruction, this thesis would not have reached its present form.

My greatest appreciation and gratitude goes to Professor Dragoslava Stojiljković. Her continuous guidance, unsurpassed knowledge, generous help and concise critical comments resulted in the completion of this thesis.

I would like to thank Professor Vojislav Novaković as the project leader of collaborative project "Sustainable Energy and Environment in Western Balkans" within which I had the opportunity to stay at the Norwegian University of Science and Technology (NTNU). Words fail me to express my appreciation to Professor Vojislav Novaković for his untiring help, guidance, generous care and the homely feeling at Trondheim.

Staying at NTNU, gave me an opportunity to meet and learn from world's leading researchers, scientists, and engineers in biomass conversion technologies. Three of them have in particular to be mentioned: Dr Morten Grønli, from NTNU, Professor Michael Jerry Antal, Jr, from University of Hawaii, USA, and Dr Gabor Várhegyi from the Hungarian Academy of Sciences, Hungary. a man with

The valuable generous scientific support, immense knowledge that I have received from all them has been crucial for the development of this thesis.

I extend my sincere thanks to all members of the Department of Process Engineering and Environmental Protection, and all those who contributed directly or indirectly to the dissertation.

Also I want to thank all my friends for their kindness and help.

Special gratitude goes to my early deceased friend Jerko Labus, who left fingerprints of grace on our lives. *"Of all the souls I have encountered in my travels, his was the most.. Human."* – James T. Kirk, *Star Trek II: The Wrath of Khan*.

Without the support of my mother, I would never finish this thesis and I would never find the courage to overcome all these difficulties during this work. My thanks go to her for her confidence and her love during all these years.

Marta R. Trninić



## **SUMMARY**

The need for energy and fuels is one of the common threads throughout human history. Energy, in its many useful forms, is a basic element that influences and limits human's standard of living and technological progress. The sustainable provision of energy that meets the needs of the present without compromising the ability of future generations to meet their needs, did not receive much attention until the middle of the twentieth century, that is, the fossil fuel era, and then usually only in crisis situations of one kind or another.

The rapid worldwide increase in the consumption of fossil fuels in the twentieth century to meet energy demand, mostly by industrialized nations, suggests that the time is not too distant before depletion begins to adversely affect oil and natural gas reserves. Also, the greenhouse effect and acid rains are mainly associated with the use of fossil fuels. The carbon cycle in nature is basically balanced, but the artificial emission of CO<sub>2</sub> by the use of fossil fuels is the cause of the increase in CO<sub>2</sub> in the air. Other gases like methane, nitrous oxide, and ozone also can be the cause of the greenhouse effect, but their weight is smaller compared to CO<sub>2</sub>. Energy and environment currently are two sides of one coin. To separate one from another, the world needs to increase usage of alternative biomass energy resources. Biomass energy is considered to be CO<sub>2</sub> neutral in so far as its production and consumption are balanced. Biomass is also noted for less S content and, thus, less likely to cause acid rain.

Biomass has historically supplied human needs for food, fibre, energy and structural material. The potential for biomass to supply much larger amounts of useful energy with reduced environmental impacts compared to fossil fuels has stimulated substantial research and development of systems for handling, processing, and converting biomass to energy.

The energy in biomass may be realised by different thermochemical methods such as: pyrolysis, gasification, liquefaction and combustion. Of these processes, pyrolysis and gasification are most promising alternative routes to convert biomass to power/heat generation and production of transportation fuels and chemical feedstock. Being more flexible than the direct combustion process, biomass gasification can be directly utilized in external and internal combustion engines or it can be converted via chemical processes to provide synthetic chemicals or liquid fuel. Also, combustion product gas does not have



useful heating value, but product gas from gasification does. Gasification packs energy into chemical bonds while combustion releases it. Pyrolysis is a viable process for efficient and economical transformation of biomass into solid charcoal, bio-oil and gases. In addition, this process has added advantages of being a clean process (low emission of sulphur, nitrogen oxides, furan and dioxin compounds and particulates), high thermal efficiency and a good degree of control.

Although numerous projects have been promoted, pyrolysis commercialization is progressing at a low pace not only in Serbia but also in Europe. Major efforts on researching are needed in order to maximize the advantages and minimize the disadvantages of this technology. The upsurge of interest in simulation and optimization of suitable reactors for thermochemical processes requires appropriate models that contemplate different operational conditions and varied feed stocks and helping to achieve a better understanding of the reactions in the corresponding processes. In this sense, a better knowledge of the pyrolysis parameters and kinetics concerning to the thermal decomposition of the biomass materials is required.

Two main research topics were thought to be of main concern at this purpose, and they were therefore discussed in this thesis: the investigation of fixed-carbon yields of charcoal from corn cob and kinetics of corn cob pyrolysis.

In first stage, a round-robin study of corn cob charcoal and fixed-carbon yields, involving three different thermogravimetric analysers, revealed the impact of feedstock size (mass) and vapour-phase reactions on the formation of charcoal. The yield of charcoal from biomass is not a meaningful metric of the efficiency of a carbonization process. Instead, the fixed-carbon yield should be used to characterize carbonization efficiency. When an elemental analysis of the feedstock is available, it can be used to calculate the yield of pure carbon that can be realized when thermochemical equilibrium is reached in a carbonizer. This theoretical yield of pure carbon can be compared to the experimental value of the fixed-carbon yield and thereby used as a meaningful metric of the efficiency of the carbonization process. The lowest fixed-carbon yields are obtained by the standard proximate analysis procedure for biomass feedstock; this yield falls in a range from 49 to 54% of the theoretical value. The fixed-carbon yields of charcoal produced by the proximate analysis procedure are about 1/2 of the theoretical value. The fixed-carbon yields of charcoal obtained from the pyrolysis of corncob in analytic thermogravimetric analysers is low but somewhat higher than that of the proximate analysis procedure. The

fixed-carbon yield is reduced to a range from 68 to 75% of the theoretical value when whole corn cobs are carbonized under nitrogen at atmospheric pressure in an electrically heated muffle furnace. In order to investigate influence of pyrolytic vapours residence time, experiments with lid were performed. Experiments show that any restriction of the ability of the pyrolytic vapours to escape from the vicinity of the charcoal product increases the fixed-carbon yield. This improvement in yield is a result of increasing heterogeneous interactions between the pyrolytic vapours and the solid charcoal together with its mineral matter, both of which may be catalytic for the formation of charcoal. Also experiments with different particle size show that larger particles offers significantly higher fixed-carbon yields than small particles within TGA instruments. Beside experimental analysis, the predictive model based on the proximate analysis of the corn input has been developed in order to evaluate the mass balance during pyrolysis. Moreover heating value of the charcoal and gases issued form the corn cob pyrolysis is calculated from the elemental analysis of corn cob. Results of modelling are in good agreement with experimental results.

In the second part of this thesis, experimental and modeling work on the pyrolysis of corn cob under regimes controlled by chemical kinetics is presented. Two different corn cob samples from were studied by thermogravimetry at linear and nonlinear heating programs in inert gas flow. The thermograms of two different corn cobs revealed different weight loss characteristics which can be attributed to their different chemical composition; the small pectin peak occurred only in one of the samples and some reactivity differences arose in the hemicellulose pyrolysis. The exploitation of the information provided by thermogravimetry, a relatively low priced, simple technique suitable for studying several reactions of interest in biomass conversion, requires the establishing of appropriate models and evaluation strategies for the various biomass materials. In the kinetic analysis, a model of independent parallel reactions was successfully used to describe the thermal degradation. A distributed activation energy model (DAEM) with three and four pseudocomponents (pectin, hemicelluloses, cellulose and lignin) was used due to the complexity of the biomass samples of agricultural origin. The reliability of the models was tested in three ways: (1) the models provided good fit for all experiments; (2) the evaluation of a narrower subset of the experiments resulted in approximately the same parameters as the evaluation of the whole series of experiments; and (3) the models allowed accurate extrapolations to higher heating rates.

The resulting models described well the experimental data. When the evaluation was based on a smaller number of experiments, similar model parameters were obtained which were suitable for predicting experiments at higher heating rates. This test indicates that the available experimental information was sufficient for the determination of the model parameters. The checks on the prediction capabilities were considered to be an essential part of the model verification. In another test, the experiments of the two samples were evaluated together, assuming more or less common kinetic parameters for both cobs. This test revealed that the reactivity differences between the two samples are due to the differences in their hemicelluloses and extractives. The kinetic parameter values from a similar earlier work on other biomasses could also be used, indicating the possibilities of a common kinetic model for the pyrolysis of a wide range of agricultural byproduct.

Overall, this research work represents a comprehensive and thorough thermokinetic study of corn cob pyrolysis that approaches the thermal behaviour by recognizing the connections between different chemical phenomena making up the pyrolytic process. The two different model proposal, finally built up in this thesis, is a contribution for understanding the process as a whole. Additionally, it can be considered as a first step toward its extension to practical applications, where additional chemical and transport phenomena need to be incorporated.

**Key words:** pyrolysis, charcoal yield, fixed carbon yield, prediction model, kinetic model, corn cob

**Scientific discipline:** Mechanical engineering

**Scientific sub-discipline:** Process and Environmental Protection Engineering

**UDC Number:** 628.475:662.63(043.3)

66.092-977(043.3)

662.63:620.9(043.3)

## РЕЗИМЕ

Развој енергетике је снажан модификатор привредне структуре и погонски фактор технолошког и економског развоја.

Стални и све виши пораст потрошње енергије, условљених како због повећања становништва тако и због повећања нивоа и стандарда живота у свим земљама света, наговестила је чињеницу да се залихе фосилних горива исцрпљују. Паралелно са суочавањем ограничености извора фосилних горива јавља се и проблем нагомилавања CO<sub>2</sub> у атмосфери и ефекат „стаклене баште“ и „киселих киша“. Дакле енергија и заштита животне средине представљају „два лица истог новчића“. У циљу задовољења свих захтева, како по погледу задовољења енергетских потреба тако и испуњење услова задатих правилима заштите животне средине, потребно је интензивније користити обновљиве изворе енергије (ОИЕ).

Енергија биомасе представља акумулирану сунчеву енергију којом се енергија трансформисала у хемијску енергију процесом фотосинтезе. С обзиром да је енергија акумулирана сунчева енергија у биомаси хемијског порекла, њеном експлоатацијом нема периода прекида рада, као у случају других ОИЕ (енергија ветра, сунчева енергија, итд.). Биомаса као се сматра за CO<sub>2</sub> неутрално гориво. Наиме, угљеник из атмосфере се потхрањује у биљке током њиховог раста, да би се током њиховог разлагањем та иста количина угљеника вратила у атмосферу, у облику CO<sub>2</sub>. Биомаса садржи мале количине сумпора и азота, који су главни елементи у формирању „киселих киша“. Из наведених разлога потпуно је јасно да се у оквиру било које политике одрживог развоја као један од основних постулата мора предвидети и коришћење биомасе за потребе генерисања енергије.

Хемијску енергије биомасе могуће је трансформисати у топлотну и/или електричну енергију, применом различитих процеса термичке конверзије биомасе као што су: сагоревање, гасификације и пиролиза. Процес пиролизе и гасификације представљају знатно флексибилније процесе од процеса сагоревања.

Процеси пиролизе и гасификације престављају ефикаснији процес термичке конверзије хемијске енергије биомасе у електричну и /или топлотну енергију, производњу био – горива, као и у широк спектар хемијских једињења. Процеси пиролизе и гасификације, спадају у групу тзв. чистих процеса (ниска емисија сумпорних једињења, азотних оксида, фурана, диоксида, честица итд.). Процес

гасификације је знатно флексибилнији процес од процеса сагоревања, с обзиром да се гасовити продукти гасификације могу директно користити у моторима на унутрашње сагоревање, за производњу електричне и/или топлотне енергије, или, путем различитих хемијских процеса произведени гас може бити коришћен као полазна сировина за добијање различитих синтетичких хемијских једињења или течног горива. Продукте сагоревања не одликује висока топлотна моћ за разлику од гаса добијеног процесом гасификације. Наиме, процесом сагоревања хемијска енергија биомасе се ослобађа у виду топлотне енергије, док се процесом гасификације, хемијска енергија биомасе остаје већим делом сачувана у хемијској енергији новонасталог гаса. Процес пиролизе, представља још ефикаснији и економичнији процес за добијање био уља (тер), био – угља (коксног остатка) и гаса. Иако постоји велики број повољних експерименталних резултата, лабораторијских реактора и пилот постројења пиролизе, комерцијализација и развој ове технологије је на ниском нивоу не само у Републици Србији већ и у Европи. У циљу интензивнијег развоја и имплементације процеса пиролизе биомасе у привреду, потребно је не само испитати потенцијално гориво већи детаљно истражити сам процес. С обзиром да је веома често економски неисплативо конструисати реакторе за пиролизу за сврхе испитивања, потребно је применити алтернативнији метод за добијење потребних информација о процесу. То је могуће оставарити применом математичког моделирања и симулацијом одабраног процеса коме подлеже одабрана биомасе. У циљу успешног дефинисања процеса пиролизе и конструисања реактора у којем ће се одабрани процес одвијати, веома је важно познавати утицаје различитих радних параметара на продукте процеса као и кинетику самог процеса. На основу успостављених корелација између утицајних параметара процеса пиролизе (режим загревања, величина и маса узорка, време задржавања, проток радног медијума) и крајњих продуката процеса пиролизе могуће је дефинисати одговарајуће математичке моделе који дефинишу дати процес. Математички модели омогућавају симулацију и оптимизацију процеса, што посредно утиче на пројектовање, конструисање, а самим тим и на усавршавање карактеристика лабораторијских и индустријских реактора.

Сходно томе, у оквиру докторске дисертације детаљно су дефинисани утицајни параметри процеса пиролизе на принос коксног остатка (и фиксног угљеника)

током пиролизе кукурузног окласка као и кинетика процеса пиролизе кукурузног окласка. У анализи су коришћене две врсте кукурузних окласака, добијених из две различите сорете кукуруза: кукуруза ZP Maize Hybrid ZP 505 (у тексту Scob) и Pioneer HiBred International (у тексту Pcob). Потребно је напоменути да процес пиролизе представља не само независан процес већ и прву фазу процеса гасификације и сагоревања, од које зависи даље одвијање ових процеса.

У оквиру првог дела докторске дисертације, анализиран је утицај масе узорка и секундарних реакција на принос коксног остатка. Као референтна вредност у односу на коју је могуће дефинисати степен ефикасности процеса пиролизе коришћена је теоријска вредност фиксног угљеника, садржаног у коксном остатку. Теоријска вредност фиксног угљеника је добијена применом StanJan програма који се базира на израчунавању продуката пиролизе при условима термохемијске равнотеже. Поређени су резултати добијени са три различита термогравиметриска анализатора и муфолне пећи. Најнижа вредност фиксног угљеника је добијена на основу техничке анализе кукурузног окласка. Вредност фиксног угљеника је нижа за 49 до 54% у односу на теоријску вредност фиксног угљеника. Вредности фиксног угљеника добијених при експериментима у термогравиметријским анализаторима показали су нешто већу вредност у односу на вредност добијену техничком анализом кукурузног окласка. Вредност фиксног угљеника добијеног из експеримента пиролизе кукурузног окласка у муфолној пећи је износила 69 до 75% вредности теоријског фиксног угљеника. У циљу дефинисања утицаја задржавања парне фазе у контакту са коксним остатком, током одвијања процеса пиролизе, на принос коксног остатка, коришћене су посуднице са поклопцем. Поклопац који има мањи прорез, успорава испирање парне фазе (волатили, тер, водена пара) са површине коксног остатка, што подстиче одвијање хетерогених секундарних реакција које резултирају повећањем приноса коксног остатка. Такође експерименти са различитим гранулацијама и масом кукурузног окласка показали су да узорци веће масе и гранулације омогућавају виши принос коксног остатка. У оквиру овог дела, а на основу експерименталних резултата дефинисан је статички модел пиролизе кукурузног окласка. Статички модел пиролизе кукурузног окласка омогућава дефинисање продуката пиролизе. Резултати моделирања су у складу са експерименталним и литературним подацима.

У оквиру другог дела докторске дисертације, верификован је универзалност примене модела расподеле активационе енергије (МРАЕ). У циљу добијања резултат, оба узорка кукурузног окласка су пиролизоване у термогравиметријском анализатору при линеарним и нелинеарним температурним режимима, а потом поређени са резултатима моделирања процеса, применом различитих математичких модела заснованих на реакцијама  $n$ -тог реда, првог и применом МРЕА. Модел расподеле активационе енергије показао резултате најприближнијим експерименталним резултатима. Модел расподеле активационе енергије садржи реакције разградње три или четири псеудокомпоненте кукурузног окласак (пектин, хемицелулоза, целулоза, лигнин). Валидност модела је проверена на три начина: (1) одређивањем грешке моделирања, (2) провером да ли се резултати добијени за ужи скуп експеримената могу користити за прорачун читаве серије експеримената, (3) примена модела при различитим условима вођења процеса, (4) примена добијених кинетичких параметара, пиролизе кукурузног окласка, за опис кинетике пиролизе других пољопривредних остатака. Резултати моделирања су показали да је модел расподеле активационе енергије могуће (са великом тачношћу) примењивати независно од услова вођења процеса пиролизе и врсте тестиране пољопривредне биомасе. На крају, модел је универзално применљив, односно могуће га је примењивати без обзира на различиту хемијску структуру пољопривредних остатака.

Уопштено речено, докторска дисертација представља детаљну и свеобухватну анализу пиролизе кукурузног окласка. Представљени математички модели омогућавају јасније разумевање целокупног процеса, развој и унапређење процеса, усавршавање лабораторијских и индустријских реактора пиролизе и гасификације.

**Кључне речи:** пиролиза, коксни остатак, фиксни угљеник, статички модел, кинетички модел, кукурузни окласак

**Научна област:** Машинство

**Ужа научна област:** Процесна техника

**УДК број:** UDK 628.475:662.63(043.3)

66.092-977(043.3)

662.63:620.9(043.3)

## TABLE OF CONTENTS

<b>1. INTRODUCTION</b> .....	<b>1</b>
<b>1.1. BIOMASS AS RENEWABLE ENERGY RESOURCE</b> .....	<b>5</b>
<b>1.2. CHEMICAL STRUCTURE OF BIOMASS</b> .....	<b>6</b>
1.2.1. STRUCTURE OF BIOMASS .....	7
1.2.2. CHEMICAL CHARACTERISATION OF BIOMASS .....	11
<b>1.3. ACTUAL AND POTENTIAL USES OF BIOMASS RESOURCES IN EU -27</b> .....	<b>18</b>
<b>1.4. ACTUAL AND POTENTIAL USES OF BIOMASS RESOURCES IN REPUBLIC OF SERBIA</b> .....	<b>26</b>
<b>2. THERMOCHEMICAL CONVERSION TECHNOLOGIES</b> .....	<b>37</b>
<b>2.1. COMBUSTION</b> .....	<b>39</b>
<b>2.2. GASIFICATION</b> .....	<b>41</b>
2.2.1. TYPES OF GASIFIERS .....	42
<b>2.3. PYROLYSIS</b> .....	<b>45</b>
2.3.1. TYPES OF PYROLYSIS REACTORS .....	46
<b>3. BIOMASS PYROLYSIS FUNDAMENTALS</b> .....	<b>48</b>
<b>3.1. OVERVIEW OF BIOMASS PYROLYSIS</b> .....	<b>49</b>
<b>3.2. HEAT AND MASS TRANSFER DURING PYROLYSIS PROCESS</b> .....	<b>52</b>
<b>3.3. TYPES OF PYROLYSIS</b> .....	<b>59</b>
<b>3.4. PYROLYSIS PRODUCTS CHARACTERISTICS</b> .....	<b>65</b>
<b>3.5. INFLUENCE OF PYROLYSIS PARAMETARS ON PRODUCTS YIELD</b> .....	<b>69</b>
<b>3.6. INFLUENCE OF CHEMICAL AND PHYSICAL CHARACTERISTICS OF BIOMASS ON PYROLYSIS PROCESS</b> .....	<b>78</b>
<b>4. MATHEMATICAL MODELLING OF PYROLYSIS – STATE OF ART</b> .....	<b>90</b>
<b>4.1. PYROLYSIS MODELLING OBJECTIVES</b> .....	<b>91</b>
<b>4.2. PYROLYSIS KINETIC MODELING</b> .....	<b>93</b>
<b>4.3 MODELING OF PRIMARY PYROLYSIS</b> .....	<b>97</b>
4.3.1. ONE STEP MODEL .....	97
4.3.2. MULTI – STEP REACTION KINETIC MODEL .....	105



<b>4.4. MODELING OF PRIMARY AND SECONDARY PYROLYSIS .....</b>	<b>109</b>
4.4.1. SEMI - GLOBAL KINETIC MODELS .....	109
4.4.2 A DISTRIBUTED ACTIVATION ENERGY MODEL FOR THE PYROLYSIS OF LIGNOCELLULOSIC BIOMASS - DEAM .....	124
<b>4.5. CONCLUSION .....</b>	<b>129</b>
<b>5. KINETIC MODELING OF CORN COB PYROLYSIS .....</b>	<b>131</b>
<b>5.1. INTRODUCTION .....</b>	<b>131</b>
<b>5.2. EXPERIMENTAL SECTION .....</b>	<b>133</b>
5.2.1. SAMPLES AND SAMPLE PREPARATION .....	133
5.2.3. EXPERIMENTAL PROCEDURE .....	136
<b>5.3. RESULT AND DISSCUSION .....</b>	<b>138</b>
5.3.1. DESCRIBING CORN COB PYROLYSIS KINETICS BY PARAMETERS OBTAINED FOR OTHER SORTS OF AGRICULTURAL RESIDUES .....	142
5.3.2. DESCRIBING KINETICS OF THE TWO CORN COB SAMPLES BY COMMON KINETIC PARAMETERS .....	149
5.3.3. MODELING WITH $n$ -ORDER KINETICS .....	152
5.3.4. PREDICTION TESTS.....	153
<b>5.4. CONCLUSIONS.....</b>	<b>154</b>
<b>6. FIXED CARBON YIELD OF CHARCOAL FROM CORN COB PYROLYSIS .....</b>	<b>157</b>
<b>6.1. EXPERIMENTAL SECTION .....</b>	<b>159</b>
6.1.1. SAMPLES AND SAMPLES PREPARATION .....	161
6.1.2. EXPERIMENTAL APPARATUS AND EXPERIMENTAL PROCEDURE .....	161
<b>6.2. EXPERIMENTAL RESULTS.....</b>	<b>165</b>
6.2.1. PYROLYSIS BEHAVIOUR OF DIFFERENT CONSTITUENTS OF A CORN COB .....	165
6.2.2. FIXED CARBON YIELDS.....	166
6.2.3. THE ELEMENTAL ANALYSIS OF CHARCOAL.....	176
<b>6.3. DISCUSSION .....</b>	<b>180</b>
<b>6.4. PREDICTIVE MODEL OF CORN COB SLOW PYROLYSIS .....</b>	<b>181</b>
6.4.1. MODEL FORMULATION .....	182
6.4.2. VALIDATION OF THE MODEL.....	196
<b>6.6. CONCLUSION .....</b>	<b>201</b>
<b>7. PYROLYSIS EXTENSION TO PRACTICAL GASIFICATION MODELS .....</b>	<b>204</b>
<b>7.1. MODELING OF CORN COB GASIFICATION – STEADY STATE MODEL .....</b>	<b>205</b>
<b>7.2. GASIFICATION MODEL VALIDATION .....</b>	<b>210</b>
7.3. CONCLUSION.....	221

<b>8. CONCLUSIONS AND FUTURE WORK .....</b>	<b>223</b>
<b>8.1 ATTAINMENT OF THE THEORETICAL YIELD OF CARBON FROM CORN COB.....</b>	<b>223</b>
<b>8.1 PREDICTIVE MODEL OF CORN COB PYROLYSIS .....</b>	<b>224</b>
<b>8.2 KINETICS OF CORN COB PYROLYSIS .....</b>	<b>225</b>
<b>8.3. FUTURE RESEARCH WORK .....</b>	<b>226</b>
<b>REFERENCES.....</b>	<b>228</b>
<b>APPENDIX A. PERFORMANCE INDICATORS.....</b>	<b>A1</b>
<b>APENDIX B ULTIMATE AND PROXIMATE ANALYSIS .....</b>	<b>A4</b>
<b>APPENDIX C TGA SPECIFICATIONS.....</b>	<b>A14</b>
<b>APENDIX D PUBLISHED SCI PAPERS RELATED TO DOCTORAL THESIS .....</b>	<b>A19</b>



## LIST OF FIGURES

Figure	CAPTER 1
Figure 1.1	The structure of plant biomass [5]
Figure 1.2	Structural formula of cellulose [1]
Figure 1.3	Structural formulas of hemicellulose`s monomers [2]
Figure 1.4	A hypothetical depiction of soft wood ligning, with basic monolignols [3]
Figure 1.5	Classification of biomass by constituent ratios [4, 5]
Figure 1.6	Van Krevelen`s diagram [6]
Figure 1.7	C-H-O ternary diagram [5]
Figure 1.8	EU-27 Electricity and Heat Production in 2011 [7]
Figure 1.9	EU-27 Electricity and Heat production from RES in 2011 [7]
Figure 1.10	Biomass use towards reaching 2020 Renewable Targets [8]
Figure 1.11	The biomass feedstock input required to reach the 2020 bioenergy targets [9]
Figure 1.12	Domestic supply by biomass type [9]
Figure 1.13	Biomass derived electricity [10]
Figure 1.14	Biomass derived heating [10]
Figure 1.15	Contribution to transport energy by biofuel type [10]
Figure 1.16	Domestic and import primary energy supply in 2013 [113]
Figure 1.17	Primary energy production detailed selected by energy sources in 2013 [113]
Figure 1.18	Energy potential of RES in the Republic of Serbia
Figure 1.19	Projected changes in the structure of fuel for electricity generation and heat production
Figure 1.20	The structure of different biomass sources
	CHAPTER 2
Figure 2.1	Biomass conversion technologies
Figure 2.2	Products of thermochemical conversion technologies and there potential end uses
Figure 2.3	The different reactions in combustion of solid fuels [13]
Figure 2.4	Diverse gasifiers: (a) Downdraught, (b) Updraft, (c) Bubbling Fluidized Bed, (d) Circulating fluidized bed [14, 132]
Figure 2.5	The concept design of some pyrolysis reactors: a) Ablative, CFB and vacuum technologies [144] b) Fluid bed, screw (auger) and rotating cone technologies [144], c) retort and kiln technologies
	CHAPTER 3
Figure 3.1	Primary and secondary pyrolysis reactions
Figure 3.2	Heat transfer during pyrolysis process [16]
Figure 3.3	Rate-controlling regimes of heterogeneous reactions [17, 18]
Figure 3.4	Effect of temperature on pyrolysis product yield [20]
Figure 3.5	Influence of pyrolysis temperature on gas composition

- Figura 3.6 Influence of heat rate and pyrolysis temperature on devolatilization, [21, 22]
- Figure 3.7 Cellulose decomposition [23]
- CHAPTER 4
- Figure 4.1 The kinetic model for cellulose pyrolysis proposed by Broido and Weinstein [24]
- Figure 4.2 Broido–Nelson (1975) model for cellulose pyrolysis [25]
- Figure 4.3 Broido-Shafizadeh model (1979) [23]
- Figure 4.4 Arrhenius's plot
- Figure 4.5 Scheme of Semi-global Pyrolysis Model [26]
- Figure 4.6 One - step semi global model
- Figure 4.7 Biomass kinetic reaction scheme Thurner and Mann [27, 28]
- Figure 4.8 Reaction scheme of Biomass Pyrolysis suggested by Koufopoulos [29]
- Figure 4.9 global mechanism for the secondary reactions of vapour-phase tar species as proposed by Antal [30, 31]
- Figure 4.10 Scheme of Biomass Pyrolysis model suggested by Chan et al [33, 34]
- Figure 4.11 Model of Srivastava et al. [35]
- Figure 4.12 Reaction scheme of Biomass Pyrolysis suggested by Di Blasi [36]
- Figure 4.13 Miller-Bellan model [37]
- Figure 4.14 Reaction scheme of Biomass Pyrolysis suggested by Rath and Staudinger [38]
- CHAPTER 5
- Figure 5.1 Schematic diagram of the TA Q600 simultaneous TGA - DTA with sample cup/sample thermocouple configuration [39]
- Figure 5.2 Temperature programs employed in the experiments: linear and stepwise [40]
- Figure 5.3 Comparison of the mass-loss rate curves and peak temperatures of the two samples of corn cob (Scob and Pcob) [40]
- Figure 5.4 Evaluations by DAEM kinetics. Part of the kinetic parameters were taken from a literature work on agricultural biomasses [40]
- Figure 5.5 Evaluation by DAEM kinetics assuming eight common parameters for the two samples. The left-hand-side (plots a and c) belongs to the regular least squares evaluation of the eight available experiments while the right-hand-side (plots b and d) [40]
- Figure 5.6 Evaluation by  $n$ -order kinetics assuming eight common parameters for the two samples. The left-hand-side (plots a and c) belongs to the regular least squares evaluation of the eight available experiments while the right-hand-side (plots b and d) [40]
- CHAPTER 6
- Figure 6.1 Experimental matrix with expected results
- Figure 6.2 Cross-sectioned view of corn cob
- Figure 6.3 Schematic illustration of TA Q 5000 furnace part [41]
- Figure 6.4 Schematic illustration of Mettler Toledo model TGA/SDTA 851e [42]

- Figure 6.5 Crucibles/pans used in pyrolysis experiments [43]
- Figure 6.6 Pyrolysis and charcoal yield behaviour of different constituents of a corn cob (Scob) thin cross-section in an open crucible
- Figure 6.7 Pyrolysis and charcoal yield behaviour of different constituents of a corn cob (Pcob) thin cross-section in an open crucible
- Figure 6.8 Effects of pressure on corn cob pyrolysis following the attainment of thermochemical equilibrium at 400 °C (results derived by StanJan software)
- Figure 6.9 Influence of different instruments on one corn cob single particle sample charcoal yield in an open crucible
- Figure 6.10 Influence of different instruments on corn cob powder sample charcoal yield in an open crucible
- Figure 6.11 Effects of open versus closed crucible on Scob and Pcob powder sample charcoal yield
- Figure 6.12 Effects of open versus closed crucible on Scob and Pcob particles sample charcoal yield
- Figure 6.13 Parity plot displaying the experimental vs theoretical values
- Figure 6.14 Particle size distributions of ground Pcob and Scob samples
- Figure 6.15 Influence of the particle size on Pcob and Scob charcoal yield (sample mass of 10 mg)
- Figure 6.16 The charcoal yields (daf) as functions of temperature
- Figure 6.17 The tar yields as functions of temperature for corn cob
- Figure 6.18 Gas yields as functions of temperature for corn cob
- Figure 6.19 Gas yields for agricultural residues as functions of temperature: a) CO, b) CO<sub>2</sub>, c) H<sub>2</sub>, d) CH<sub>4</sub>
- Figure 6.20 Overall mass balance to the biomass pyrolysis process. The presented quantities (Y) are mass ratios referred to the dry ash-free part of biomass (scheme based on Neves et al. [44] mass balance scheme)
- Figure 6.21 The yield of charcoal, gas and tar yield compared with literature data a) charcoal yield, b) gas yield and c) tar yield
- Figure 6.22 Yield of gas composition given by model and compared with literature data a) CO yield, b) CO<sub>2</sub> yield and c) CH<sub>4</sub> yield
- CHAPTER 7
- Figure 7. 1 Overall mass balance to the biomass gasification process. The presented quantities (Y) are mass ratios referred to the dry ash-free part of biomass
- Figure 7.2 Composition of the dry product gas predicted by model compared with experimental results
- Figure 7.3 Influence of Equivalence Ratio on Gasification Temperature
- Figure 7.4 Influence of Equivalence Ratio on Gas Composition and LHV, for corn cob gasification with a moisture content of 5%

- Figure 7.5 Influence of Air Temperature on Gas Composition and LHV<sub>gas</sub>, for gasification of corn cob with moisture content of 5% and  $\lambda = 0.3$
- Figure 7.6 Influence of Oxygen Amount on Gas Composition and LHV<sub>gas</sub>, for gasification of corn cob with moisture content of 5% and  $\lambda = 0.3$
- Figure 7.7 Influence of Oxygen on Gas Composition and LHV<sub>gas</sub>
- Figure 7.8 Influence of Biomass Moisture on Gas Composition and LHV<sub>gas</sub>
- APPENDIX B
- Figure B.1 Functional diagram vario MACRO CHNS [388]

## LIST OF TABLES

Table	CHAPTER 1
Table 1.1	Major groups of biomass and their sub classifications [5, 46]
Table 1.2	Cellulose, hemicellulose and lignin share in some biomass tips
Table 1.3	Ash content in some agricultural residues
Table 1.4	Alkali oxides in some agricultural residues [47, 48]
Table 1.5	EU-27 RES in Transport in 2011 [7]
Table 1.6	EU Polices for renewable energy implementation
Table 1.7	Wood biomass energy potentials [122]
Table 1.8	Estimated quantities of Agricultural residues
Table 1.9	Biomass production in orchards and vineyards in Serbia
Table 1.10	Biomass production in livestock breeding and energy potential of their manure in Serbia
Table 1.11	Energy potentials of Agricultural residues in Serbia
Table 1.12	Energy density and heating value of several types of fuels [52]
	CHAPTER 2
Table 2.1	Advantages and disadvantages of some gasifier reactors [138, 139]
Table 2.2	Advantages and disadvantages of some pyrolysis reactors [143, 145]
	CHAPTER 3
Table 3.1	Pyrolysis technology variant [5, 16, 53, 54, 177]
Table 3.2	Yield of products of the individual components [55]
Table 3.3	Yield of products samples of synthetic biomass with different ratios of cellulose and lignin [55]
	CHAPTER 4
Table 4.1	Values of the corn cob parameters
Table 4.2	A survey of kinetic data for Biomass Pyrolysis [2]
Table 4.3	Kinetic parametars used by Thurner and Mann [27, 28]
Table 4.4	Kinetic parametars, Koufopoulos et al. [8, 93]
Table 4.5	Kinetic Parametars used by Chan et al [33, 34]
Table 4.6	Kinetic parameters used by Di Blasi [36]
Table 4.7	Kinetic parametars for the pyrolysis reactions [37]
Table 4.8	Kinetic Parametars of three parallel reaction of tar decomposition [27, 38]
	CHAPTER 5
Table 5.1	Proximate Analysis, Heating Value, and Fixed Carbon Yield of corn cobs
Table 5.2	Ultimate Analyses of corn cobs
Table 5.3	Evaluation of Scob and Pcob by DAEM reactions [40]
Table 5.4	List of the model parameters for seven selected evaluations [40]
Table 5.5	Simultaneous evaluation of samples Scob and Pcob [40]
	CHAPTER 6
Table 6.1	Specifications of Instruments and Their Crucibles/Pans [43]



Table 6.2	Temperature regime of Pyrolysis Experiment [43]
Table 6.3	Charcoal and Fixed-Carbon Yields Realized in the TA Q600 [43]
Table 6.4	Charcoal and fixed-carbon yields realized in a muffle furnace
Table 6.5	Fixed-carbon yields realized by different approach (theoretical and experimental)
Table 6.6	Ultimate Analyses of Wcorn cobs
Table 6.7	Proximate Analysis, Heating Value, and Fixed Carbon Yield of corn cobs
Table 6.8	Fixed-carbon yields realized by different approach (theoretical and experimental)
Table 6.9	SEM EDX Analyses of Scob charcoal, (wt %)
Table 6.10	Fixed-carbon yields realized by different approach (theoretical and experimental) of corn cob and some type of wood [43, 56]
Table 6.11	Characteristics of agricultural residues (literature data and results from present study)
Table 6.12	Experimental details used in this study
Table 6.13	Comparison of present study results with literature data
	CHAPTER 7
Table 7.1	Tar Ultimate Analysis [13]
Table 7.2	Gas composition as a results of corn cob downdraft gasification modeling
Table 7.3	Gas composition after corn cob downdraft gasification, literature review
Table 7.4	Influence of Equivalence Ratio on Gas Composition and LHV
Table 7.5	Influence of Air Temperature on Gas Composition and LHV <sub>gas</sub>
Table 7.6	Influence of oxygen amount on gas composition and LHV <sub>gas</sub>
Table 7.7	Influence of Biomass Moisture on Gas Composition and LHV <sub>gas</sub>
	APPENDIX A
Table A.1	The influence of pyrolysis process parameters on the pyrolysis products
	APPENDIX B
Table B.1	Table B.1 High heating value of corn cob (measured and calculated value)
	APPENDIX C
Table C.1	Table C.1 Technical specifications of TA Q 5000
Table C.2	Table C.2 Technical specifications of TA Q600
Table C.3	Table C.3 Technical specifications of Mettler Toledo TGA/SDT 851e

## NOMENCLATURE

Although most of the symbols are explained in the place where they appear, this section is a quick reference to the reader for the notation used along this work.

### *Greek characters*

$\alpha_j$	Fraction of the remaining component $j$	
$\alpha$	reacted biomass fraction	
$\beta$	heating rate	$^{\circ}\text{C}/\text{min}, \text{K}/\text{s}$
$\lambda$	coefficient of convection	$\text{W}/\text{m}^2\text{K}$
$\rho$	Bulk density	$\text{kg}/\text{m}^3$
$\sigma$	Standard deviation	
$\tau$	Reaction time constant	

### *Acronyms and abbreviations*

$A$	Surface area of the particle	$\text{m}^2$
$A$	Frequency factor (pre-exponential factor)	$1/\text{s}$
$A_1$	Pre-exponential factor for hemicellulose	$1/\text{s}$
$A_2$	Pre-exponential factor for cellulose	$1/\text{s}$
$A_3$	Pre-exponential factor for lignin	$1/\text{s}$
$A_j$	Pre-exponential factor of component $j$	$1/\text{s}$
$B_i$	Biot number	
$C$	Carbon mass fraction in biomass	wt % db
$c_p$	Specific heat capacity of a sample	$\text{kJ}/(\text{kmol}), \text{kJ}/(\text{kgK})$
$C_{ter,i}$	Tar concentration	$\text{mg}/\text{gm}^3$
$E$	Activation energy	$\text{kJ}/\text{mol}$
$E_j$	Activation energy of component $j$	$\text{kJ}/\text{mol}$
$E_1$	Activation energy hemicellulose	$\text{kJ}/\text{mol}$
$E_2$	Activation energy cellulose	$\text{kJ}/\text{mol}$
$E_3$	Activation energy lignin	$\text{kJ}/\text{mol}$
$H$	Hydrogen mass fraction in biomass	wt % db
$h$	Coefficient of conduction	$\text{W}/\text{m}^2\text{K}$
$h_k$	Height of an experimental curve that strongly depend on the experimental conditions	$1/\text{s}$
$k$	Temperature-dependent reaction rate constant	
$k_i$	Temperature-dependent reaction rate constant of $i$ th pyrolysis product	
$k$	Indicates the experiments of the series evaluated	
$L$	Particle characteristic length	$\text{m}$
$m$	Normalized sample mass	$\text{kg}$
$m_B$	Biomass mass	$\text{kg}$

$m_{char}$	Final mass after reaction has finished (relatively charcoal rate)	kg
N	Nitrogen mass fraction in biomass	wt % db
$N_{exp}$	Number of experiments in a given evaluation	
$N_k$	Number of evaluated data on the $k$ th experimental curve	
O	Oxygen mass fraction in biomass	wt % db
$p$	Pressure	kPa, bar
$P_y$	External Pyrolysis Number	
$P_y^I$	Internal Pyrolysis number	
Q	Energy	kW
R	Universal gas constant, $8.3143 \times 10^{-3}$ kJ/(molK)	
$r_i$	Rate of pyrolysis reaction	mg/gm <sup>3</sup> s <sup>1</sup>
$r_{ter,i}$	Tar rate	mg/gm <sup>3</sup> s <sup>1</sup>
S	Sulphur mass fraction of biomass	wt % db
S	Particle surface	m <sup>2</sup>
$S_N$	Goal function	
T	Temperature	°C, K
$T_o$	Initial temperature	°C, K
t	Time	s
$t_i$	time values in which the discrete experimental values were taken	
$t_r$	Pyrolysis reaction time	
V	Particle volume	m <sup>3</sup>
$v$	Mass of volatiles present at any time t	
$v_f$	Total mass of volatiles evolved during the reaction	
x	Fraction of the initial unreacted material	
$X_{obs}$	Observed values	
$X_{model}$	Modelled values at place $i$	
y	product yield	
$y_i$	$j$ th product of the pyrolysis reaction	
$Y_{j,i}$	Yield coefficient	g/g

### ***Subscripts and Superscripts***

a	Carbon content in pyrolysis products
b	Hydrogen content in pyrolysis products
c	Oxygen content in pyrolysis products
fc	Fixed carbon
$i$	Pyrolysis products (volatile, charcoal, gases)
$i$	Biomass pseudocomponent (hemicellulose, cellulose, lignin))
$i$	Digitized point on an experimental curve
$j$	Reaction component

$n$	Reaction order
$n$	Carbon mass content in biomass
$m$	Hydrogen mass content in biomass
$p$	Oxygen mass content in biomass
$th$	Theoretical yield

### ***Abbreviations***

daf	Dry ash free
db	Dry basis
wt	Water free
RMS	Rootmean-square value

$\Sigma_j$  - width-parameter (variation)

## CHAPTER 1

*“The great thing in the world is not so much where we stand,  
as in what direction we are moving.”  
Oliver Wendell Holmes*

### 1. INTRODUCTION

Ever increasing energy demand and the climate change problem caused by anthropogenic greenhouse gas emissions have resulted in the worldwide effort to find a sustainable and environmentally friendly alternative to today's fossil fuels dominated energy supply. The potential offered by biomass for solving some of the world's energy and environmental problems is widely recognised as environmentally friendly and renewable energy source. Biomass is very useful to meet different kinds of energy needs, including fuelling vehicles, providing process heat for industrial facilities, generating electricity and heating homes [58]. Examples of such biomass include agricultural residues, forest residues and food processing waste.

Agricultural residues, a widely available energy source, are especially interesting for energy production by means of different thermochemical processes. Corn cobs, as an agricultural residues, are particularly desirable as a sustainable biomass for energy feedstock because of its widespread availability and sufficient volumetric energy. The worldwide yearly corn production is around 800 million ton [38]. For every 1 kg of dry corn grains produced, about 0.15 kg of cobs, 0.22 kg of leaves and 0.50 kg of stalks are produced [59]. This results the production of about 120 million tonnes of corncobs. Also, the final report of a recent feasibility study [60] lists the advantages of corn cob utilization as: “Cobs represent a small, 15% portion of corn stover remaining on the field and cob removal has negligible impact on organic carbon depletion from the soil; Cobs have limited nutrient value to the soil. Whole and ground cobs have excellent flow properties and can be handled with conventional conveyors.” Therefore, there is need to research into a suitable corn cobs energy conversion technology applicable for widespread use.

Immerged technologies, although some have not attained a mature status, are able to convert the energy in the biomass not only to heat and power but also to solid fuels, fuel gas and liquid fuels that can be used in the transportation sector, chemicals with a high market value and hydrogen [12]. Although there are several methods of converting

biomass into energy, pyrolysis is highly promising thermochemical processes due to the possibility of converting the biomass into three constituents: solid (charcoal), liquid (tar and other heavy hydrocarbons) and gas ( $\text{CO}_2$ ,  $\text{CO}$ ,  $\text{H}_2$ ,  $\text{CH}_4$ ,  $\text{H}_2\text{O}$  etc.). Pyrolysis products in particular may be readily integrated into the energy infrastructures of both industrialised and developing countries [61].

At present time, more and more efforts have been put into extracting a higher form of energy from biomass. For example, recently, scientist leaders in field of biomass pyrolysis (Antal, Gronli, Varhegyi [38, 41, 57, 62-71] has focussed their attention onto production of well-characterized charcoals, from many different biomass feedstocks, for a wide variety of research endeavours, including carbon fuel cell studies, metallurgical charcoal applications, activated carbon production, and terra preta research.

In spite of the evident importance of charcoal to the world economy, the science of charcoal production is still in its infancy. According to Antal and Mok [72] and Várhegyi et al [73], traditional methods for charcoal production in developing countries realize yields of 20 wt % (even less), and modern industrial technology offers yields of only 25 - 37 wt % [68, 73]. This charcoals has a fixed - carbon content of about 70 - 80 wt % and offers a fixed - carbon yield of about 20 - 24 wt % [67]. From a theoretical perspective, charcoal production should be efficient and quick. Thermochemical equilibrium calculations indicate that carbon is a preferred product of biomass pyrolysis at moderate temperatures, with byproducts of  $\text{CO}_2$ ,  $\text{H}_2\text{O}$ ,  $\text{CH}_4$ , and traces of  $\text{CO}$  [69, 71]. Antal et al. [68, 72, 74, 75] based on thermochemical equilibrium calculations, pointed that, at 1MPa and 400°C, the maximum yield of carbon from cellulose is 27.7 wt % (i.e., 62.4 mol % of cellulose carbon is converted into biocarbon). More detailed calculations, based on the actual composition of the sample, led Antal et al [68] to the conclusion that the theoretical yield of charcoal from most biomass feeds, at 1MPa and 400°C, should be in the approximate range 55 (corn cobs with a carbon content of 45%) to 71% (Macadamia nut shells with a carbon content of 58%).

In this study, slow pyrolysis was chosen for charcoal maximisation. The product yields and properties of final products of slow pyrolysis are highly dependent on biomass type, moisture content of biomass, chemical and structural composition of the biomass, temperature, heating rates, reactors, particles size, residence time and others. To achieve an advanced pyrolysis process for improving product yields and quality from pyrolysis of selected corn residues, in-depth studies on the slow pyrolysis are needed.

## **OBJECTIVES OF THIS RESEARCH**

The main purpose of this thesis was to evaluate the potential of converting corn cob by slow pyrolysis to energy products. In order to achieve this, the following objectives are defined:

1. Determination of the chemical and physical properties, and thermal behaviour of corn cobs with the aim of predicting their pyrolytic behaviour and finding their suitability as feedstock for slow pyrolysis for charcoal production.
2. Establishing the effects of varying process parameters, including effects of particle size, sample size, and vapour-phase residence time on the formation of charcoal.
3. Validation of a distributed activation energy model (DAEM) as a best kinetic model for the description of the global decomposition of biomass compositions.
4. Development of a steady model of slow pyrolysis, in order to characterise physical and chemical properties of pyrolysis products and to determine the effect of biomass properties.

## **RESEARCH HYPOTHESES**

1. Hypothesis - increasing particle size substantially improves fixed-carbon yields. This improvement in yield is a result of increasing heterogeneous interactions between the pyrolytic vapours and the solid charcoal together with its mineral matter, both of which may be catalytic for the formation of charcoal.
2. The DEAM provides good fits for a wide range of experimental conditions. The DEAM is suitable to predict the behaviour of the samples outside of those experimental conditions at which the model parameters were determined.
3. Hypothesis - elevated pressure enables the carbonization of liquid bio-oil before it can vaporize and escape the solid matrix.

In general, this work addresses thermokinetic approaches for the detailed description of corn cob pyrolysis.

The aim of this work is to define in detail thermokinetic mechanisms of corn cob pyrolysis and to identify pyrolysis process conditions that improve the yield of charcoal from corn cob. Regarding to these, this work includes experimental and modelling work on the slow pyrolysis of corn cob and experimental and modelling work on the pyrolysis of corn cob under regimes controlled by chemical kinetics.

With regard to the main aims and objectives of this work, the thesis is developed in the following parts:

**Chapter 1** is the brief overview the actual and potential uses of renewable energy sources in EU-27 and Serbia, with special emphasis on biomass. Also, before treating biomass as a fuel, basic knowledge about its physical as well as its chemical properties is of high importance. Physical properties deal with the relationship between the solid biomass and moisture content [3]. The chemical properties refer to carbohydrate and lignin structures that are related to the decomposition and reactivity of the biomass [3]. Regarding to this a general introduction to the biomass structure and chemical composition.

**Chapter 2** is the brief overview of the biomass conversion technologies: combustion, gasification and pyrolysis.

**In Chapter 3**, fundamentals of biomass pyrolysis process are introduced. Types of pyrolysis, pyrolysis mechanism and influence of different working parameters on product yield are detail presented.

**Chapter 4** consists in a detailed bibliography review of the most significant issues around pyrolysis kinetics and product distribution. The kinetic approaches in this thesis and the mathematical procedures for reliable determination of the kinetic parameters that describe the pyrolysis process are introduced.

**Chapter 5** experimental and kinetic modelling work on the pyrolysis of corn cob under regimes controlled by chemical kinetics are presented in detail.

**Chapter 6** is the thorough discussion of the experimental results from the corn cob slow pyrolysis, concerning the mass loss process, yield of the products (charcoal, gas and tar) with the varied experimental conditions, variation of the compositions in the gas products. An experimental study on mechanisms influencing yield of charcoal and fixed carbon. Also, modelling work on the pyrolysis of corn cob under regimes of slow pyrolysis are presented in detail.

**Chapter 7** presents pyrolysis extension to practical gasification applications and addresses future work. In terms of engineering purposes, pyrolysis can be used as an independent process for the production of useful energy and chemicals. It also occurs as the first step in a gasification or combustion process. Considering mentioned, developed steady pyrolysis model (from chapter 5) is used for steady gasification model developing. This model considers gasification as a staged process divided into six different steps: drying, pyrolysis, volatiles combustion, charcoal combustion, charcoal gasification and



equilibrium reactions. These is able to predict phenomena in a wide range of experimental conditions and for different type of biomass material.

Finally, **Chapter 8** summarizes the thesis contribution. This chapter also includes recommendations for future work which will give deeper insight into the pyrolysis and gasification reaction mechanism and therefore improve pyrolysis and gasification process further.

All the work that has been performed for this study was published in scientific papers that can be found in APPENDIX D.

### **1.1. BIOMASS AS RENEWABLE ENERGY RESOURCE**

Biomass<sup>1</sup> is a general term used to describe the non-fossilized solid hydrocarbon material originating from plants and animals. Biomass sources include various natural and derived materials, such as wood and wood wastes (from forest thinning and harvesting), agricultural crops and their waste by products, animal wastes and wastes from food processing operations, municipal solid waste, animal wastes, waste from food processing, aquatic plants and algae and industrial and energy crops grown for biomass.

A generally accepted definition is difficult to find. The one of often used biomass definition are:

1. "Biomass - material of biological origin excluding material embedded in geological formations and transformed to fossil" (CEN/TS 14588) [76, 77].
2. "Biomass residues - biomass originating from well-defined side streams from agricultural, forestry and related industrial operation" (CEN/TS 14588) [76, 77].
3. "Biomass - renewable energy source, organic matter of vegetable or animal origin - wood, straw, vegetable residues from agricultural production, manure, the organic part of municipal solid waste" (Directive 2001/77/EC) [77, 78].

However, the one used by the Renewable Energy Directive (Directive 2009/28/EC) is relevant here:

*"Biomass means the biodegradable fraction of products, waste and residues from biological origin from agriculture (including vegetal and animal substances), forestry and related industries including fisheries and aquaculture, as well as the biodegradable fraction of industrial and municipal waste" [79].*

---

<sup>1</sup> biomass - Greek *bio* meaning life + *maza* meaning mass

Biomass does not include organic materials that over many millions of years have been transformed by geological processes into substances such as coal, oil or natural gas.

According to Basu [1] common sources of biomass are:

1. *Agricultural*: food grain, bagasse (crushed sugarcane), corn residues, straw, seed hulls, nutshells, and manure from cattle, poultry, and hogs;
2. *Forest*: trees, wood waste, wood or bark, sawdust, timber slash, and mill scrap;
3. *Municipal*: sewage sludge, refuse-derived fuel (RDF), food waste, waste paper, and yard clippings;
4. *Energy*: herbaceous woody crops - perennial grasses (switchgrass, miscanthus, bluestem, elephant grass, and wheatgrass), short rotation woody crops (poplars, willows, eucalyptus, cottonwood, silver maple, black locust), starch crops (corn, wheat and barley), grasses, sugar crops (cane and beet), forage crops (grasses and clover), oilseed crops (soyabean, sunflower, safflower).
5. *Biological*: animal waste, aquatic species, biological waste.

Table 1.1 lists a range of biomass types, grouping them as virgin or waste. Primary or virgin biomass comes directly from plants or animals. Waste or derived biomass comes from different biomass-derived products.

Table 1.1 Major groups of biomass and their sub classifications [1, 44]

Virgin	
Terrestrial biomass	forest biomass, grasses, energy crops, cultivated crops
Aquatic biomass	algae, water plant
Waste	
Municipal waste	municipal solid waste (MSW), bio solids, sewage, landfill gas
Agricultural solid waste	livestock and manures, agricultural crop residue
Forestry residues	bark, leaves, floor residues
Industrial wastes	black liquor, demolition wood, waste oil or fat

## 1.2. CHEMICAL STRUCTURE OF BIOMASS

The systematic identification, quantification and characterization of chemical and phase composition of a given solid fuel are the initial and most important steps during the investigation and application of such fuel (biomass). This composition is a fundamental code that depends on various factors and definite properties, quality and application

perspectives, as well as technological and environmental problems related to any fuel [39]. This composition is a unique fundamental code that characterizes and determines the properties, quality, potential applications and environmental problems related to any fuel, [39].

Understanding of the chemical structure and major organic components in biomass is highly important in the development of processes for producing derived fuels and chemicals. Biomass has a complex chemical composition, and both organic and inorganic constituents are important to the handling and conversion processes. Knowledge of the physical and chemical characteristics of biomass influences the choice of operating parameters of thermochemical processes, as well as the design and construction of reactors for thermochemical conversion of biomass (pyrolysis, gasification, combustion reactor).

This chapter includes a brief description of chemical characteristics and energy potential of biomasses.

### 1.2.1. STRUCTURE OF BIOMASS

Biomass is a complex mixture of organic materials such as carbohydrates, fats, and proteins, along with small amounts of minerals such as sodium, phosphorus, calcium and iron. The main components of plant biomass are extractives, fiber or cell wall components, and ash, (Figure 1.1).

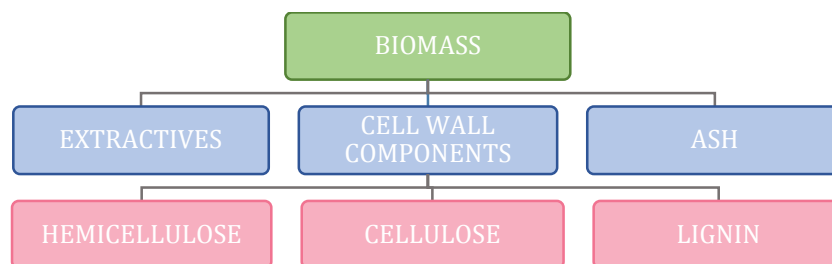


Figure 1.1 The structure of plant biomass [1]

#### **EXTRACTIVES**

Extractives are substances present in vegetable or animal tissue that can be separated by successive treatment with solvents and recovered by evaporation of the solution. The extractives are compounds of varying chemical composition such as gums, fats, resins, sugars, oils, starches, alkaloids and tannins. The composition varies according to species

as well as from sapwood to heartwood in a given stem. They contain lipophilic and hydrophilic substances (proteins, oils, sugar, starch, etc.). Extractives are classified into four major groups namely primary constituents as: steroid and terpenoid extracts, fats and waxes, phenolic compounds, and inorganic compounds. The extractives are responsible for the characteristic colour and odour of various species, or, in some biomasses, for resistance to decay and insect attack [80].

The polymeric composition of the cell walls and other constituents of a biomass vary widely, but they are essentially made of three major polymers: cellulose, hemicellulose, and lignin [1].

### **CELLULOSE**

Cellulose,  $(C_6H_{10}O_5)_n$ , is the primary structural component of cell walls in biomass. Its amount varies from 90 wt % in cotton to 33 wt % for most other plants. Cellulose is a long chain polymer with a high degree of polymerization ( $\sim 10,000$ ) and a large molecular weight ( $\sim 500,000$ ) [1]. It has a crystalline structure of thousands of units, which are made up of many glucose molecules, connected to each other by 1-4- $\beta$ -glycosidic bond, Figure 1.2. This structure gives it high strength, permitting it to provide the skeletal structure of most terrestrial biomass [1, 37].

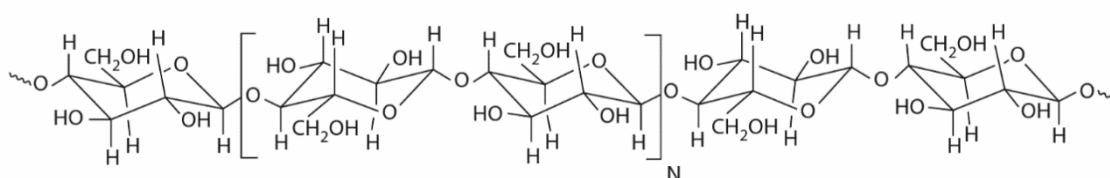


Figure 1.2 Structural formula of cellulose [2]

### **HEMICELLULOSES**

Hemicelluloses are heteropolysaccharides, in contrast to cellulose, which is a homopolysaccharide. Hemicellulose consists of a mixture of polymers: pentoses (xylose and arabinose) with the general formula  $(C_5H_8O_4)_n$  and hexoses (glucose, mannose and galactose) with the general formula  $(C_6H_{10}O_5)_n$  [32, 81]. The monomeric components of hemicellulose are primarily D-glucose, D-mannose, D-galactose, D-xylose, L-arabinose but to some extent it can be L-rhamnose in addition to D-glucuronic acid, D-galacturonic acid, and 4-O-methyl-D-glucuronic acid [82]. Its amount varies from 20-30 % (by weight)

in most plants. Figure 1.4 shows the molecular arrangement of a typical hemicellulose molecules.

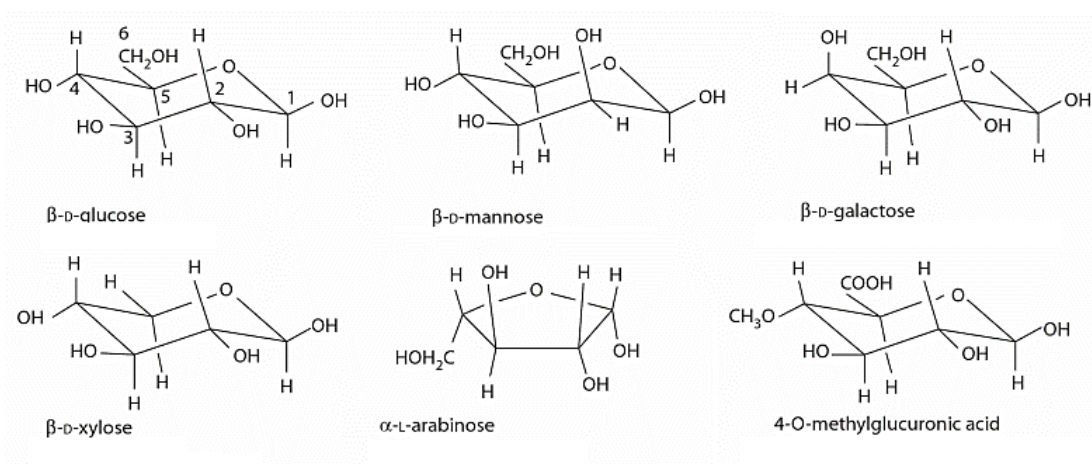


Figure 1.3 Structural formulas of hemicellulose's monomers [3]

### **LIGNIN**

Lignin is a complex highly branched polymer of p-hydroxyphenyl, guaiacyl and syringyl [83]. The structure varies among different plants. Softwood lignin is composed principally of guaiacyl units stemming from the precursor trans-coniferyl alcohol [80]. Hardwood lignin is composed mostly of guaiacyl and syringyl units derived from trans-coniferyl and trans-sinapyl alcohols [80]. Grass lignin contains p-hydroxyphenyl units deriving from trans-p-coumaryl alcohol [80]. Almost all plants contain all three guaiacyl, syringyl, and p-hydroxyphenyl units in lignin. A partial structure of softwood lignin is shown in Figure 1.4. The lignin contents on a dry basis generally range from 10% to 40% by weight in various herbaceous species [80, 84].

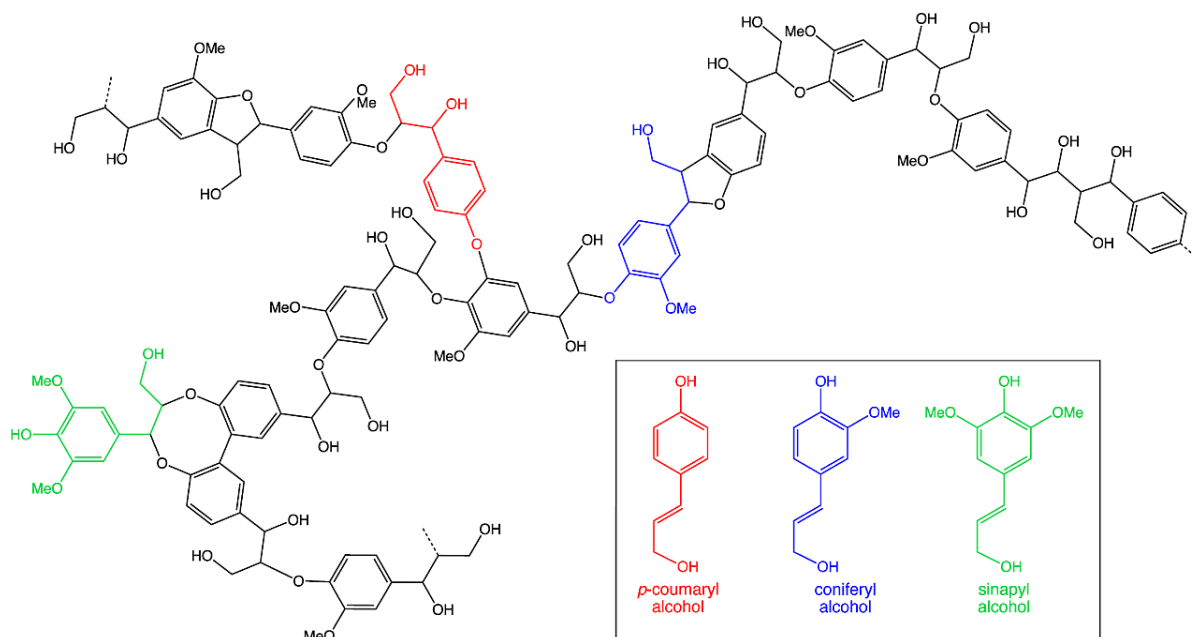


Figure 1.4 A hypothetical depiction of soft wood ligning, with basic monolignols [4]

In Table 1.2 is presented share of cellulose, hemicellulose and lignin share in some biomass tips. It can be seen, corn stover compered to corn cobs, wheat straw and grass, has lowest amount of lignin, which make its suitable for bioethanol production [81].

Table 1.2 Cellulose, hemicellulose and lignin share in some biomass tips

Biomass	Hemicellulose (wt %)	Cellulose (wt %)	Lignin (wt%)	Extractives (wt%)	Ref.
corn cob	26.2	34.1	18.50	5.1	[85]
corn leaves	19.1	33.8	18.4	11.5	[85]
corn stalks	18.5	40.7	23.0	9.9	[85]
wheat straw	27.3	27.3	16.4	7.4	[86]
sunflower seed hull	18.4	26.7	27	NA	[67]
rice straw	35.7	32	22.3	10	[87]
rice husk	28.6	28.6	24.4	18.4	[87]
grape residues	17.2	17.2	30.4	15.6	[86]
olive husks	18.5	18.5	28.0	8.7	[86]
pine wood	28.5	40	27.7	3.5	[88]
birch wood	32.4	41	22	3	[88]
spruce wood	30.6	39.5	27.5	2.1	[88]

Biomass can also be classified on the basis of its relative proportion of cellulose, hemicellulose, and lignin. For example, the behaviour of a biomass during pyrolysis can

be predicted from knowledge of these components [1, 5]. The ratio of hemicellulose to lignin vs the ratio of cellulose to lignin is presented in Figure 1.5.

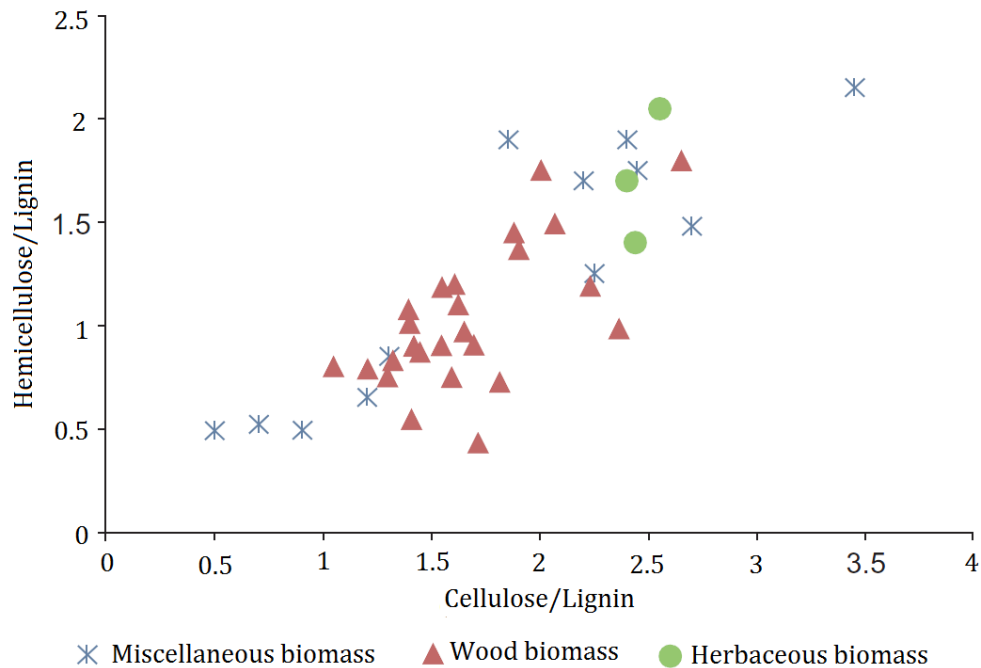


Figure 1.5 Classification of biomass by constituent ratios [1, 5]

In spite of some scatter, certain proportionality can be detected between the two. Biomass falling within these clusters behaves similarly irrespective of its type. For a typical biomass, the cellulose–lignin ratio increases from  $\sim 0.5$  to  $\sim 2.7$ , while the hemicellulose–lignin ratio increases from 0.5 to 2.0.

### 1.2.2. CHEMICAL CHARACTERISATION OF BIOMASS

The elements are present in solid biomass at varying concentrations depending on the origin and type of biomass. Carbon (C), Hydrogen (H) and Oxygen (O) are the main components of biomass. The content of C and H contributes positively to the Heating Value, the content of O negatively [89]. The C contents of wood fuels are higher than those of herbaceous biofuels, which explains the slightly higher higher Heating Value of wood fuels [89]. Variation in Heating Value between different biomass types is in direct correlation with the atomic ratio between oxygen-to-carbon (O/C) ratio and hydrogen-to-carbon (H/C) ratio. The heating value is very different: bituminous coal has 30.20 MJ/kg, where hardwoods have 19.80 MJ/kg (dry) and agricultural residues average about 18.00 MJ/kg (dry). The reason for that is the higher carbon content of the coal. As the

carbon content of the fuel increases, the heating value also increases. The atomic ratio is based on the hydrogen, oxygen, and carbon content of the fuel. Figure 1.6 plots the atomic ratios H/C against O/C on a dry ash free basis for all fuels, from carbon-rich anthracite to carbon-deficient woody biomass. This plot, known as van Krevelen diagram, shows that biomass has much higher ratios of H/C and O/C than fossil fuel [1]. For example, the higher heating value (HHV) of a biomass correlates well with the O/C ratio reducing from 8 to about 15 MJ/kg while the O/C ratio increases from 0.1 to 0.7 [1]. When the H/C ratio increases, the effective heating value of the fuel reduces, [1]. For a large range of biomass, the H/C ratio might be expressed as a linear function of the O/C ratio [1, 5].

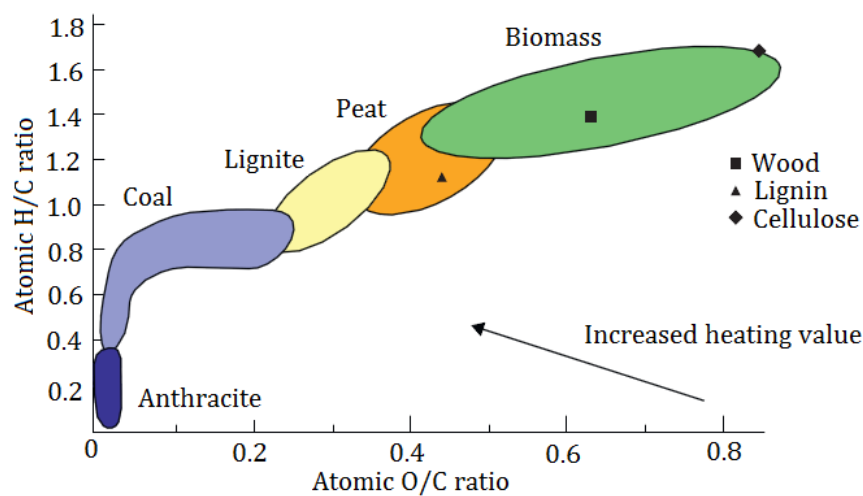


Figure 1.6 Van Krevelen`s diagram [6]

Biomass has higher H/C ratio and O/C ratio compared to fossil fuels. Biomass has higher oxygen content what results in higher reactivity and contains high amounts of volatile matter compared with coal [6, 90]. The energy content is very different: bituminous coal has 30.2 MJ/kg, where hardwoods have 19.8 MJ/kg (dry), and agricultural residues average about 18.0 MJ/kg (dry, [6]. Among all hydrocarbon fuels biomass is highest in oxygen content. Oxygen, unfortunately, does not make any useful contribution to heating value and makes it difficult to transform the biomass into liquid fuels. The high oxygen and hydrogen content of biomass results in high volatile and liquid yields, respectively [1]. High oxygen consumes a part of the hydrogen in the biomass, producing less beneficial water, and thus the high H/C content does not transform into high gas yield [1]. Also, tar decreases with O increases.

Most virgin or fresh biomass contains little to no sulphur (S). Biomass-derived feedstock such as municipal solid waste (MSW) or sewage sludge does contain S, which requires



limestone ( $\text{CaCO}_3$ ) for the capture of it. Interestingly, such derived feedstock also contains small amounts of calcium (Ca), which intrinsically aids S capture [1]. Gasification from coal or oil has an edge over combustion in certain situations. In combustion systems, S in the fuel appears as sulphurdioxide ( $\text{SO}_2$ ), which is relatively difficult to remove from the flue gas without adding an external sorbent [1]. In a typical gasification process 93 to 96% of the S appears as hydrogen sulfide  $\text{H}_2\text{S}$  with the remaining as carbonyl sulfide (COS) [1, 91].

According to Obernberger et al [89], coniferous and deciduous wood has the lowest N content. Higher concentrations are found in bark, logging residues, short rotation coppice (willow and poplar) and straw from wheat, rye and barley [89]. The concentrations are usually still higher in rape straw (wheat, rye and barley straw can also have N contents in this range), miscanthus and fruit residues (e.g. olive or grape cakes, kernels, shells) [89]. Grains and grasses usually show the highest values of N. Also, a combustion system firing fossil fuels can oxidize the N in fuel and in air into nitric oxide (NO), the acid rain precursor, or into nitrous oxide ( $\text{N}_2\text{O}$ ), a greenhouse gas [1]. Both are difficult to remove. In a gasification system, nitrogen appears as either nitrogen gas ( $\text{N}_2$ ) or ammonia ( $\text{NH}_3$ ), which is removed relatively easily in the syngas-cleaning stage. Emission of  $\text{N}_2\text{O}$  results from the oxidation of fuel nitrogen alone. Measurement in a biomass combustion system showed a very low level of  $\text{N}_2\text{O}$  emission [1, 92].

The Figure 1.8, called ternary diagram [1], is not a tool for biomass classification, but it is useful for representing biomass conversion processes.

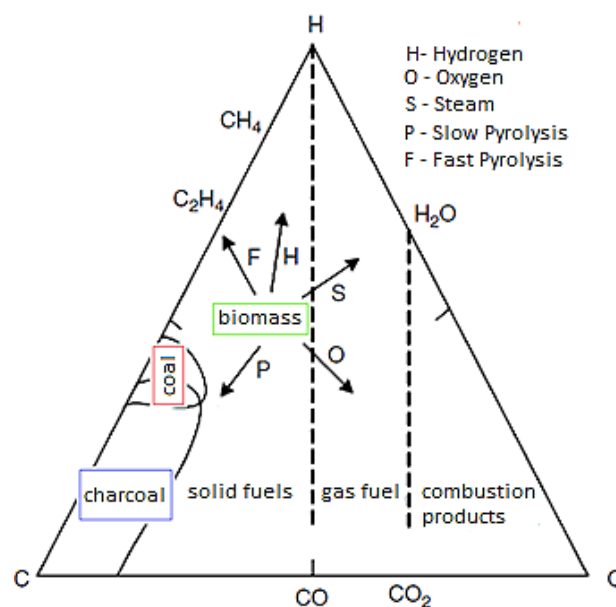


Figure 1.7 C-H-O ternary diagram [1]

The three corners of the triangle represent pure C, O and H that is 100% concentration [1]. Points within the triangle represent ternary mixtures of these three substances. The side opposite to a corner with a pure component (C, O or H) represents zero concentration of that component [1]. For example, the horizontal base in Figure 1.7 opposite to the hydrogen corner represents zero hydrogen— that is, binary mixtures of C and O [1].

A biomass fuel is closer to the H and O corners compared to coal [1]. This means that biomass contains more H and more O than coal contains. Lignin has lower amount of O and higher C compared to cellulose or hemicellulose. Peat is in the biomass region but toward the carbon corner, implying that it is like a high-C biomass. Peat is the youngest fossil fuel formed from biomass. Coal resides further toward the carbon corner and lies close to the oxygen base in the ternary diagram, suggesting that it is very low in O and much richer in C [1]. Anthracite lies furthest toward the C corner because it has the highest C content. The diagram can also show the geological evolution of fossil fuels, [1]. With age the fuel moves further away from the H and O corners and closer to the C corner [1].

The ternary diagram can depict the conversion process. For example, carbonization or slow pyrolysis moves the product toward carbon through the formation of solid charcoal; fast pyrolysis moves it toward H and away from O, which implies higher liquid product [1]. Oxygen gasification moves the gas product toward the O corner, while steam gasification takes the process away from the C corner [1].

### ***VOLATILE MATTER***

Volatile matter (VM) during thermal degradation is released as gases consisting of light hydrocarbons ( $C_nH_m$ ), carbon monoxide (CO), carbon dioxide ( $CO_2$ ), hydrogen ( $H_2$ ), moisture ( $H_2O$ ) and tars [12]. The volatiles involve:  $H_2$ , CO,  $C_nH_m$  (combustible gases) and also  $N_2$ ,  $O_2$ ,  $CO_2$ ,  $H_2O$  (incombustible gases). Biomass typically has high volatile matter content (up to 80 %), whereas coal has a low volatile matter content (less than 20 %). For example, bituminous coal has approximately 30–40% of volatile matter, and lignite has approximately 40–50% of volatile matter. The ignition temperature of biomass samples is lower than that of coal, which can be explained by the higher amount of volatiles and higher H/C and O/C ratio. Also, the amount of devolatilized products during the pyrolysis stage of combustion increases with increasing hydrogen to carbon ratio and, to some

extent, with increasing O/C [12]. Biomass has a high volatile content which makes it easier to ignite even at low temperature. Since volatiles get released relatively fast during thermal degradation (90% of its mass in its first stage of combustion), its fraction in biomass becomes a decisive parameter in designing reactors. In combustion, one has to ensure enough residence time for the devolatilized products in order to ensure complete combustion and to ensure low pollutant emissions (CO and PAH<sup>2</sup>) [12].

### **MOISTURE**

High moisture content is a major characteristic of biomass. It varies over a wide range from 10 – 70 % (wt) [12]. Higher moisture content, rendering the material putrifiable, which in turn presents storage problems [82]. Moisture content influences the heating value of the fuel (biomass) as it decreases with higher moisture values. The high moisture content causes significant energy loss in thermochemical processes, mainly as latent heat of steam<sup>3</sup>, which leads to higher fuel usage. During thermochemical processes, moisture content in biomass influences on the physical properties and quality of the products and results in larger equipment flue gas handling. Biofuels have normally a high moisture content which can cause ignition problems and reduce the combustion temperature [12]. Based literature review, any moisture content exceeding 20-40% will reduce efficiency of thermochemical process. Fuel (biomass) should therefore be dry, even if separate drying before use is necessary.

### **ASH**

Ash is the inorganic part of the fuel (biomass) that is left after thermal conversion process. It contains the bulk of the mineral fraction of the original biomass [12]. The ash content in the biomass varies with different types and can vary from 0.5 % (wood) and up to 20 % (some agricultural residues), Table 1.3. The major ash elements found in biomass include silicon, calcium, magnesium, potassium, sodium, phosphorus, sulphur, chlorine, aluminium, iron, manganese (Si, Ca, Mg, K, Na, P, S, Cl, Al, Fe, Mn), also traces of heavy metals such as copper, zinc, cobalt, molybdenum, arsenic, nickel, chromium, lead, cadmium, vanadium, mercury (Cu, Zn, Co, Mo, As, Ni, Cr, Pb, Cd, V, Hg) and N.

---

<sup>2</sup> PAH - Polycyclic Aromatic Hydrocarbons

<sup>3</sup> Heating value drops dramatically with increased moisture since the heat of vaporization of the water can't be recovered during thermochemical conversion

Table 1.3 Ash content in some agricultural residues

	<b>Ash content</b> (wt % db)	<b>Reference</b>
corn cob	0.3 - 4.31	[67, 69, 85, 87, 93]
corn leaves	2.0- 8.3	[85, 93, 94]
corn stalks	0.5-5.9%	[85, 93, 95]
wheat straw	5.5 – 9.6	[86, 94, 96]
sunflower seed hull	≈ 1.62	[67]
rice straw	6 – 10.1	[87, 94]
rice husk	15.30 - 41.34	[67, 69, 86, 87]
grape residues	≈ 5	[86]
olive husks	2.0 – 4.0	[86, 92, 97]
pine wood	≈ 0.3	[67]
birch wood	≈ 0.2	[67]
spruce wood	≈ 0.3	[67]

For most types of biomass, the contents of N, S and Cl is less than 1 wt% (db) [98]. K and P are two essential nutrients that promote plant root growth, increase grain yields, and enhance the strength of fibre structures [99]. Moreover, K and P fertilizers are currently being used to improve the soil quality and grain production, enhancing the K and P concentrations in agricultural residues [99]. Corn cobs, wheat straw have a relatively high content of these alkali metals (K, Na) Table 1.4 [45, 46].

It is commonly accepted that the concentration and behaviour of elements such as Ca, Cl, K, Na, P, S, Si and heavy metals (more precisely trace elements) are mostly responsible for many technological and environmental problems during biomass processing [39]. The release of ash particles during thermal treatment can occur due to ash volatility or reaction with the organic fraction of biomass, [12]. Ash elements that become volatile at high temperatures are derivatives of some of the alkali and alkaline earth metals, most notably K and Na [12]. Other nonvolatile elements such as Ca and Mg can be released by convective transport during a fast devolatilization stage. The ash composition has a great effect on the ash melting point. K and Si for instance yield lower ash melting point while Mg and Ca increase it. Chlorides and low melting alkali- and aluminosilicates may also significantly decrease the ash melting point [89]. This can cause sintering or slag formation in the reactor (reduced plant availability and lifetime). In addition, melts occurring in fly ash particles may cause hard deposit formation on cooled reactor walls or heat exchanger tubes [89]. Hard deposit formation due to sticky fly ash particles can be accelerated by alkali and heavy metal salt mixtures (mixtures of alkali chlorides and

sulphates with Zn and Pb chlorides) [89]. Straw, cereal, grass and grain ashes, which contain low concentrations of Ca and high concentrations of Si and K, start to sinter and melt at significantly lower temperatures than wood [89]. Together with Cl and S, K and Na play a major role in corrosion mechanism. Moreover, low melting mixtures of alkali and heavy metal chlorides can also cause corrosion by sulphation reaction [89]. Certain fuels such as demolition wood contain heavy metals such as Cd, Cr, Cu, Pb, and Hg. Such elements are regarded hazardous for the environment and are normally found in the fly ash in combustion plants.

Table 1.4 Alkali oxides in some agricultural residues [45, 46]

<b>Biomass</b>	<b>Ash content</b> (wt % db)	<b>Alkali oxides in Ash</b> (Na <sub>2</sub> ,K <sub>2</sub> O) [wt % db]	<b>Alkali oxides in Biomass</b> (wt % db)
corn cob	2.62	30.60	0.80
wheat straw	6.60	14.80	0.98
rice straw	18.67	13.26	2.47
rice husk	23.7	0.98	0.23
barks	4.31	2.67	0.12
wood sawmills	1.28	4.67	0.60

The varying chemical properties of the different biomass mentioned emphasise the necessity of reliable methods for their characterisation as well as of the standardisation of these methods and of the biomass themselves. Moreover, an appropriate biomass characterisation is of great relevance in order to be able to adapt the thermochemical conversion technology and flue gas cleaning technology to the fuel accordingly and to be able to define and also control acceptable quality deviations for a certain biomass.

### **FIXED CARBON**

Fixed Carbon (fC) represents the solid carbon in the biomass that remains in the charcoal in the pyrolysis process after devolatilization.

Since fC depends on the amount of VM, it is not determined directly [1]. VM also varies with the rate of heating. In a real sense, then, fixed carbon is not a fixed quantity, but its value, measured under standard conditions, gives a useful evaluation parameter of the fuel [1].

For gasification analysis,  $f_C$  is an important parameter because in most gasifiers the conversion of fixed carbon into gases determines the rate of gasification and its yield [1]. This conversion reaction, being the slowest, is used to determine the size of the gasifier [1].

Knowledge of the physical and chemical characteristics of biomass influences the choice of operating parameters of thermochemical processes, as well as the design and construction of reactors for thermochemical conversion of biomass (pyrolysis, gasification, combustion reactor).

The characteristics of biomass greatly influence the performance of thermochemical reactors. A proper understanding of the physical and the chemical properties of biomass feedstock is essential for the design of thermochemical reactors to be reliable.

Many of the characteristics of biomass or other fuels are determined using ASTM<sup>4</sup> procedures or standard analytical methods. These include Proximate (moisture content, volatile content, ash content and fixed carbon) and ultimate analyses (C, H, N, O and S), trace metal content, ash, ash fusion temperature, and materials-handling. This will be presented in the following chapters (when will be corn cobs characterized as a bioenergy feedstock).

### **1.3. ACTUAL AND POTENTIAL USES OF BIOMASS RESOURCES IN EU -27**

Production of primary<sup>5</sup> energy in the European Union (EU-27) from 802.94 Mtoe in 2011, decreased to 794.34 Mtoe in 2012 [100]. The general downward trend of **EU-27** production may, at least in part, be attributed to supplies of raw materials becoming exhausted and/or producers considering the exploitation of limited resources uneconomical. In 2011, the share of fossil fuels represented 50.68 % (406.92 Mtoe) in the total primary production, followed by nuclear energy 29.14 % (234.01 Mtoe) and renewable energy (RE<sup>6</sup>) 20.18 % (162.01 Mtoe) [100]. Among RE, the most important source in the EU-27 was biomass and waste, accounting for just over two thirds (108.01 Mtoe) of primary renewables production in 2011 [100].

---

<sup>4</sup> **ASTM International**, formerly known as the American Society for Testing and Materials (ASTM), is a globally recognized leader in the development and delivery of international voluntary consensus standards.

<sup>5</sup> Any kind of extraction of energy products from natural sources to a usable form is called primary production

<sup>6</sup> Primary production of biomass, hydropower, geothermal energy, wind and solar energy are included in renewable energies

Gross inland consumption of primary energy<sup>7</sup> in the European Union (EU-27) from 1699.53 Mtoe in 2011, decreased to 1682.93 Mtoe in 2012 [100]. In 2011, the share of fossil fuels represented 77.11 % (1356.47 Mtoe) in the gross primary energy consumption, followed by nuclear energy 13.30 % (234.01 Mtoe) and RE 9.92 % (168.65 Mtoe) [100]. Among renewable energies, the most important source in the EU-27 was biomass and waste, accounting 68.63% (105.24 Mtoe) of primary renewables consumption in 2011 [100].

Figure 1.8 shows the EU-27 electricity and heat production in 2011, breakdown by different energy sources. Gross electricity generation in 2011 was 3279.27 TWh. The share of fossil fuels represented 60.48 % (1983.43 TWh) in the gross electricity generation, followed by nuclear energy 27.65 % (906.8 TWh) and RE 11.72 % (699.56 TWh).

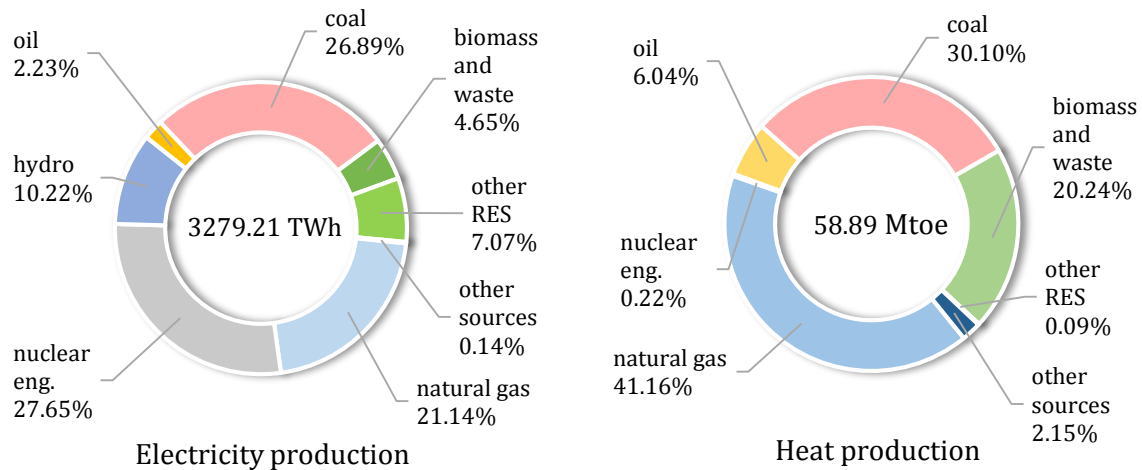


Figure 1.8 EU-27 Electricity and Heat Production in 2011 [7]

It can be observed how biomass represented  $\approx 5\%$  and  $\approx 20\%$  of the total production of electricity and heat respectively.

Among the renewable resources represented in Figures 1.9 and Table 1.5 it can be seen how biomass represents an important share in the renewable electricity, heat production and transport (of year 2011) [101].

Table 1.5 EU-27 RES in Transport in 2011 [7]

Energy Source	Consumption (Mtoe)
biomass	12.01
<b>Sum</b>	<b>12.01</b>

<sup>7</sup> Gross inland consumption is defined as primary production plus imports (It therefore reflects the energy necessary to satisfy inland consumption within the limits of national territory)

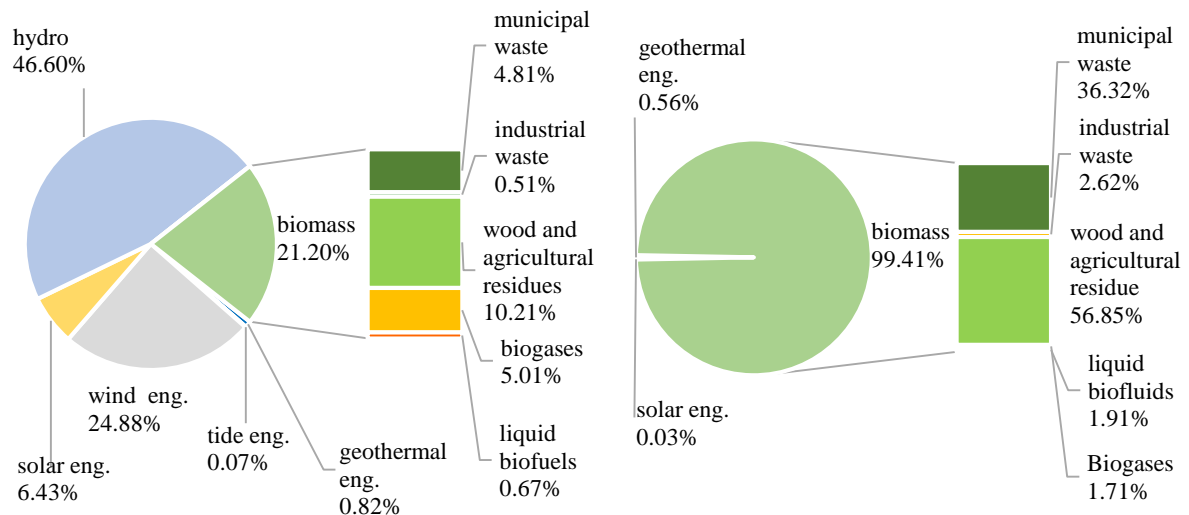


Figure 1.9 EU-27 Electricity and Heat production from RES in 2011 [7]

In order to reduce energy dependence on imported fossil fuels and thereby reduce emissions of GHG<sup>8</sup> gases, renewable energy is a key element in energy policy of every country.

The EU's renewable energy policy started in 1997, when the European Commission published a white paper "Energy for the future: renewable sources of energy" (EC 1997) stating a target for the EU to double the European Union's renewable energy share of the gross domestic energy consumption to 12% by 2010 [102]. The 1997 White Paper included a renewable energy strategy and action plan. Following legislation Directive 2001/77/EC (Renewable Energy Supply–Electricity (RES-E)) set indicative national targets for electricity produced from renewable sources. The target for the whole European Union was set to 21% of electricity consumption from renewable energy sources by 2010, and the Member States' targets ranged from Luxembourg's 5.7% to Sweden's 60% [100, 103, 104].

On May 2003, the EU-27 adopted Directive 2003/30 EC (The promotion of the use of biofuels or other renewable fuels for transport) to promote the use of biofuels and renewable fuels in transport. The Directive required Member States to, by 2003, set indicative targets for a minimum proportion of biofuels to be placed on the market: 2% in 2005 and 5.75% in 2010. The share of RES in the transport sector in 2005 and 2009

<sup>8</sup> GHG – greenhouse gas is a gas in an atmosphere that absorbs and emits radiation within the thermal infrared range. This process is the fundamental cause of the greenhouse effect. The primary greenhouse gases in the Earth's atmosphere are water vapor, carbon dioxide, methane, nitrous oxide, and ozone.



was 1.4 % and 4 % respectively. Following this trend, it can be estimated that target of 5% share of RES in transport will be achieved in 2020,

In January 2007, the European Commission (EC) proposed following targets [105]:

1. Reduce unilaterally GHG by 20% in 2020 compared to 1990 levels,
2. Supply 20% of energy needs by 2020 from RES, including the use of 10% renewable energy in transport,
3. Give priority to energy efficiency in all energy domains.

On January 2008 the EC proposed a full policy package of implementation measures to meet these objectives, the Directive 2009/28/EC. This package, The EU climate and energy package (“Directive 20-20-20”), for the first time sets mandatory national targets for integrating energy from renewable sources in to the gross final consumption of energy, [106]. The aims of Directive 2009/28/EC were:

1. To reduce emissions of greenhouse gases by 20% by 2020,
2. To increase energy efficiency to save 20% of EU energy consumption by 2020,
3. To reach 20% of renewable energy in the total energy consumption in the EU by 2020,
4. To reach 10% of biofuels in the total consumption of vehicles by 2020.

Figure 1.10 shows the expected share of biomass in final energy consumption in the EU-27, according to the objectives of the Directive 2009/28/EC.

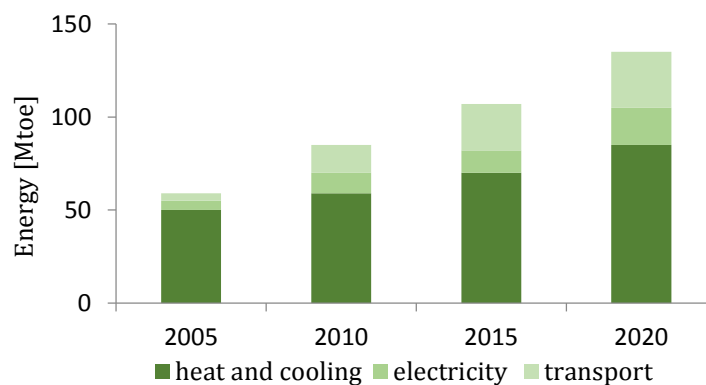


Figure 1.10 Biomass use towards reaching 2020 Renewable Targets [8]

As indicated in the Figure 1.10, member states expect that use of bioenergy will increase from 100.36 Mtoe in 2010 to 135.00 Mtoe in 2020. The greatest increases are in the electricity and transport sector, where bioenergy use is expected to double, from 10.7 Mtoe to 20.00 Mtoe in the electricity sector and 12.00 to 28.00 Mtoe in the transport sector.

On March 2011 the European Commission adopted the White Paper "The Transport 2050 roadmap to a Single European Transport Area" [107]. The roadmap includes 40 concrete initiatives for the next decade which will dramatically reduce Europe's dependence on imported oil and cut carbon emissions in transport by 60% by 2050 [108]. One of the White paper goals is to halve the use of 'conventionally fuelled' cars in urban transport by 2030; phase them out of cities by 2050; achieve CO<sub>2</sub>-free city logistics in major urban centres by 2030 [107]. Clearly, by 2020 the shift toward a transport system using much less energy, a significant part of which comes from renewable sources, should have been initiated [107]. EU Policies for renewable energy implementation, are presented in Table 1.6.

The present EU biomass supply is estimated at 429 Mtoe [109]. The bioenergy targets set in the Members States' NREAP<sup>9</sup>s can in principal be met through utilization of around 167 Mtoe biomass in 2020, which is only 40% of the domestic supply [109, 110]. Figure 1.11 illustrates the feedstock input to reach the 2020 bioenergy targets.

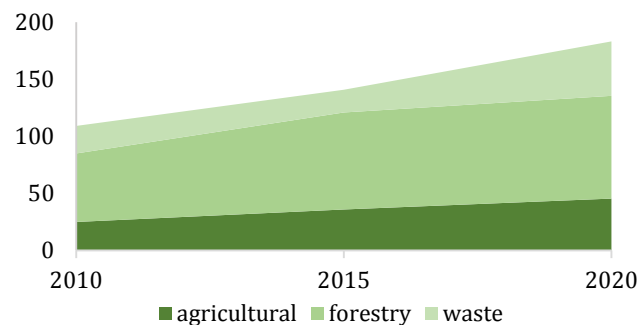


Figure 1.11 The biomass feedstock input required to reach the 2020 bioenergy targets [9]

The primary biomass use in comparison to the potentials for the different feedstock categories is presented in Figure 1.12. Among the biomass feedstocks current roundwood production, additional harvestable roundwood, straw, grassy perennials and dry manure are the largest unutilized feedstocks while the cheapest resources such as industrial wood residues, black liquor, post-consumer wood, used fats and oils are fully utilised [9]. Current roundwood and the additional harvestable roundwood remain very expensive (>400 €/toe) in comparison to the alternatives such as imported wood pellets [9]. Between 2010 and 2030 total import comprises around 12-15 % of the total demand

<sup>9</sup> National Renewable Energy Action Plans (NREAPs) were published by all Member States of the European Union in 2010. These plans provide detailed road maps of how each Member State expects to reach its legally binding 2020 target for the share of renewable energy in their total energy consumption, as required by the renewable energy Directive (2009/28/EC)

[9]. These imports mainly consist of wood pellets, feedstock for biofuel production and biofuels.

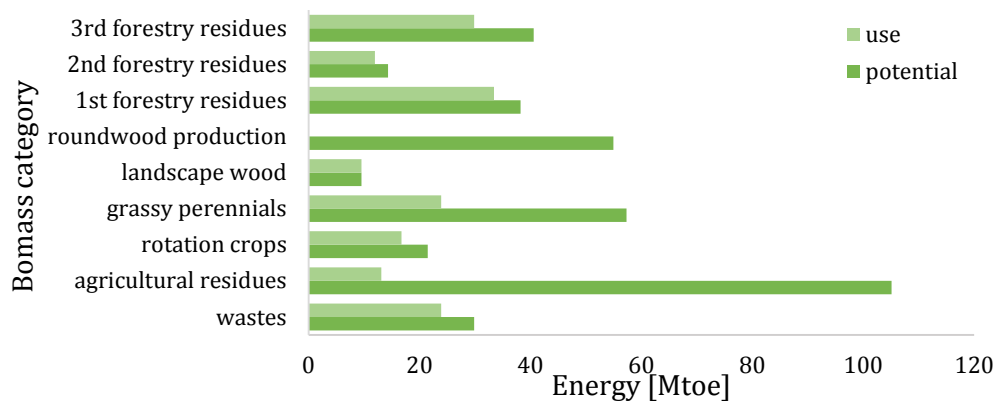


Figure 1.12 Domestic supply by biomass type [9]

Figure 1.13, 1.14 and 1.15 illustrates the total electricity production, heat and biofuels, for the EU-27 based on the policy measures promoted by the Member States in their NREAPS. In 1997 the EU agreed a strategy and target to double the share of renewable energies in gross domestic energy consumption, from 6% to 12% by 2010 [90]. In 2001, member states agreed national (non-binding) targets for electricity production from renewable sources, to expand the aggregate proportion of electricity from renewable sources in the EU from 13.9% in 1997 (3.2% excluding large hydro) to 22.1% by 2010 (12.5% excluding large hydro) [91]. The EU is making progress towards meeting the 2020 target of 20% renewable energy in gross final energy consumption. In 2010, the renewables share in the EU was 12.7% compared to 8.5% in 2005 [91]. In the period 1995-2000 when there was no regulatory framework, the share of renewable energy grew by 1.9% a year [91]. Following the introduction of indicative targets (2001-2010), the share of renewable energy grew by 4.5% per annum. With legally binding national targets growth has increased but needs to average 6.3% per year to meet the overall 2020 target. The share of renewables in transport reached 4.7% in 2010 compared to only 1.2% in 2005 [91]. In the heating and cooling sector, renewable energy continues to grow and its share should nearly double by 2020. However, new measures will be needed for most Member States to achieve their 2020 targets reflecting the scaling back of support schemes and more difficult access to finance in the context of the economic crisis [91].

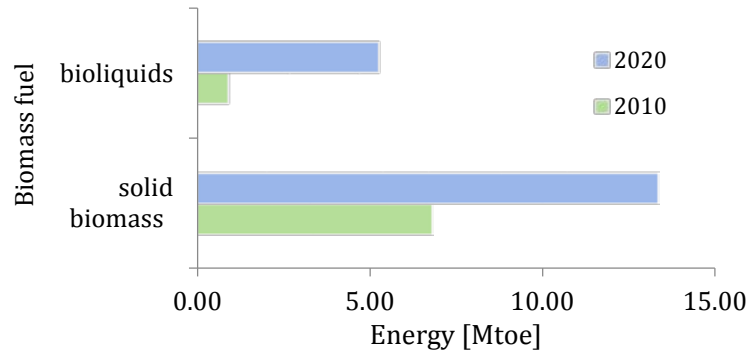


Figure 1.13 Biomass derived electricity [10]

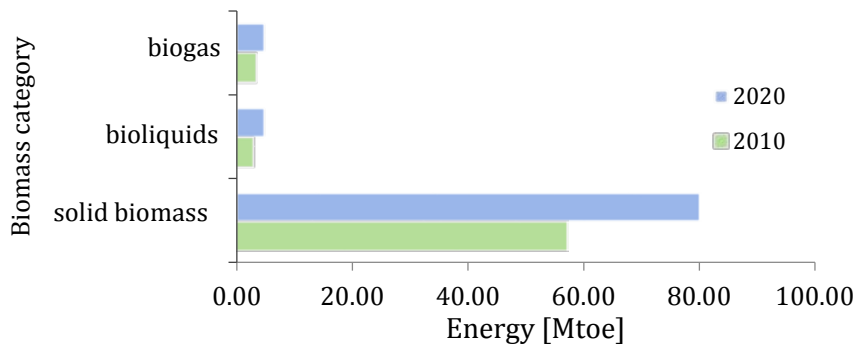


Figure 1.14 Biomass derived heating [10]

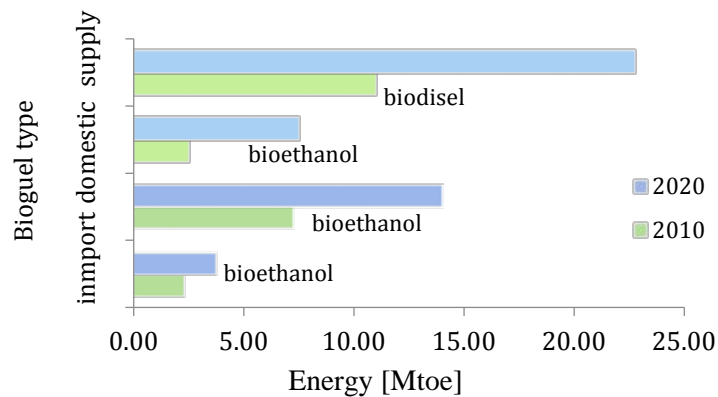


Figure 1.15 Contribution to transport energy by biofuel type [10]

Among the renewable resources, biomass represents an important share in the renewable electricity and heat production. The main benefits of the use of biomass over conventional fuels can be summarized as follows: renewable and recyclable energy source, widespread availability in Europe and abroad, decreased reliance on imported energy sources, less waste directed to landfills can be stored and used on demand, CO<sub>2</sub>, SO<sub>2</sub> and other emissions [111]. In addition to the many benefits common to any renewable energy use, biomass is the only other naturally available energy containing

carbon resource known that is large enough to be used as a substitute for fossil fuels [82]. In addition, bioenergy is unique in its potential to service all three of the major energy demand sectors for heat, electricity, and transport fuels. Moreover, biomass has a great potential to provide feed stocks to make a wide range of chemicals and materials or bio-products [99]. For these reasons, the role of bioenergy in achieving EU energy targets is crucial. However, its complexity and inter-sectorial nature, along with limited attention by policy makers compared to that given to photovoltaics and wind, are some of the reasons that have resulted to lower growth of bioenergy compared to other RES [112]. Other reasons are relatively high costs of the technologies of upgrading; the investment costs can be twice as high compared to fossil-fired plants (the low energy density requires larger plant sizes, the wide variety of fuel characteristics and the objective to achieve a clean combustion require higher efforts in conversion and clean-up technology) [80]. There is also a high effort necessary for transportation and storage of biofuels because of the low energy density and a reliable market for biofuels has not yet been established [99].

Table 1.6 EU Polices for renewable energy implementation

<b>Document</b>	<b>Goal</b>
White paper "Energy for the future: renewable sources of energy"	- 12% of gross inland energy consumption from renewables for the EU-15 by 2010.
Directive 2001/77/EC "Renewable Energy Supply- Electricity -RES-E"	- 21% RES contribution to electricity production.
Directive 2003/30 EC "The Promotion of the use of biofuels and other renewable fuels for transport"	- 2% of all transport fossil fuels (petrol and diesel) replaced with biofuels by 2005. - 5.75% of all transport fossil fuels (petrol and diesel) replaced with biofuels by 2010.
Directive 2009/28/EC "The Renewable Energy Directive"	- 20% reduced emissions of greenhouse gases by 2020. - 20% of EU energy consumption reduced by 2020. -10% of biofuels in the total consumption of vehicles by 2020. - reduced primary energy consumption by 2020 by 20%.
White Paper "The Transport 2050 roadmap to a Single European Transport Area"	- 30% of road freight over 300 km should shift to other modes such as rail or waterborne transport by 2030, and more than 50% by 2050, facilitated by efficient and green freight corridors.

## 1.4. ACTUAL AND POTENTIAL USES OF BIOMASS RESOURCES IN REPUBLIC OF SERBIA

Production of primary energy in the Republic of Serbia from 10.77 Mtoe in 2012, increased to 11.39 Mtoe in 2013, although last years shows a downward trend in primary energy production (11.16 Mtoe in 2011) [11, 113]. The gross inland primary energy consumption in 2013, in Republic of Serbia, was 15.16 Mtoe out of which domestic production accounted for 75.44% (11.44 Mtoe), and import for 24.56% (3.72 Mtoe) [11]. Figure 1.16 indicates that the balance of domestic production compared with import of energy depends on the source of fuel.

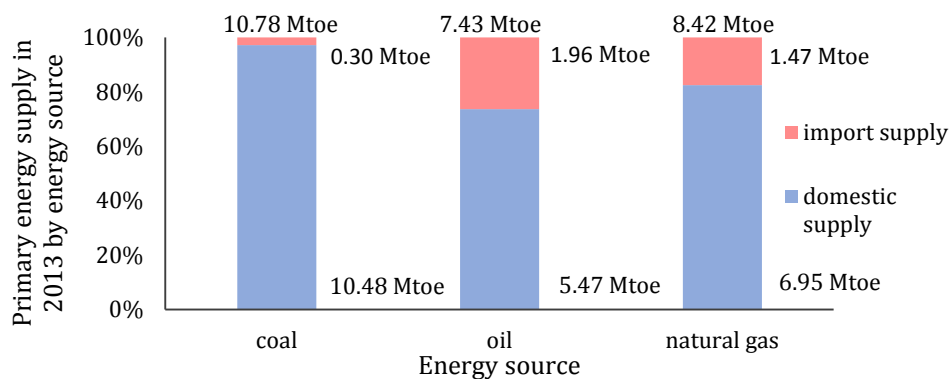


Figure 1.16 Domestic and import primary energy supply in 2013 [11]

Serbia has very diverse energy supply sector, composed of coal extraction, coal and hydro electricity generation and oil and gas production. According to the data of the Ministry of Energy, Development and Environmental Protection of Republic of Serbia, the share of coal in the structure of primary energy production in 2013 was 67.75%, oil 11.44%, natural gas 4.01% and renewable energy sources 16.80 % (hydro potential 7.53 %, biomass 9.21 % and geothermal energy 0.05 %) [11]. Figures 1.17 show the Serbian primary energy production in 2013, breakdown by different energy sources. On other hand, the Republic of Serbia has high-quality of RES (Figure 1. 18), it clearly states that it should be one of the main pillars of the energy sector in the future. Renewable energy sources with an estimated technically usable potential of about 5.63 Mtoe per annum (Figure 1.18) can have a considerable contribution to a lesser utilization of fossil fuels and achievement of defined targets (subchapter) regarding the share of renewable sources in the energy consumption, as well as regarding the improvement of environment [114]. In the previous period, the use of renewable energy sources was

based on the electricity generation from large river flows and the use of biomass mostly for household heating and to a lesser part in industry.

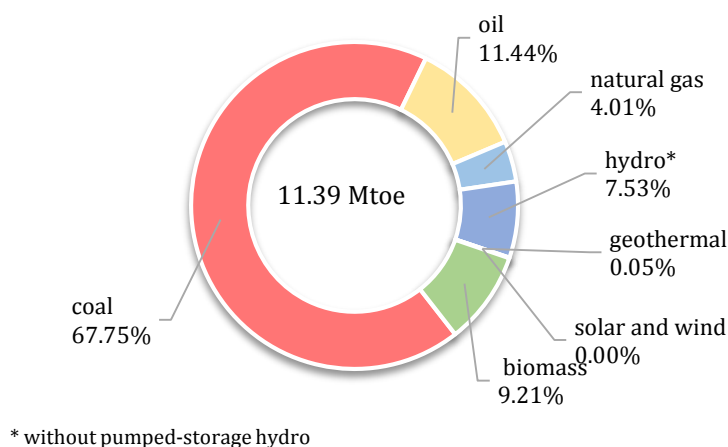


Figure 1.17 Primary energy production detailed selected by energy sources in 2013 [11]

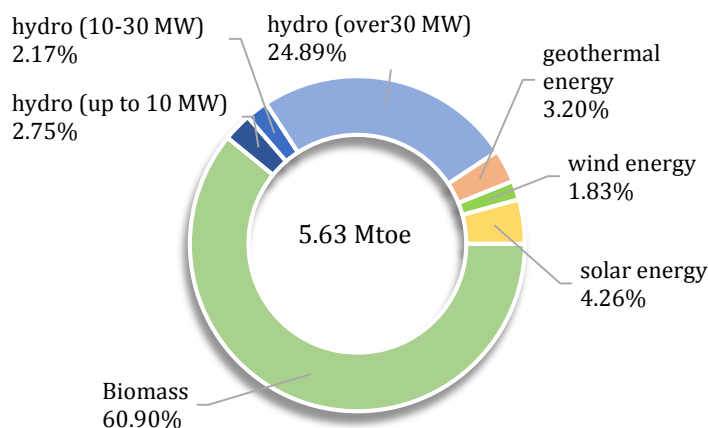


Figure 1.18 Energy potential of RES in the Republic of Serbia

### **NATIONAL ACTION PLAN FOR RES BY 2020**

With ratification of Energy Community Treaty the Republic of Serbia also assumed obligation from Directives 2009/28/EC on the promotion of the use of energy from renewable sources and on promotion of use of bio fuel or other fuel from renewable energy sources for transport [114]. For intensive use of renewable sources the Republic of Serbia joined countries that subsidised electricity generation from renewable sources and introduced the widely used model feed/in tariff with the period of guaranteed supply of electricity of 12 years [114]. The Republic of Serbia adopted the National Action Plan for RES as a frame work for promotion of energy sources and set mandatory national

goals for share of renewable energy in gross final consumption of energy (27%) as well as the share of RES in transport (10%) by 2020 [114]. Taking into account the currently available capacities for the production of second generation biofuels from biomass which meets the parameters regarding greenhouse emissions, as well as the non-existence of the legislation and the relevant infrastructure for its application in the field of biofuels, the Republic of Serbia will have to plan import of biofuels in 2018 [114].

The Action Plan is prepared in accordance with the EU methodology and standards EU, on the basis of all relevant data in the field of energy and renewable energy sources in the Republic of Serbia.

In order to achieve adopted national goals installation of larger capacities is envisaged for electricity generation by using wind, biomass and sun, as well higher share of RES in heat and cooling sector. To achieve its targets in the electric power sector, the Republic of Serbia will install additional 1092 MW until 2020 [114]. In Figure 1.19 the share of different types of RES in electricity and heat production is presented.

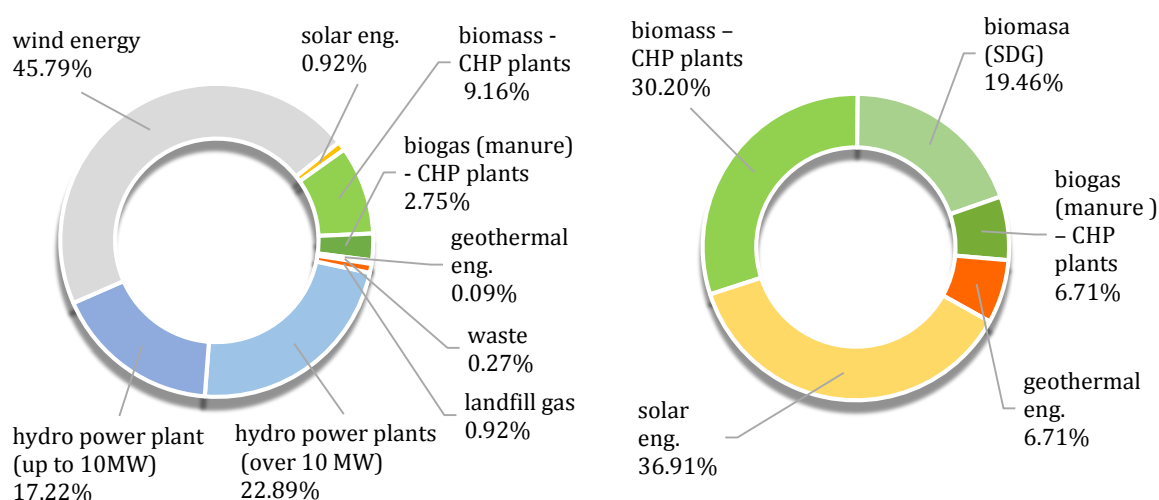


Figure 1.19 Projected changes in the structure of fuel for electricity generation and heat production

In the transport sector, renewable energy sources were existent at the market but only in form of biodiesel and was used in agriculture [114]. Biofuel were not existent at the market in mixtures with the oil-based fuels for motor vehicles, in line with allowed quantities pursuant to the relevant standards for motor petrol and diesel fuel [114]. Depending on the energy consumption in traffic sector, and in compliance with the agreements achieved in the Energy Community, mandatory goal for the share of



renewable energy sources in the transport sector amounts to 10 % in 2020 [114]. The quantity of renewable energy sources in the transport sector will amount to 267 ktoe in 2020, which is 2.6% of renewable energy sources in gross final energy consumption [114]. The Republic of Serbia currently has capacities for production of bio fuels from biomass of first generation, which do not full fill conditions regarding greenhouse gases emissions and could not contribute to achieving mandatory share of 10% 2020. Having in mind that currently there are no facilities for the production of biofuels from biomass of second generation, the absence of legal regulation in this field and very short period for achieving this very demanding goal, the Republic of Serbia has to plan the import of bio fuel [114]. Therefore it is necessary to stimulate the production of biofuels in the country[114].

### ***BIOMASS ENERGY POTENTIALS IN REPUBLIC OF SERBIA***

The total surface area of Serbia is 8.83 million ha, without Kosovo and Metohija (as defined under UNSCR 1244) is around 7.75 million ha [115]. Agricultural land covers approximately 5.49 million ha (central Serbia 66.7% and Vojvodina 33.3% [116]). Total area of forests in Serbia is 2.25 million ha (state-owned 52.89 % and privately owned 47.11 % [115]) [117]. This indicates that largest RES energy source is biomass. According to Brkić, et. al. [118] the annual amount of biomass produced is totally 26.4 million tons. Since the Republic of Serbia has high-quality of biomass, it clearly states that it should be one of the main pillars of the energy sector in the future.

In order to be able to evaluate the sustainability of present consumption patterns and the feasibility of introducing modern biomass fuel-based applications, an assessment of the resources and its availability for energy has been done. It should be noted that this overview only considers: residues generated by agricultural production (crop residues, farming, fruit growing, viticulture, and livestock waste), wood residues (from logging, wood-processing such as saw-milling and manufacturing of plywood and particle board) and additional biomass resources (energy crops and municipal solid waste), Figure 1.20.

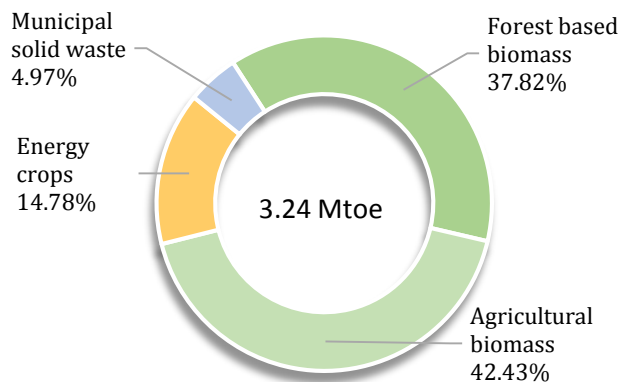


Figure 1.20 The structure of different biomass sources

### FOREST BIOMASS

As it is mentioned, an area of 2.25 million ha in the Republic of Serbia is covered with forests, which accounts around 29.1 % of the total area of the Republic of Serbia [119]. Every year 6.84 million m<sup>3</sup> (1.53 Mtoe ) of forest (wood) biomass is available for energy use every year. According to Glavonjić [120] about 5.52 milion m<sup>3</sup> represents fuel wood, with heating value of 1.15 Mtoe. Besides fuel wood, as a kind of forest assortments, there are different kinds of biomass residues associated with tree felling in forests and with processing of wood. As results of tree felling about 58% of the total mass of the tree are different wood assortments for the market, for industry, different technical purposes, and for heating as fuel wood [121, 122]. The rest of 42% of the total mass of the tree are different bio mass residues which do not have any value at the market (bark, small branches, tree stumps, etc.) [121]. The estimation is that these forest residues account for about 0.57·10<sup>6</sup> m<sup>3</sup>, which has an energy value of 0.16 Mtoe [120]. Residues of wood processing in saw mills, resulting from the production of veneer, boards, and furniture, and residues in pulp and paper and chemical industry, consist of small and large pieces (shavings, chips, cutting edge and bark) [121]. Estimated annual yield of these wood residues is about 0.63 10<sup>6</sup> m<sup>3</sup>, with energy value of 0.18 Mtoe [120]. Besides statistically registered forest felling, there is an unregistered tree felling as well. It encompasses not only un registered tree felling in forests, but also tree felling near local roads, small rivers, channels, and trees surrounding arable land [121]. A rather uncertain estimation indicates that around 0.12 million m<sup>3</sup> represents wood from trees outside the forest with energy value of 0.18 Mtoe. Table 1.7 shows estimated energy potential of forest biomass and fuel wood.

Table 1.7 Wood biomass energy potentials [47]

<b>Wood assortment</b>	<b>Amount (million m<sup>3</sup>)</b>	<b>Available energy (Mtoe)</b>
fuel wood	1.55	1.15
forest residues	1.78	0.03
wood from trees outside the forest	0.12	0.18
wood processing industry residue	0.63	0.16
<b>Sum</b>	<b>4.08</b>	<b>1.52</b>

## ACRICULTURAL BIOMASS

The waste biomass, generated in the agriculture, can be divided according to the agriculture branches on biomasses from field crops cultivation, or from orchards and vineyards, and that from the livestock cultivation [123, 124].

The field crops cultivation biomass is the largest potentially available biomass and it is contained in the residues obtained during the primary harvesting of the field products. The agricultural biomass residues are coming from cereals, mostly corn, wheat and barley, and from industrial crops mostly sunflower, soya, and rapeseed.

The estimation of the total potentials of the biomass residues, from field crops cultivation, is obtained by the application of annual yield of the main species of crop farming and known values of the mass ratio between grains and residues of specified cultures.

Table 1.8. shows the annual yield of main species in crop farming, annual yield of postharvest residues, and annual energy potential of biomass residues from field crops cultivation. It is estimated that every year in Serbia a total amount of 9.45 million tons of agriculture biomass is produced. However, according to the analyses of experts from different fields there is a conclusion that it is not justified to use all the biomass resulting from agricultural production residues for energy purposes [125]. It can be said that among farmers, cattle breeders, technologists, mechanical engineers, economists and other potential users of biomass in agriculture there are conflicting opinions for what purposes it could be most useful to use biomass [125]. Farmers believe that most of the biomass should be plowed, and thus increase soil fertility, cattle breeders in turn argue that biomass should be used for the production of animal feed, thermal engineers believe that biomass should primarily be used to produce heat energy, etc. On the other hand, it is known that there is biomass in huge quantities, that it is renewed every year and irrationally used. Postharvest residue is mostly burned directly in the field, which is

prohibited by law [125]. The accustomed burning of the postharvest residues means not only wastes of the organic substances and of considerable energetic value contained in it, but also the destruction of humus and annihilation of microorganisms from the surface layer of soils. Also, the postharvest residues burning releases not only carbon into the atmosphere, but also the other significant biogenic elements, such as nitrogen and phosphorus [124]. As a compromise solution it could be regulated that one third of biomass should be plowed or as sheet taken back to field, one third used for animal feed, one third used for heating facilities and for other purposes (industries of alcohol, furniture, construction materials, paper, packaging, cosmetics and others) [126-128].

Table 1.8 Estimated quantities of Agricultural residues

<b>Culture</b>	<b>Area (ha)</b>	<b>Yield of grain (t/ ha)</b>	<b>Mass of grain (t/ year)</b>	<b>Ratio grain/post-harvest residues (t/t)</b>	<b>Yield of straw (t/ha)</b>	<b>Total residues (10<sup>3</sup>t/year)</b>	<b>Residues for energy use (10<sup>3</sup> t) 1/3 of total</b>	<b>Energy potential (toe)*</b>
Wheat	566,277	3.52	1,994,068	1:1	3.52	1,994.07	658.04	220,081.08
Rye	6,178	2.13	13,139	1:1.2	2.55	15.77	5.20	1,740.06
Barley	100,698	2.96	298,569	1:1	2.96	298.57	98.53	32,952.43
Oats	44,952	1.98	89,183	1:1	1.98	89.18	29.43	9,842.94
Corn	1,000,752	5.59	5,591,972	1:1	4.47	4,473.58	1,476.28	493,739.38
Corn cob <sup>1</sup>	–	–	–	1:0.2	1.12	1,118.39	369.07	123,434.79
Sunflower	185,825	2.04	379,313	1:2	2.86	531.04	175.24	58,609.55
Shell <sup>2</sup>	–	–	–	1:0.3	1.22	227.59	75.10	25,118.41
Soybean	137,827	2.41	332,726	1:2	4.83	665.45	219.60	73,444.54
Rapeseed	6,937	2.42	16,796	1:2	4.84	33.59	11.08	3,707.15
Tobacco (leaf, stem)	7,605	1.49	11,349	1:0.35	0.52	3.97	1.31	438.16
Total/mean value	2,057,051	4.24	8,727,115		4.71	9,451.20	3,118.89	1,043,108.48

\* 1 toe – ton of oil equivalent = 41.87 GJ

One of main activity in fruit growing and viniculture is pruning of small branches, and these cut small branches can be available for energy purposes. The quantity of pruned branches depends on species and sort of fruit, ranging from 1 kg per tree for some sorts of apple, up to 7 kg per tree for some sorts of peach and plum [123]. Also, stones of plums, cherries, peaches, and apricots together with peels and seeds of apples, pears, and grapes are wastes derived from processing of fruit and also can be available for energy purposes. According to Ilić et al. [123] additional source of biomass residues in fruit growing and viticulture is replacement of old trees with new ones. This replacement occurs each 10 to 25 years, depending on fruit types that are cultivated. The annual energy potential of fruit trees and vines that are extracted with roots is about 245,000 toe. In Table 1. 9 biomass production in orchards and vineyards in Serbia are presented.

Table 1.9 Biomass production in orchards and vineyards in Serbia

<b>Species</b>	<b>Number of trees (10<sup>3</sup> ha)</b>	<b>Fruit production (t/year)</b>	<b>Biomass residues (t)</b>	<b>Annual energy equivalent (toe)*</b>
Plum	50,630	382,400	393,500	131,605.35
Apple	17,570	198,400	36,200	12,107.02
Cherries	12,280	99,500	55,000	18,394.65
Pear	7,080	70,000	14,000	4,682.27
Peach	4,450	44,400	35,100	11,739.13
Apricot	1,900	27,500	15,500	5,183.95
Walnuts	2,100	21,500	55,000	18,394.65
Grape	77,390	213,000	515,000	172,240.80
<b>SUM</b>				<b>374,347.83</b>
replacement of old trees				245,000
<b>OVERALL SUM</b>				<b>619,347.83</b>

\* Average low heating value – 14 MJ/kg

The only biomass waste from livestock breeding is cattle, pigs and poultry manure. In spite to the fact that animal manure represents waste directly originated by the animals, owing to the fact that it contains organic substances that basically are of the plant origin, it is considered to be the biomass [118, 123]. Because of high water content (up to 90%) these slurries are usually treated by anaerobic digestion for biogas production. The present state of main species of livestock is given in the Table 1.10.

Table 1.10 Biomass production in livestock breeding and energy potential of their manure in Serbia

<b>Livestock</b>	<b>Number of heads</b>	<b>Manure</b> (10 <sup>3</sup> m <sup>3</sup> /year)	<b>Biogas</b> (10 <sup>3</sup> m <sup>3</sup> /year)	<b>Available energy</b> (toe)
Cattle	260,300	1,923.55	38,471,000	21,137.91
Pigs	1,655,100	1,664.40	33,288,000	16,989.97
Poultry	2,350,000	175.20	8,760,000	4,813.19
<b>Sum</b>	<b>4265400</b>	<b>3763.15</b>	<b>80,519,000</b>	<b>42,941.07</b>

### MUNICIPAL SOLID WASTE AND ENERGY CROPS

According to Stojiljković [129] annual energy potential of municipal solid waste and energy crops is 199,876 toe and 594,134 toe, respectively.

From the above analysis it can be concluded that the total energy potential of biomass residues from agricultural production is 1.71 Mtoe (Table 1.12). Total primary energy production (according to data from 2013) in Serbia was 11.39 Mtoe, while the data in Table 1.11 indicate that the energy potential of agricultural biomass is approximately 15 % of total primary energy consumption.

Table 1.11 Energy potentials of Agricultural residues in Serbia

<b>Agricultural crops</b>	<b>Available Energy (toe)</b>
Agriculture crops	1,043,108.48
Orchards and vineyards	619,347.83
Livestock manure	42,941
<b>Sum</b>	<b>1,705,397.31</b>

From Table 1. 9 can be seen that the most widely planted agricultural crops in Serbia are corn cob and wheat (planted area of 2.2 million ha). Corn covers an area of about 1.35 million ha, while wheat covers an area of about 0.85 million ha [125].

Corn cobs, leaves and stalks are important residues of corn processing and consumption. It is estimate that for every 1 kg of dry corn grains produced, about 0.15 kg of cobs, 0.72 kg of corn stover (0.22 kg of leaves and 0.50 kg of stalks) are produced [93]. The volumetric energy density of an energy feedstock is significant when considering the volume of biomass needed to be harvested, transported, stored and utilized in an energy production process. The higher the energy density, the less volume of biomass needed to produce a given amount of energy. Corn stalks and leaves have high volume, and lower

energy density. Volumetric energy of the corn stalks and leaves can be achieved by pelletization, [130]. Pelletization process requires additional energy and equipment. Corn cobs are sufficiently dense and therefore do not require densification. As it is mentioned corn cobs are dense and relatively uniform, and have a high heat value, low N and S contents harvest. As a direct heat source, corn cobs have a high heat value of about 18.25-19.18 [MJ/kg] (d.b)<sup>10</sup>. Table 1.12 presents a comparative view of energy density and heating value for several types of fuels.

Table 1.12 Energy density and heating value of several types of fuels [48]

	<b>Corn cob</b>	<b>Corn stover</b>	<b>Wheat straw</b>	<b>Wood pallets</b>	<b>Antracite</b>	<b>Fuel oil</b>
HHV* [MJ/kg] (d.b)	18.25-19.18	17.00	17.99	19.00	34.00	43.50
Energy density [MJ/m <sup>3</sup> ] (d.b)	4960 - 5210	2550	3994	12400	17,200 – 23,300	38,600

\* HHV - High Heating Value

Corn cobs are characterized by a higher energy density, higher heating value and lower bulk density compared to corn straw.

Considering availability of corn cobs, its characteristics and the fact that the corn cob is in general treated as an agriculture waste, which is often left on the field or used in some conventional appliances for household heating, in this study corn cob is analysed in detail as a potential energy feedstock which can be used in pyrolysis process, one of the modern thermochemical technologies, for producing energy and chemical products.

Before use of biomass as a source of energy, it should be understood the performance characteristics of biomass in order to avoid possible problems and utilize the biomass effectively. Several characteristics affect the performance of biomass fuel, including the heat value, moisture level, chemical composition, ash content, susceptibility to slagging and fouling, and percent volatiles) and size and density of the fuel.

This fact sheet presents some of the more important characteristics of solid biomass fuel and explains their significance

<sup>10</sup> d.b. -dry basis



**CHAPTER 2**

*“Without continual growth and progress, such words as improvement, achievement, and success have no meaning.”  
Benjamin Franklin*

**2. THERMOCHEMICAL CONVERSION TECHNOLOGIES**

Biomass can be converted to energy by the use of thermochemical, biochemical and physicochemical processes, Figure 2.1.

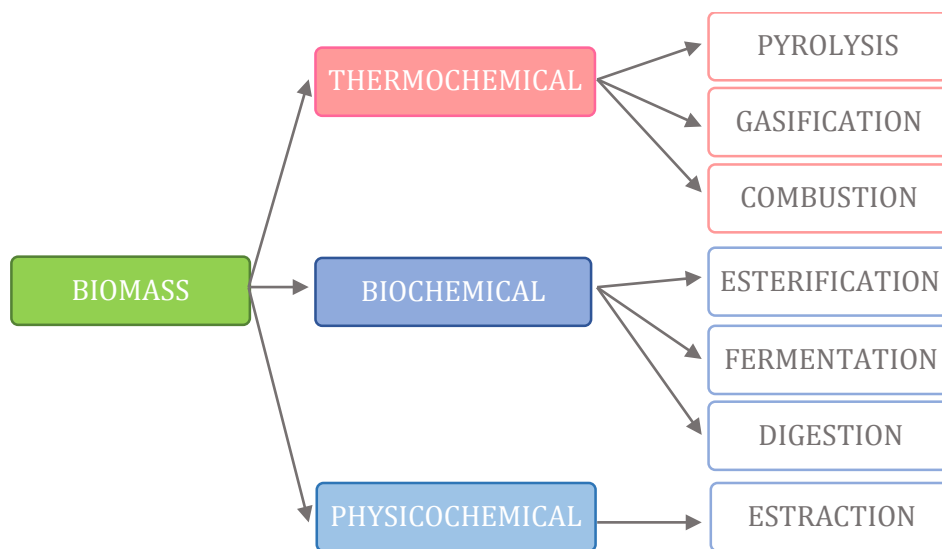


Figure 2.1 Biomass conversion technologies

In practice, combinations of two or more of these routes may be used [80]. Biochemical and physicochemical processes are beyond the scope of this thesis. Briefly explained, these technologies include fermentation for the production of alcohol, anaerobic digestion processes for the production of gas rich in methane and carbon dioxide and oil and hydrocarbon extraction [12, 80, 92]. Biochemical and physicochemical processes are in general more intended to upgrade biomass components and produce higher value products [80]. Thermochemical processes includes combustion, gasification and pyrolysis, along with a number of variants involving microwave, plasma arc, supercritical fluid, and other processing techniques [80]. Thermochemical processes can, as biochemical and

physicochemical processes, also be used in as in the indirect production of methanol via gasification [80].

The primary products from these conversion technologies may be in the form of energy carriers such as charcoal, oil or gas, or as heat [92]. An overview of these technologies, their respective primary products and their end uses are shown in Figures 2.2.

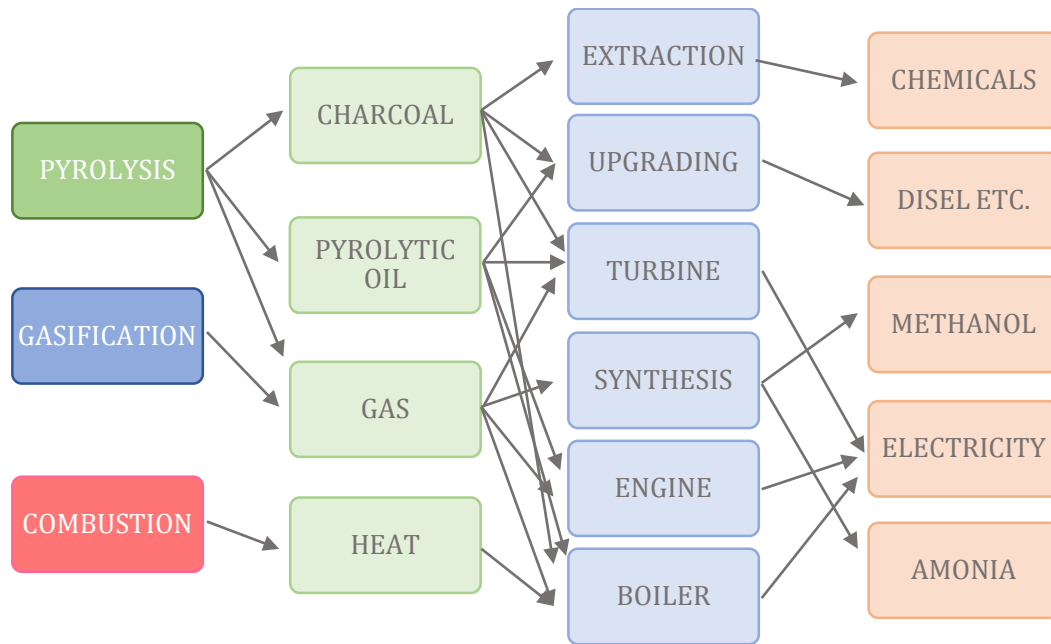


Figure 2.2. Products of thermochemical conversion technologies and there potential end uses

The conversion strategies are integrally coupled to the properties of the biomass. In many cases, the properties of the biomass necessary for engineering design have not been properly characterized prior to commercial implementation of a technology.

## **2.1. COMBUSTION**

Combustion represents perhaps the oldest utilization of biomass, given that civilization began with the discovery of fire. The burning of forest wood taught humans how to cook and how to be warm [1]. Combustion is an exothermic reaction between oxygen (by using excess air) and the hydrocarbon in biomass. Chemical energy of biomass is converted by combustion process into thermal energy of product gases, which can be used for heating or combined heat and power production.

The process of biomass combustion involves a number of physical and chemical aspects of high complexity. Combustion is a complex process that consists of both homogenous and heterogeneous reactions. The nature of the combustion process depends both on the fuel properties and the combustion application [92]. The combustion process has several different zones where drying, pyrolysis, oxidation of char and gasification. Several parameters in the combustion zone are quite crucial to the combustion process; among these are reactor technology, combustion temperature, size and moisture content of the fuel [12]. Drying, pyrolysis and gasification will always be the first steps in a solid fuel combustion process. The relative importance of these steps will vary, depending on the combustion technology implemented, the fuel properties and the combustion process conditions [92]. Although combustion is quite conventional compared to other thermal processes, research and technological improvements are still an ongoing activity. The main objectives are to reduce NO<sub>x</sub> and particle emissions. The main concern is the reduction of pollutants such as sulphur, nitrous and heavy metal compounds [12]. Such pollutants are not only hazardous to nature and the human life but they also create problems during the thermal conversion (e.g. slagging and corrosion). The most relevant constituents in native biomass are nitrogen as a source of NO<sub>x</sub>, and ash components (e.g., K and Cl as a source of KCl) that lead to particulate emissions [131]. Also, the content of alkali metals such as potassium (K) and chlorine (Cl) react and form potassium chloride (KCl) which condensates at low temperature and create process and environmental related problems [12]. Native wood is usually the most favourable biomass for combustion due to its low content

of ash and N. Herbaceous biomass such as straw, miscanthus, switch grass, etc., have higher contents of N, S, K, Cl, etc., that lead to higher emissions of NO<sub>x</sub> and particulates, increased ash, corrosion, and deposits [131]. NO<sub>x</sub> formation in combustion of biomass can originate from the nitrogen content in the fuel (fuel NO<sub>x</sub>), or the oxidation of the nitrogen found in the air (thermal NO<sub>x</sub>) [12]. Many primary and secondary measures for combating pollutions and optimizing the combustion process exist. One of the successful methods for combating nitrous compounds (NO<sub>x</sub>) is staged combustion (Figure 2.3), which gives a better control over the temperature profile in the combustion chamber [12]. The idea is to gain control over temperature gradients inside the combustion chamber and by that decreasing the formation of thermal NO<sub>x</sub> [12].

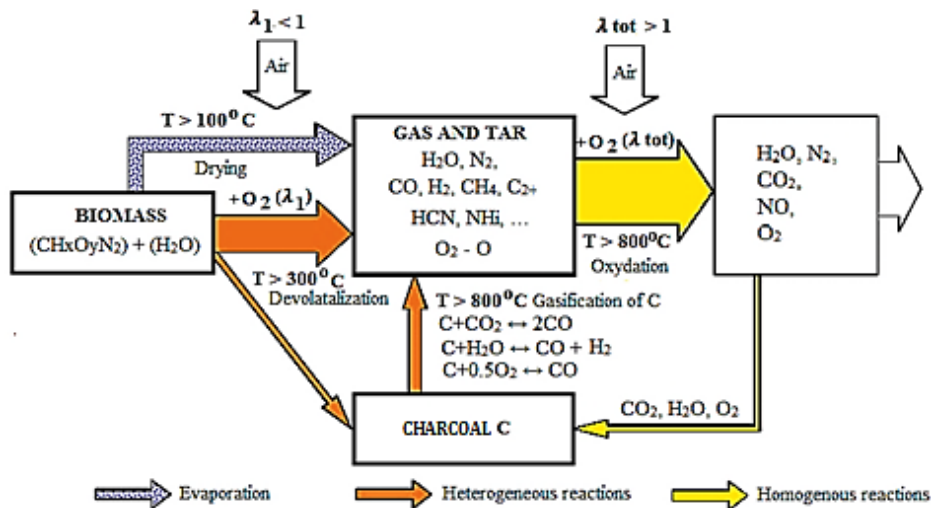


Figure 2.3 The different reactions in combustion of solid fuels [12]

Two-stage combustion is applied with primary air injection in the fuel bed and consecutive secondary air injection in the combustion chamber. In addition to conventional two-stage combustion, primary air needs to be understoichiometric ( $\lambda$  primary < 1). Further, a relevant residence time (and hence a reduction zone in the furnace thus leading to an enlarged furnace volume) is needed between the fuel bed and the secondary air inlet. Secondary air needs to be  $\lambda$  secondary > 1.

This enables good mixing of combustion air with the combustible gases formed by devolatilization and gasification in the fuel bed [131]. If good mixing is achieved, the concentrations of unburnt pollutants can be reduced to levels close to zero (e.g., CO < 50 mg/m<sup>3</sup> and C<sub>x</sub>H<sub>y</sub> < 5 mg/m<sup>3</sup> at 11 vol % O<sub>2</sub>) [131]. Optimized conditions are

usually attainable by having a good control over three parameters, temperature, turbulence and time. NO<sub>x</sub> reduction could also be achieved through secondary measure such as the direct injection of ammonia (NH<sub>3</sub>) in the boiler [12].

The hot gases from the combustion may be used for direct heating purposes in small combustion units, for water heating in small central heating boilers, to heat water in a boiler for electricity generation in larger units, as a source of process heat, or for water heating in larger central heating systems.

Drying, pyrolysis and gasification will always be the first steps in a solid fuel combustion process.

## **2.2. GASIFICATION**

Gasification is a well-established technology which reached a peak during the World War II when up to a million downdraft gasifiers were used for motive power [132]. Gasification is an endothermic process, which converts fossil or nonfossil fuels (solid, liquid, or gaseous) into useful gases and chemicals. Since gasification is an endothermic process, the energy needed to drive the chemical reactions forward are usually provided by feeding the reactor the necessary understoichiometric amount of oxygen [12]. Medium for gasification process include air, oxygen, steam, carbon – dioxide or a mixture of these. The process temperature of gasification is usually quite high (850 – 1500 °C) compared to pyrolysis (400 – 800 °C) [12]. The high temperature is needed to drive the main gasification reactions forward. The resultant mixture of gases produced during gasification process is called product gas, which contains carbon - monoxide (CO), hydrogen (H<sub>2</sub>), carbon - dioxide (CO<sub>2</sub>), methane (CH<sub>4</sub>), and nitrogen (N<sub>2</sub>) and is combustible. The raw biogas also contains tar and particulate matter, which have to be removed depending on the application. Due to the existence of several reacting agents, biomass gasification is quite complex where a number steps occur simultaneously, regardless of the technology used. These steps include: biomass drying, pyrolysis of biomass to condensable vapours (heavy hydrocarbons), gas and charcoal fractions, subsequent thermal cracking of heavy hydrocarbons to gas and charcoal, partial oxidation of combustible gases and charcoal, gasification of charcoal through reactions with CO<sub>2</sub> and H<sub>2</sub>O [12]. Emissions of sulphur and nitrogen compound (mainly their oxides), particles, furans

and dioxins are significantly reduced by use of gasification process. The lack of oxygen during the gasification process prevents the formation of free chlorine from hydrogen chloride (HCl). This prevents contact of hydrogen chloride gas comes with moisture, and formation of hydrochloric acid, which is very corrosive substance. Depending on the gasification process and the processing of the produced gas, several end products can be generated: syngas can be upgraded to produce methanol and other transport fuels and by steam reforming of product gas hydrogen can be produced. Heat and electrical power can be produced by direct utilization of the produced gas in boilers (hot water and steam production), combustion engines, gas turbines (heat and electricity) as well as solid oxide fuel cells (electricity and heat).

### 2.2.1. TYPES OF GASIFIERS

Gasification processes can be categorized into three groups: entrained flow, fluidised bed and moving bed (fixed-bed). Figure 2.4 shows the main types of gasifiers. Characteristics of some gasifier reactor types are summarised in Table 2.1.

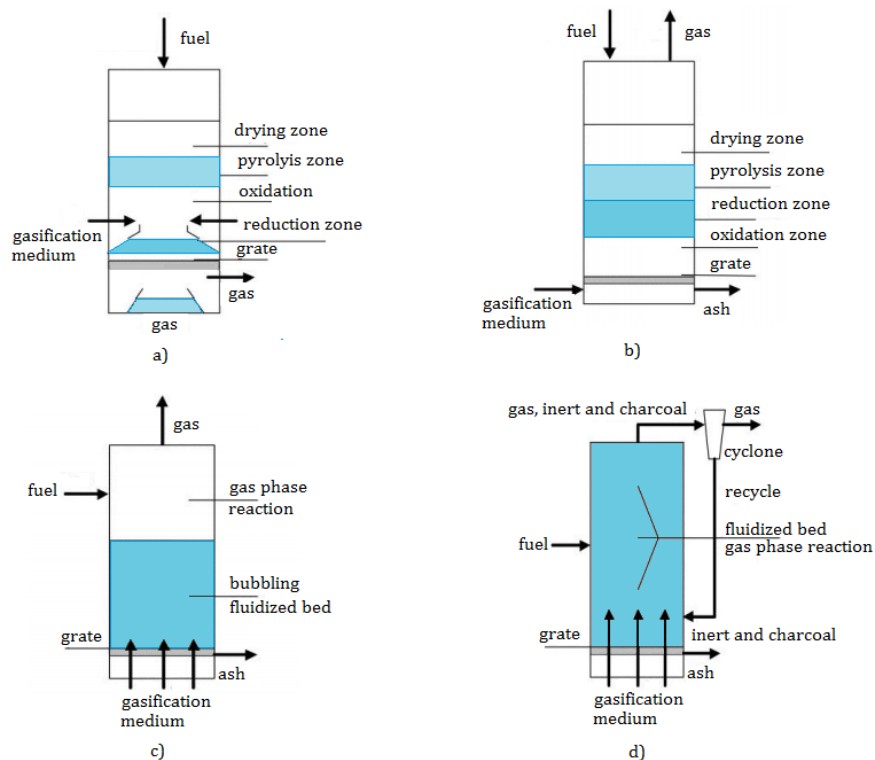


Figure 2.4 Diverse gasifiers: (a) Downdraft, (b) Updraft, (c) Bubbling Fluidized Bed, (d) Circulating fluidized bed [13, 14]

Fixed-bed gasifiers are the most suitable for biomass gasification. Fixed-bed gasifiers involve reactor vessels in which the biomass material is either packed in or moves slowly as a plug, with gases flowing in between the particles [130]. Fixed-bed gasifiers are usually fed from the top of the reactor and can be designed in either updraft or downdraft configurations. With fixed bed updraft gasifiers, the air or oxygen passes upward through a hot reactive zone near the bottom of the gasifier in a direction countercurrent to the flow of solid material [130, 133]. They can be scaled up; however, they produce a product gas with very high tar concentrations [130]. Fixed-bed downdraft gasifiers are limited in scale and require a well-defined fuel, making them not fuel flexible [130, 133]. Small scale fixed-bed downdraft gasifier installations (150 kW<sub>e</sub>–1 MW<sub>e</sub>) can be employed for on-site conversion of biomass to electricity and heat [130]. In a downdraft gasifier the feed and the oxidant move in a downwards (co-current) direction. The primary advantage of this type of gasifier is that all the decomposition products of pyrolysis pass through the hottest region of the gasifier [132]. This results in the cracking (thermal degradation) of tars to non-condensable gases and water to give a product gas with a low tar content [132].

Fluidized-bed gasifiers are a more recent development that takes advantage of the excellent mixing characteristics and high reaction rates of this method of gas–solid contacting [130, 133]. Fluidized-bed gasifiers are typically operated at 800–1000°C (limited by the melting properties of the bed material) and are therefore not generally suitable for coal gasification, as due to the lower reactivity of coal compared to biomass, a higher temperature is required (>1300 °C) [130].

The bubbling fluidized-bed gasifier tends to produce a gas with tar content between that of the updraft and downdraft gasifiers [134]. The circulating fluidized-bed gasifiers employ a system where the bed material circulates between the gasifier and a secondary vessel [130]. The circulating fluidized-bed gasifiers are suitable for fuel capacity higher than 10 MW<sub>th</sub> [130].

The gasifier types have been extensively reviewed (e. g. Kaupp [135]; Bridgwater [136]; Knoef; Milligan [132]; Basu [1]; McKendry [137]). The downdraft fixed bed gasifier are considered in this thesis (Chapter 7).

Table 2.1 Advantages and disadvantages of some gasifier reactors [49, 50]

Advantages	Drawbacks/Considerations
<b>Downdraft Gasification</b>	
Up to 99.9% of the tar formed is consumed, requiring minimal or no tar cleanup Minerals remain with the char/ash, reducing the need for a cyclone Proven, simple and low cost process	Requires feed drying to a low moisture content (<20%) Syngas exiting the reactor is at high temperature, requiring a secondary heat recovery system 4-7% of the carbon remains unconverted
<b>Updraft Gasification</b>	
Simple, low cost process Able to handle biomass with a high moisture and high inorganic content (e.g., municipal solid waste) Proven technology	Syngas contains 10-20% tar by weight, requiring extensive syngas cleanup before engine, turbine or synthesis applications
<b>Entrained Flow</b>	
High-temperature slagging operation; Relatively large oxidant requirements; Large amount of sensible heat in the raw syngas; Ability to gasify all biomass regardless of rank, caking characteristics or amount of fines.	Entrainment of some molten slag in the raw syngas;
<b>Circulating Fluidized Bed</b>	
Suitable for rapid reactions High heat transport rates possible due to high heat capacity of bed material High conversion rates possible with low tar and unconverted carbon	Temperature gradients occur in direction of solid flow Size of fuel particles determine minimum transport velocity; high velocities may result in equipment erosion Heat exchange less efficient than bubbling fluidized-bed
<b>Bubbling fluidized-bed gasifier</b>	
Yields a uniform product gas Exhibits a nearly uniform temperature distribution throughout the reactor Able to accept a wide range of fuel particle sizes, including fines Provides high rates of heat transfer between inert material, fuel and gas High conversion possible with low tar and unconverted carbon	Large bubble size may result in gas bypass through the bed



### **2.3. PYROLYSIS**

Pyrolysis is an endothermic process where the solid fuel in the absence of oxidant (air, oxygen, carbon – monoxide, steam, etc.), degrades to form a mixture of liquid (tarry composition), gases and a highly reactive carbonaceous charcoal of which the relative proportions depend very much on the method used. Conditions that will influence the distribution and the characteristics of the pyrolysis products are; temperature, pressure, heating rate and residence time of both the fuel and the devolatilized products, environment or medium in which the pyrolysis is carried [1, 12]. In addition, the chemical and physical characteristics of the fuel type used can also have an influence on product distribution [12]. Depending on the process parameters such as medium, pressure, heating rate, pyrolysis temperature, there are a several variation of pyrolysis process. Given specific operating conditions, each process has its characteristic products and applications [1]. There are three primary types of pyrolytic reaction, which are differentiated by temperature and the processing or residence time of the biomass: slow, fast and flash pyrolysis

Pyrolysis process is most capable of competing with and eventually replacing non – renewable fossil fuel resources [138]. This process is the most efficient process for biomass conversion as it produces energy fuels with high fuel – to feed ratio [139]. For example, the pyrolysis process can be adjusted to maximize charcoal, pyrolytic oil, gas or methanol production with 95. 5% fuel – to feed efficiency [140]. Pyrolysis should be also viewed as complementary to gasification as a liquid/charcoal is produced that can be stored and transported to the point of use and can be used intermittently as well as continuously.

Although numerous projects have been promoted, pyrolysis commercialization is progressing at a low pace not only in Europe but also globally [80]. Major efforts on researching are needed in order to maximize the advantages and minimize the disadvantages of this technology. The upsurge of interest is to explore, define the processes that follow the process of pyrolysis (heat transfer, hydrodynamics (for fluidized systems), preparation of biomass, mass transport, yield and quality of relevant products, secondary reactions, various technical issues (scaling process monitoring and process control), etc.

### 2.3.1. TYPES OF PYROLYSIS REACTORS

In pyrolysis the heart of the process is the reactor, where the most important transformation of feedstock occurs [51]. As a consequence, its mechanical design, temperature control and heat transfer is crucial to pyrolysis performance. Based on type of pyrolysis process, the typical reactor configurations are:

1. for conventional pyrolysis: Fixed Bed and Vacuum Reactors
2. for fast pyrolysis: Ablative, Auger, Fluidized Bed, Circulating Fluidized Bed Reactors
3. for flash pyrolysis: Fluidized Bed, Circulating Fluidized Bed, Downer Reactors

In Figure 2.5 the Concept Design of Pyrolysis Reactor are presented. Characteristics of some pyrolysis reactor types are presented in Table 2.2.

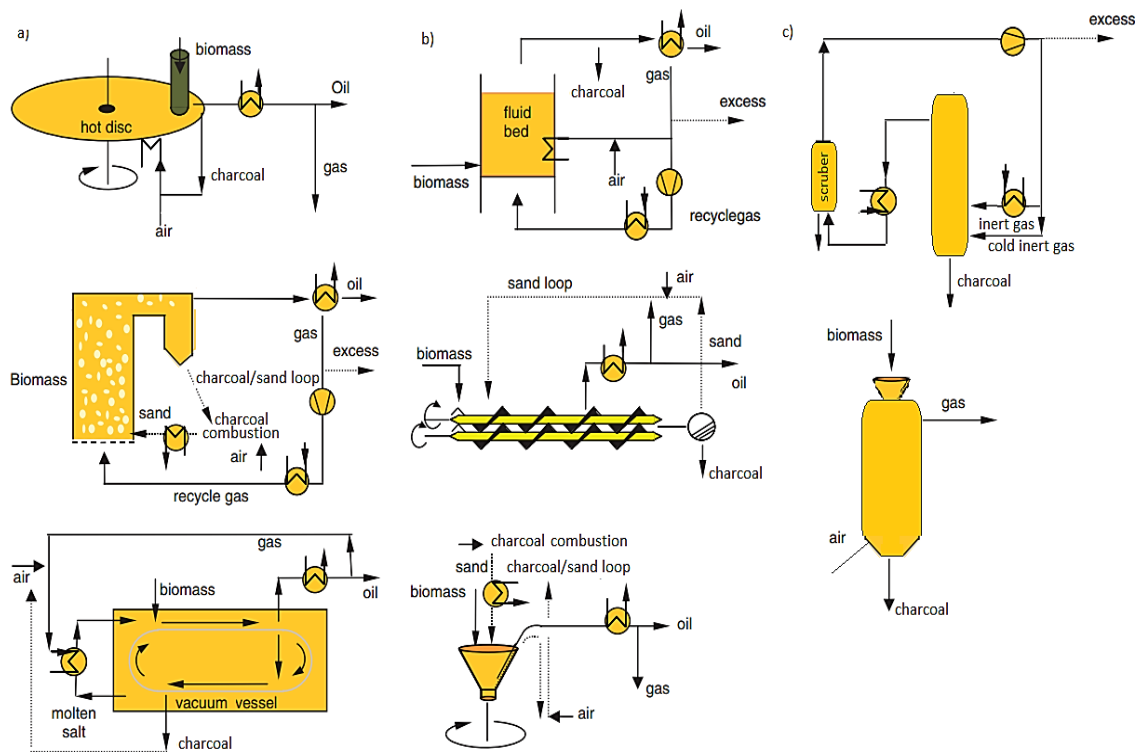


Figure 2.5 The concept design of some pyrolysis reactors: a) Ablative, CFB and vacuum technologies [15] b) Fluid bed, screw (auger) and rotating cone technologies [15], c) retort and kiln technologies

Table 2.2. Advantages and disadvantages of some pyrolysis reactors [51, 52]

Advantages	Drawbacks/Considerations
<b>Fixed Fluid Bed</b>	
Simple construction and operation Easy scaling Good temperature control High liquid yields of typically 70-75%wt db	Very small size particle is required ( $\leq 3$ mm.) Rapid charcoal separation is needed to avoid vapor cracking reactions Residence time of solids and vapors is controlled by the fluidizing gas flow rate Large-scale systems have to be studied carefully due to scale-up limitations
<b>Circulating Fluid Bed</b>	
Good temperature control Residence time for the charcoal is almost the same as for vapors and gas They are suitable for very large throughputs	Hydrodynamics more complex Charcoal combustion in a second reactor requires careful control Heat transfer in large-scale systems have to be studied carefully
<b>Rotating Cone Reactor</b>	
Feedstock is heated rapidly and the gases have short residence time The products are usually 75 wt % bio-oil and only 15 wt% charcoal and gas	It requires size particles $< 6$ mm, moisture content $< 10$ wt % Carrier gas in the reactor are much less needed than for fluid beds however, gases are required for the combustion of charcoal as well as the transportation of sand.
<b>Moving Bed Vacuum Reactor</b>	
It can process larger particles. Less charcoal in the liquid products as a results of lower gas velocities There is no need of carrier gas however, a nitrogen is used to avoid any leakage of air to the reactor Liquids yields of 35-50% on dry feed are obtained.	Heat transfer to the feedstock is much lower than in other reactors It is a relatively complicated mechanical process
<b>Ablative Reactor</b>	
Allows the use of large particle sizes Inert gas is not required	The reactor is more complex mechanically It can be costly at high scales due to surface area requirements Reaction rates are limited by heat transfer to the reactor

## CHAPTER 3

*"Nothing in life is to be feared. It is only to be understood."  
Marie Curie*

### 3. BIOMASS PYROLYSIS FUNDAMENTALS

The art of pyrolysis of biomass is as old as our natural habitat [1]. Magnificent charcoal drawings in the Grotte Chauvet, which are over 38,000 years old, bear witness to Cro-Magnon man's artistic creativity and native chemical engineering talents [69]. Prehistoric finds (back to the Middle Palaeolithic) have shown that arrow-heads were attached to their shafts by employing wood tar, a material then obtainable only by the charring of wood [141, 142]. From Mesolithic and Neolithic dwelling sites in northern Europe, there is much evidence that birch bark pitch used for cleaning teeth [142]. Egyptian papyri from around 1,500 BC<sup>11</sup> describe the use of charcoal to adsorb malodorous vapours from putrefying wounds. Also, ancient Egyptians practice wood pyrolysis to produce tars and pyroligneous acid for use in embalming procedures.

Also, man employed shallow pits of charcoal to smelt tin needed for the manufacture of bronze tools [69]. Founder's hoards of the Bronze age scattered throughout Europe indicate that shallow pits of charcoal were used to smelt tin before the dawn of recorded history [68]. Extensive investigation has proved that in Europe charcoal-making had already become an important industry for the recovery of iron and other metals from their ores around 1,100 BC [67, 68, 141]. Charcoal from wood via pyrolysis was essential for extraction of iron from iron-ore in the pre-industrial era. This practice continued until wood supplies nearly ran out and coal, produced inexpensively from underground mines, replaced charcoal for iron production [1]. Also, charcoal has also been used in agriculture for thousands of years. The prehistoric Amazonians added large amounts of charcoal to their wet desert soil to render it fertile [69]. The fertile *terra preta* (dark earth) had and still have long-lasting fertility that has been related to the stability of carbon in the soil. The modern

---

<sup>11</sup> BC - Before Christ

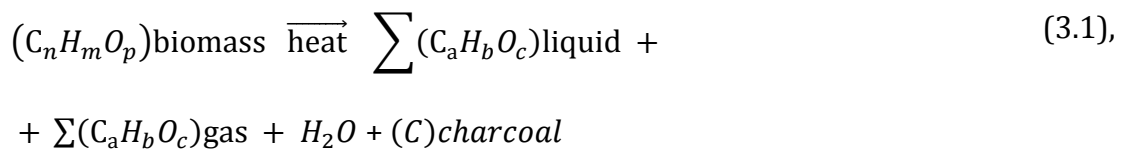
petrochemical industry owes a great deal to the invention of a process of kerosene production using pyrolysis (in the mid-1840s, Abraham Gesner). The kerosene is the first transportable liquid fuel. It is also interesting that the first gas mask used in warfare (First World War) had a replaceable filter cartridge filled with activated carbon (made from charcoal).

As Antal and Grønli [69] said, that pyrolysis products charcoal and tar, was the first synthetic materials produced by man. At the end of 20. Sanctuary and at the beginning of 21. Sanctuary, global warming and political instability in some oil-producing countries gave a fresh momentum to pyrolysis The threat of climate change stressed the need for moving away from carbon-rich fossil fuels [1]. Pyrolysis came out as a natural choice for conversion of renewable carbon-neutral biomass into gas [1].

This section describes basic concepts related to the pyrolysis process, the physical characteristics of the process, pyrolysis of biomass components (hemicellulose, cellulose, lignin, extracts), primary and secondary reactions, heat transfer, products quantity and products composition.

### 3.1. OVERVIEW OF BIOMASS PYROLYSIS

Pyrolysis is a thermal degradation process of organic biomass compounds (hemicellulose, cellulose and lignin), in the absence of oxygen. This process is irreversible and generally produces numerous chemical species in the form of pyrolysis vapours, aerosols and solid residue. The condensation of pyrolysis vapours and aerosols yields a tar (bio – oil, pyrolitic liquids, bio-crude oil or pyrolytic oil, etc). Noncondensable fraction of pyrolysis vapours usually consists of mixtures of different gases species (e.g., CO, CO<sub>2</sub>, CH<sub>4</sub>, H<sub>2</sub>). Solid residue is named as charcoal. Pyrolysis process can be presented by with equation [1]:



Where  $n$ ,  $m$ ,  $p$  presents the number of carbon, hydrogen and oxygen content in biomass and  $a$ ,  $b$ ,  $c$  presents the number of carbon, hydrogen and oxygen content in biomass pyrolysis products

The pyrolysis process, is a complex process. It involves many physical and chemical processes such as heat transfer, moisture evaporation and mass transfer. combination of successive endothermic and exothermic reactions, decomposition kinetics, heat of pyrolysis, pressure build up in the solid, changes in material properties with the extent of pyrolysis and temperature, anisotropic property behaviour, among others.

Examples of the more Antal [64, 143] has pointed out in his excellent reviews of biomass pyrolysis theory and experimentation that a particle undergoing thermal decomposition must pass through certain temperature zones regardless of the final reaction temperature. Boundaries between this temperature stages are not sharp; there is always some overlap.

*First phase* - Drying ( $\leq 200$  °C). During the initial phase of biomass heating at low temperature, the free moisture and some loosely bound water is released, and the heat is conducted into the biomass interior [1]. Also, some of volatile products such as acetic acid and formic acid are released, noncondensable gases such as CO and CO<sub>2</sub> are also evolved [64, 143-145].

*Second phase* – Initial Stage (200 - 270°C). Decomposition is more vigorous with the release of pyroligneous acids, water, and noncondensable gases (CO, CO<sub>2</sub>). Separation of tar is also observed [64, 143-145].

*Third phase* - Intermediate Stage or Primary pyrolysis (270 - 600 °C) [1]. This is endothermic chemical decomposition of biomass main components (cellulose, hemicelluloses, lignin and extractives). Large molecules of biomass particles decompose into charcoal (primary charcoal), with release of combustible volatile products (CO, CH<sub>4</sub>, and H<sub>2</sub>) and formaldehyde, formic acid, methanol, and acetic acid occur [64, 143-145].

During this phase, the pores of the solid are enlarged, and the solid particle merely becomes more porous because the biomass converts into gases [146]. The enlarged pores of the pyrolyzing solid offer many reaction sites to the volatile and gaseous products of pyrolysis and favour their interaction with the hot solid [147]. Small

molecules (H<sub>2</sub>, CH<sub>4</sub>, CO, H<sub>2</sub>O) and small radicals (H, CH<sub>3</sub>, C<sub>2</sub>H<sub>5</sub>) easily escape porous structure of the sample before undergoing further decomposition. Large molecules of free radicals and tar cannot easily flow through porous sample structure and may undergo further decomposition [148].

*Forth phase* - Final stage or Secondary pyrolysis ( $\leq 900$  °C). If the reaction products are not removed from the reaction zone as soon as they are formed, secondary reactions begin and charcoal-gas reactions start (decomposition of volatiles into charcoal and noncondensable gases) [149]. If condensable gases reside in the biomass long enough, relatively large-molecular-weight condensable gases can decompose, yielding additional charcoal (called secondary charcoal) and gases [1]. If condensable gases are removed quickly from the reaction site, condense outside in the downstream reactor as tar [1]. All of these reactions are also severely affected by the catalytic effect exerted by the minerals present in biomass and charcoal. From above, it can be concluded that pyrolysis of biomass consist of two kind of reactions, primary and secondary reactions Figure 3.1.

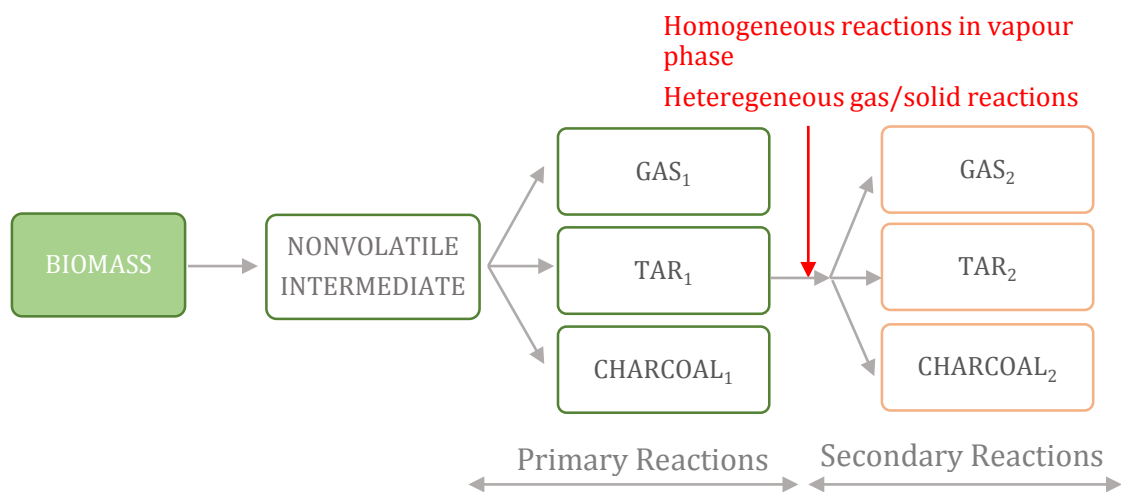


Figure 3.1. Primary and secondary pyrolysis reactions

Based on the information found in the literature it can be concluded that:

1. The importance of secondary reactions increases with longer residence time of vapour phase (volatile gases and tar) and lower heating rate. With long residence time and low heating rate, formation and escape of vapour phase will be slower and contact between vapour phase and charcoal will be extended,

2. Tars decompositions is catalysed by the charcoal (formed by primary reactions) [150],
3. The presence of H<sub>2</sub>O and/or CO<sub>2</sub> increases the tar decomposition rate [151],
4. The presence of H<sub>2</sub> depresses the tar decomposition rate [151],
5. High pressure results in greater tar decomposition [151],
6. Raising the temperature pressure results in greater tar decomposition,
7. The mineral matter and trace elements (such as Ca, K, Na, Mg, and Fe), catalyse tar thermal decomposition reactions [152].

### **3.2. HEAT AND MASS TRANSFER DURING PYROLYSIS PROCESS**

As biomass particle size increases, the time required for heat and mass transfer increases until these processes become rate controlling processes instead of chemical kinetics [153]. According to Yang et al. [154] isothermal assumption is no longer valid with biomass particles exceeding 250  $\mu\text{m}$ . The larger temperature gradients through the sample occurs also as secondary reactions. Mass transfer can account for some variations in the volatile yields of pyrolysis due to possible secondary reactions; however, it does not normally control the rate of pyrolysis of small or porous particles [155]. The reaction regimes for pyrolysis can be defined as thermally thin, thermally thick. In the thermally thin case the temperature is assumed to be constant across the particle (negligible temperature gradient), and this is the situation normally assumed to be the case in the heating-up step for small biomass particles (powder or sawdust samples). The thermally thick case predominantly applies when there is large biomass particles involved and considerable thermal gradients. It can be concluded that for small biomass particles the kinetics are sufficient to predict the reaction rate. However, there are not many thermochemical conversion process that use biomass in the form of sawdust and powder as feedstock (beside pulverized fuel combustors) [3]. Combustors, gasifiers and wood stove use feedstock with a certain size (thermally thick samples), which have effective temperature gradient within the solid during the thermal stage [3]. Temperature profiles within the core of biomass particles, subjected to pyrolysis, exhibit a thermal sink, followed by a sharp peak, which overtakes the surface thermal profile. This could be explained on the basis of the process kinetics, which



is described by both endothermic and exothermic reactions. A first endothermic stage corresponds to a primary release of volatile species, and a second exothermic period mainly corresponds to the successive transformations of the solid residue to final charcoal [156]. For this samples both the physical and the chemical changes are essential for obtaining a global pyrolysis rate [16]. To formulation an analytical pyrolysis model, the known parameters that can influence the pyrolysis process must be considered.

When a solid particle of biomass is heated in an inert atmosphere the following phenomena occur [16]:

1. Heat transfer from the reactor environment to the particle surface by convection, and/or radiation and and/or conduction,;
2. Heat transfer from the outer surface of the particle into the interior of the particle by conduction and in a few situations to a lesser degree by convection;
3. Primary pyrolysis occurs which leads to conversion of the biomass to gas, charcoal and a primary liquid product;
4. Convective heat transfer between the volatile reaction products leaving the reaction zone and the solid matrix ;
5. Condensation of some of the volatiles in the cooler parts of the particle to produce tar;
6. Secondary pyrolysis leads to conversion of the primary product to a gas, charcoal and a secondary liquid product which then forms primary and secondary products;
7. Changes in physical properties, enthalpy and heats of reaction of the biomass changes in the enthalpy of the pyrolysis products;
8. Diffusion of volatiles out of the solid and away from the particle surface.

### ***HEAT TRANSFER***

The heat changes due to the chemical reactions and phase changes contribute to a temperature gradient as a function of time, which is nonlinear [157]. Inside the pyrolyzing particle, heat is transmitted by the following mechanisms [157]:

1. Conduction inside solid particle,
2. Convection inside the particle pore,

3. Convection and

4. Radiation from the surface of the solid particle.

Heat transfer during pyrolysis process is shown in Figure 3.2. Pressure gradients may also occur due to vapour formation in larger particles.

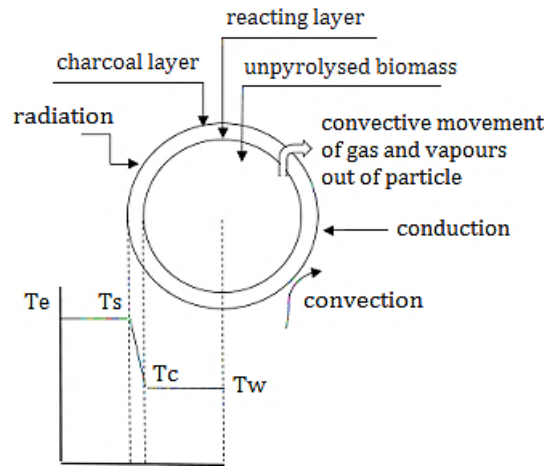


Figure 3.2 Heat transfer during pyrolysis process [16]

In the initial stages of pyrolysis, the temperature profile is very steep near the wall (refer to the temperature profile), and as the time progresses, the steepness in the temperature profile near the wall decreases. This can be explained by the fact that when the heat transfer takes place by both the mechanisms of convection and radiation from the wall surface, the resistance offered for heat transfer near the wall at the initial stages of pyrolysis is very high. On the contrary, when heat transfer from the wall surface takes place only by convection and with no radiation, the resistance offered for heat transfer near the wall is not as high as in the above case. The Biot number, defined as in equation (3.2) is a useful ratio to evaluate the extent of the temperature gradients [156]:

$$B_i = \frac{hL}{\lambda} \quad (3.2)$$

Where  $h$  ( $W/m^2K$ ) is the coefficient of conduction,  $\lambda$  ( $W/m^2K$ ) is the coefficient of convection,  $L$  (m) is the particle characteristic length.

$$L = \frac{6V}{A} \quad (3.3)$$

With  $V$  and  $A$  being the particle volume and surface, respectively.

When the Biot number is very small e.g.  $< 10^{-3}$  then the material conducts heat rapidly to provide a uniform temperature throughout the sample. However for biomass samples the Biot number often has values much higher than 0.2, and consequently there are large temperature gradients within the solid biomass material [158]. Thus, at high external heat fluxes with large particles (of  $> 2$  cm thick), the surface rapidly reaches the external temperature, while the centre of the particle is still cold [158]. For example Overend [158] uses Biot<sup>12</sup> number as indicator of heat transfer through sample. For a 1 cm<sup>3</sup> cube of wood, a very high heating rates of 100 K min<sup>-1</sup> ( $Bi = 0.3$ ), would result in a large thermal gradient. Reasons for this temperature gradient, is the fact that the particle surface is heated not only by convection and radiation but also by heat released from chemical reaction, while centre of the sample is heated only by conduction [32]. Gvero [32] also concluded that at temperature range lower than 400°C, temperature gradients through sample area are relatively uniform, while at temperatures very close to 400°C, temperature gradients decreases. In the pyrolysis process, the reactions that take place at low conversions (which practically means the temperature below 400°C even below 300°C) conversions are endothermic in nature [159]. At temperatures of 400-450 °C, the temperature gradient increases again, even exceeding the initial temperature (temperature of the centre is higher than the temperature of the environment even for 50°C) [28, 32]. The reactions that take place at high conversions (temperature above 400°C) are exothermic [28, 32]. The higher is the temperature, the faster will be the pyrolysis rate. Upon reaching ambient temperature, there is a decrease in the temperature on the surface of the sample, due to the passage of gas through the formed pattern to the surface. For a 1 cm<sup>3</sup> cube of wood, a very slow heating rate of 0.01 K min<sup>-1</sup> ( $Bi = 10^{-5}$ ) would result in an isothermal situation throughout the cube. In this case, the drying of the wood would take place independently of the pyrolysis process [159]. If  $Bi=1$ , the heat transfer through the inside of of the sample requires a lot of time and secondary reaction occur. Secondary reactions occurs between primary pyrolysis products

---

<sup>12</sup>Biot number is a dimensionless ratio of surface convective heat transfer to internal heat conductivity

themselves and with the original feedstock molecules. Primary pyrolysis products decompose through partial oxidation, re-polymerization and condensation [160].

### **MASS TRANSFER**

During pyrolysis, biomass particle is converted in homogeneous and heterogeneous reactions. When charcoal is generated, charcoal is further converted in heterogeneous reactions. The reactivity of biomass particle and charcoal depends on total surface area, the number of reactive sites per unit surface area, and the local gaseous reactant concentration. Consequently, biomass particle and charcoal reactivity depends on three important characteristics of the sample [161]:

1. Chemical structure: the chemical structure of the biomass/charcoal surface provides active sites,
2. Mineral matter: inorganic constituents promote catalytic activity and create further dislocations,
3. Physical biomass/charcoal structure: the pore structure determines the total surface area accessible for reaction; it influences diffusion and therefore the local gas concentration within the biomass/charcoal particle.

The conversion of a biomass/charcoal particle is a series of reaction and diffusion processes that can be separated in several reaction steps:

1. Diffusion of reactants across the stagnant gas film around the particle surface (external diffusion) [17]
2. Diffusion of gas into the particle pore (pore diffusion) [17]
3. Adsorption on the charcoal surface [161]
4. Chemical reaction on the particle surface [161]
5. Desorption of the products from the charcoal surface [17, 161]
6. Diffusion within the particle pores to the outer particle surface [17]
7. Diffusion of products across the stagnant film to the gaseous reaction environment [17]

In practical applications generally a combination of several steps has a controlling influence [17, 18] [161]. In this sequence of reaction steps, one or more can be identified as the slowest step and the step that controls rate of the overall process [17]. The degree of limitation by chemical reaction or diffusion is mainly a function

of reaction temperature. The dependence of the reaction rate on temperature is usually shown as an Arrhenius plot of reactivity (logarithmic) versus temperature (inverse), as shown in Figure 3.3 the relation between chemical reaction and mass transport limitation is classified in three regimes.

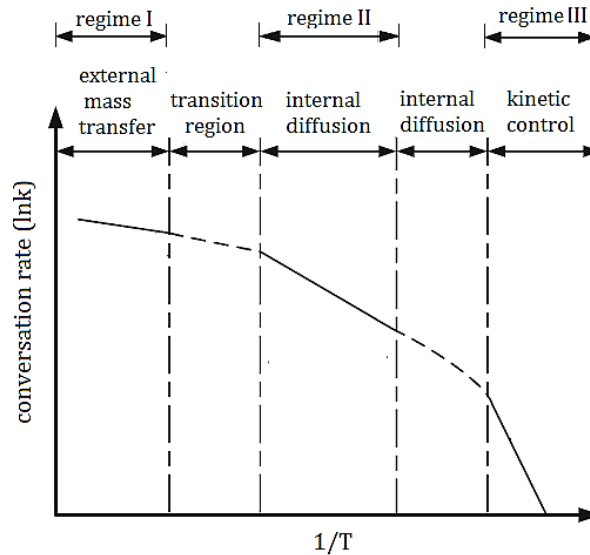


Figure 3.3 Rate-controlling regimes of heterogeneous reactions [17, 18]

The chemical reaction is a strong function of temperature (typically exponentially). In *Regime I* at low temperature the chemical reaction rate at the particle surface is very slow and determines the overall reaction rate. The gas concentration is uniform within the particle and the bulk gas phase. With increasing temperature the chemical reaction rate increases exponentially and becomes comparable to the pore diffusion rate within the particle. As the reactant is consumed at the inner particle surface, a concentration gradient develops within the particle.

Under ideal *Regime II* conditions, the reactant concentration is equal to the bulk concentration at the outer particle surface and zero at the particle centre. Under *Regime II* conditions the reaction rate is influenced by the chemical reaction rate and the pore diffusion rate. When the temperature is increased further, the chemical reaction is very fast and reactants are consumed at the outer particle surface before reaching the pore system. The overall rate is controlled by the mass transfer between bulk phase and particle outer surface and a concentration gradient is formed in the boundary layer. As diffusion processes are only slightly influenced by temperature, the slope of the curve approaches zero. There are two transition zones

(between Regime I and II and between Regime II and III) where the overall rate is influenced by a combination of the adjoining regimes. In fact, in real pyrolysis systems a combination of chemical reaction and both internal and external mass transfer limitations are likely. The surface reaction as well as diffusion phenomena have to be considered. The transition temperature from Regime I to Regime II conditions is dependent on particle properties and reaction conditions. When continuously increasing the temperature in an experiment, the reaction rate increases. The transition to Regime II conditions is typically observed by a decreasing temperature influence, i.e. the slope in the Arrhenius plot (Figure 2.5) decreases. The reaction temperature during pyrolysis of small and medium sized particles is significantly lower and charcoal conversion is expected to occur under Regime I. The reaction temperature during pyrolysis of larger particle, diffusion pathways within the particles are long, internal and external mass transfer is expected to play an important role.

In general, there are two mass transfer phenomena: transfer of formed volatiles through sample and transfer from sample surface to sample surroundings (pyrolysis reactor) [148].

It should be noted that for thick biomass particles, internal pressure generation is also an important factor influencing the pyrolysis process and the temperature. Pressure gradient drives the volatiles out of the particle and high internal pressure may also split a partially pyrolyzed biomass particle [162]. Pressure splitting of thick particles may be desirable because it obviates the need to make small particles [162]. This natural formation of small particles enhances the biomass conversion speed and increases the yield of liquid products [162]. It also reduces the residence time of the volatiles in the pores reducing tar cracking that would otherwise be promoted by high pressure. According to Park et al [162] at high temperatures, a thick wood particle may split by combination of high internal pressure and weakened structure. On the other hand, a thick wood particle does not split during low temperature pyrolysis. Therefore, pressure becomes more important for the high temperature fast pyrolysis process.

### 3.3. TYPES OF PYROLYSIS

Based on heating rate, pyrolysis may be broadly classified as:

1. Slow,
2. Mild (torrefaction) and
3. Fast pyrolysis.

According to Basu [1] pyrolysis process is considered slow if the time ( $t_{\text{heating}}$ ) required to heat the fuel to the pyrolysis temperature is much longer than the characteristic pyrolysis reaction time ( $t_r$ ) and vice versa [1]:

- Slow pyrolysis:  $t_{\text{heating}} \gg t_r$
- Fast pyrolysis:  $t_{\text{heating}} \ll t_r$ .

In slow pyrolysis, the residence time of vapour in the pyrolysis zone (vapour residence time) is on the order of minutes or longer [1]. Slow pyrolysis is used primarily for charcoal production and is divided into two types:

- Carbonization
- Conventional

Carbonization is a slow pyrolysis process, in which the production of charcoal is the primary goal. It is the oldest form of pyrolysis, in use for thousands of years. The biomass is heated slowly in the absence of oxygen to a relatively low temperature of around 400 - 600 °C over an extended period of time, which in ancient times ran for several days to maximize the charcoal yields (about 35 wt % ) [1, 163]. Carbonization allows adequate time for the condensable vapours to be converted into charcoal and noncondensable gases [1].

Conventional pyrolysis heats the biomass at a moderate rate to a moderate temperature, with vapour residence times of 0.5 to 5 minutes. Conventional pyrolysis gives approximately equal proportions of gas liquid and solid products [1]. It can be conclude: low temperature and slow heating rate maximizes charcoal formation, while high temperature promotes tar cracking which in return produce lighter hydrocarbons [12]. Pyrolysis conditions not only influences the distribution of the main products but also their chemical composition. For the charcoal residue, the pyrolysis condition can affect its yield, physical characteristics and reactivity [12]. For example, slow heating rate during pyrolysis will produce charcoal which is

less reactive compared to charcoal produced at fast heating rate [12]. This is mostly due to an increased specific area in the charcoal produced at high heating rate and a more spread out distribution of the catalytic elements in the charcoal matrix [12]. The structure of the charcoal matrix is therefore a key element in the determination of charcoal reactivity.

Torrefaction process (named for the French word for roasting), is a milder form of pyrolysis carried out at temperatures around 200-300°C without presence of oxygen. During this process, biomass is slowly heated to within a specified temperature range and retained there for a stipulated time such that it results in near complete degradation of its hemicellulose content while maximizing mass and energy yield of solid product [164]. Typically the heating rate of torrefaction is less than 50°C/min<sup>13</sup> [164]. Torrefaction is an important pre-processing step to improve the quality of biomass in terms of physical properties and chemical composition. This thermal pre-treatment of biomass improves its energy density, reduces its oxygen-to-carbon (O/C) ratio, and reduces its hygroscopic nature [1].

The initial heating of biomass during torrefaction removes unbound water [165]. Further heating results in the removal of bound water through chemical reactions. It is assumed that most of the bound water is removed by a thermo-condensation process, which occurs above 160°C when the formation of CO<sub>2</sub> begins [165, 166]. Further heating between 180–270°C results in an exothermic reaction and initiates the decomposition of the hemicellulose, which causes the biomass to change colour due to loss of water, CO<sub>2</sub>, and large amounts of acetic acid and phenols [165]. The energy values of these compounds are relatively low, resulting in a significant increase in the energy density of the biomass. The process becomes completely exothermic at temperatures greater than 280°C, resulting in significant increases in the production of CO<sub>2</sub>, phenols, acetic acid, and other higher hydrocarbons [166]. For example, the biomass, during the process of torrefication can lost 31 to 38% of its original mass and to increase its energy density 29 to 33% (energy per unit mass) of the biomass [1]. It also greatly reduces its weight as well as its hygroscopic

---

<sup>13</sup> A higher heating rate would increase liquid yield at the expense of solid products as is done for pyrolysis



nature, thus enhancing the commercial use of wood for energy production by reducing its transportation cost [1].

Torrefaction is primarily used as a pretreatment of biomass to improve its energy density, reduce the O/C and H/C ratio and reduce its hygroscopicity [54]. Such biomass will absorb less moisture while stored than regular biomass. Also, biomass becomes brittle (through the decomposition of the hemicellulose molecules of the biomass) and easy to mill (reduces the handling costs). Also, in raw biomass, high oxygen content prompts its over oxidation during gasification, increasing the thermodynamic losses of the process [54]. Torrefaction could reduce this loss by reducing the oxygen in the biomass [1]. Torrefaction also increases the relative carbon content of the biomass. The properties of a torrefied wood depend on torrefaction temperature, time, and on the type of wood feed. For example, torrefied wood has a density of about 0.25 kg/dm<sup>3</sup>, heating value of about 20 900 kJ/kg, a fixed-carbon content between 35 and 40%, and it is highly friable [167].

The primary goal of fast pyrolysis is to maximize the production of liquid fuel (known as bio-oil, tar, etc.). The biomass is heated so rapidly that it reaches the peak (pyrolysis) temperature before it decomposes (short vapour residence times of typically less than 1 second or 500 ms) [1, 163]. The heating rate can be as high as 1000 to 10,000 °C/s, but the peak temperature should be below 650 °C if bio-oil is the product of interest (up to 85 wt % (wet basis) or up to 70% (dry basis) [1]. Therefore, fast pyrolysis has two main types:

- Flash
- Ultra-rapid

In flash pyrolysis biomass is heated rapidly in the absence of oxygen to a relatively modest temperature range of 450 to 600 °C. The product, containing condensable and noncondensable gas, leaves the pyrolyzer within a short residence time of 30 to 1500 ms [1, 163]. Upon cooling, the condensable vapour is condensed into a liquid fuel. Such an operation increases the liquid yield (70 to 75% of the total pyrolysis product) while reducing the charcoal production [1].

In the ultra-rapid pyrolysis, a hot inert gas and/or hot solid particles are bombarded against fine particles of biomass (extremely fast mixing). The retention time is very small and the heat rates are very high, favouring the formation of liquid products. A

rapid quenching of the primary product follows the pyrolysis, occurring in its reactor. A gas – solid separator separates the hot heat - carrier solid particles from the noncondensable gases and primary product vapours, and returns them to the mixer [1]. The products are suddenly cooled and removed from the system. Liquid yield is high, since the heat transfer is high and residence time is low. To maximize the product yield of gas, the pyrolysis temperature is around 1000 °C for gas (gas yields at up to 80 wt % ) and around 650 °C for liquid [1].

It should be noted that there are a few other variants of pyrolysis process depending on the medium and pressure at which the pyrolysis is carried out [1].

Vacuum pyrolysis is typically carried out at a temperature of 400-500°C and a total pressure of 2-20 kPa [127] This conditions allow the pyrolysis products to be rapidly withdrawn from the hot reaction chamber, thus preserving the primary fragments originating from the thermal decomposition [168]. Conversely, the liquid yields are higher than in slow pyrolysis technologies because the vapours are removed quickly from the reaction zone, thus minimizing secondary reactions [169]. This pyrolysis process enables the production of large quantities of pyrolysis oils and charcoal product. The products obtained in this manner are of superior quality because their chemical characteristics are often closely related to those of the complex molecules which make up the original organic matter [170]. The main advantages of the process are that it can process larger particles than most fast-pyrolysis reactors, there is less charcoal in the liquid product because of the lower gas velocities, and no carrier gas is needed [169].

Slow and fast pyrolysis are carried out generally in the absence of a medium, while there is other types of pyrolysis process which are conducted in a specific medium:

- Hydrous pyrolysis (in H<sub>2</sub>O)
- Hydro pyrolysis (in H<sub>2</sub>)
- Methano-pyrolysis (in CH<sub>4</sub>)

In hydro pyrolysis, thermal decomposition of biomass takes place in an atmosphere of high-pressure hydrogen. Hydrogen is used because the hydrogen molecules bind to the decomposed hydrocarbons in a manner that increases the volatile yield and the proportion of lower-molar-mass hydrocarbons. Higher volatile yield is

attributed to hydrogenation of free-radical fragments sufficient to stabilize them before they repolymerize and form charcoal [1].

Hydrous pyrolysis is the thermal cracking of the biomass in high-temperature water. It is used to convert biomass into light hydrocarbon that can be used for production of bio-oil with reduced oxygen, fertilizer, or chemicals.

Methane pyrolysis occurs in the temperature range 1000°-1200°C in an atmosphere of methane. The main reaction products are hydrogen and carbon, though very small amounts of higher hydrocarbons, including aromatic hydrocarbons are formed [171]. This pyrolysis process is usually used for hydrogen and chemical production. The characteristics of some pyrolysis processes are presented by Table 3.1.

Table 3.1 Pyrolysis technology variant [1, 16, 53-55]

Pyrolysis Process	Residence Time	Heating Rate	Final Temperature (°C)	Product yield (wt %)		
				Charcoal	Bio-oil	Gas
Carbonization	hot vapour residence time 5 s solids residence times minutes, hours or days	0.01°C/s to up to 2°C/s	400-600	25-35	30 - 45	25-35
Conventional	hot vapour residence time less than 5 s long solids and volatiles residence times up to one minute, (vapour residence times of 0.5 to 5 minutes ; solids residence times can be longer)	2-10°C/s	600	20-25	20	40-35
Torrefaction	solids residence time 30-90 min	<50°C/min	200-300	80-90	0	10-20
Fast	short vapour residence times of typically less than 1 second or 500 ms	1,000 - 10,000 °C/s	<650	12	75	13
Flash	hot vapour residence time 30 to 1500 ms	10-1,000°C/s	450-600	n/a	n/a	up to 80
Ultra-rapid	hot vapour residence time <0.5 s	very high	~1,000 (for gas) ~ 650 (for liquid)	n/a	n/a	up to 90

### **3.4. PYROLYSIS PRODUCTS CHARACTERISTICS**

As mentioned earlier, pyrolysis involves a breakdown of large complex molecules into several smaller molecules. Its product is classified into three principal types: charcoal, tar and gas (CO<sub>2</sub>, H<sub>2</sub>O, CO, C<sub>2</sub>H<sub>2</sub>, C<sub>2</sub>H<sub>4</sub>, C<sub>2</sub>H<sub>6</sub> etc.). Figure 3.4, summaries pyrolysis products and applications.

#### ***CHARCOAL***

Charcoal consists of dehydration, condensation and repolymerization products of the nonvolatile fragments of hemicellulose, cellulose and lignin that are produced during pyrolysis [172]. Charcoal, though a carbon residue of pyrolysis or devolatilization, is not pure carbon; it is not the fixed carbon of the biomass [1]. Charcoal contains some volatiles and ash in addition to fixed carbon [1]. Relative to their fossil fuel cousins, charcoal are very low in nitrogen. Unlike fossil fuels, biomass contains very little inorganic ash [1], and virtually no sulphur or mercury [69]. Also, charcoal contain some oxygen and hydrogen [1, 38, 41]. Consequently, many carbonized charcoals are purer forms of carbon (~85%) than most graphites [69]. Unlike graphite, charcoals are extremely reactive and highly porous [69]. Antal and Grønli [69] explained charcoal reductivity. The transformation of biomass to charcoal involves the loss of approximately 60% of the substrate's mass with the evolution of nearly 4 mol of gas per mole of monomer [69]. During this transformation, the molecular framework of the sugar moieties composing biomass is grossly rearranged to form aromatic structures. Because the transformation does not involve a liquid phase, many bonds are left dangling, giving rise to a carbonaceous solid that is inherently porous at the molecular level and highly reactive [69]. Bulk density of the charcoal is around 130 and 300 kg/m<sup>3</sup> [173]. The lower heating value (LHV) of biomass charcoal is about 32 MJ/kg, which is substantially higher than that of virgin biomass (19.50–21.00 MJ/kg) or its liquid product and lignite (6.2 – 14.3 MJ/kg) [1, 173, 174]. The carbon atoms in charcoal molecules are strongly bound to one another, and this makes charcoal resistant to attack and decomposition by microorganisms. By contrast, the carbon in most

organic matter is a rapidly (1-2 years) returned to the atmosphere as CO<sub>2</sub> through respiration.

Charcoal is used as an active carbon, as a reducing agent in the metallurgical industry (e.g. to smelt metal ores). As a premium solid fuel, charcoal is used for the refining of metals (copper, bronze, steel, silicon, nickel, aluminium, and electro-manganese). For example, wood charcoal (as well as coal and coke) is used to reduce silicon dioxide to silicon. Very high purity silicon is used to manufacture semiconductors (silicon with impurities in the parts per billion range) and photovoltaic cells (silicon with impurities in the parts per million range) [67]. Silicon is also used as an alloy in the production of steel, cast iron, aluminium, and other metals (copper (Cu), nickel (Ni), aluminium (Al), manganese (Mn)). For example, Norwegian ferrosilicon industry consumes 300,000 t/year of charcoal. Currently, the Norwegian ferrosilicon industry imports charcoal from Asia and South America (Brazil) at a price (including transportation costs) of about 250 €/t of fixed carbon [67]. Despite its high price, wood charcoal is able to compete with fossil carbons because of its relative purity (low ash content) and high reactivity. Also, charcoal is used as an active carbon, for domestic cooking (e.g. as a barbecue charcoal), as a fuel in households, as an adsorbent, as a s raw material for the production of chemical compounds (carbon - disulphide (CS<sub>2</sub>), calcium - carbide (CaC<sub>2</sub>), silicon - carbide (SiC), sodium cyanide (NaCN), fertilizers, carbon black, various pharmaceutical compounds, etc.) [67, 68, 72, 84, 175]. Also, charcoal is used as soil fertilizer. The most well-known is fertile terra preta soils in the Amazonian region. Terra preta soils contain up to 70 times more black carbon than the adjacent soils. Due to its polycyclic aromatic structure, black carbon is chemically and microbially stable and persists in the environment over centuries [176]. There is some evidence that *terra preta* can reduce the run off of agricultural inputs such as nitrates as well as suppressing NO<sub>2</sub> and CH<sub>4</sub> emission from the soil to atmosphere [177]. These all characteristics of charcoal and charcoal manufactured carbons are preferred adsorbents for air and water treatment. For examples, activated charcoal is used on an enormous scale in both vapour-phase and liquid-phase purification processes. It is widely used in respirators, as well as in air-conditioning systems and in the clean-up of waste gases from industry. In the liquid-phase, its largest single application is

the removal of organic contaminants from drinking water. Many water companies in Europe and the USA now filter all domestic supplies through granular activated carbon filters, and household water filters containing activated carbon are also in widespread use

Packed bed of carbonized charcoal conducts electricity nearly as well as a packed bed of graphite particles. Coutinho et al. [178, 179] emphasizes use of biocarbons to form electrodes.

In contrast with other renewable fuels (e.g., hydrogen and ethanol), charcoal is easy to store, cheap to produce, and when compared with other conventional fuels, charcoals are environment-friendly.

### **TAR**

The tar is a mixture of organic compounds and water. The tar has a dark brown to reddish colour and is a free-flowing organic liquid with a distinct smoky odor. Tar is composed of a very complex mixture of oxygenated hydrocarbons and consists of more than 180 compounds and they are often grouped as acids, alcohols, ketones, aldehydes, phenols, alkenes, furans, guaiacols, oxygenates and sugars [180]. From literature review it is learnt that: water content of tar usually varies from 15-30% depending upon the feedstock and processing conditions; oxygen is present in most of the species present in tar, together with water, this accounts for overall oxygen content of 35-40% of tar; tar show wide range of volatility distribution; viscosity of bio-oil can vary over a wide range (0.035-1 Pas at 40°C); tar is unstable and results in phase separation over time; tar is corrosive due to presence of organic acids (2 - 3 pH) [172]. While the virgin biomass has an LHV in the range of 19.5 to 21 MJ/kg dry basis, its liquid yield has a lower LHV, in the range of 13 to 18 MJ/kg wet basis, whereas the values for methanol (CH<sub>3</sub>OH) and ethanol (C<sub>2</sub>H<sub>5</sub>OH) vary between 22.7 and 29.7 MJ/kg [1, 174]. Although bio-oil is the most easily obtainable liquid product from biomass, its applicability becomes limited due to its above mentioned physicochemical properties (acidity, low energy value, high viscosity, and instability) needs to be upgraded to more stable and desirable form prior to using directly as heating fuel or as a feedstock for upgrading into transportation fuels [172, 181, 182]. Tar can be used for heating and/or electricity production, chemicals

and pharmaceuticals, including a food additives, methanol, ammonia, hydrogen, glues, paint, fertilizers, etc.

## **GAS**

Primary decomposition of biomass produces both condensable gases (vapor) and noncondensable gases (primary gas) [1]. The vapors, which are made of heavier molecules, condense upon cooling, adding to the tar yield of pyrolysis. The gas pyrolysis products are mainly composed of carbon - monoxide (CO), carbon - dioxide (CO<sub>2</sub>), hydrogen (H<sub>2</sub>), methane (CH<sub>4</sub>), acetylene (C<sub>2</sub>H<sub>2</sub>), ethylene (C<sub>2</sub>H<sub>4</sub>), ethane (C<sub>2</sub>H<sub>6</sub>), benzene (C<sub>6</sub>H<sub>6</sub>), water, various alcohols, and traces of higher hydrocarbons [1, 172]. Additional noncondensable gases produced through secondary cracking of the vapour are called secondary gases. The final noncondensable gas product is thus a mixture of both primary and secondary gases. [12]. In addition to the gas release, saturated compounds such as water and alcohols will be present in the gas phase. Due to the nitrogen content in the fuel, trace elements of nitrous compounds such as ammonia (NH<sub>3</sub>) and hydrogen cyanide (HCN) are also present [12]. These will react to form NO<sub>x</sub> under the presence of an oxidizing agent for example during combustion. Other trace gas elements that are present due to the sulphur content in the raw fuel are hydrogen sulphide (H<sub>2</sub>S) and carbonyl sulphide (COS). These sulphur compounds are likely to be produced in gasification processes and are undesirable since they reduce process efficiency, [12]. Other trace elements such as potassium chloride (KCl), hydrogen chloride (HCl) and many more are quite normal to be found in the devolatilized products as well due to the alkali metals found in biomass, [12].

The LHV of primary gases is typically 11 MJ/Nm<sup>3</sup>, but that of pyrolysis gases formed after severe secondary cracking of the vapour is much higher 20 MJ/Nm<sup>3</sup> [1, 174]. The combustion characteristic of gas differs from natural gas. The H<sub>2</sub> content of gas is quite high, which is critical from the point of view of knock, and it has very low LHV which is critical from the point of view of power [183]. Due to the high H<sub>2</sub> content of gas the direct use in IC engine<sup>14</sup> is not recommended, the gas has to be

---

<sup>14</sup>IC engine - internal combustion engine



mixed with natural gas in ratio 40:60 [183]. Also, gas can be used as a raw material for synthetic natural gas production or for production of liquid fuels (e.g. synthetic diesel, methanol, etc.).

Depending on the pyrolysis conditions (heating rate, temperature, particle size etc.) the pyrolysis product distribution can be adjusted and optimized.

### **3.5. INFLUENCE OF PYROLYSIS PARAMETARS ON PRODUCTS YIELD**

Pyrolysis is thermochemical conversion routes to recover energy from biomass and waste fuels. Pyrolysis is not only an independent conversion technology but also part of the gasification process, which can be broadly separated into two main stages, solid devolatilization (pyrolysis) and charcoal conversion (combustion and gasification). The product of pyrolysis depends on the design of the pyrolyzer, the physical and chemical characteristics of the biomass (fuel particle size and fuel composition), and important operating parameters (temperature, pressure, and heating rate), presence or absence of catalytically active substances, retention time of the products in the zone of the pyrolysis process. The process parameters has an important influence on the course of thermal degradation of biomass macromolecules as well as on the primarily product distribution through hot charcoal zone [148]. The primarily formed products passes a hot charcoal zone, where they are converted by so-called secondary reactions. These reactions control the products content and composition. If the major mechanisms of the secondary reactions are known, products mass and composition can be controlled by choosing appropriate reactor conditions. Retention time and reaction rate depends on rate of diffusion - distribution. The diffusion - distribution does not have influence on gases with small molecular weight and with low reactivity (hydrogen (H<sub>2</sub>), methane (CH<sub>4</sub>), carbon - monoxide (CO), steam (H<sub>2</sub>O)), on small radicals (hydrogen (H), methyl group (CH<sub>3</sub>), ethyl group (C<sub>2</sub>H<sub>5</sub>)) which are very reactive and quickly forms gases which easily passes through biomass micropores [148]. Diffusion- distribution has a high impact on large radicals and tar molecules [148]. Radicals and tar delays the escape from the carbon matrix. This delay offers additional opportunities for residual tarry vapours to suffer secondary reactions with the solid carbon and increases the yield of fixed carbon [69].

In summary, reactor temperature together with the material flow rates (both solid and gas phase) control the key parameters of heating rate, peak temperature, residence time of solids and contact time between solid and gas phases. These factors affect the product distribution and the product properties.

### **PYROLYSIS TEMPERATURE**

The temperature profile is the most important aspect of operational control for pyrolysis processes. The pyrolysis temperature affects both composition and yield of the product. Numerous studies have investigated the effect of temperature on the final pyrolysis product yields [180, 184-190].

Peak temperature (highest temperature of pyrolysis process) has an unequivocal effect on the yield and the quality of the charcoal product. Both the yield and the quality of the charcoal product are strongly influenced by the peak temperature of the pyrolysis process [72]. Higher temperatures lead to lower charcoal yield in all pyrolysis reactions (Figure 3.4). The effect can be thought of as more volatile material being forced out of the charcoal at higher temperatures reducing yield but increasing the proportion of carbon in the charcoal.

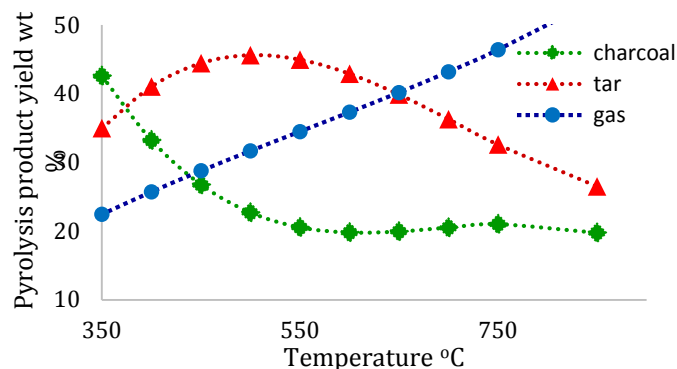


Figure 3.4 Effect of temperature on pyrolysis product yield [19]

Antal and Mok [72], and later Gronli and Antal [69], compiled a succinct summary of the trends of many important properties of charcoal with increasing peak temperature. As the peak temperature increases above 200 °C, the solid pyrolytic residue changes from *toasted wood* to *torrefied wood* to *pyrochar* to conventional charcoal [72]. The process of torrefaction involves heating the biomass substrate to a peak temperature between 200 and 280 °C, with a preferred value between 240

and 260 °C. In this temperature-time domain the hemicelluloses are thermally degraded (not destroyed), acetyl groups are cleaved, and acetic acid is formed as a gaseous product [72]. Some degradation of the lignin must also occur [167]. Torrefied wood has a heating value of about 20 900 kJ/kg and a fixed-carbon content between 35 and 40%, with density about 0.25 kg/dm<sup>3</sup>, and it is highly friable [72]. When the biomass is further heated to higher temperatures, but not exceeding about 350 °C, a pyrochar is produced [72]. This material is formed in about 50% yield and has lost the fibrous character of the biomass feedstock (has a heating value of 26 000 kJ/kg and a volatile matter content of about 35%) [72]. Pyle [191] reported that the pyrolysis reactions become exothermic when the percentage volatile matter contained in the pyrochar reaches 35-45%. Also, Emrich [192] and Bourgeois [167] also reported the final stages of charcoal formation to be exothermic. Above 350°C conventional charcoal, having a volatile matter content of less than 35%, is formed from the biomass sample [72]. Pyle [191] and Bourgeois [167] indicated that it is difficult to control the peak temperature in this regime because of the exothermicity of the pyrolysis reactions in industrial - scale reactors (the peak temperature usually is not defined within narrow limits) [14]. Consequently, the peak temperature range employed to produce conventional charcoal is usually not defined within narrow limits. Charcoal yields decrease rapidly as the temperature increases to 500°C and then decrease very slowly to 800°C, when the devolatilization is almost completed [193]. Temperature also has an effect on charcoal composition. The carbon content of the charcoal increases sharply with increasing temperature while that of H and O decrease [194]. It can be concluded, charcoal produced at higher temperatures having higher carbon contents both total - and fixed -carbon [69].

Liquid yields are higher with increased pyrolysis temperatures up to a maximum value, usually at 450 to 600°C but dependent on equipment and other conditions [180, 194]. For fast pyrolysis the peak liquid yields are generally obtained at a temperature of around 500°C [163]. Peak liquid yields for slow pyrolysis are more variable. Peak liquid yields of 28-41% at temperatures between 377°C and 577°C, depending on feedstock, when using a laboratory slow pyrolysis technique [195]. Above this temperature secondary reactions causing depolymerisation of tar become more dominant and the condensed liquid yields are reduced.

Gas yields are generally low with irregular dependency on temperature below the peak temperature for liquid yield; above this gas yields are increased strongly by higher temperatures, as the main products of vapour decomposition are gases [194]. The composition of the gas varies significantly with temperature, in particular the concentration of CH<sub>4</sub> is the highest between 600°C and 700°C, concentrations of CO and H<sub>2</sub> are rising while CO<sub>2</sub> decreases uniformly with the temperature [56]. The high temperature favours the formation of H<sub>2</sub> at the expense of heavy hydrocarbons that are dehydrogenated from cracking (Figure 3.5).

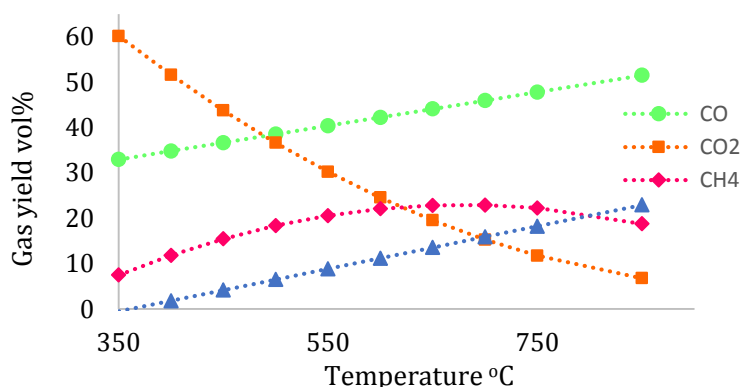


Figure 3.5 Influence of pyrolysis temperature on gas composition

It is difficult to control the peak temperature in this regime because of the exothermicity of the pyrolysis reactions in industrial-scale reactors. Consequently, the peak temperature range employed to produce conventional charcoal is usually not defined within narrow limits. These variations in temperature result in a variation in the quality of charcoal.

### **HEATING RATE**

Numerous studies have investigated the effect of heating rate on the final pyrolysis product yields [180, 193, 196-198]. The length and intensity of heating of the biomass has an important influence on the yield and composition of the pyrolysis products. Heating rate has intensity affect the rate and extent of pyrolytic reactions, the sequence of these reactions, and composition of the resultant products [197]. Pyrolytic reactions proceed over a wide range of temperatures; hence, products formed earlier tend to undergo further transformation and decomposition in a series of consecutive reactions [197]. Long heating periods allow the sequence of

secondary reactions to take place, whereas rapid heating (flash pyrolysis) tends to reduce these secondary reactions and the further degradation of the earlier formed products [197]. The effect of heating rate can be viewed as the effect of temperature and residence time. As the heating rate is increased, the residence time of volatiles at low or intermediate temperatures decreases [197]. Most of the reactions at which tar convert to gas, occurs at higher temperatures. At low heating rates, the volatiles have sufficient time to escape from the reaction zone before significant degradation can occur. If heat is supplied fast enough during flash pyrolysis (heating rates up to  $10^4$ °C/min), little or no charcoal results and subsequent processing is greatly simplified and provide maximum yields of pyrolysis oils. At slow pyrolysis (heating rates in the order of  $10$ °C/min) and low temperature, charcoal is the dominant product followed by steam. During slow heating, a slow or gradual removal of volatiles from the reactor permits a secondary reaction to occur between charcoal particles and volatiles, leading to a secondary charcoal formation. The yield of volatile products (gases and liquids) increases with increasing heating rate while solid residue decreases [197]. For example, Debdoubi [199] observed that, when the heating rate increased from  $5$  to  $250$  °C/min to  $400$  to  $500$  °C/min, the liquid yield increases from  $45$  to  $68.5\%$ . The maximum rate of devolatilization increases almost linearly with increasing heating rate, [200]. At the lower heating rates, the maximum rates of mass losses were relatively low. When the heating rate was increased, maximum rates of mass losses also increases (extensive thermal fragmentation of biomass). A high heating rates may shift the pyrolysis reaction to a much higher temperature range and affect the shape of the DTG peaks. Increase in the heating rate shifts the peak on the DTG profile to the lower temperatures as shown in Figure 3.6 [20, 21]. At low heating rates, resistance to mass or heat transfer inside the biomass particles occurs, which results in a low total mass loss values and thus lower conversion of biomass to liquid or gaseous products [180]. Also, heating rate is a function of the biomass samples. The rate of thermal diffusion within a particle decreases with increasing particle size, thus resulting in lower heating rate [197]. Liquid products are favoured by pyrolysis of small particles at high heating rates and high temperature, while charcoal is maximized by pyrolysis of large particles at low heating rates and low temperatures as mentioned earlier [197].

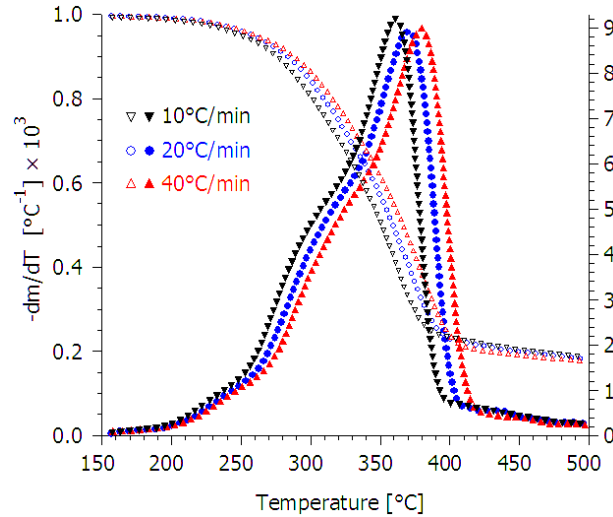


Figure 3.6 Influence of heat rate and pyrolysis temperature on devolatilization, [20, 21]

Consequently, it is often assumed that the charcoal yield will continue to improve as the heating rate continues to be reduced [72]. Unfortunately, this assumption is not true: usually an asymptote is reached beneath which a decrease in heating rate does not improve the charcoal yield [72]. In 1851, Violette [69] reported a charcoal yield of 18.87 wt % (with carbon content of 82.1%) from wood heated slowly over a 6-h period. The charcoal yield decreased to 8.96 wt % when the wood was heated quickly, and the product was light and friable with a carbon content of 79.6% [69]. Years later, Klar (in 1925) [69] presented a table of wood distillation products that displayed the effects of heating rate on yields. A change from slow to rapid carbonization decreased measured charcoal yields from 2 to 10 wt %, depending on the species [69]. MacKay and Roberts [201], reported an increase from 22 to 32% in the yield of charcoal from redwood when the heating rate was reduced from 200 to 1 °C/min [69]. The accurate thermogravimetric studies reported by Varhegyi et al. [202, 203] revealed no influence on the charcoal yield from bagasse when the heating rate was decreased from 80 to 10 °C/min [72]. These findings were largely corroborated by complementary thermogravimetric studies on bagasse conducted in the Renewable Resources Research Laboratory (R<sup>3</sup>L) of the University of Hawaii [72]. A decrease in heating rate from 2 to 0.5 °C/min resulted in no significant change in the charcoal yield at 541 °C; however, a small increase in yield was detected between 20 °C/min and 2 °C/min [72].

### **RESIDENCE TIME**

The residence time of volatiles in the hot reactor, determines the extent of exothermic secondary volatile reactions [74, 204].

Even today, many researchers still assume that charcoal is solely a product of primary (solid-phase) pyrolytic reactions. In reality, charcoal contains both primary charcoal and secondary charcoal that is a coke derived from the decomposition of the organic vapours (tars) onto the solid carbonaceous solid [29]. This decomposition is probably catalysed by the charcoal [41, 202, 205, 206]. Remarkably, secondary charcoal is as reactive as primary charcoal. Low gas flows provide increased opportunities for reactive volatile matter to interact with the solid carbonaceous residue of pyrolysis and produce more charcoal. Varhegyi et al. [202], conducted TG studies of Avicel cellulose pyrolysis in open and covered sample pans. A small sample (0.5 mg) was hermetically sealed in an aluminium DSC crucible and a pinhole of about 0.2 mm diameter was punctured in the top. This arrangement affected both the decomposing sample and the evolving vapours: the decomposition occurs in the presence of the vapours, and these vapours spend a longer time at a higher partial pressure in the hot zone above the sample [202]. The charcoal yield in the open sample pan was typically about 7%. When pyrolysis was conducted in a covered pan with a pinhole, charcoal yield dramatically increased to 19% [202]. The closed vessel prevents the quick escape of the products from the hot zone; thus, these vapours may undergo further decomposition and form additional quantities of H<sub>2</sub>O, CO, CO<sub>2</sub> and charcoal.

These striking results clarify the beneficial effects of both prolonged vapour-phase residence times and increased concentrations of vapours on the carbonization chemistry.

Generally speaking, pyrolysis classification is based on heating rate and residence time. The operating parameters of a pyrolyzer are adjusted to meet the requirement of the final product of interest. Tentative design norms for heating in a pyrolyzer include the following [1]:

1. To maximize charcoal production, use a slow heating rate (<0.01–2.0 °C/s), a low final temperature, and a long gas residence time.

2. To maximize liquid yield, use a high heating rate, a moderate final temperature (450–600 °C), and a short gas residence time.
3. To maximize gas production, use a slow heating rate, a high final temperature (700–900 °C), and a long gas residence time.

Production of charcoal through carbonization uses the first norm. Fast pyrolysis uses the second to maximize liquid yield. The third norm is used when gas production is to be maximized.

### ***PRESSURE***

Pressure has a significant influence on pyrolysis of biomass.

Violette [41] in 1853 released the first paper concerning the production and properties of charcoal produced under pressure. Violette heated wood samples weighing about 1g in sealed glass tubes to high temperatures (temperature at which that caused some of the tubes to explode). At the highest temperature employed in his work, Violette reported a charcoal yield of 79.1 wt % with a carbon content of 77.1% [69]. Violette's observations are intriguing, and his experiments remain novel even today. Palmer (in 1914) [207], presented the first thorough study of the effects of elevated pressures on wood distillation. From a practical standpoint, the most interesting effect of pressure is in connection with the yield of soluble tar [207]. Charcoal at 60 lbs (4 bar) pressure, 8% more charcoal was obtained than at atmospheric pressure, and at 120 lbs (8 bar) there was an increase of 11% over atmospheric distillations [207]. At 4 bar and 8 bar the yield of total tar was 60 to 65% less than at atmospheric pressure [207]. Mok et al. [204] found that an increase in pressure from 0.1 to 1.0 MPa (at constant purge gas velocity) increases the charcoal yield up to 41%. Several decades later, Antal and Mok [204], used DSC in conjunction with stainless steel pressure vessels was to investigate the effects of pressure and purge gas flow rate (gas phase residence time) on the heat demands of cellulose pyrolysis. High pressure and low flow rate reduce the heat of pyrolysis and increase charcoal formation [204]. They observed an increase from 12 to 22% in the yield of charcoal from cellulose with an increase in pressure from 0.1 to 2.5 MPa at low gas flow [69, 204]. The improved yield of charcoal was accompanied by the formation of additional CO<sub>2</sub>, H<sub>2</sub>, and C<sub>2</sub>H<sub>6</sub> and lesser quantities of CO, CH<sub>4</sub>, and C<sub>2</sub>H<sub>4</sub>



[69, 204]. Ward and Braslaw [208] in experiments with unmilled wild cherry wood at 300°C observed a higher rate of weight loss at 1 atm and at  $4 \times 10^4$  atm. After a reaction time of 50 min, the samples under 1 atm and  $4 \times 10^4$  atm pressure lost about 55% and 40% of their weight, respectively [197, 208]. Blackadde and Rensfelt [209] in experiments with wood, lignin, and cellulose in a pressurized thermobalance, found that at a given temperature, charcoal residue increased pressure in each case [197, 210]. Cellulose, however, displayed the strongest pressure dependency and lignin the weakest. Bhattacharya et al. [211] reported that at temperatures in excess of 400 °C (preferably above 535 °C), and pressures exceeding 6.8 MPa, the biomass substrate is rapidly transformed into a charcoal [72, 212]. The yield of charcoal is 25-35% with a fixed-carbon content of 62-86% and a volatile matter content of 8-17%. The charcoal has a heating value of 26.7 - 35 MJ/kg [72, 212]. Richard and Antal, [213], presented results of thermogravimetric studies of cellulose pyrolysis in flowing nitrogen at elevated pressures. In this work the charcoal yield varies from 6% to 41% and is strongly influenced by process conditions [213]. Decreasing the velocity of purge gas passing through the sample increases the charcoal yield from about 6% to more than 21% at 0.1 MPa [213]. Increasing the pressure from 0.1 MPa to 1.0 MPa (with a constant purge gas velocity) further increases the charcoal yield to a value of 41% [213]. Antal et al. [68], executed experiments using the laboratory reactor to identify the effects of operating pressure on charcoal yields from Macadamia nut shells. The pressure of only 0.4 MPa is sufficient to realize an attractive yield of 40.5%, and further increases in pressure improve the yield to a value of 51% (3.3 MPa) [68].

Under pressure, the tarry pyrolytic vapours have a smaller specific volume; consequently, their residence time within the particle and in the near vicinity of the particle increases [69]. Also, the partial pressure of the tarry vapour within and in the vicinity of the particle is higher [69]. These effects are magnified when the flow of gas through the particle bed is low as is the case at elevated pressure [69, 204, 213, 214]. Furthermore, the formation of secondary carbon from the tarry vapour is catalysed by the charcoal [69, 215, 216], and water vapour or chemisorbed moisture can act as an autocatalytic agent for carbon formation at elevated pressures [68, 75, 217]. Molecular diffusivities are also affected by increasing pressure and can

influence the escape of the tarry vapour from the solid particle. The tarry vapours is composed of a complex reactive mixture of organic compounds including vapour phase sugars, and anhydrosugars and their oligomers, fragments of sugars, and lignin moieties that are highly unstable at elevated temperatures [69]. These tarry vapours rapidly decompose on the surface of charcoal, producing secondary charcoal and a gas composed primarily of water, carbon dioxide, methane, hydrogen, and carbon monoxide [69].

#### ***EFFECT OF AMBIENT ATMOSPHERE AND MEDIUM FLOW***

During pyrolysis, the ambient atmosphere affects the heat transfer and nature of the secondary reactions [145]. The ambient atmosphere may either be a vacuum or an inert or reactive surrounding. In a vacuum, primary products are rapidly removed or thinned out in the gas phase, and thus are not available for further decomposition and reaction, while the presence of water or steam is known to speed up the breakdown and degradation of molecules by way of hydrolysis of the biomass and rearrangement of the intermediate products [145]. This hydro-thermolysis may be catalysed by acid or alkali reagents.

Gas flow rate through the reactor affects the contact time between primary vapours and hot-charcoal and so affects the degree of secondary charcoal formation. Low flows favour charcoal yield and are preferred for slow pyrolysis; high gas flows are used in fast pyrolysis, effectively stripping off the vapours as soon as they are formed [194].

The influence of pyrolysis process parameters on the pyrolysis products are summarised and presented in APPENDIX A.

### **3.6. INFLUENCE OF CHEMICAL AND PHYSICAL CHARACTERISTICS OF BIOMASS ON PYROLYSIS PROCESS**

The composition, size, shape, and physical structure of the biomass exert some influence on the pyrolysis product through their effect on heating rate. The composition of the biomass, especially its hydrogen to carbon (H/C) ratio, has an important bearing on the pyrolysis yield [218]. As biomass is heated, its components

(hemicellulose, cellulose and lignin) become chemically unstable and thermally degrade or vaporise. Each of the three major constituents of a biomass has its preferred temperature range of decomposition. A number of studies [16, 219-223] have shown that the main components of most biomass types, i.e. cellulose, hemicellulose and lignin, are chemically active at temperatures as low as 150°C. A review of the possible reaction pathways and mechanisms which the pyrolysis of biomass may follow depending upon the reaction conditions are presented below.

### ***BIOMASS SAMPLE MASS***

The pyrolysis pathways, duration of the process, kinetics of the process, quantity and quality of products are also influenced by the mass of the observed biomass.

The biomass is often treated in the form of pellets or fragment of a certain size. The sample size and/or sample mass during pyrolysis can cause spatial gradients of temperature (a process taking place under nonnegligible effects of internal heat transfer) [160]. This implies that gradients of temperature exist in the biomass and that the temperature variation is generally slower inside [224].

The biomass particle influenced by heat transfer is a factor in the diffusion of volatile products out of the biomass particle. Furthermore, the products generated by decomposition of biomass components must diffuse into the mass of matter. Several studies [31, 225] have in fact shown an influence of the sample size on the amount of tar and gas yields both for cellulose.

The influence of sample size on pyrolysis products is directly connected with the mass and heat transfer from the reactor environment to the particle surface, from the outer surface of the particle into the interior of the particle and transfer between the volatile reaction products leaving the reaction zone and the solid matrix.

Finer biomass particles offer less resistance to the escape of condensable gases, which therefore escape relatively easily to the surroundings before undergoing secondary cracking. This results in a higher liquid yield. Larger particles, on the other hand, facilitate secondary cracking due to the higher resistance they offer to the escape of the primary pyrolysis product [218].

Micro particle pyrolysis involves biomass materials with samples sizes (thermally thin) sufficiently small that diffusion effects become negligible and the pyrolysis is

kinetically controlled. This is a desirable situation for experiments focusing on identification of kinetic schemes. Critical particle size estimates for kinetic control are generally 100 a 1000 micrometres [35]. In the case of large biomass particles (thermally thick), the chemistry of decomposition is influenced by heat and mass transfer effects.

The effect of the sample size can be explained as follows:

1. The size of the particles affects the heating rate [148]. The heat flux and the heating rate are higher in small particles than in large particles. The rate of thermal diffusion within a particle decreases with increasing particle size, thus resulting in lower heating rate and longer residence time of vapour phase in solid.
2. Longer residence time of vapour phase (volatile gases and tar) and lower heating rate stimulates the secondary reaction to occur. Formation and escape of vapour phase will be slower and contact between vapour phase and charcoal will be extended [148]. The higher heating rate favours a decrease of the charcoal yield.

The effect of particle size is important parameter for pyrolysis with regard to the product yield distribution. For an example, small samples give less charcoal than larger samples. The sample size influence on the charcoal yield is explained by the residential time of the volatiles, which react with the charcoal layer when flowing out the particle to form charcoal [226]. The long residence time of the vapour phase inside large particles explains the formation of higher charcoal yield. It takes longer time for the volatiles to leave a large particle than a small [226]. Lower charcoal yield for small sample masses (powder and single particle samples), could be explained by the bigger surface area that interacts with the pyrolysis medium. Formed volatile products leave the sample without undergoing secondary cracking reactions [227]. Scott et al. [193] have reported over 60 wt % liquid products and 10% charcoal below 600°C in fast pyrolysis of maple wood (120 µm). Aarsen [228] reported that the pyrolysis of 1 µm wood particles in a fluidized bed at 800°C produces less than 10%wt of charcoal. Also, for small sizes, above certain temperatures, the time for total conversion become shorter than times needed for the reactor (TGA) to

attain the final temperature [229]. In the case of larger particles, secondary cracking reactions could be dominant, leading to additional charcoal and tar formation.

### **BIOMASS MOISTURE CONTENT**

The moisture content in biomass also has negligible impact on the final pyrolysis products, since that initial pyrolytic degradation reactions include depolymerisation, hydrolysis, oxidation, dehydration, and decarboxylation, [230]. Gray et al [231] investigated the influence of moisture on the thermal degradation of wood waste at pyrolysis temperature between 320 and 470° at about 300°C/min heating rate. The presence of moisture increased the charcoal yield by as much as 5 wt. % within the temperature range of 390 - 460 °C [231]. The moisture also decreased the liquid (tar) yield from ash-free wood waste by as much as 10 wt. % [231]. They proposed that the decrease in the tar yield and the increase in the charcoal yield are probably due to the free-radical reactions between tar and moisture such as depolymerisation and trapping [231]. The formation of gases, however, was not affected by the presence of moisture. Demirbas [230], investigated the effects of initial moisture contents on the yields of total liquid (tar) products from conventional pyrolysis of spruce wood, hazelnut shell and wheat straw were studied. Moisture percentage of the biomass species varied from 41 to 70%. It was found that, in general, the yields of liquid products (wt. %,dry feed basis) increase with increasing pyrolysis temperature from 575 to 700 °C then it decreases with increasing temperature [230]. The yield of total liquid also increases with increasing the initial moisture content of the sample. The yields of total liquid products of spruce wood (moisture content: 6.5 %), hazelnut shell (moisture content: 6.0 %) and wheat straw (moisture content: 7.0 %) increase from 8.4, 6.7 and 6.2 % to 33.7, 30.8 and 27.4 %, respectively, by increasing the pyrolysis temperature from 575 to 700 °C [230]. Qualitative observations show that dry feed material led to the production of very viscous liquid, particularly at higher reaction temperatures. It is desirable to use fuel with low moisture content because heat loss due to its evaporation before thermal conversion (pyrolysis, gasification and combustion) is considerable. For example, for fuel at 25<sup>0</sup>C and raw gas exit temperature from

reactor at 300<sup>o</sup>C, 2875 KJ/kg moisture must be supplied by biomass to heat and evaporate moisture [232]. The high moisture content also puts load on cooling and filtering equipment by increasing the pressure drop across these units because of condensing liquid. Thus in order to reduce the moisture content of biomass some pre-treatment of fuel is required. Generally desirable moisture content for biomass should not exceed 20-40% [232].

### ***BIOMASS MINERAL MATTER CONTENT***

Biomass is carbon based and is composed of a mixture of organic molecules (containing hydrogen, usually including atoms of oxygen, often nitrogen) and also small quantities of other inorganic atoms (including alkali, alkaline earth and heavy metals). The inorganic composition and content varies for different biomasses and woody materials. The inorganic concentration in wood is often low (< 1 wt %) compared to the herbaceous biomass and agricultural residues which can be up to 15 wt % [84]. The presence of inorganic materials (minerals) either as additives or natural ash content, strongly affects the pyrolysis of biomass; the effect is more pronounced with alkaline compounds and acidic reagents [145]. In biomass inorganic materials generally remain as salts or are organically bound [1]. Even the natural impurities and ash content can produce significant effects, which can be made clearer by lowering the process temperature and increasing charcoal formation [145]. Inorganic matter also affects pyrolysis, giving charcoal of varying morphological characteristics [1]. Potassium and sodium catalyse the polymerization of volatile matter, increasing the charcoal yield; at the same time they produce solid materials that deposit on the charcoal coal pores, blocking them [1, 233]. During subsequent oxidation of the charcoal, the alkali metal catalyses this process. Polymerization of volatile matter dominates over the pore-blocking effect [1, 233]. A high pyrolysis temperature may result in thermal annealing or loss of active sites and thereby loss of charcoal reactivity [1, 233]. The acidic catalysts also enhance the condensation of intermediate compounds and affect some of the charcoal properties [145]. Most affected is the nature of charcoal oxidation. It should be noted, however, that the effect of catalysts is great during cellulose and wood

pyrolysis, but almost negligible when lignin is pyrolyzed [145]. The presence of catalysts suppress the release of combustible volatiles such as tar, thus suppressing flaming combustion. Tsuchiya and Sumi [234], studied the pyrolysis of untreated and salt treated cellulose under vacuum and at temperatures ranges of 320-520°C. The presence of inorganic compounds ( $K_2CO$ ,  $KHCO_3$ ,  $ZnCl_2$ ,  $PO_4$ , and  $H_3PO_4$ ) decreased the yield of tar fraction and increased charcoal [234]. Yields of  $CO$ ,  $CO_2$ , and  $H_2O$  were enhanced;  $CO$  was more pronounced with alkali salts. Nassar et al. [235] investigated the effects of four inorganic salts ( $NaCl$ ,  $KHCO$ , borax, ammonium phosphate) on the major products of pyrolysis of black spruce sawdust at 500°C under vacuum. Their results show a decreased yield of total flammable gases, especially  $CO$ , decreased tar fraction, and increased water and charcoal yields.  $H_2$  and hydrocarbon gases yields were reduced but  $CO_2$  was increased [235]. Nassar and MacKay [236], carried out studies on lignin treated with inorganic salts. The results show that lignin is almost inert to the effect of salts during pyrolysis [236]. Utioh et al. [237], report increased yields in synthesis gas with the addition of 15%  $K_2CO$  during the pyrolysis of grain screenings.  $H_2$  and  $CO_2$  production were enhanced while  $CO$  yields were decreased [237]. Impregnation of biomass with monobasic ammonium phosphate salts reportedly reduce decomposition temperature and increase weight loss during the pyrolysis even at temperatures below 350°C [237]. The salts also enhance charcoal production and reaction rates. Biomass materials composed predominantly of holocellulose, lignin, extractives and inorganic components. These constituents have different rates of degradation and preferred temperature ranges of decomposition. The holocellulose is the carbohydrate fraction of lignocellulose that includes cellulose and hemicellulose, and composes from 70% to 85% of most woody biomass [29]. The reaction rates, products, and other thermal behaviour of biomass pyrolysis are considered a combination of the behaviour of its main components. The thermal degradation of each component occurs at different temperature by different pathways. The basic knowledge of the role and behaviour of the three principal components of biomass (cellulose, hemicelluloses and lignin) during pyrolysis is important for understanding and controlling this process.

### **BIOMASS THERMAL AND THERMODYNAMIC PROPERTIES**

The most important thermal and thermodynamic properties are thermal conductivity, heat transfer coefficient, emissivity and etc. The dependence of average product concentrations and conversion time on these properties during convective/radiant pyrolysis is applicable to both gasification and pyrolysis units [58]. The thermal and thermodynamic properties are important mainly for large particles (thermally thick regime) [58]. For example, high charcoal concentration is associated with high thermal conductivity.

### **SHRINKAGE**

According to Di Blasi [34], the shrinking of the solid biomass particle effects on: the medium properties (porosity, permeability, density, mass diffusivity, specific heat capacity and thermal conductivity), the volume occupied by volatiles (gas and tar), the volume occupied by solid (biomass and charcoal), and consequently the total volume of the particle also change continuously [58].

Shrinkage occurs because of a loss of water mass or as a result of the pyrolysis reactions. Shrinkage due to a loss of water mass typically accounts for a 5 –10% reduction in particle size [238]. Shrinkage also occurs in the charcoal layer during the pyrolysis reactions because of a rearrangement of chemical bonds and the coalescence of graphite nuclei within the biomass particle [238]. The amount of charcoal shrinkage is a function of biomass species, heat flux and temperature. Charcoal shrinkage increases as the temperature increases and also increases with the amount of time at a given temperature [238]. Roughly one-half of the charcoal shrinkage occurs during the rapid devolatilization of the biomass, with continued chemical rearrangement following the devolatilization process [238]. As a result of restructuring during pyrolysis, the charcoal density increases. Also, the temperature profile of the particle (biomass and charcoal) changes due to increased density and decreases distance across the pyrolysis regions [58, 238].



### ***SURFACE CRACKS***

The surface cracking affects on heat transfer through biomass sample. For example, while the total heat transfer remains the same, heat is transported more quickly to the interior due to the presence of cracks on the sample surface. This causes the changes in the local porosity and permeability, affecting the fluid flow inside. According to Kansa et al [58, 239] the internal heat transfer coefficient had its greatest effect on the fluid temperature at temperatures around 430 °C and pore size (cracks) 1mm in diameter . At temperatures close to 930 °C, and pores become large and radiant transfer through the solid matrix may become more important than thermal conduction [58]

### ***HEMICELLULOSE***

Hemicelluloses are the most reactive major component of biomass decomposing in the temperature range 200 - 260°C [145]. The thermal instability of hemicelluloses is due to their lack of crystallines. Decomposition of hemicellulose under pyrolytic conditions is postulated to occur in two steps [240]. First is the breakdown of the polymer into water soluble fragments followed by conversion to monomeric units, and finally decomposition of these units to volatiles [240]. Compared to cellulose, the charcoal yield from hemicellulose is rather higher, normally in the range of 20-30 wt % [241]. The relatively high charcoal yield may partly be due to salts and minerals in the hemicellulos [241]. Yang et al. [242] found that xylan (main hemicellulose component) started its decomposition easily with the weight loss mainly happened at 220-315 °C and the maximum mass loss rate (0.95 wt % /°C) at 268 °C with 20%wt solid residue. However there is still 20 % solid residue left even at 900 °C [242].

### ***CELLULOSE***

Of the principal components of biomass, cellulose is the most widely studied. This is mainly because it is the major component of most biomass (43%). Cellulose also appears naturally almost in its pure state (e.g., cotton). In addition, it is the least complicated, best defined component of biomass. Cellulose is the major source of

the combustible volatiles that fuel flaming combustion [145]. At a temperature of 120 °C, cellulose becomes thermally unstable but thermal decomposition starts at higher temperatures [26]. The decomposition of cellulose begins at temperature below 300 °C, normally at 280 up to 380°C [180, 242-244]. Decomposition of cellulose is a complex multistage process. A large number of models have been proposed to explain it. The Broido-Shafizadeh model is the best-known and can be applied, at least qualitatively, to most biomass [1, 22]. The model includes an initial step (with high activation energy) during which cellulose initially gives rise to a compound called *active cellulose* that subsequently decomposes according to two concurrent processes giving respectively rise to volatile tars and charcoal [245]. The two competing first-order reactions are:

1. Dehydration - dominates at low temperature ( $\approx 300^\circ\text{C}$ ) and slow heating rates. The following chemical reactions may occur: reduction of molecular weight, the appearance of free radicals, oxidation, dehydration, decarboxylation, and decarbonylation, The products are mainly CO, CO<sub>2</sub>, H<sub>2</sub>O, and a charcoal [1, 145].
2. Depolymerization - dominates at higher temperatures ( $>300^\circ$ ) and at fast heating rates. This phase involves depolymerization and scission, forming vapours including tar and condensable gases [1]. As the temperature is increased from 300°C to 500°C, the amount of tarry products increases while the proportion of charcoal component diminishes [145].

The condensable vapour, if permitted to escape the reactor quickly, can condense as tar. On the other hand, if it is held in contact with biomass within the reactor, it can undergo secondary reactions, cracking the vapour into secondary charcoal, tar, and gases [1]. Stages of degradation of cellulose are simplified presented in Figure 3.7.

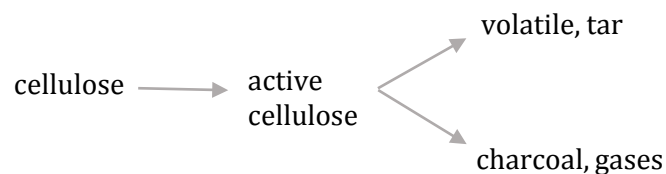


Figure 3.7 Cellulose decomposition [22]

So far, numerous studies based on the cellulose have been carried out. Antal et al [246], investigated in the same thermogravimetric analyzer (TGA) under identical

conditions, samples of pure, ashfree cellulose (i.e., Avicel PH-105, Whatman CF-11, Millipore ash-free filter pulp, and Whatman#42) obtained from different manufacturers undergo pyrolysis at temperatures which differ by as much as 30 °C. The Avicel powder is much less stable than the Whatman#42 filter paper: it pyrolyzes at temperatures 30 °C below the Whatman cellulose at 1 °C/min [246]. Equally disconcerting is the range in charcoal yields: 2-6% at 65°C/min and 7-10% at 1 °C/min [246]. This difference cannot be ascribed to the ash content of the celluloses, since they are all low-ash materials [246]. Evidently, there are “hidden variables” which exert a strong influence on the pyrolysis behavior of cellulose and have not yet been identified [246]. These hidden variables may include the crystallinity and degree of polymerization of the cellulose substrate [246]. Jansen et al., found that the pyrolysis of micro crystalline cellulose at a heating rate of 10 °C/min showed a maximum weight loss rate at 377 °C and it was completely pyrolyzed at 410 °C with a remaining of 4 wt. % of solid charcoal [243]. Also, they found that the presence of inorganic species in the cellulose material alters the rate of decomposition and its final products. When KCl was added to cellulose, increase in charcoal yield was observed of 4.0 to 17.5 %, [243].

### ***LIGNIN***

Lignin is full of aromatic rings with various branches, the activity of the chemical bonds in lignin cover an extremely wide range, which lead to the degradation of lignin occurring in a wide range of temperature and with a lower decomposition rate than cellulose and hemicellulose [180]. Lignin thermally decomposes over a broad temperature range, because various oxygen functional groups from its structure have different thermal stability, their scission occurring at different temperatures [247]. Due to its complex composition and structure, the thermal degradation of lignin is strongly influenced by its nature and moisture content, reaction temperature and degradation atmosphere, heat and mass transfer processes, with considerable effect on conversion and product yields, as well as on the physical properties and quality of the pyrolysis products [247]. Thermal decomposition of lignin occurs in the temperature range 250°C to 500°C, although some physical and/or chemical changes (e.g., depolymerization, loss of some methanol) may occur

at lower temperatures [1, 28]. Lignin is the least reactive component of biomass. Wenzel [1, 248] reported that, at a slow heating rate, lignin loses only about 50% of its weight when the pyrolysis is stopped at 800°C. Jensen et al. [243] investigated structure of lignin using mass spectrometry to determine various lignin pyrolysis products. At temperature of 300 °C, degradation of lignin initially breaks relatively weak aliphatic bonds releasing large fragments of tar. Some of these fragments are relatively reactive free radicals which can undergo a variety of secondary reactions such as cracking and repolymerization. Simultaneously, the various functional groups are decomposed to form low-molecular-weight gaseous species such as CO<sub>2</sub> from carboxyl, H<sub>2</sub>O from hydroxyl, CO from carbonyl, methanol from methoxy and light hydrocarbons from aliphatics [243]. Degradation studies performed on different types of lignin by thermal analysis (DTA) showed an endothermic peak at 100-180 °C, corresponding to the elimination of humidity, followed by two broad exothermal peaks, the first one from 280 to 390 °C and the second one at higher temperatures, with a peak around 420 °C and a long tail beyond 500 °C [249-253]. The DTG curves of lignin decomposition show wide and flat peaks with a gently sloping baseline<sup>26</sup> that makes it impossible to define an activation energy for the reaction [249, 254]. Pyrolysis of lignin typically produces about 55% charcoal, 15% tar, 20% aqueous components (pyroligneous acid (methanol (CH<sub>3</sub>OH), acetone ((CH<sub>3</sub>)<sub>2</sub>CO), acetic acid (CH<sub>3</sub>COOH), water, etc.), and about 12% gases [1, 240]. Thermal decomposition of lignin, compared to the thermal decomposition of cellulose results in 1.5 times higher amount of charcoal and 2 times higher amount of tar [32, 255].

Different studies presented by Caballero et al [256] and Raveendran [241] show that each kind of biomass has unique pyrolysis characteristics, by virtue of the specific proportions of the components present in it. Caballero et al [256] studied the thermal decomposition of two biomass materials (olive stones and almond shells) using dynamic TG at heating rates between 2 and 25°C/min at atmospheric pressure. The TGA analysis results indicate a qualitative relationship between the thermal decomposition of the original biomass and degradation of hemicellulose, cellulose and lignin. Raveendran [241] shown results from thermogravimetric experiments with isolated biomass components as well as synthetic biomass.

Thermogravimetric studies show that each kind of biomass has unique pyrolysis characteristics, by virtue of the specific proportions of the components present in it. Results from this experiments are shown in Tables 3.2 and 3.3.

Table 3.2 Yield of products of the individual components [56]

<b>Components</b>	<b>Charcoal (wt %)</b>	<b>Tar (wt %)</b>	<b>Gas (wt %)</b>
Cellulose	11.10	46.80	43.00
Lignin	41.70	26.80	30.50

Table 3.3 Yield of products samples of synthetic biomass with different ratios of cellulose and lignin [56]

<b>Ratios of Cellulose and Lignin</b>	<b>Charcoal (wt %)</b>	<b>Tar (wt %)</b>	<b>Gas (wt %)</b>
3:1	18.1	40.5	41.3
1:1	29.8	33.1	37.0
1:3	36.1	31.5	32.8

Thermal degradation of cellulose produces minimal yield of charcoal and maximum yield of tar and gas while thermal degradation of lignin alone produces a high yield of charcoal and less of gas and tar. The yields of products depend directly on the initial composition of the mixture. The increase of the cellulose content will decrease the charcoal yield but increase the tar and gas yield. Consequently, cellulose is primarily responsible for the formation of the volatile fraction of the products while lignin mainly contributes to the formation of the solid fraction.

It can be concluded that lignin represents a major source of charcoal, while cellulose and hemicellulose are the main sources of volatiles, gases and tar [152].

At high heating rate decomposition of biomass is carried out at a narrow temperature range. The partial peaks in DTG curves (decomposition of biomass components) are often overlapped which further complicate the analysis of the biomass pyrolysis process. Also, mineral matters catalyse biomass decomposition. Várhegyi et al. [257] showed that the mineral matter present in the biomass samples can highly increase the overlap of the partial peaks in DTG curves.

## CHAPTER 4

*“All models are wrong, but some are useful.”  
George E. P. Box*

### **4. MATHEMATICAL MODELLING OF PYROLYSIS – STATE OF ART**

The development of thermochemical processes for biomass conversion and proper equipment design requires knowledge and good understanding of the chemical and physical mechanisms that are interacting in the thermal degradation process. The upsurge of interest in simulation and optimization of the reactors for thermochemical processes requires appropriate models that help to achieve a better understanding of the governing pyrolysis mechanisms, the determination of the most significant pyrolysis parameters and of their effect on the process and knowledge of the kinetics.

In general the modelling of pyrolysis process can be divided into two groups:

1. Modelling of pyrolysis process of biomass under regimes controlled by chemical kinetics,
2. Modelling of pyrolysis process of biomass under regimes controlled by heat and mass transfer.

This chapter presents the state of the art in modelling chemical and physical processes of biomass pyrolysis. The review includes different mechanisms of kinetic modelling of the biomass pyrolysis process. Numerous models exist for the pyrolysis process, each with their advantages and disadvantages. They range in complexity from simple first-order models to more mathematically complex models incorporating various factors which influence the kinetics of pyrolysis.

Following the trends and challenges found from the analysis of the current approaches, the specific objectives of the thesis are formulated. These models are analysed and compared, and the most suitable model for the pyrolysis of the particular sample is utilized for the purposes of this thesis.

#### **4.1. PYROLYSIS MODELLING OBJECTIVES**

As it is mentioned earlier, pyrolysis consisting of biomass thermal degradation in the absence of oxidizing agents, is a possible thermochemical conversion route, resulting in the production of a huge number of chemical compounds. However, for engineering applications, reaction products are often lumped into three groups: permanent gases, a tar and charcoal, or simply into volatiles and charcoal [160]. Reaction products result from both primary decomposition of the solid fuel and secondary reactions of volatile condensable organic products into low-molecular weight gases and charcoal, as they are transported through the particle and the reaction environment [160]. The proportions of the product yields depend on process parameters which also has impact on the mechanism and kinetics of pyrolytic reactions. The most significant parameters in biomass pyrolysis are temperature, pressure, solid and volatile residence time, particle size, biomass composition and heating conditions. Increasing the temperature and the solid residence time favours the formation of volatile and gaseous products [160]. As the particle size increases, the time necessary to achieve a certain conversion level at a certain temperature also increases. The volatile residence time may influence the process, as the volatile products may produce secondary interactions with the hot charcoal which acts as a catalyst [67-69, 160]. Under pressure, tarry vapours have a smaller specific volume, so that their intraparticle residence time is prolonged, favouring their decomposition, as they escape the biomass particle [74, 160]. Also the concentration (partial pressure) of tarry vapours is higher, thus increasing the decomposition reaction rate. Changes in heating conditions may modify the actual pathway and the rate of the reactions and affect the pyrolysis yields. Also, the biomass components react independently and, therefore the thermal behaviour of biomass is also reflected by the individual behaviour of the biomass components. Each kind of biomass has unique pyrolysis characteristics, by virtue of the specific proportions of the components present in it. Even the same chemical species may have differing reactivity if their pyrolysis is influenced by other species in their vicinity (chemical composition, ash content and composition, particle size and shape, density, moisture content, etc.) and/or by different process parameters.

In spite of the great number (several hundred) of published papers, no consensus is presently reached in the literature. A great portion of publications have presented contradictory

results, which induced a great deal of pessimism about the applicability of reaction kinetics for the evaluation of biomass pyrolysis [258]. The cause of the problem must be searched mainly in the application of oversimplified kinetic equations for processes composed from several chemical, physical, and physicochemical subprocesses [258]. Careless experimental work (e.g. kinetic parameters may vary according to the laboratory device, difficulties in measuring the actual biomass reaction temperature) and poor mathematical evaluation techniques have also contributed to the wrong performance of the reaction kinetics in this field [258].

What should we expect from a good kinetic model? The answer of this question depends obviously on the interest of the investigator and on the properties of the studied samples [21]. The objectives of a mathematical pyrolysis model should include:

1. The development of a diagnostic tool in order to define the behaviour of the samples in a wide range of experimental conditions (particle size, heat of pyrolysis (reaction) and thermal properties of the feedstock and products) and to reveal similarities and differences between different biomass samples [16, 21]
2. The prediction of the behaviour outside the domain of the given set of observations, in order to aid optimization of the pyrolysis process [16, 21]
3. The development and establishment of better reactor design techniques in order to specify reactor type and size [16].

Biomass pyrolysis involves numerous extremely complex reactions and end up with large number of intermediates and end products, devising an exact reaction mechanism and kinetic modelling for biomass pyrolysis is extremely difficult, hence, pyrolysis models are modelled on the basis of visible kinetics [259]. From a theoretical point of view, an endless variety and complexity of reactions forming a network can be assumed in biomass pyrolysis. Hence even today it is difficult to develop a precise kinetic model taking into account all the parameters concerned.

The assumption, that biomass decompose through primary and secondary reactions and assumption of a distribution on the reactivity of the biomass components, frequently helps in the kinetic evaluation of the pyrolysis of complex organic samples. Mathematical model can be identified and validated by experimental, theoretical and by both experimental and theoretical data.



## **4.2. PYROLYSIS KINETIC MODELING**

A large variety of experimental techniques have been adopted for the study of pyrolysis process. The most frequently applied techniques used to study biomass pyrolysis are: thermogravimetric analysis (TGA), [3, 21, 38, 57, 67, 72, 80, 202, 225, 246, 250, 254, 257, 258, 260-271], differential thermal analysis (DTA) and differential scanning calorimeter (DSC) [3, 74, 80, 204, 266, 272].

Degradation kinetics of biomass can be studied in either dynamic or static conditions [273, 274]. Static conditions are achieved by maintaining the selected constant temperatures in the pyrolyzing reactor [273]. During dynamic conditions, biomass particles submitted in pyrolyzing reactor experience an increase in temperature with time according to an assigned heating rate [273]. In the static analysis, tests are carried out according to two different methodologies to attain the isothermal stage; in the first methodology, the small dynamic stage consists of very slow heating rates to avoid spatial gradients of temperature, while in the second methodology very fast, external, heat transfer rates to keep short the first dynamic stage are used [273]. However, in the first case, the weight loss is not negligible during heating and the subsequent interpretation of the data may be lacking an important part of the whole process, while in the second case, the results may be seriously affected by heat transfer limitations; unless an accurate control of the sample temperature is accomplished [273]. Static TGA cannot be used for studies over 600°C [274]. In the dynamic analysis, the biomass weight is continuously recorded as a function of the temperature attained by the sample with the reactor temperature rising steadily at a linear rate; or static, in which case the biomass sample weight is recorded as a function of time while the reactor temperature remains constant [261, 272, 275, 276]. The study of biomass pyrolysis using a dynamic temperature technique has several advantages over the isothermal method [274]:

1. Kinetic data (weight vs time) over a broad temperature range can be obtained in only a few minutes,
2. The problem of decomposition before reaching the desired test temperature is not encountered in the dynamic method since the test may be initiated well below the incipient decomposition temperature,
3. Different heating rates may be studied.

Thermogravimetric curves (TGA and DTG<sup>15</sup>), measured for dynamic or isothermal conditions are source of information for the formulation of different kinetic mechanisms for description of thermal decomposition of biomass. Many kinetic models for wood pyrolysis have been reported in the literature; a good review is given by Di Blasi [160], Grønli [3], Гверо [26], Diaz [80], Antal et al [246], Várhegyi et al [21, 250, 269], etc. The kinetic models make use of an Arrhenius dependence on temperature, (equation (3.1)), thus introducing the parameters activation energy ( $E$ ) and pre-exponential factor ( $A$ ), and a linear or power law dependence on the component mass fraction, which may lead to additional parameters (the exponents) [160].

The numerous pyrolysis models can be divided into two principal categories:

1. *Modeling of primary pyrolysis*

1.1. *Single reaction kinetic model (one step kinetic model)*. This model is simplified description of primary decomposition processes, usually adopted for isothermal conditions or fast heating rates. This models considers pyrolysis as a single step first order reaction. The usefulness of single-step global models, however, is limited by the assumption of a fixed mass ratio between pyrolysis products (i.e., volatiles and charcoals), which prevents the forecasting of product yields based on process conditions [160, 277, 278],

1.2. *Multiple step kinetic models*. This reaction mechanisms are also proposed where each reaction takes into account the dynamics of several zones or pseudo-components in the measured curves of weight loss [160]. The majority of multi-component mechanisms simply consist of devolatilization reactions, which can be applied to predict only the rate of weight loss, provided that the total amount of matter to be released in the gas/vapour phase is already known (assigned or measured) [160],

2. *Modeling of Primarily and Secondary Pyrolysis*

2.1. *Semi - global models*. This model considers pyrolysis to be a two stage reaction, in which the products of the first stage break up further in the presence of each other to produce secondary pyrolysis products [273]. This technique is a suitable tool for correlating and evaluating kinetic data from different biomass types under similar reaction conditions,

---

<sup>15</sup> DTG - Derivative Thermogravimetric

but it is ill-suited for comparisons of thermal decomposition data obtained from dissimilar reaction conditions [278, 279].

2.2. *distributed activation energy model (DAEM)*. This model assumes that the thermal decomposition of numerous components is described by a distribution of activation energies. The DAEM is a powerful tool for the determination of the kinetic properties of a biomass. It allows the identification of different degradation steps and also the determination of the activation energies of these steps. It is possible to use the kinetic data obtained to recalculate the weight loss for any temperature profile.

The Arrhenius law, Biot number and Pyrolysis number are important parts of these models [280].

### **ARRHENIUS LAW**

In chemistry the Arrhenius law commonly is used to describe a reaction. Therefore most pyrolysis models use this Arrhenius law to model the reaction as well [280]. The Arrhenius law is given by equation [280]:

$$k(T) = A \exp\left(-\frac{E}{RT}\right) \quad (4.1)$$

Where  $k$  is the temperature dependent reaction rate constant,  $A$  is the frequency factor (pre-exponential factor),  $R$  (8.314 J/Kmol) is the universal gas constant,  $E$  (kJ/mol) is the activation energy of the reaction,  $T$  (K) is the temperature.

### **BIOT AND PYROLYSIS NUMBER**

Depending on the particles size of the fuel different pyrolysis models are to be used. The difference is a thermally thin regime or a thermally thick regime and this is controlled by the ratio of external heat transfer to the internal heat transfer coefficient, [280]. The dimensionless ratio of convection and conduction coefficient is called the Biot number [280]:

$$Bi = \frac{hL}{\lambda} \quad (4.2)$$

Where  $h$  (W/m<sup>2</sup>K) is the coefficient of conduction,  $\lambda$  (W/m<sup>2</sup>K) is the coefficient of convection. The particle characteristic length  $L$  (m) is:

$$L = \frac{V}{A} \quad (4.3)$$

Where  $V$  ( $m^3$ ) is the particle volume and  $A$  ( $m^2$ ) is surface area of the particle.

In case of thermally thick samples effective temperature gradient within the solid during the thermal stage will occur. This temperature gradient will cause a deviation between the temperature of the different particles in the sample [280]. This will also influence the measured temperature at the thermocouple (measured temperature and temperature of the sample are different). In a thermally thin particle ( $Bi \ll 1$ ) the heat transfer to the surface of the particle is faster than the heat flow into the particle. In this case there will be a temperature gradient across the particle and the drying and pyrolysis will take place simultaneously [281].

#### **INTERNAL AND EXTERNAL PYROLYSIS NUMBER**

The Internal Pyrolysis number gives a measure of the internal conduction and the reaction time constant [280]:

$$Py = \frac{\lambda}{k\rho cpL^2} \quad (4.4)$$

$$1/k = \tau - \text{reaction time}$$

Where  $\rho$  ( $kg/m^3$ ) is the bulk density,  $cp$  ( $kJ/kgK$ ) is the specific heat capacity of a sample.

The External Pyrolysis number is the product Biot and Internal Pyrolysis number [280]:

$$Py^I = BiPy \quad (4.5)$$

$$Py^I = \frac{h}{k\rho cpL} \quad (4.6)$$

In case of small samples, the Biot number is small and the Pyrolysis number is high, and the reaction rate is controlled by kinetics. Typical values for corn cob are shown in Table 4.1.

Table 4.1 Values of the corn cob parameters

Parameter	Symbol	Value	Ref.
Coefficient of convection	$\lambda$ (W/mK)	$\approx 0.13$	[280]
Bulk density	$\rho$ (kg/m <sup>3</sup> )	282.38	[93]
Specific heat capacity	$cp$ (kJ/kgK)	$\approx 1.67$	[280]
Coefficient of conduction	$h$ (W/m <sup>2</sup> °C)	$\approx 8.4$	[280]

## 4.3 MODELING OF PRIMARY PYROLYSIS

### 4.3.1. ONE STEP MODEL

The biomass weight loss curves, obtained under dynamic or isothermal conditions, present different reaction zones mainly corresponding to component decomposition, which tend to merge as the heating conditions become more severe. For example, for heating rates at sufficiently slow or moderate temperatures, several zones appear in the weight loss curves, which can be associated with component dynamics. As the heating rate is increased, given that the range of the degradation temperatures of components is relatively narrow, the different peaks in the degradation rate tend to merge and the characteristic process temperatures tend to become progressively higher [160]. Furthermore, if temperatures are sufficiently high, significant degradation rates are simultaneously attained by all the components.

One step models were used during the initial stages of the modelling of pyrolysis process. These one-step models decompose the organic fuel into volatiles and a fixed charcoal yield [160]. These models consider pyrolysis as a single step first order reaction, where the rate of mass loss depends on mass and temperature according to the following equation [3]:

$$k(T) = A \exp\left(-\frac{E}{RT}\right) \quad (4.7)$$

This model is adopted for isothermal conditions or fast heating rates [26].

The one step model is used to predict the overall rate of devolatilization from the biomass sample (i.e. mass loss). This mechanism does not separately predict the production of

condensable and gas from volatile products. The dependence of product yields on reaction conditions cannot be predicted, as a constant ratio between volatiles and charcoal is assumed.

The composition, and rate of formation of the products are highly dependent on the employed biomass composition and pyrolytic condition. Since dry biomass fuels typically consist of about 50% cellulose by weight, the study on pyrolysis of cellulose would be particularly beneficial for achieving the better understanding of the pyrolytic mechanism of biomass and facilitating its direct applications in terms of fuels, chemicals and bio-materials. Regarding to this, cellulose is the most widely studied substance in the field of wood and biomass pyrolysis. Pyrolysis of cellulose proceeds by alternative pathways involving a variety of reactions which provide different products, [282]. The kinetics of these reactions are highly dependent on the experimental conditions, [282].

Historically, it was perhaps that Broido's group firstly called attention to the intriguing phenomena of cellulose pyrolysis and proposed the established kinetic scheme in 1960s [23, 24, 269, 282]. Only the virgin cellulose and the end products are taken into account. As described Figure 4.1, the decomposition of cellulose can be represented through two competing reactions: the first step is estimated to be important at low temperatures and slow heating rates, accounting for the slight endothermic formation of anhydrocellulose below 280 °C [24, 283]. At about 280 °C a competitive, more endothermic unzipping reaction is initiated for the remained cellulose, leading to the tar formation [283]. The third step presents the exothermic decomposition of anhydrocellulose to charcoal and gas.

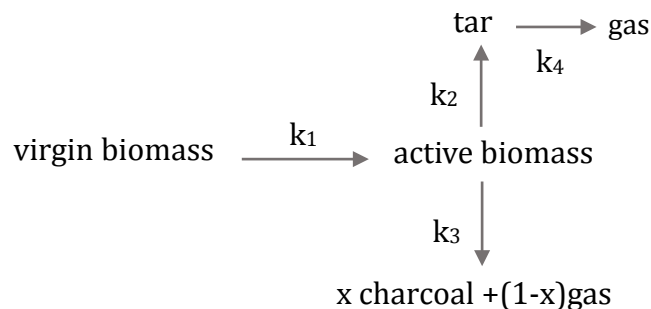


Figure 4.1 The kinetic model for cellulose pyrolysis proposed by Broido and Weinstein [23]

It is worthily noting that the formation of the anhydrocellulose as an intermediate product is undetectable in the experiments, and no kinetic data for the charcoal forming reaction are reported in the above publications [283]. Broido and Nelson examined the effect of thermal pretreatments at 230-275 °C on the cellulose charcoal yields varying from 13% (no thermal pretreatment) to over 27% [254]. They employed the large samples of cellulose (100 mg of shredded cellulose, and 7 cm × 3 cm sheets, individually wrapped several layers deep around a glass rod), which might incur the charcoal formation from solid - vapour interactions during the prolonged thermal pretreatment. Broido and Nelson used these results to rationalize the competitive reaction model for cellulose pyrolysis displayed in Figure 4.2

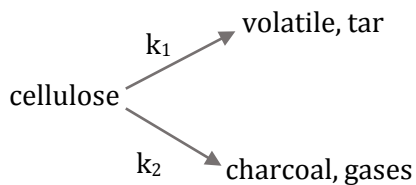


Figure 4.2 Broido–Nelson (1975) model for cellulose pyrolysis [24]

Below approximately 250 °C, the formation of charcoal and permanent gas is assumed to be favoured while above 280 °C, it is the formation of tar, which is favoured, because of the predominant depolymerisation reactions associated to the breakage of glycosidic bonds. Subsequent researchers and reviewers alike (for example Antal [64, 143, 254]) overlooked the fact that Broido and Nelson employed large samples of cellulose (100 mg of shredded cellulose, and 7 cm x 3 cm sheets, individually wrapped several layers deep around a glass rod), that could have incurred charcoal formation from vapour - solid interaction during the prolonged thermal pretreatment. This mechanism did not differentiate between charcoal and gaseous compounds, it was later modified by Bradbury et al [22, 265]. Three years after Broido published his work, Shafizadeh's laboratory undertook a kinetic study of cellulose pyrolysis in vacuum by batchwise heating of 250 mg samples of cellulose at temperatures ranging between 259 and 407°C [22, 265]. A numerical integration of the ordinary differential equations resulting from the model given in Figure 4.3 was able to fit their weight loss data. Bradbury stated that the cellulose had to enter an activated state before reacting.

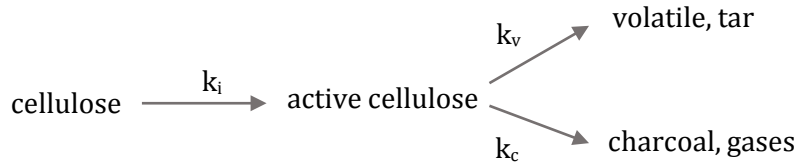


Figure 4.3 Broido-Shafizadeh model (1979) [22]

According to this model (titled as Broido-Shafizadeh model), at the low temperatures (259-295 °C), the initiation period (characterized by an accelerating rate of weight loss) has been explained as a formation of “active cellulose” through the depolymerization process [283]. Then, the active cellulose easily degraded into tar, charcoal and gases through three single step reactions. They also speculated the secondary charcoal formation from the re-polymerization of components of tar; however could not provide evidence based on the thermogravimetric data [172]. The rate of mass loss depends on mass and temperature according to the following equation [284]:

$$k_i = A_i \exp\left(-\frac{E}{RT}\right) \quad (4.8)$$

Where  $i$  represents pyrolysis products: volatile, charcoal, gases

The argument between Antal and Várhegyi [250, 268, 269] and Broido-Shafezadeh [23] is remarkable, concerning the existence of “active cellulose” during the pyrolysis of cellulose. Antal and Várhegyi, performed thermogravimetric analyses of Avicel cellulose involving prolonged thermal pretreatments of small samples (0.5-3 mg). The weight loss curves were simulated by modern numerical techniques using the Broido-Safizadeh and other related models. Results were not consistent with the presence of an initiation reaction, but they did strongly confirm the role of parallel reactions in the decomposition chemistry [57]. In other words this model is partially true, this step (initiation reaction) proceeded at an immeasurably high rate at conditions of interests, or it does not exist [217].

The mechanisms of global decomposition describe the thermal degradation by means of an irreversible and single step reaction to predict the overall rate of volatiles release (i.e., mass loss), but without separately predict the production of condensable and gas from volatile



product, (see equation 4.9) [254]. The corresponding experimental studies have been mostly carried out with small particles, employing thermogravimetric systems.

$$\frac{d\alpha}{dt} = A \exp\left(-\frac{E}{RT}\right) (1 - \alpha)^n \quad (4.9)$$

Where  $n$  the reaction order.

Most of the work done in this field has been reviewed by Antal and Várhegyi [246, 254, 269, 285]. From diverse thermogravimetric studies they established that the primary pyrolysis of a small, homogeneous sample of pure<sup>16</sup> cellulose at low to moderate heating rates, was an endothermic process, modelled reasonably well by a simple first-order reaction, under conditions which minimize vapour-solid interactions and heat transfer intrusions.

In spite of the great number (several hundred) of published papers, no consensus is presently reached in the literature. A great portion of publications have presented contradictory results. The cause of the problem must be searched mainly in the potential role of different sample characteristics employed (size and wood variety), the mathematical treatment of the experimental data. To specify the serious trouble that supposes those experimental errors, Grønli et al. [268] coordinated the realization of a round-robin kinetic study for the cellulose pyrolysis (Avicel PH-105) in eight European laboratories. Results confirmed the theories of Antal et al. [285] and evidenced the potential role of varied systematic errors in temperature measurement among the various thermobalances used by researchers.

Single-step global models have provided reasonable agreement with experimentally observed kinetic behaviour [279, 286, 287]. The pyrolysis of many different cellulosic substrates can be adequately described by an irreversible, single-step endothermic reaction that follows a first order rate law. The usefulness of single-step global models, however, is limited by the assumption of a fixed mass ratio between pyrolysis products (i.e. volatiles and charcoals), which prevents the forecasting of product yields based on process conditions, [278, 288]. The assumption of one component behaviour for composite fuels, such as biomass, unavoidably produces inaccuracies in the details of the decomposition rates (and conversion time). Most pyrolysis systems the kinetic pathways are simply too complex to yield a meaningful global apparent activation energy [278, 287].

---

<sup>16</sup> Pure cellulose - cellulose free from inorganic contaminants (ash free), with a well-defined degree of polymerization and crystallinity

The kinetics of biomass decomposition is routinely predicated on a single reaction [278, 289, 290]. Biomass materials composed predominantly of holocellulose, lignin, extractives and inorganic components. The reaction rates, products, and other thermal behaviour of biomass pyrolysis are considered a combination of the behaviour of its main components. The thermal degradation of each component occurs at different temperature by different pathways. The basic knowledge of the role and behaviour of the three principal components of biomass (cellulose, hemicelluloses and lignin) during pyrolysis is important for understanding and controlling this process. Several studies [80, 291, 292] suggest that primary decomposition rates of biomass can be modelled taking into account the thermal behaviour of the main components and their relative contribution in the chemical composition.

The pyrolysis of wood and related biomass substances is frequently described by a single reaction [3]:

$$\frac{d\alpha}{dt} = k(T)f(\alpha) \quad (4.10)$$

The variation of the temperature-dependent reaction rate constant is approximated by the Arrhenius rate expression [3]:

$$k(T) = A \exp\left(-\frac{E}{RT}\right) \quad (4.11)$$

It should be noted that every kinetic model proposed employs a rate law that obeys the fundamental Arrhenius rate expression.

The function  $f(\alpha)$  is approximated by [3]:

$$f(\alpha) = (1 - \alpha)^n \quad (4.12)$$

Where  $(1 - \alpha)$  is the remaining fraction of volatile material in the sample and  $n$  is the reaction rate.

If the original mass is  $m_o$ , the final mass after reaction has finished (relatively charcoal rate) is  $m_f$  and the mass at any time is  $m$ , than a fraction reacted (conversion fraction)  $\alpha$  is defined as:

$$\alpha = \frac{m_o - m}{m_o - m_f} = \frac{v}{v_f} \quad (4.13)$$

Where  $v$  is the mass of volatiles present at any time  $t$ , and  $v_f$  is the total mass of volatiles evolved during the reaction.

From equations 4.8, 4.9 and 4.10, the following equation can be written:

$$\frac{d\alpha}{dt} = A \exp\left(-\frac{E}{RT}\right) (1 - \alpha)^n \quad (4.14)$$

For the determination of the kinetic parameters ( $E$ ,  $A$ ,  $n$ ), in literature can be find several methods.

### ***KINETIC EVALUATION METHODS***

When the kinetic evaluation methods are classified based on the form of experimental data, they are grouped into [34]: integral, differential and special methods.

#### ***Differential Method***

The devolatilization dynamics of biomass pyrolysis are frequently expressed as a first order decomposition process [278]. Assuming a first order reaction, equation 4.12 can be written [3]:

$$\frac{d\alpha}{dt} = A \exp\left(-\frac{E}{RT}\right) (1 - \alpha) \quad (4.15)$$

Dynamic thermogravimetry is often carried out at constant heating rate [3]:

$$T = T_o + \beta t \rightarrow \beta = \frac{dT}{dt} \quad (4.16)$$

When the natural logarithm of equation (3.13) is taken and the resulting equation is rearranged, one obtains the traditional and often applied differential method [3]:

$$\ln \left[ \frac{d\alpha/dt}{(1 - \alpha)} \right] = \ln A - \frac{E}{RT} \quad (4.17)$$

By using experimental values for  $\alpha$  and  $d\alpha/dt$  as a function of temperature, a plot of  $\ln[(d\alpha/dt)/(1 - \alpha)]$  versus  $1/T$  should ideally give straight line with a slope of  $(-E/R)$ , with an intercept of  $\ln A$ , Figure 4.4.

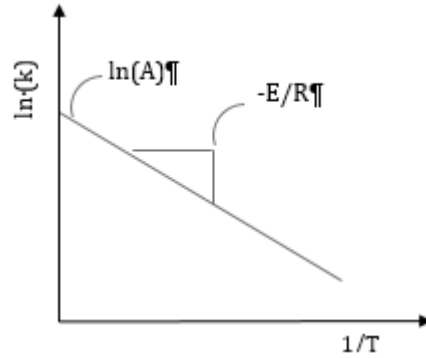


Figure 4.4 Arrhenius's plot

### ***Integral Method***

Integrating equation 4.15:

$$\int_0^\alpha \frac{d\alpha}{(1-\alpha)} = \frac{A}{\beta} \int_{T_0}^T \exp(-E/RT) dT \quad (4.18)$$

On the right side of the equation (3.16) temperature containing integral has no exact solution [3]. For solution of temperature containing integral, in the literature, several expansions and semi-empirical approximations have been suggested.

Table 4.2 [3] gives a survey of kinetic data for different biomass species where a single step reaction model have been used. The activation energy (Table 4.2), ranges from 83 to 260 kJ/mol for cellulose, from 125 to 260 kJ/mol for hemicellulose, from 37 to 125 kJ/mol for lignin and from 60 to 235 kJ/mol for wood. The reason for this diversity may be attributed to different experimental conditions, e.g.: sample size, measurement temperature, heating rate and atmosphere [3]. Also the reason for this differences, can be caused by different extraction procedures and to lack of accuracy caused by the approximations used in the different computational methods [3].

### ***Special Method***

Special methods are generally based on particular couples of experimental data, e.g. data from different heating rates, or data evaluated from graphical plots [3]. The special methods give worst accuracy.

Today, with developed software and computers, there is no need for simplifying approximations, if  $\alpha$  and  $d\alpha/dt$  is known (results from TGA experiments), the kinetic parameters ( $E, A, n$ ) can be calculated by non – linear curve fitting of equation (3.12) [3].

The dependence of product yields on reaction conditions cannot be predicted, as a constant ratio between volatiles and charcoal is assumed. The global decomposition is used to predict the overall rate of devolatilization (volatiles release) from the biomass sample (i.e. mass loss). This mechanism does not separately predict the production of condensable and gas from volatile products. The corresponding experimental studies have been mostly carried out with small particles, employing thermogravimetric systems.

#### 4.3.2. MULTI – STEP REACTION KINETIC MODEL

It is basically and essentially important to study the pyrolysis characteristics of whole biomass, including all three main biomass components (cellulose, hemicellulose and lignin) for a better understanding of biomass thermal chemical conversion. The proposed multi-step reaction kinetic model assume that each individual component of virgin biomass (cellulose, hemicellulose, and lignin) decomposes directly to each reaction product  $i$ , except tar, by a single independent reaction, Figure 4.5 [3, 26, 279, 288].



Figure 4.5 Scheme of Semi-global Pyrolysis Model [25]

The kinetics can be modeled through a unimolecular first-order reaction:

$$\frac{dV_i}{dt} = A_i \exp\left(-\frac{E_i}{RT}\right) / (V_i^* - V_i) \quad (4.19)$$

Where  $V_i$  is the yield of the product  $i$ ,  $V_i^*$  is ultimate attainable yield of the species  $I$  (the yield at high temperatures for long residence times).

Theoretical curves, obtained by best fit values of kinetic parameters, correlate well with experimental measurements [25]. However, since at high temperatures and long residence times secondary reactions effects are not negligible, the values of the kinetic parameters are valid only for correlating experimental data under the operative conditions from which they

were derived and not representative of the true physicochemical processes governing the degradation of solid [25]. The rigorous kinetic model should include multi-step reactions for both the primary and the secondary stage of the degradation.

Table 4.2 A survey of kinetic data for Biomass Pyrolysis [3]

Experiment condition					Kinetic parameters			Ref.
Apertures	Heating rate	Temperature (°C)	Aatmosphere	Biomass feedstock	n	log A (logs <sup>-1</sup> )	E (kJ/mol)	
TGA and DTA	0.23 – 5 °C/min	250 – 330	N <sub>2</sub> (vacuum)	cellulose	1	15	224	Akita and Kase [11][3]
		280 – 325		pine	1	5.5	96.3	
		325 - 350			1	16.8	226.1	
TGA	3°C/min	240-308	(vacuum)	cellulose	1	9.8	146.5	Tang [77] [3]
		308 - 360			1	17.6	234.5	
		280 - 344		lignin	1	5.2	87.9	
		344 - 435			1	-0.03	37.7	
Heated Grid	400 – 1000°C/s	250 - 1000	He	cellulose	1	9.8	139.8	Lewellen et al [78][3]
TGA	7°C/min	284 - 337	N <sub>2</sub>	cellulose	1	18.6	248	Fairbridge et al [75][3]
		290 - 360	air		1	27.5	343	
TGA	1-5 °C /min	200-400	N <sub>2</sub>	Filter paper Whatman	0.5	11.3	153.2	Rogers et al [79][3]
TGA	10°C /min	220-460	N <sub>2</sub>	spruce	1	5.8	98.4	Lee [80][3]
	160°C/min				1	5.5	86.3	
	10°C /min				redwood	1	2.8	

Experiment condition					Kinetic parameters			Ref.
Apertures	Heating rate	Temperature (°C)	Aatmosphere	Biomass feedstock	n	log A (logs <sup>-1</sup> )	E (kJ/mol)	
	160°C/min				1	3.2	58.6	
TGA	1°C/ min	200-600	He	cellulose	1.13	16.6	213	Cooley et al [81] [3]
	2°C/ min				0.99	16.8	216.3	
	5°C/ min				1.02	17.5	225.5	
TGA	10°C/min	200-400	Ar	cellulose	1	17.6	234	Várhegyi et al [42] [3]
	80°C/min				1	15.1	205	
TGA	5°C/ min	230-360	He	pine	1	4.7	87.6	Grønli et al [82] [3]
		220-400		spruce	1	7.2	92.4	
TGA	5-100°C/min, (dynamic heating)	100-850	He	almond shell	1		92.9	Balci et al [83]
	1.210 <sup>6</sup> °C/min, (stationar heating)	100-900		almond shell	1		99.7	
	20°C/min, (dynamic heating)	100-800		almond shell	1		92.4	
	10°C/min, (dynamic heating)	100-500		almond shell	1		77.6 – 123.3	
	120°C/min, (dynamic heating)	150-625		almond shell	1		89.8 – 128.6	



## **4.4. MODELING OF PRIMARY AND SECONDARY PYROLYSIS**

### **4.4.1. SEMI - GLOBAL KINETIC MODELS**

The semi-global models, is used to describe primary and secondary solid degradation by means of experimentally measured rates of weight loss. Though one step models can predict the characteristic time of the pyrolysis process, for the formulation of engineering models with a view of reactor optimization and design, semi-global mechanisms appear to be more promising, because competitive chemical pathways are described, which allow product distribution to be predicted on dependence of reaction conditions [277]. The degradation of the three main biomass components is described through a kinetic mechanism, which deviates from the original Broido – Shafizadeh mechanism for the introduction of a linked tar and gas formation [277]. Then the degradation rate of biomass is considered as the sum of the contribution of its main components, cellulose, hemicelluloses and lignin [277]. The extrapolation of the thermal behaviour of main biomass components to describe the kinetics of complex fuels is however, only a rough approximation because it has not been possible to establish exact correlations [277, 293]. This is probably due to: the presence of inorganic matter in the biomass structure, which acts as a catalyst or an inhibitor for the degradation of cellulose, purity and physical properties of cellulose, which play an important role in the degradation process, noticeable differences in the hemicellulose and lignin, depending on the biomass type [277]. In addition, as it is impossible to isolate biomass components without affecting to varying extents their chemistry and structure, differences can be expected in the degradation mechanisms on dependence of the separation technique [277].

As well as for cellulose, wide interest in the primary pyrolysis of whole biomass has appeared in the literature (the pyrolysis of hemicelluloses and lignin). Várhegyi et al. [257, 294], performed several thermogravimetric experiments using: Avicel cellulose, 4-methyl-Pglucurono-D-xylan (hemicellulose) and sugar cane bagasse, in the presence and absence of catalysts (inorganic salts). The three major DTG peaks were observed during the experiments resulted from decomposition of cellulose, hemicellulose, and lignin (main constituents of lignocellulosic materials). Thermogravimetric analysis showed a distinct DTG peak resulting from the decomposition of cellulose, than a lower DTG peak at lower temperature range resulting from hemicellulose pyrolysis, and an attenuated

shoulder that can be attributed to lignin decomposition. Várhegyi et al. [257], showed that the mineral matter present in the biomass samples can highly increase the overlap of the partial peaks in DTG curves. Sometimes the first peaks merge into one very broad peak [80]. Várhegyi et al. [257, 263, 294], showed that pretreatments have influence on pyrolysis behaviour of lignocellulose materials. Thermal pretreatment destroys the hemicellulose component of the lignocellulose material but doesn't enhance the charcoal yield. Várhegyi, Grønli et al. [263], evidenced the ability of pretreatments to separate merged peaks, to displace reaction zones toward higher temperatures, decrease the charcoal yield and increase peak reaction rates [263, 291]. The water washing, as one of pretreatments type, is preferred because it results in less hydrolysis and solubilisation of the holocellulose [80]. Also the acid washes appeared to decrease the measured activation energy of cellulose pyrolysis [80].

As it is said, generally, from the thermogravimetric analysis (observing DTG curve) can be seen that temperature domains of moisture evolution and hemicellulose, cellulose and lignin decomposition more or less overlap each other. Considering this and also the results from experiments with biomass different pretreatments, it can be concluded that general biomass pyrolysis behaves as a superposition of the independent kinetics of the primary components (hemicellulose, cellulose, and lignin). The inability to predict the kinetic behaviour of biomass under different process conditions has encouraged researchers for developing complex multi-component models. It assumes that the true reaction system is too complex to be characterized in any fundamental way, so the reaction is described in terms of pseudo species, which are themselves complex materials or mixtures [292]. Absolute concentration is not important, as all species are characterized in terms of the fraction of their initial or final value [292].

The basic building block for all reactions is a pseudocomponent reaction [292]:

$$-\frac{dx}{dt} = \frac{\sum a_i dy_i}{dt} = kf(x) \quad (4.20)$$

where  $x$  is the fraction of the initial material *unreacted*,  $f(x)$  is a mathematical function of the unreacted initial material,  $y_i$  is the  $i$ th product of the reaction, and  $\sum a_i = 1$ .

The simplest case is that of a pseudo-first-order reaction, for which  $f(x) = x$ . Other more complex functions will be discussed later. The  $y_i$  values represent, for example, a partitioning into gaseous, liquid, and solid products. The pseudocomponents reactions can be presents as [292]:

$$-\frac{dx}{dt} = \frac{\sum_i \sum_j \frac{a_{ij} dy_{ij}}{dt}}{dt} = \sum a_j k_j f(x_j) \quad (4.21)$$

where  $j$  represents the  $j$ th component of  $x$ ,  $\sum a_j x_j = x$ ,  $y_{ij}$  is the  $i$ th product of reaction component  $j$ ,  $\sum_i \sum_j a_{ij} = 1$ , and  $\sum_i a_{ij} = a_j$ .

According to Di Blasi [26], there are two different approaches in pyrolysis of biomass modeling.

*The first approach* assumes that the biomass is composed of three chemical components, (hemicellulose, cellulose and lignin), which react independently and, therefore, the thermal behaviour of biomass is also reflected by the individual behaviour of the biomass components, Figure 4.6. Each kind of biomass has unique specific proportions of the components present in it.

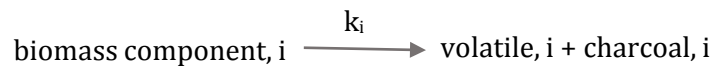


Figure 4.6 One - step semi global model [26]

Thurner and Mann [26, 27], investigated the kinetics of wood (oak sawdust) pyrolysis into gas, tar, and charcoal, to determine the reaction rate parameters, and to identify the composition of the pyrolysis products. It has been found that, in the range investigated, wood decomposition into gas, tar, and charcoal can be described by three parallel first-order reactions as suggested by Broido-Shafizadeh. They proposed the model which is an upgrade of the Broido-Shafizadeh model, Figure 4.7.

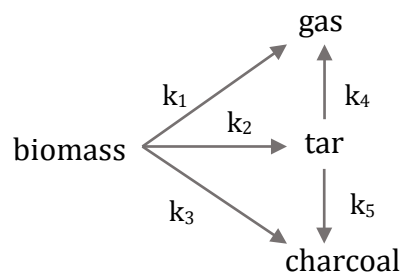


Figure 4.7 Biomass kinetic reaction scheme Thurner and Mann [26, 27]

According to the model, wood is pyrolyzed into gas, tar, and charcoal according to three parallel reactions (reaction  $k_1, k_2, k_3$ ), called primary reactions, and the tar decomposes into gas and charcoal according to two parallel reactions (reaction  $k_4, k_5$ ), called secondary reactions [27]. Each product in Figure 3.10 represents a sum of numerous

components which are lumped together to simplify the analysis. The composition of each product, especially the distribution between the gas and the tar, depends, among other things, on the conditions under which the products are collected [27]. In principle, the reaction rate constants of these five reactions can be determined by measuring the amount of each product as a function of time. When the tar is removed from the reaction zone the secondary reactions are avoided and the reaction rate constants of the primary reactions can be determined directly from these measurements [27]. Table 4.3 presents evaluated kinetic parameters.

Table 4.3 Kinetic parameters used by Thurner and Mann [26, 27]

<b>reaction rate constant</b> [s <sup>-1</sup> ]	<b>A</b> (s <sup>-1</sup> )	<b>E</b> (kJ/mol)
k <sub>1</sub>	1.43·10 <sup>4</sup>	88.6
k <sub>2</sub>	4.12·10 <sup>6</sup>	112.7
k <sub>3</sub>	7.37·10 <sup>5</sup>	106.5

Koufopoulos et al [28] attempted to correlate the pyrolysis rate of the biomass with its composition. Koufopoulos et al [28], proposed kinetic model based on experimental results performed experiment of pyrolysis of fine particles of lignocellulosic materials (below 1 mm) in size. In this case, the possible effects of heat and mass transfer phenomena are drastically decreased and the process is controlled by kinetics. The good fit of the kinetic model to experimental data obtained under different heating conditions and over a wide temperature range suggests that the pyrolysis rate of fine particles can be interpreted in terms of pyrolysis temperature and solid residence time [28]. This model is presented in Figure 4.8. This model uses an intermediate step (initial reaction k<sub>1</sub>) to get an activated sample. This initial reaction (k<sub>1</sub>) describes the overall results of the reactions prevailing at lower pyrolysis temperatures (below 473 K) [259]. This first step is considered to be of zero-order and is not associated with any weight loss. The intermediate formed further decomposes through two competitive reactions, to charcoal (reaction k<sub>3</sub>) and to gaseous/volatile products (reaction k<sub>2</sub>) [259]. This model is relatively simple and can predict the final charcoal yield in different heating conditions.

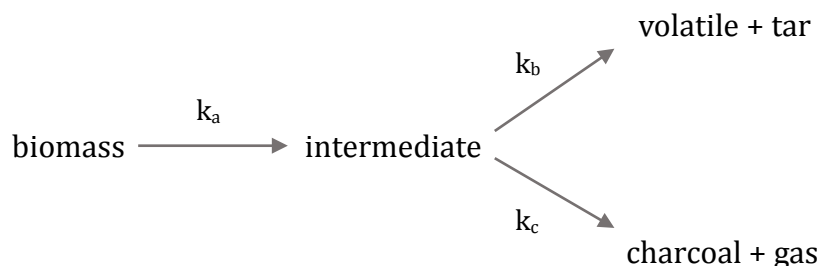


Figure 4.8 Reaction scheme of Biomass Pyrolysis suggested by Koufopoulos [28],  
a, b, c – share of biomass components

Kinetic parameters used by Koufopoulos are presented in Table 4.4

Table 4.4 Kinetic parameters, Koufopoulos et al. [8, 93]

Biomass component	First reaction			Second reaction			Third reaction		
	n	A (s <sup>-1</sup> )	E (kJ/mol)	n	A (s <sup>-1</sup> )	E (kJ/mol)	n	A (s <sup>-1</sup> )	E (kJ/mol)
cellulose	0	2.2·10 <sup>14</sup>	167.5	1.5	94·10 <sup>15</sup>	216.5	1.5	3.110 <sup>13</sup>	196
hemicellulose	0	3.3·10 <sup>6</sup>	72.4	1.5	1.1·10 <sup>14</sup>	174.1	1.5	2.510 <sup>13</sup>	172
lignin	0	3.3·10 <sup>12</sup>	147.7	1.5	8.6·10 <sup>8</sup>	137.1	1.5	4.410 <sup>7</sup>	122

The proposed kinetic model for the pyrolysis of lignocellulosic materials is relatively simple and predicts with sufficient accuracy both the reaction rate (expressed in terms of weight-loss) and the charcoal yield, also model can be used for the interpretation of experimental data and for the design of biomass thermochemical conversion apparatus, [28]. Another set of conclusions emerging from this work relates to the relationship between the biomass pyrolysis rate and the biomass composition; it was found to be possible to analyse biomass pyrolysis by considering the biomass as the sum of its main components: cellulose, lignin and hemicellulose [28].

One of first researches who introduce this idea of pseudocomponents was Orfao et al [295] proposed a method to determine biomass composition based on experimental results. The behaviour of biomass components (cellulose, hemicelluloses and lignin) was experimentally studied thermogravimetrically with linear temperature programming, under nitrogen and air [295]. Three commercial products were taken as representative

of biomass components: cellulose (Avicel PH101, FMC Corporation), xylan<sup>17</sup> (code X0627, Sigma) and lignin from pine wood (Westvaco Co.), sawdust from pine wood (*Pinus pinaster*), eucalyptus (*Eucalyptus globulus*) and pine bark [295]. Small particle sizes were chosen in order to avoid mass and heat transfer resistances. The pyrolysis of biomass was successfully modelled by a kinetic scheme consisting of three independent first order reactions of three pseudo components (hemicellulose, cellulose and lignin). In the model, the kinetic parameters of the second pseudo component, which were previously determined, were fixed. They noted that thermal decomposition of xylan and lignin could not be modelled with acceptable errors by means of simple reactions (minimum deviations were 15% and 10%, respectively) [295]. Orfao et al. [295] defined three pseudocomponents for describing the primary thermal decomposition of pine and eucalyptus woods and pine bark. The pyrolysis of lignocellulosic materials was successfully modelled by a kinetic scheme consisting of three independent first-order reactions of three pseudocomponents. The first and the second pseudocomponents correspond to the fractions of hemicellulose and cellulose which are reactive at low temperatures and the third includes lignin and the remaining fractions of the carbohydrates [295]. Reasonable agreement was obtained between the activation energies calculated for the other pseudocomponents and reported values [295]. Reasonable agreement was obtained between the activation energies calculated for the other pseudo components and reported values. Later, Manyà et al. [267] the thermal decompositions of sugarcane bagasse and waste-wood samples studied using thermogravimetric analysis. First, an irreversible first order reaction model was assumed for each pseudocomponent, but results showed that the model simulated curves do not fit well to the experimental data. Manyà et al. [267] with kinetic study presented that pyrolysis of lignin is better described by a third-order reaction rate law. The reformulation of the lignin kinetic model, and its subsequent implementation in the summative model (for the third pseudocomponent), has allowed one to reach a good agreement between simulated and experimental data [291]. Later, Mészáros et al. and Diaz [80, 267] showed satisfactory results when several partial reactions for corresponding pseudocomponents were assumed in the decomposition of a wide variety of biomass materials.

---

<sup>17</sup> Xylan - representative component of hemicelluloses

The goal of the kinetic evaluation is to obtain better, more informative results from the experiments. In the attempt to better identify the zones associated with the devolatilization of the biomass components and their overlapped kinetics, different  $T(t)$  heating programs have been employed [80]. Mészáros et al. [267] increased the information content of the experiments by involving successive non-isothermal steps into their study. The wider range of the experimental conditions reveals more of the chemical inhomogeneities of the biomass components [267]. Linear and stepwise heating programs were employed to increase the amount of information in the series of experiments [38]. Employing non isothermal experiments, not only identification of pseudo-components or zones were possible to made (hemicellulose, cellulose and lignin), but also, the contribution of extractives or more than one reaction stage in the decomposition of components, especially hemicellulose and lignin, could be also taken into pyrolysis kinetic analysis account.

Experimental measurements of the pyrolytic behaviour of biomass have been the focus of extraordinary interest in the research community, but practical problems associated with these measurements have often been overlooked. The most important errors are connected to problems of temperature measurements and to the self-cooling/self-heating of samples due to heat demand by the chemical reaction [80]. A consequence of these limitations is that the single step activation energy measured at high heating rates is almost always lower than its true value [80]. Another consequence is that weight loss is reported at temperatures much higher than it actually occurs [80]. All mentioned, are possible reasons for gross disagreements in the literature concerning the kinetics of pyrolysis.

For example, Antal and Várhegyi [254] concluded that the pyrolysis of a small sample of pure cellulose is characterized by an endothermic reaction governed by a first-order rate law with a high activation energy (ca. 238 kJ/mol). Almost immediately after the paper was published, these conclusions were contradicted by the findings of Milosavljevic and Suuberg [296], claim that the cellulose thermal degradation can be well described by a two-stage mechanism: the first at a low-temperature range with high activation energy (218 kJ/mol) and the second at a high-temperature range with reduced activation energy (140-155 kJ/mol). Antal et al. [246] measured the rates of pyrolysis of the same cellulose employed by Milosavljevic and Suuberg [296], in Antal's laboratory equipment. Also, the kinetics of other cellulose samples was studied to learn if different pure celluloses

evidence markedly different pyrolysis behaviour. The mass used for samples by Milosavljevic and Suuberg (30 mg) causes diffusion effects and, subsequently, an increase in the residence time for the vapour fraction, which promotes secondary reactions [246]. Also, the thermal lag (between the thermocouple lecture and the real temperature of the sample) accentuates the compensation effect [246]. This phenomenon causes an erratic estimation for the kinetic parameters [246]. If heat transfer effects cannot be neglected, then the kinetic model may not be adequate for describing the behaviour of the process involved, and must be combined with heat transfer equations [80]. It is difficult to combine a realistic modeling of the heat transfer phenomena with complex chemical kinetic models [80]. An alternative way is the empirical assessment of systematic errors [80]. To specify the serious trouble that supposes the experimental error, Grønli et al. [268] coordinated the realization of a round-robin kinetic study for the cellulose pyrolysis (Avicel PH-105) in eight European laboratories.

Results confirmed the theories of Antal et al. [246] but also alerted the scientific community about the convenience of carrying out this experiment (under standard conditions) in order to be able to quantify their own experimental errors [268, 291].

*The second approach* involves biomass as a single homogeneous sample whose thermal decomposition takes place according to semi - global model [26]. A model is based on Shafizadeh's model, Figure 3.10.

Compared with primary reactions, secondary reactions are less investigated and evaluations of the kinetic constants are essentially available only for the cracking process. The least understood aspect of pyrolysis is the interaction of the nascent, hot pyrolysis vapours with the decomposing solid, which vapours must traverse during their escape to the environment [80]. That process has been identified as secondary decomposition. At high temperatures and given sufficiently long residence times, secondary reactions of primary tar vapours also become active [29, 30, 160, 297]. These alter both the yields and composition of the biomass pyrolysis products. They may occur in the pores of the particles, while undergoing primary degradation, homogeneously in the vapour phase and heterogeneously over the charcoal surfaces and the extra-particle surfaces [160]. Secondary reactions of tar vapours include processes such as cracking, partial oxidation, re-polymerization and condensation. It is worth to mention that extensive research on biomass gasification confirm the catalytic effects exerted by different materials on the cracking of tarry components.



However, despite the quantitative understanding about the chemical composition of this class of products, the most cited mechanism simply consists of two competing reactions [160], as reported in Figure 4.9.

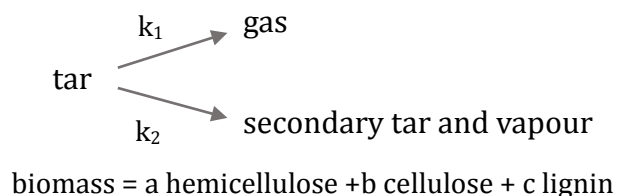


Figure 4.9 A global mechanism for the secondary reactions of vapour-phase tarry species as proposed by Antal [29, 30]

The reactive volatile matter is assumed to be consumed by two competitive reactions leading to the formation of permanent gases and a refractory condensable material. The competition between the chemical paths of gas and refractory tar formation has important implications from the point of view of process development [160].

The kinetics of secondary tar reactions is also of paramount importance in biomass gasification. The amount of tar produced and its composition depend on the type of gasifier and the process conditions. In principle, producer gas with a low tar content can be obtained if a high-temperature zone can be created where the volatile products of pyrolysis are forced to reside sufficiently long to undergo secondary gasification [160]. However, the discovery of a refractory tar product of secondary reactions has motivated extensive research activities on catalytic pyrolysis for the vapour phase products which, as anticipated, have been reviewed [160].

Chan et al [31, 32], have also included dehydration reactions along with the tar cracking to the competing reaction model. Model of independent parallel reactions was successfully used to describe the thermal decomposition of biomass. Model includes three independent parallel reaction of gas, charcoal and tar formation, and one reaction of tar decomposition to gas and secondary charcoal, Figure 4.10. Kinetic parameters are evaluated by use of this kinetic model are presented in Table 4.5.

Table 4.5 Kinetic Parametars used by Chan et al [31, 32]

Reaction	A (s <sup>-1</sup> )	E (kJ/mol)	Δh (kJ/kg)
1	1.3·10 <sup>8</sup>	140.3	209.3
2	2.0·10 <sup>8</sup>	133.1	209.3
3	1.1·10 <sup>7</sup>	121.4	209.3
4	1.48·10 <sup>6</sup>	114.3	-2009.3
5	5.13·10 <sup>6</sup>	88.0	2257

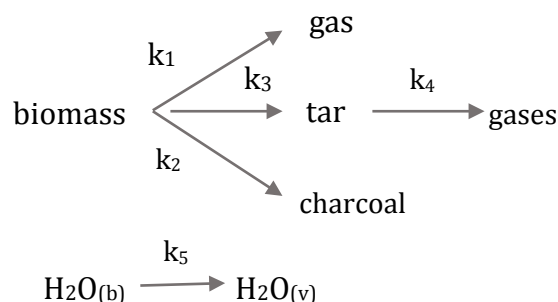


Figure 4.10 Scheme of Biomass Pyrolysis model duggedsted by Chan et al [31, 32]

The interaction involves an exothermic reaction which leads to the formation of charcoal. The role of such reactions is minimized by conditions which facilitate rapid mass transfer Antal and Grønli [69]. The majority of studies dealing with secondary reactions have been based on sensitivity analysis but a few number of practical models have included it. Srivastava et al. [33] extended the Koufopoulos mechanism. Proposed kinetic model based on experimental results of pyrolysis of different biomass in isothermal and non-isothermal conditions. The operative temperature ranges from 573 to 973 K for isothermal conditions and, for non-isothermal conditions, the heating rate ranges from 5 to 80 K/min [33]. It was found that the model developed was in excellent agreement with the experimental data. The pyrolysis model is presented in Figure 4.11.

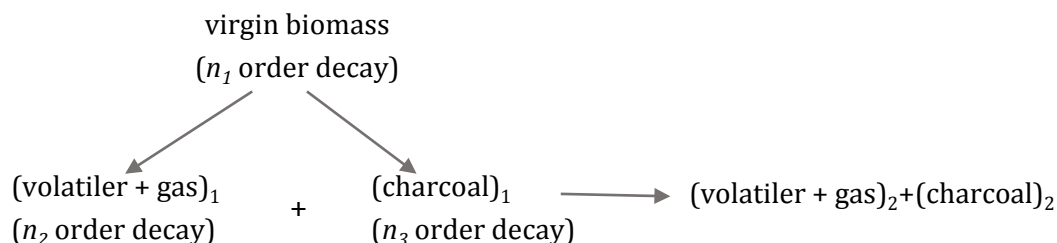


Figure 4.11 Model of Srivastava et al. [33]

This model indicates that the biomass decomposes to volatiles, gases and charcoal. The volatiles and gases may further react with charcoal to produce different types of volatiles, gases, and charcoal where the compositions are different. Therefore, the primary pyrolysis products participate in secondary interactions (reaction  $k_3$ ), resulting in modified final product distribution. It suggests that the gases and volatiles can react with the charcoal to produce different types of volatiles, gases and charcoals. When the volatiles and gases are transported by a gas flow, the secondary reaction will be affluent. Concerning kinetic modelling, Di Blasi [34] presented an approach describing the kinetics according to a competitive reaction scheme (Figure 4.12). In this model biomass decomposes via three competing reactions into gas, charcoal and tar. The secondary reaction takes place in the gas/vapour-phase within the pores of the charcoal. Consecutively the tar is converted by two secondary reactions into secondary gasses and charcoal. The rate of the reaction is proportional with the concentration of the tar vapours. Kinetics parameters are presented in Table 4.6.

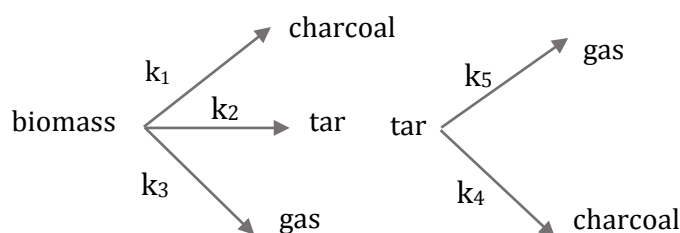


Figure 4.12 Reaction scheme of Biomass Pyrolysis suggested by Di Blasi [34]

Table 4.6 Kinetic parameters used by Di Blasi [34]

Reaction	A ( $s^{-1}$ )	E (kJ/mol)	$\Delta h$ (kJ/kg)
1	$5.16 \cdot 10^6$	100	418
2	$1.49 \cdot 10^{10}$	121	418
3	$2.66 \cdot 10^{10}$	112	418
4	$4.28 \cdot 10^6$	108	-42
5	$1.00 \cdot 10^6$	108	-42

The Miller - Bellan model shown in Figure 4.13.

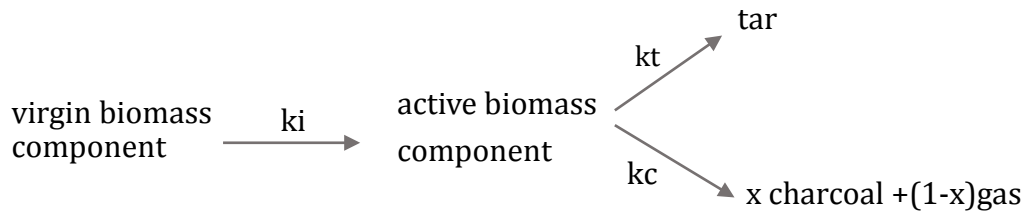


Figure 4.13 Miller-Bellan model [35]

The chemical pyrolysis reactions are modelled using the modified Broido - Shafizadeh scheme. This model has the advantage that it is one of the most complete models available. The scheme provided by Miller and Bellan [35] is able to deal with varying heating rates through the different reaction paths, and the model can deal with variations in fuel composition since it uses three fuel species instead of one model specie for biomass. In this two-step scheme the virgin fuel is first converted into an activated variant, which on its turn is converted into pyrolysis products. The scheme is applied for all three biomass model components with different kinetic constants. Kinetics parameters are listed in Table 4.7.

Table 4.7 Kinetic parameters for the pyrolysis reactions [35]

	Cellulose		Hemicellulose		Lignin	
	A (s <sup>-1</sup> )	E (kJ/mol)	A (s <sup>-1</sup> )	E (kJ/mol)	A (s <sup>-1</sup> )	E (kJ/mol)
ki	2.80E19	242.4	2.10E16	186.7	9.60E8	107.6
kt	3.28E14	196.5	8.75E15	202.4	1.50E9	143.8
kc	1.30E10	150.5	2.60E11	145.7	7.70E6	111.4

Compared with primary reactions, secondary reactions are less investigated. Most of the kinetic models are based on the primary pyrolysis analysis, only few models includes secondary reactions which take place outside of the biomass samples. Gvero [26], Rath and Staudinger [36], emphasize that the main product of the primary pyrolysis is tar, complex mixture of different organic compounds. Secondary reactions of tar vapours are classified as homogeneous and heterogeneous and include processes such as cracking, partial oxidation, re-polymerization and condensation. The complex chemical composition of tarry products would require a huge number of chemical reactions to describe the details of the transformations [160]. The existence of the second reaction is inferred from the gas yield data, which display an asymptotic behaviour (after residence times of about 5 s) that is strongly dependent on temperature; higher temperatures result

in dramatic increases in the asymptotic yields of all the light permanent gases produced [160]. The temperature-dependent asymptotes require the existence of the second reaction in order to explain the disappearance of carbon atoms in the gas phase when the gas phase temperature is reduced [160].

Borson et al [298], the homogeneous vapour phase cracking of newly formed wood pyrolysis tar studied at low molar concentrations as a function of temperature (773–1073 K), at residence times of 0.9–2.2 s [298]. Quantitative yields and kinetics were obtained for tar cracking and resulting products formation. The tar yield at 1 K/s and temperature of 600°C is 30 wt % , while at 800 °C is 80 wt % . The major tar conversion product was carbon monoxide, which accounted for over two-thirds of the tar lost (even up to 50 – 70 wt % ) at high severities [298]. Corresponding ethylene and methane yields were each about 10% of the converted tar; charcoal formation was negligible and weight-average tar molecular weight declined with increasing tar conversion [298].

Morf [299, 300], the change of mass and composition of biomass tar due to homogeneous secondary reactions experimentally studied by means of a lab reactor system that allows the spatially separated production and conversion of biomass tar. Homogeneous secondary tar reactions without the external supply of oxidising agents were studied in a tubular flow reactor operated at temperatures from 500 to 1000 °C and with space times below 0.2 s [300]. It is shown that, under the reaction conditions chosen for the experiments, homogeneous secondary tar reactions become important at temperatures higher than 650 °C, which is indicated by the increasing concentrations of the gases CO, CH<sub>4</sub>, and H<sub>2</sub> in the pyrolysis gas [300]. The gravimetric tar yield decreases with increasing reactor temperatures during homogeneous tar conversion. The highest conversion reached in the experiments was 88% at a reference temperature of 990 °C and isothermal space time of 0.12 s [300]. Hydrogen is a good indicator for reactions that convert the primary tar into aromatics, especially PAH. Soot appears to be a major product from homogeneous secondary tar reactions [300].

Innovative approach to secondary reaction kinetic modelling is presented by Rath and Staudinger [36]. Model is presented in Figure 4.14. Applying a coupling of a TGA and a tubular reactor, the investigation of the particular cracking characteristics of tar from pyrolysis of spruce wood as a function of the temperature was done.

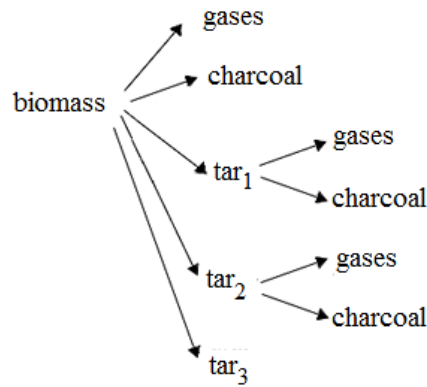


Figure 4.14 Reaction scheme of Biomass Pyrolysis suggested by Rath и Staudinger [36]

The experimental results showed that the extent of tar cracking is not only dependent on the conditions in the cracking reactor (temperature and residence time) but also on the temperature at which the tar was formed. During fast biomass pyrolysis, relatively high amount of tar is produced. This tar, which may reach up to 70%, is an extremely complex mixture. The tar could be classified, as a result of biomass pyrolysis, into three major classes: primary, secondary and tertiary tars. Primary tar is formed due to the presence of oxygen compounds in a temperature range of 400-700 °C. Secondary tar is formed in a temperature range of 700-850 °C, and it includes phenolics and olefins. Tertiary tar products appear in the temperature regime of 850-1000 °C and are characterized by aromatics. Sometimes, these three main classes are divided into sub-classes as well. During thermal biomass pyrolysis, the tar classes are formed and cracked hereafter. However, some of such tar classes and in particular their compounds are not fully cracked at pyrolysis process where some of which are left and they are so called non-reactive tars. Their values are mainly attributed to the structure of biomass and type of pyrolysis process (slow or fast).

Primary tars 1 and 2 cracking according a simple first order over all kinetic model (equation 4.17). Primary tar 3 does not crack.

$$-r_{ter,i} = A_i e^{-E_i/RT} C_{tar,i} \quad (4.22)$$

Where  $r_{ter,i}$  (mg/gm<sup>3</sup>s<sup>1</sup>) is tar rate, and  $C_{tar,i}$  (mg/gm<sup>3</sup>) tar concentration.

It was assumed that there exists a linear correlation between the rate of tar cracking and the rate of carbon - monoxide formation from tar cracking. This assumption was extended to all gaseous components. Therefore the formation of the individual product gases  $j$  from

tar cracking can be described according to equation 4.18 using the rates of tar cracking (cracking of tars  $i=1$  and  $i=2$ , tar 3 does not crack) and constant yield coefficients  $Y_{j,i}$ .

$$r_i = \sum_{j=1}^2 (-r_{tar,i})Y_{j,i} \quad (4.24)$$

Where  $r_j$  (mg/gm<sup>3</sup>s) is the rate of reaction and  $Y_{j,i}$  (g/g) is the yield coefficient.

Table 4. 8 shows the kinetic parameters calculated for the vapour phase cracking of the tars from pyrolysis of birch wood determined within this work.

Table 4.8 Kinetic Parametars of three parallel reaction of tar decomposition [26, 36]

	<b>E</b> (kJ/mol)	<b>A</b> (s <sup>-1</sup> )
primary tar	66.3	3.076 · 10 <sup>3</sup>
secondary tar	109	1.13 · 10 <sup>6</sup>
tertiary tar	no cracking	

The simplest models were based on a single decomposition reaction, and they do not allow to predict the influence of pyrolysis conditions on the amount of products [160]. Other models assume some parallel reactions to predict the production kinetics of gas tar and charcoal. More complex reaction schemes were also adopted, involving a further decomposition of tar in the gas phase or an intermediate product deriving from primary decomposition of biomass, giving rise to gas, tar charcoal. Most of these models were developed on the basis of experimental results obtained by pyrolysis of few mg of biomass in powder, often with a very high increase of temperature.

Based on the literature review, there are two approaches in biomass pyrolysis modelling. The first approach takes into account that the biomass is composed of three pseudocomponents (hemicellulose, cellulose and lignin), which thermally decompose independently of each other. Thermal decomposition of pseudocomponents are explain by single range reactions. This approach results in large number of experimental data ( $k_i$ ,  $E_i$ ,  $A_i$ ). The second approach, comprises multicomponential devolatalisation reactions, and include the primary and secondary reactions.

#### **4.4.2 A DISTRIBUTED ACTIVATION ENERGY MODEL FOR THE PYROLYSIS OF LIGNOCELLULOSIC BIOMASS - DEAM**

The complex composition of biomass materials, the conventional linearization techniques of the nonisothermal kinetics are not suitable for the evaluation of the TGA experiments. As it is mentioned several times, biomass contain a wide variety of pyrolyzing species. Even the same chemical species may have a different reactivity if its pyrolysis is influenced by other species in its vicinity [38]. As biomass is heated, its components (hemicellulose, cellulose and lignin) become chemically unstable and thermally degrade or vaporise. The thermal degradation of each component occurs at different temperature by different pathways. The decomposition of the hemicellulose is carries out at temperatures 200-260°C, cellulose 240-350°C and lignin 280-500°C, [144, 301]. The basic knowledge of the role and behaviour of the three principal components of biomass (cellulose, hemicelluloses and lignin) during pyrolysis is important for understanding and controlling this process. The assumption of a distribution in the reactivity of the decomposing species frequently helps the kinetic evaluation of the pyrolysis of complex organic samples [38, 302]. The chemical complexity of both the biomass and the related pyrolysis products motivate the introduction of kinetic models based on kinetic laws different from those presented above. The distributed activation energy model (DAEM) is the best way to represent mathematically the physical and chemical inhomogeneity of a substance [38, 260, 302].

The concept of a distributed activation energy as originally proposed by Vand [303] was adapted to the problem of coal devolatilization by Pitt [304]. Pitt [304], first treated the coal as a mixture of a large number of species decomposing by parallel first order reactions with different activation energies. The pyrolysis behaviour of coal is described as a complex of first-order reactions, each with its own rate constants. Further work carried out by Anthony and Howard [305], and Braun and Burnham [306], modified the model developed by Pitt and extended its use to coal, biomass and even blends of the two. Distributed activation energy models have been used for biomass pyrolysis kinetics since 1985, when Avni et al. [302] applied a DAEM for the formation of volatiles from lignin. Later this type of research was extended to a wider range of lignocellulose materials. Saidi et al. [307], employed DAEM-based kinetic models in establishing an actual combustion model of a burning cigarette. A three-dimensional model for a puffing cigarette was



constructed using the principles of the conservation of mass and momentum. To do this, an average temperature–time history of a burning cigarette was derived using existing experimental data for the temperature distribution in a cigarette [307].

Várhegyi et al. [270] was studied decomposition of two tobacco blends by thermogravimetry–mass spectrometry (TGA–MS) at slow heating programs under well-defined conditions. The kinetic evaluation was based on a distributed activation energy model (DAEM). The complexity of the studied materials required the use of more than one DAEM reaction [270]. The resulting models describe well the experimental data and are suitable for predicting experiments at higher heating rates. Várhegyi et al. [270, 308], Becidan et al. [271], Trninic et al. [38], based DAEM kinetic studies on the simultaneous evaluation of experiments with linear and stepwise temperature programs. The model parameters obtained in this way allowed accurate prediction outside of the domain of the experimental conditions of the given kinetic evaluations [38]. The determination of the unknown model parameters and the verification of the model were based on the least squares evaluation of series of experiments [308]. This approach led to favourable results and allowed predictions outside the experimental conditions of the experiments used in the parameter determination [260, 308].

The distributed reactivity is usually approximated by a Gaussian distribution of the activation energy due to the favourable experience with this type of modelling on similarly complex materials [38]. According to this model, the sample is regarded as a sum of  $M$  pseudocomponents, where  $M$  is usually between 2 and 4 [38]. Here pseudocomponent is the totality of those decomposing species which can be described by the same reaction kinetic parameters in the given model [38]. The reactivity differences are described by different activation energy values. On a molecular level, each species in pseudocomponent  $j$  is assumed to undergo a first-order decay [38].

### ***DERIVATION OF DAEM***

The key concept of the DAEM is to compress the manifold diversity (appearing in composition, structure, reaction complexity) into a proper set of kinetic parameters [309]. The biomass sample is assumed to contain  $1, 2, \dots, j, \dots, M$  distinguishable constituents (pseudocomponent). In the pyrolysis. Regard to this, denote the unreacted constituent of biomass represented by the  $j$ th kinetic equation as  $\alpha_j$ . The normalized biomass mass  $m$  is the linear combinations of  $\alpha_j(t)$ :

$$m(t) = 1 - \sum_{j=1}^M c_j \alpha_j(t) \quad (4.25)$$

Where a weight factor  $c_j$  is equal to the amount of volatiles formed from a unit mass of pseudocomponent  $j$ .  $M$  denotes the number of partial reactions contributing to the given measured quantities. If  $M=1$ , there is only one  $c$ , which is a proportionality factor between the reaction rate and the observed quantity. When  $M>1$  (i.e., when the observed curve is composed of overlapping partial curves)  $c_j$  represents the contribution of the  $j$ th partial reaction to the measured quantity [260].

The following boundary conditions apply to functions  $\alpha_j(t)$  [260]:

$$\alpha_j(t = 0) = 1 \text{ (mass of pseudocomponent } j \text{ at the beginning of the process)}$$

$$\alpha_j(\infty) = 0 \text{ (mass of pseudocomponent } j \text{ at the end of the process)}$$

The derivative of the normalized sample mass  $m$ :

$$-\frac{dm}{dt} = \sum_{j=1}^M c_j d\alpha_j/dt \quad (4.26)$$

The overall reaction rate is a linear combination of these partial reactions  $d\alpha_j/dt$ , [121, 198]:

$$-\frac{dm^{calc}}{dt} = \sum_{j=1}^M c_j d\alpha_j/dt \quad (4.27)$$

Each partial reaction is approximated by an Arrhenius equation. The corresponding rate constant  $k$  and mean lifetime  $\tau$  are supposed to depend on the temperature by an Arrhenius formula:

$$\frac{d\alpha_j}{dt} = A_j \exp(-E_j/RT)(1 - \alpha_j)^{n_j} \quad (4.28)$$

Where  $A_j$  and is the preexponential factor of the  $j$ th pseudocomponent and  $E_j$  is the activation energy of the  $j$ th pseudocomponent.

If  $\alpha_j(t, E)$  is the solution of the corresponding first-order ( $n=1$ ), kinetic equation. at a given  $E$  and  $T(t)$  with conditions  $\alpha_j(0, E) = 1$  and  $\alpha_j(\infty, E) = 0$ , became [260]:

$$-\frac{d\alpha_j(t, E)}{dt} = A_j \exp\left[-\frac{E}{RT(t)}\right] [1 - \alpha_j(t, E)] \quad (4.29),$$

Where  $T(t)$  is the temperature of the reacting particle.

The density function of the species differing by  $E$  within a given pseudocomponent is denoted by  $D_j$ . The overall reacted fraction of the  $j$ th pseudocomponent,  $\alpha_j(t)$ , is obtained by integration [260]:

$$\alpha_j(t) = \int_0^{\infty} D_j(E_a) X_j(t, E_a) dE \quad (4.30)$$

$D_j(E)$  is approximated by a Gaussian distribution with mean  $E_{0j}$  and width-parameter (variation)  $\sigma_j$ , [38, 260]:

$$D_j(E) = (2\pi)^{1/2} \sigma_j^{-1} \exp \left[ -(E - E_{0j})^2 / 2\sigma_j^2 \right] \quad (4.31)$$

The  $d\alpha_j/dt$  curves, based on equations (4.89) and (4.90), can be written as [260]:

$$\frac{d\alpha_j(t)}{dt} = \int_0^{\infty} D_j(E) d\alpha_j(t, E) / dt dE \quad (4.32)$$

Due to the fact that there is an inner  $dT$  integral and outer  $dE$  integral in the DAEM, it is very difficult to obtain the exact analytical solution of the DAEM. Since it is difficult to analytically solve the DAEM, the numerical techniques has been employed.

### **NUMERICAL SOLUTION**

The integration in equations 4.30 and 4.32 goes from  $E=0$  to  $E=\infty$ . The change of the lower limit of integration enables us to employ generally available mathematical techniques for the integration, without affecting the results, as outlined below, [38, 260]:

$$\alpha_j(t) = \int_0^{\infty} D_j(E) X_j(t, E) dE_a \cong \int_{-\infty}^{\infty} D_j(E) \alpha_j(t, E) dE \quad (4.33)$$

Introducing a variable:

$$\epsilon_j = (E - E_0) / \sqrt{2\sigma_j} \quad (4.34)$$

Equation 4.33 can write as [260]:

$$\begin{aligned}\alpha_j(t) &\cong (2\pi)^{-1/2} \sigma_j^{-1} \int_{-\infty}^{\infty} \exp[-(E - E_0)^2 / 2\sigma_j^2] \times \alpha_j(t, E) dE \\ &= \pi^{-1/2} \int_{-\infty}^{\infty} \exp(-\epsilon_j^2) \alpha_j(t, \epsilon_j) d\epsilon_j\end{aligned}\quad (4.35)$$

Where  $\alpha_j(t, \epsilon_j)$  is  $\alpha_j(t, E)$  expressed as a function  $\epsilon_j$ .

The equation 4.35 can easily be evaluated by a Gauss - Hermite quadrature formula [260, 310, 311]:

$$\alpha_j(t) \cong \pi^{-1/2} \sum_{i=1}^N w_i \alpha_j(t, \epsilon_{ij}) \quad (4.36)$$

Where  $w_i$  is weight factors and  $\epsilon_{ij}$  is the abscissas of the quadrature formula [38]

These quantities can be determined by well-known Fortran library functions [311].

Derivative of the equation (4.35):

$$d\alpha_j/dt \cong \pi^{-1/2} \int_{-\infty}^{\infty} \exp(-\epsilon_j^2) d\alpha_j(t, \epsilon_j) dt d\epsilon_j \cong \pi^{-1/2} \sum_{i=1}^N w_i d\alpha_j(t, \epsilon_{ij})/dt \quad (4.37)$$

Donskoi and McElwain [20, 260, 312], suggested that the energy domain of the integration should be rescaled by a factor of 0.5-0.3 to increase the efficiency of the Gauss-Hermite quadrature formula. Here rescaling factor of 1/2 is introduced by introducing a variable  $\mu_j$  [260]:

$$\mu_j = 2\epsilon_j = 2(E - E_{0,j})/\sqrt{2} \sigma_j \quad (4.38)$$

Substituting  $\mu_j$  variable into equation (4.35) and employing the Gauss-Hermite quadrature, [260]:

$$\begin{aligned}\alpha_j(t) &\cong 1/2 \pi^{-1/2} \int_{-\infty}^{\infty} \exp(-0,25\mu_j^2) X_j(t, \mu_j) d\mu_j \\ &\equiv 1/2 \pi^{-1/2} \int_{-\infty}^{\infty} \exp(-\mu_j^2) \exp(0,75\mu_j^2) \alpha_j(t, \mu_j) d\mu_j \\ &\cong 1/2 \pi^{-1/2} \sum_{i=1}^N w_i \exp(0,75\mu_{ij}^2) \alpha_j(t, \mu_{ij})\end{aligned}\quad (4.39)$$

Here  $\alpha_j(t, \mu_j)$  is  $\alpha(t, E)$  expressed as a function of  $\mu_j$ , and  $w_i$  and  $\mu_{ij}$  are the weight factors and abscissas of the Gauss-Hermite quadrature formula.

Considering above mentioned, equation (4.37) become:

$$d\alpha_j/dt \cong 1/2 \pi^{-1/2} \sum_{i=1}^N w_i \exp(-0,75\mu_{ij}^2) dX_j(t, \mu_{ij})/dt \quad (4.40)$$

The performance of the present computers allows the application of high  $N$  values. Várhegyi and Szabó [260] employed  $N=80$  in their calculations. In their calculations the relative precision of the Gauss-Hermite quadrature at  $N=80$  proved to be better than  $10^{-7}$  in this way. The high precision can ensure that all features of the calculated curves will reflect the properties of the model employed, [260]. Várhegyi and Szabó, [260], calculated equation 4.96 without the rescaling and observed oscillations superposed on some of our simulated curves. It is known, however, that such oscillations appear when the numerical solution of the DAEM employs an insufficient precision [260].

The unknown model parameters can be estimated using the least squares method. The method for solving DEAM is explained in the Chapter 5.

#### 4.5. CONCLUSION

In the 1960s people started to model the pyrolysis [23, 24, 269, 282]. They started with simple kinetic models and over time the models were changed and improved. Kinetic models range in complexity from simple first-order models to more mathematically complex models incorporating various factors which influence the kinetics of pyrolysis. Well-chosen kinetic models fit the thermal decomposition data for complex biomass samples over a wide range of times and temperatures. The key to finding a model that will extrapolate well outside its calibration temperature range is to thoroughly decouple the effects of time, temperature, and extent of reaction [292].

The most versatile distributed reactivity models have a discrete energy distribution that is able to conform to the subtleties of the pyrolysis profile [292]. The conventional discrete distribution assumes the same frequency factor for all parallel reactions. However, the uniform frequency factor approximation is not always valid. Regarding, these methods are not as accurate for determining reactivity distribution parameters [292]. Consequently, a new method has been derived in which the discrete activation-energy distribution is derived by assuming a linear relationship between the logarithm of the frequency factor and the activation energy [26, 29, 97][260, 292]. This model provides improved accuracy for the initial and final stages of the reaction for some

samples when the kinetics are extrapolated far outside their range of calibration. This extension is most important for flash coal pyrolysis and natural gas generation.

The distributed activation energy model (DAEM) is the best way to represent mathematically the physical and chemical inhomogeneity of a substance.

## CHAPTER 5

*“Mathematical models enable us to obtain amazing new insights into the way in which nature operates”*  
*Melvin Schwartz*

# 5. KINETIC MODELING OF CORN COB PYROLYSIS

## 5.1. INTRODUCTION

The chemistry of biomass pyrolysis has been the subject of intense scientific research for many decades, and several review-articles are available in the literature (Beall and Eicicner [313]; Antal [63, 64, 246, 254, 284, 285], Várhegyi [20, 202, 203, 217, 250, 257, 260, 269, 270, 294, 308, 314-317], Broido [23, 24, 261, 275], Koufopoulos [28, 318], Di Blasi [25, 86, 160, 225, 277, 319, 320], Branca [205, 206, 321, 322], etc.). The review of literature shows various kinetic approaches developed with different assumptions, simplifications, and with different levels of complexity and different treatments of pyrolysis products. The determination of kinetic mechanisms and rate constants for the pyrolysis process has been mainly carried out under regimes controlled by chemical kinetics, by using very small samples in powder form so that effects of transport phenomena such as heat and mass transfer can be neglected. This was the subject of this chapter, where experimental and modeling work on the pyrolysis of corn cob under regimes controlled by chemical kinetics and under different heating programs is presented. In this chapter, a distributed activation energy model (DAEM) was used due to the complexity of the corn cob. Biomass and residues contain a wide variety of pyrolyzing species. Even the same chemical species may have differing reactivity if their pyrolysis is influenced by other species in their vicinity. The assumption of a distribution in the reactivity of the decomposing species frequently helps the kinetic evaluation of the pyrolysis of complex organic samples [38]. The most promising results seem to be obtained with kinetic schemes consisting of sets of independent simultaneous reactions. In these kinetic schemes, it is assumed that the biomass components react independently and, therefore, that the global thermal behaviour

reflects the individual behaviour of the components, weighed by the composition [295]. The relative amounts of the components can be determined and, therefore, it is possible to establish the composition of the materials under pyrolysis [295, 323-325]. The distributed activation energy model (DAEM), assumes that the decomposition of complex pseudocomponents (hemicellulose, cellulose, and lignin) occurs through a series of reactions that have a range of activation energies. The distributed activation energy models (DAEM) have been used for biomass pyrolysis kinetics since 1985, when Avni et al [38, 302] applied a DAEM for the formation of volatiles from lignin. The use of DAEM in pyrolysis research was subsequent extended to a wider range of biomasses and materials derived from plants [38, 260, 271, 315, 326-331]. Due to the complexity of the investigated materials, the model was expanded to simultaneous parallel reactions (pseudocomponents) that were described by separate DAEMs [270, 308, 315, 329, 330]. The increased number of unknown model parameters required least-squares evaluation on larger series of experiments with linear and nonlinear temperature programs [21, 308, 316, 317]. The model parameters obtained in this way allowed accurate prediction outside of the domain of the experimental conditions of the given kinetic evaluations [21, 308, 316, 317]. The prediction tests helped to confirm the reliability of the model.

The present work aims at testing the applicability of this approach on a biomass of high applicability potential. Two types of corn cob were analysed in order to discern the peculiarities of their decomposition kinetics. The models and evaluation strategies outlined in a Várhegyi's [316] work. Particular emphasize was taken to discern the similarities and differences between the behaviour of the present samples and the kinetics established on other sorts of biomasses: corn stalk, rice husk, sorghum straw, and wheat straw (published in Várhegyi's [316] work). The presently available works on the pyrolysis kinetics of corn cobs [332-334] are far from the models and evaluation methods of the present work.

**Trninic et al** [38] have been already published most of the results and discussion presented in this chapter.



## **5.2. EXPERIMENTAL SECTION**

This chapter exposes the experimental procedure followed in the thermogravimetric studies carried out along this work. The experimental system is defined by the type of biomass, as well as the different thermogravimetric apparatus and experimental procedures employed in this chapter.

### **5.2.1. SAMPLES AND SAMPLE PREPARATION**

#### ***SAMPLE ORIGIN***

Grab samples of corn cobs were obtained from Serbia (ZP Maize Hybrid, ZP 505, denoted here as Scob) and Hawaii, USA (Pioneer HiBred International denoted here as Pcob).

#### **5.2.1.1. DRYING AND MILLING**

After receiving the corn cobs, they were put into a drying oven at 105 °C for about three days. Then the corn cobs were taken out of the drying chamber and prepared for the milling procedure. The aim was to get a particle size less than 1 mm for good mixing conditions. Because of their big size, corn cobs had to be milled in a two-step milling procedure with a big and a small cutting mill. In the first step the corn cobs were milled up with the big cutting mill into small elongate pieces with a maximum diameter of approximately mm. In the second step the corn cobs were milled up to a particle size less than 1 mm with the small cutting mill. After that, corn cob samples were stored in closed plastic bags.

To guarantee that corn cob samples are without any moisture, a necessary amount was taken out of the bags or bottles and stored in glass crucibles in the drying oven (Termaks) at 105 °C for 24 hours before every experiment.

#### **5.2.1.2. CHARACTERIZATION OF CORN COB**

The first step in analysis and understanding of feedstock thermochemical behaviour is samples characterisation.

## PROXIMATE ANALYSIS

Proximate analysis gives the composition of the biomass in terms of gross components such as moisture (M), volatile matter (VM), ash (A), and fixed carbon (fC). All corn cob samples were subjected to proximate analysis according to the appropriate standards:

1. ASTM<sup>18</sup> E871 - the moisture content analysis [335]
2. ASTM E872 - the volatile matter analysis [336]
3. ASTM D1102 - the ash content analysis [337]

A procedure to estimate proximate analysis of corn cob samples is explained in APENDIX B. Table 5.1 presents proximate analysis of corn cob.

Table 5.1 Proximate Analysis, Heating Value, and Fixed Carbon Yield of corn cobs

<b>Proximate analysis (wt % db)</b>					
Sample	<b>MC*</b>	<b>VM</b>	<b>A</b>	<b>fC</b>	<b>HHV (MJ/kg)</b>
Scob	5.18	81.08	1.45	17.47	18.63
Pcob	6.40	79.65	2.61	17.75	18.87

\*As received (moisture content on a wet mass basis)

## ULTIMATE ANALYSIS

Ultimate analysis gives the composition of the biomass in terms of gross components such as weight percentages of carbon (C), hydrogen (H), oxygen (O), nitrogen (N), and sulphur (S).

All corn cob samples were subjected to proximate analysis according to according to the appropriate standards:

1. ASTM E 777 – the carbon and hydrogen analysis
2. ASTM E 778 – the nitrogen analysis
3. ASTM E 775 – sulphur analysis

The oxygen content was determined by the difference of 100% and the sum of the ash, C, H, N, and S contents.

Elemental analyses of the feed samples were conducted by use of an elemental analyzer (Vario MACRO Elementar).

---

<sup>18</sup> ASTM - American Society for Testing and Materials

The procedures for Ultimate analysis are shown summarized in APENDIX B.

Table 5.2 presents ultimate analyses of corn cobs samples.

Table 5.2 Ultimate Analyses of corn cobs

Sample	Ultimate analysis [wt % db]						Sum
	C	H	O	N	S	ASH	
Scob	47.60	6.30	43.90	0.55	0.60	1.45	100.0
Pcob	47.00	6.40	43.40	0.50	0.10	2.61	100.0

### 5.2.2. EXPERIMENTAL APPARATUS AND EXPERIMENTAL PROCEDURE

The experimental apparatus used for experimental analyses consisted of a Thermal Instrument TA Q600 thermobalance, supported by a computer and software for control and data handling.. A schematic diagram of the pyrolysis experimental instrumentation is shown in Figures 5.1.

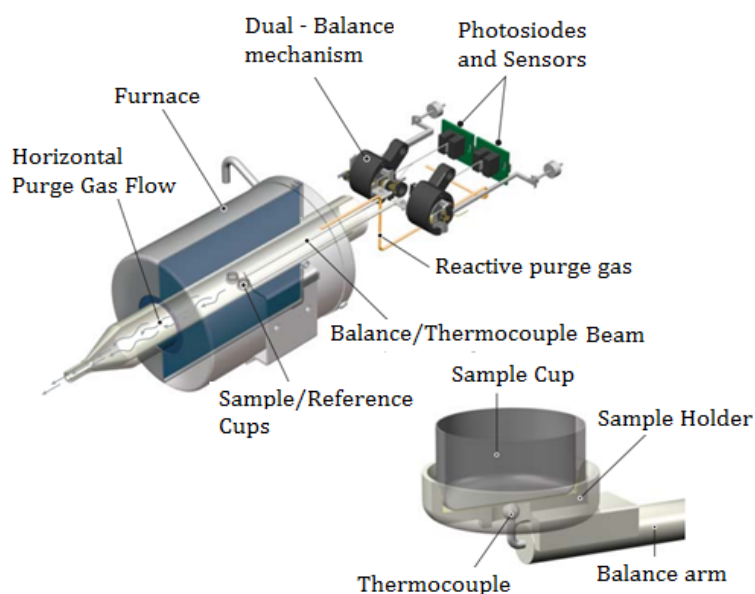


Figure 5.1 Schematic diagram of the TA Q600 simultaneous TGA - DTA with sample cup/sample thermocouple configuration [37]

The thermobalance is kept at a constant temperature of 40 °C [39] in a chamber that is insulated and purged with gas, usually nitrogen. At the end of the horizontal balance arm, there is the “hang-down wire” ending in a hook, at which the crucible (also called sample holder or sample pan) can be placed. According to TA

Instruments the weighting accuracy of the balance is +/- 0.1 % and the weighting precision +/- 0.01 %. [39]. The accuracy is the error made by the balance, difference between the measured weight and the real weight, in other words the ability of the balance to show the real weight of the sample. The precision concerns the reproducibility of the measurement, the ability of the balance to show the same mass for the same sample in every measurement.

Technical specifications of TA Q600 can be found in APENDIX C.

### **5.2.3. EXPERIMENTAL PROCEDURE**

All the experiments were performed under atmospheric pressure.

The sample material (5mg) was spread in a uniform layer in an alumina sample holder of  $\varnothing$  6 mm which was placed on the sample holder attached to the balance arm. The use of small particle sizes ensures the kinetic control by eliminating diffusion and heat transfer problems inside the particles. The omission of the finest particles eliminated the problem of dusts blown out by the gas stream during the experiments [271]. The purging<sup>19</sup> (99.99% pure nitrogen with a flow rate of 500 ml/min) was switched on and after 30 minutes isothermal hold at ambient temperature, the temperature was raised to 120°C and maintained for 30 minutes to ensure an atmosphere free of oxygen and that no moisture was left in the sample. The purging (99.99% pure nitrogen with a flow rate of 100 ml/min) was switched on and after 30 minutes isothermal hold at ambient temperature, the temperature was raised to 105°C and maintained for 30 minutes to ensure an atmosphere free of oxygen and that no moisture was left in the sample. Each TGA experiment was normalized by the initial dry sample mass. For this purpose, the sample mass measured at 120°C was selected. The sample mass normalized in this way is denoted by  $m(t)$ . The sample was then heated up to 550°C at the preselected heating programs and maintained for 5 minutes after which the experiment was terminated.

---

<sup>19</sup> The TGA instrument must be purged in order to give meaningful results. It is important to sweep away the generated sample volatiles with an adequate purge flow rate.

## HEATING PROGRAMS

Linear and stepwise heating programs were employed to increase the amount of information in the series of experiments. The aim of the stepwise experiments was to include isothermal sections and relatively fast temperature rises in the kinetic evaluation [271]. Heating rates 5, 10, and 20°C and a stepwise program were employed for both samples. A stepwise program consisted of 30 min isothermal sections at a stepwise experiment was carried out for each sample. It consisted of 30 min isothermal sections at 200, 250, 300, 350, 400, and 450°C. The corresponding steps were selected for each interesting region in the pyrolysis process: at the low temperature phenomena, at the start of the main hemicellulose decomposition and at the start of the main cellulose decomposition. The stepwise experiments took place in longer time intervals than the ones at linear temperature programs. Their DTG peak maxima were than values of the corresponding linear T(t) experiments at higher heating rates. Accordingly the peak values of the heat flux required by the endothermic reaction were also much lower in the stepwise experiments. The T (t) programs of the present work are shown in Figure 5.2.

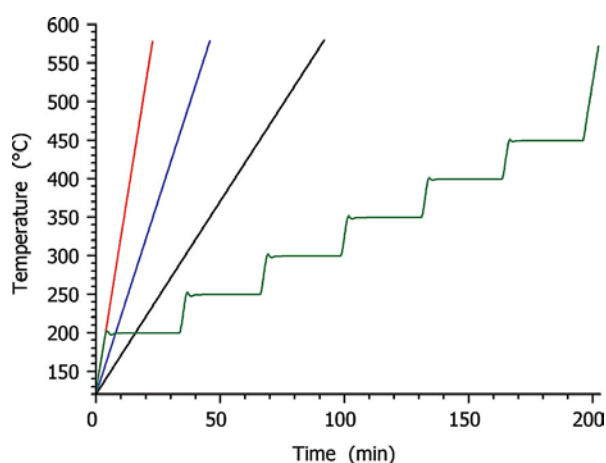


Figure 5.2 Temperature programs employed in the experiments: linear and stepwise [38]

The system for the analysis of corn cob pyrolysis kinetics included: two corn cob samples (Scob and Scob), one initial sample mass (5mg), one purge gas velocity

(100ml/min), four temperature programs (three linear heating programs and one stepwise) and one thermobalance (TA Q600).

At least three repetitions of the experiments in a given apparatus were also performed, in order to obtain reliable results.

In order to eliminate buoyancy effect, before each experiment with sample, an experiment with empty crucible was performed (blank test) and a “blank” curve was obtained, which was subtracted as baseline from the curve obtained with sample. The Buoyancy Phenomenon in TGA Systems is explained in APENDIX C.

### **5.3. RESULT AND DISSCUSION**

The Distributed Activation Energy Model (DAEM) is used to predict and characterize the underlying distribution of reactions occurring during the corn cob pyrolysis process. The DAEM was successfully applied to determine the Activation Energy ( $E$ ), and Pre-exponential Factor ( $A$ ), for each reaction during the pyrolysis of corn cob. Two of the samples were analysed to discern the peculiarities of their decomposition kinetics.

Particular emphasize was taken to discern the similarities and differences between the behaviour of the present samples and the kinetics established on other sorts of biomasses: corn stalk, rice husk, sorghum straw, and wheat straw [308]. The checks on the prediction capabilities were considered to be an essential part of the model verification [38].

In another test, the experiments of the two samples were evaluated together, assuming more or less common kinetic parameters for both cobs. This test revealed that the reactivity differences between the two samples are due to the differences in their hemicelluloses and extractives [38]. The kinetic parameter values from a similar earlier work on other biomasses presented by Várhegyi et al [308], could also been used, indicating the possibilities of a common kinetic model for the pyrolysis of a wide range of agricultural by product [308].

The present work aims at testing the applicability of this approach on a biomass of high applicability potential.

### NUMBER OF THE PSEUDOCOMPONENTS

In the attempt to get a better approach to the subtle changes in the mechanism, the fit to the DTG curves were we evaluated in a further calculation.

Figure 5.3 compares the decomposition of the samples (Scob and Pcob) at 20 °C/min heating rate.

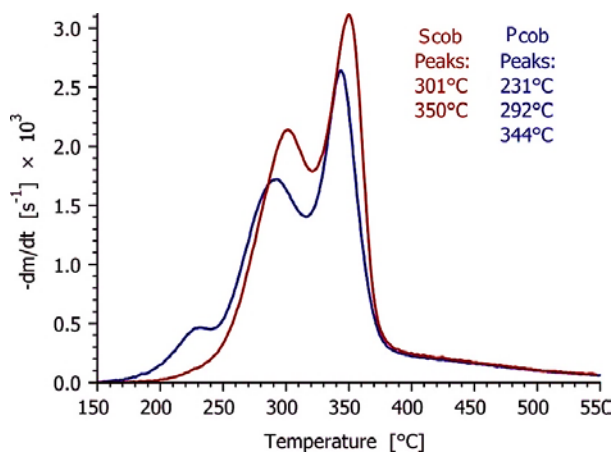


Figure 5.3 Comparison of the mass-loss rate curves and peak temperatures of the two samples of corn cob (Scob and Pcob) [38]

The main difference is the presence of a low temperature partial peak on the DTG curve of sample Pcob with peak top at 231°C [38]. This peak can be due to pectin which is a regular constituent of corn cob; its typical abundance is about 3%wt [38, 121, 338]. The rest of the decomposition is similar for the two cobs, though the hemicellulose and cellulose peaks occur at somewhat lower temperatures for the Pcob. This can be due to the higher ash content of the Pcobs, because some minerals may lower the peak temperatures of the hemicellulose and cellulose pyrolysis in agricultural by-product due to their catalytic activity [38]. The Scob could be described well by assuming three pseudocomponents, in the same way as in an earlier work on agricultural residues with similar models and methods (e.g. Várhegyi's works [271, 308, 316, 317]). The model for the Pcob, however, required an additional pseudocomponent for the low temperature peak.

### **EVALUATION BY THE METHOD OF LEAST SQUARES**

The unknown model parameters and the scale factors described in Chapter 4 were evaluated from series of experiments by use of the nonlinear least squares.

The unknown model parameters were evaluated from a series of 3–8 experiments by minimizing sum  $S_N$ , where  $N$  is the number of experiments evaluated together [20, 21, 38, 72, 80, 250, 254, 258, 270, 314, 339]:

$$S_N = \sum_{k=1}^{N_{exp}} \sum_{i=1}^{N_k} \left[ \left( \frac{dm}{dt} \right)_k^{obs} (t_i) - \left( \frac{dm}{dt} \right)_k^{calc} (t_i) \right]^2 / N_k h_k^2 \quad (5.1)$$

Where:

$S_N$  -The goal function which depends on  $\left( \frac{dm}{dt} \right)_k^{obs}$  and  $\left( \frac{dm}{dt} \right)_k^{calc}$  (for  $i = 1, 2, \dots$ ).

Function  $\left( \frac{dm}{dt} \right)_k^{calc}$  is determined when goal function reaches minimum.

$k$  - Indicates the experiments of the series evaluated

$i$  -Digitized point on an experimental curve

$\left( \frac{dm}{dt} \right)_k^{obs} (t_i)$  , - Derivated normalized sample mass- given by experiment

$\left( \frac{dm}{dt} \right)_k^{calc} (t_i)$  - Calculated derivative of the normalized sample mass

$N_{exp}$  - Number of experiments in a given evaluation,

$N_k$  - Number of evaluated data on the  $k$ th experimental curve  $R=$  gas constant ( $8.3143 \times 10^{-3} \text{ kJ mol}^{-1} \text{ K}^{-1}$ ),

$t_i$  - Denotes the time values in which the discrete experimental values were taken

$h_k$  - Height of an experimental curve that strongly depend on the experimental conditions, ( $\text{s}^{-1}$ )

$$h_k = \max \left( \frac{dm}{dt} \right)_k^{obs} \quad (5.2)$$

The normalization by  $h_k$  proved to be useful to evaluate simultaneously experiments having strongly differing magnitudes [38, 260]. As Várhegyi and Szabó [260] explained in their work, if the heights of the DTG peaks in experiments 1 and 2 were  $1.6 \times 10^{-4}$  and  $6.5 \times 10^{-4} \text{ s}^{-1}$ , respectively, due to the different heating rates



employed; without normalization by  $hk$ , experiment 2 would have a approximately 16 times higher representation in the least-squares sum than experiment 1.

If the objective function in its integral form is chosen, the data collected in the apparatus does not need more treatment, and can be used almost as they were collected [80]. However the weight fraction curves are not very sensitive to processes that can superpose partially or even go unnoticed [80]. The differential objective is much more sensitive to these changes but care must be taken in the calculation of the derivative because small experimental errors or deviations can produce large errors with respect to the actual derivative curve [340]. Here, the DTG curves were determined by spline smoothing. In most of the cases, the root mean square difference between the TG curves and the smoothing splines was small ( $\approx 0.01\%$ ) accordingly the differentiation itself did not introduce considerable systematic error into the evaluation [80].

For each group of experiments evaluated simultaneously a fit quantity was calculated [260]:

$$fit(\%) = 100 \left( \sum_{i=1}^{N_k} \frac{\left[ \left( \frac{dm}{dt} \right)_k^{obs} - \left( \frac{dm}{dt} \right)_k^{calc} \right]^2}{N_k} \right)^{\frac{1}{2}} / h_k \quad (5.3)$$

When the fit for a single experiment is given, the same formula is used with  $N_k = 1$ . Similar formulas can be used to express the repeatability of the experiments in quantitative form [80]. In this case, the mean square root difference between two repeated experimental DTG curves is calculated and normalized by the peak maximum [80]. In this way the average relative error is 1% for the repeatability of the non-isothermal experiments.

The experimental data were processed by MATLAB R2013b, FORTRAN 90 and C++ programs. FORTRAN 90 and C++ programs is developed by Gábor Várhegyi [20, 21, 38, 202, 246, 250, 257, 258, 260, 263, 270, 339]. In the MATLAB program, the differential equations are solved by a variable order method (stiff problems solver [80, 341]). The minimum fit is determined by a Nelder-Mead direct search method [80, 342]. The programs FORTRAN 90 and C++ developed by Gábor Várhegyi were

employed for the numerical calculations and for graphics handling, respectively [38]. The kinetic evaluation was based on the least-squares evaluation of the  $-dm/dt$  curves. The method used for the determination of  $-dm/dt$  does not introduce considerable systematic errors into the least-squares kinetic evaluation of experimental results [38]. For the FORTRAN 90 and C++ programs, the differential equations of the model are solved by a high precision ( $10^{-10}$ ) numerical solution. The least-squares parameters are determined by a modified Hook-Jeeves minimization, which is a safe and stable direct search method [20]. Each minimization was repeatedly restarted from the optimum found in the previous run of the algorithm until no further improvement was achieved.

The general data processing and graphic programs developed by G. Várhegyi were used in many of the figures and data processing steps in several points of the thesis.

### **5.3.1. DESCRIBING CORN COB PYROLYSIS KINETICS BY PARAMETERS OBTAINED FOR OTHER SORTS OF AGRICULTURAL RESIDUES**

This step in the modeling was the clarification of the similarities and differences between the present corn cob samples and other agricultural residues that were studied by the same models and evaluation techniques presented by Várhegyi et al. [308, 315]. Várhegyi et al. [315] the different agricultural residues (stalk, rice husk, sorghum straw, and wheat straw) were described by more or less common kinetic parameters. The different kinetic parameters were assumed to be common for corn stalk, rice husk, sorghum straw, and wheat straw [38]:

1. Activation energy -  $E_0$ ,
2. Activation energy and deviation -  $E_0$  и  $\sigma$ ,
3. Activation energy, deviation and preexponential factor -  $E_0$ ,  $\sigma$  и  $A$ .

Common  $E_0$  and  $\sigma$  were searched for the corn stalk, rice husk, sorghum straw, and wheat straw in one of the approaches employed (Várhegyi's work [316]). In this case, the shape and width of the partial curves were identical. The preexponential factors, however, depended on the type of the biomass. At given  $E_0$  and  $\sigma$  values, the increase of the preexponential factor moves the corresponding partial curve to a lower temperature [38]. In this way, the preexponential factors can express the different amounts of catalytic minerals in the different biomasses [38]. The  $c_j$

weight factors of Equation 5.5, which define the sizes (areas) of the partial peaks, also differed for the biomasses; hence, the  $c_j$  values expressed the compositional differences between the biomasses [38]. The  $E_{a0}$  and  $\sigma$  values obtained in this approach were used as constants in evaluations Scob<sub>2</sub> and Pcob<sub>2</sub> of the present work. The results obtained are shown in rows Scob<sub>2</sub> and Pcob<sub>2</sub> of Table 5.1 and columns Scob<sub>2</sub> and Pcob<sub>2</sub> of Table 5.2. The  $E_{02}$ ,  $E_{03}$ ,  $E_{04}$ ,  $\sigma_2$ ,  $\sigma_3$ , and  $\sigma_4$  values taken from the earlier work are listed in Table 5.2. The low temperature peak did not occur in corn stalk, rice husk, sorghum straw, and wheat straw samples; hence,  $E_{a01}$  and  $\sigma_1$  were free parameters in evaluation Pcob<sub>2</sub> [38, 316].

The use of predefined, constant parameters obviously decreases the number of free parameters,  $N_{param}$ . For a comparison with the evaluations from a higher number of Table 5.1.

Besides the quality of fit, an additional test was also used to check the validity of the models. In this test, the experiments with the highest heating rate of the study were compared to predictions obtained from the evaluation of the slower experiments. The goodness of the model can be assessed by the fit quality and the prediction tests together [38]. In the present work,  $fit_{20^\circ C/min}$  and  $fit_{20^\circ C/min}^{pred}$  show the fit quality of the 20°C/min experiments in the regular evaluations and in the prediction tests, respectively. The difference of the parameters obtained from a smaller and a larger set of the experiments may be used to check the possibility of ill-definition problems in the evaluation.  $||\Delta E_{a0}||$ ,  $||\Delta\sigma||$ , and  $||\Delta c||$  are the *rms* differences between the results of the evaluations based on the slower experiments and on all available experiments. The occurrence of a high value for  $||\Delta E_{a0}||$ ,  $||\Delta\sigma||$ , or  $||\Delta c||$  would indicate that the lower number of the experiments is not sufficient for the unique determination of the kinetic parameters. However, none of the calculations with the DAEM model indicated such a problem in the present study. Table 5.3 lists these differences for the evaluations carried out on both 3 and 4 experiments. The evaluation of the Scob and Pcob samples without special restrictions on the parameters, are rows Scob<sub>1</sub> and Pcob<sub>1</sub> in this table. The highest  $||\Delta E_{a0}||$  in the table, 10 kJ/mol, belongs to evaluation Scob<sub>1</sub> [38]. The  $||\Delta\sigma||$  and  $||\Delta c||$  values are negligible [38]. The differences between the  $fit_{20^\circ C/min}$  and  $fit_{20^\circ C/min}^{pred}$  pred values

are also low indicating that the prediction tests and the regular least-squares evaluations resulted in similar fit qualities for the 20 °C/min experiment [38].

Table 5.3 Evaluation of Scob and Pcob by DAEM reactions [38]

No.	values for other biomasses [38, 308]	$\frac{N_{par}}{N}$	fit <sub>4</sub> (%)	fit <sub>20°C/min</sub> (%)	fit <sub>20°C/min</sub> <sup>pred</sup> (%)	$  \Delta E_0  $ ( $\frac{kJ}{mol}$ )	$  \Delta\sigma  $ ( $\frac{kJ}{mol}$ )	$  \Delta c  $
Scob <sub>1</sub>	-	3	1.9	2.4	2.9	10	0.8	0.002
Scob <sub>2</sub>	$E_0$	2.3	2.0	2.6	3.1	-	0.4	0.006
Scob <sub>3</sub>	$E_0, \sigma$	1.5	2.5	3.5	3.7	-	-	0.007
Scob <sub>4</sub>	$E_0, \sigma, A$	0.8	4.1	5.4	5.5	-	-	0.003
Pcob <sub>1</sub>	-	4	1.7	1.7	2.0	3	0.2	0.002
Pcob <sub>2</sub>	$E_{02}, E_{03}, E_{04}$	3.3	1.8	2.1	2.4	1 <sup>b</sup>	0.2	0.001
Pcob <sub>3</sub>	$E_{02}, E_{03}, E_{04}, \sigma_2, \sigma_3, \sigma_4$	2.5	2.2	2.6	2.8	1 <sup>b</sup>	0.3 <sup>b</sup>	0.002
Pcob <sub>4</sub> <sup>c</sup>	$E_{02}, E_{03}, E_{04}, \sigma_2, \sigma_3, \sigma_4, A_2, A_3, A_4$	1	6.3	7.1	7.2	-	-	0.004

a - Scob<sub>1</sub> - Scob<sub>4</sub> are evaluations of sample Scob assuming three partial reactions

Pcob<sub>1</sub> - Pcob<sub>4</sub> are evaluations of sample Pcob assuming four partial reactions

b - Difference between the parameters of the first peak only (because the corresponding values of the other peaks were not changed)

c - the kinetic parameters of the low-temperature peak ( $A_1, E_{a01}$ , and  $\sigma_1$ )

In another approach all kinetic parameters were assumed to be common for corn stalk, rice husk, sorghum straw, and wheat straw. Such  $A$ ,  $E_0$ , and  $\sigma$  values were searched which were applicable for the four materials together. In this method, the differences between the biomasses were expressed only by the  $c_j$  weight factors of Equation 5.5, which define the sizes (areas) of the partial peaks [38]. The  $A$ ,  $E_0$ , and  $\sigma$  values obtained in this way were used as constants in evaluations Scob<sub>3</sub> and Pcob<sub>3</sub> of the present work. The corresponding results are shown in rows Scob<sub>3</sub> and Pcob<sub>3</sub> of Table 5.3 and columns Scob<sub>3</sub> and Pcob<sub>3</sub> of Table 5.4. The values taken from the work published by Várhegyi et al. [315] are  $A_2, A_3, A_4, E_{02}, E_{03}, E_{04}, \sigma_2, \sigma_3$ , and  $\sigma_4$  in Table 5.4, as noted there in a table footnote. In Evaluation Pcob<sub>3</sub>, the free variation of the kinetic parameters of the low temperature peak resulted in a false convergence; accordingly, the  $E_{01}, \sigma_1$ , and  $A_1$  values of evaluation Pcob<sub>2</sub> were employed in evaluation Pcob<sub>3</sub> as constants [38]. Accordingly, only the  $c_i$  factors were

varied in  $Scob_3$  and  $Pcob_3$ , as the low  $N_{param}/N$  indicates in Table 5.3. The partial curves and the fit quality is shown for the  $S_2$ ,  $P_2$ ,  $S_3$ , and  $P_3$  evaluations at  $20^\circ\text{C}/\text{min}$  heating rate in Figure 5.4.

The first, low temperature peak of magenta colour occurs only in sample  $Pcob$  and was identified as pectin decomposition, as outlined above. The second and third peaks (red and blue colours) are due to hemicellulose and cellulose pyrolysis, respectively. The last process (colour green in the figures) in a very wide temperature domain describes the lignin decomposition as well as the slow carbonization of the chars formed in the pyrolysis [315]. These are only approximate assignments, however, because more than one biomass component can contribute to a given pseudocomponent.

Plots (a) and (c) in the left-hand-side of Figure 5.4 display a reasonable fit quality. However, the calculated curves (black solid lines) show too high overlap in plots (b) and (d) of Figure 5.3 because the preexponential factors were not allowed to vary in the corresponding evaluations. Accordingly, the *rms* differences between the observed and calculated points are higher here, as the *fit 1* values in the graphic fields indicate [38]. Nevertheless, these calculated curves with lower fit quality still can be employed as models with rougher approximation. The omission of the low temperature peak from the model of the  $Pcob_3$  results only in a moderate worsening of the fit quality: *fit 4* increases to 6.8 from 6.3% while *fit 20°C/min* changes from 7.1 to 7.5% [38]. These observations suggest that it is possible to describe a wide range of biomass materials in a rough approximation by a common model of three partial DAEM reactions in which only the areas of the partial peaks differ.

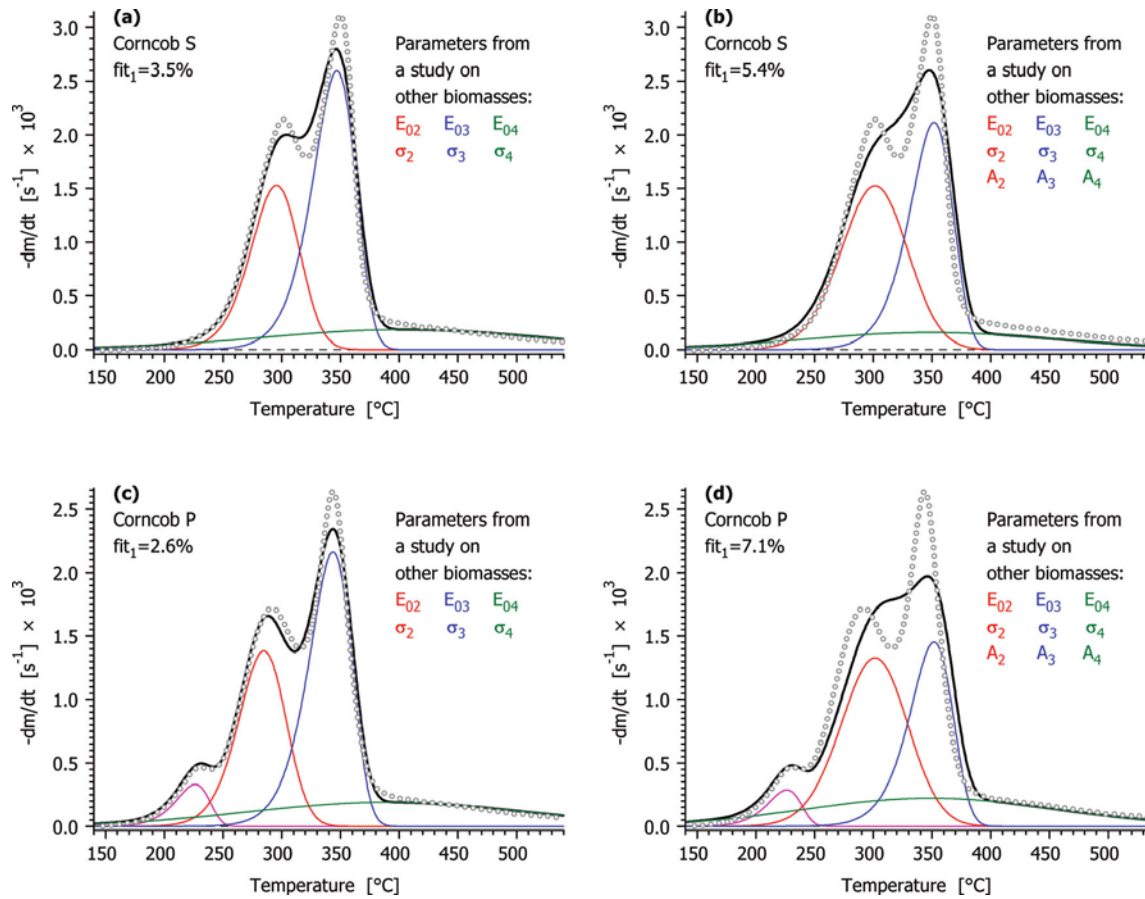


Figure 5.4 Evaluations by DAEM kinetics. Part of the kinetic parameters were taken from a literature work on agricultural biomasses [38]

*Notation:* grey circles - observed mass loss rate curve; black solid line - its calculated counterpart; thin solid lines of different colors - and partial reactions

Table 5.4 List of the model parameters for seven selected evaluations [38]

model	DAEM		DAEM		DAEM		DAEM		n-order	
	Scob <sub>3</sub>	Pcob <sub>3</sub>	Scob <sub>4</sub>	Pcob <sub>4</sub>	DAEM <sub>2</sub>		DAEM <sub>3</sub>		n_order <sub>3</sub>	
Sample	Scob	Pcob	Scob	Pcob	Scob	Pcob	Scob	Pcob	Scob	Pcob
Figures	3a	3c	3b	3d	-	-	4a	4c	5a	5c
$fit_8$		2.1		5.3		1.9		2.4		2.5
%										
$E_{01}$	-	142	-	142 <sup>b</sup>	-	141	-	141	-	138
$E_{02}$		177 <sup>c</sup>		176 <sup>c</sup>		180 <sup>d</sup>		180 <sup>d</sup>		173 <sup>d</sup>
$E_{03}$		185 <sup>c</sup>		185 <sup>c</sup>		196 <sup>d</sup>		187 <sup>d</sup>		186 <sup>d</sup>
$E_{04}$		194 <sup>c</sup>		189 <sup>c</sup>		205 <sup>d</sup>		225 <sup>d</sup>		261 <sup>d</sup>
$\sigma_1$	-	0.1	-	0.1 <sup>b</sup>	-	1.3	-	2.7	-	-
$\sigma_2$		4.3 <sup>c</sup>		7.1 <sup>c</sup>		4.2 <sup>d</sup>		3.9 <sup>d</sup>	-	-
$\sigma_3$		1.9 <sup>c</sup>		1.7 <sup>c</sup>		0.0 <sup>d</sup>		0.2 <sup>d</sup>	-	-
$\sigma_4$		34.6 <sup>c</sup>		32.7 <sup>c</sup>		29.2 <sup>d</sup>		31.3 <sup>d</sup>	-	-
$\log_{10} A_1/s^{-1}$	-	13.3	-	13.2 <sup>b</sup>	-	13.1	-	13.01	-	12.77
$\log_{10} A_2/s^{-1}$	14.4	14.8		14.13 <sup>c</sup>		14.8	15.1	14.8	15.0	14.2
									14.44	

<b>model</b>	<b>DAEM</b>		<b>DAEM</b>		<b>DAEM</b>		<b>DAEM</b>		<b>n-order</b>	
Evaluation	Scob <sub>3</sub>	Pcob <sub>3</sub>	Scob <sub>4</sub>	Pcob <sub>4</sub>	DAEM <sub>2</sub>		DAEM <sub>3</sub>		n_order <sub>3</sub>	
Sample	Scob	Pcob	Scob	Pcob	Scob	Pcob	Scob	Pcob	Scob	Pcob
Figures	3a	3c	3b	3d	–	–	4a	4c	5a	5c
$\log_{10} A_3/s^{-1}$	13.9	13.96	13.71 <sup>c</sup>		14.8	14.9	14.11 <sup>d</sup>		14.00 <sup>d</sup>	
$\log_{10} A_4/s^{-1}$	12.9	13.3	13.9 <sup>c</sup>		14.5	14.7	16.25 <sup>d</sup>		19.52 <sup>d</sup>	
$n_1$	–	–	–	–	–	–	–	–	–	2.14
$n_2$	–	–	–	–	–	–	–	–	–	1.90 <sup>d</sup>
$n_3$	–	–	–	–	–	–	–	–	–	0.94 <sup>d</sup>
$n_4$	–	–	–	–	–	–	–	–	–	10.38 <sup>d</sup>
$c_1$	–	0.04	–	0.03	–	–	–	0.05	–	0.07
$c_2$	0.24	0.21	0.33	0.28	0.25	0.21	0.23	0.21	0.29	0.25
$c_3$	0.37	0.31	0.30	0.21	0.33	0.27	0.34	0.29	0.32	0.27
$c_4$	0.17	0.17	0.13	0.18	0.18	0.18	0.20	0.16	0.19	0.14

<sup>a</sup> See Tables 5.1 and 5.3 for the meaning of these abbreviations

<sup>b</sup>  $E_{01}$ ,  $\sigma_1$  and  $A_1$  had fixed values in evaluation Pcob<sub>4</sub>. (They were taken from evaluation Pcob<sub>3</sub>.)

<sup>c</sup> values taken from work published by Várhegyi et al. [308]

<sup>d</sup> Parameters forced to have the same values for samples Scob and Pcob



### 5.3.2. DESCRIBING KINETICS OF THE TWO CORN COB SAMPLES BY COMMON KINETIC PARAMETERS

The next step in the modeling was the clarification of the similarities and differences between the two corn cob samples. For this purpose, the eight experiments of the two samples were evaluated simultaneously and the number of common parameters values were gradually increased [38]. The processes and the characteristics of the performance of the evaluations are summarized in Table 5.5. The present quantities are calculated from the corresponding values of the Scob and Pcob together. Hence,  $fit_8$  shows the fit quality of the eight experiments together;  $fit_{20^\circ\text{C}/\text{min}}$  is the root-meansquare of the  $fit_1$  values of the  $20^\circ\text{C}/\text{min}$  experiments on the Scob and Pcob;  $fit_{20^\circ\text{C}/\text{min}}^{pred}$  is a similar value calculated from the prediction tests, and  $||\Delta E_0||$ ,  $||\Delta\sigma||$ , and  $||\Delta c||$  are rms differences between the values determined from all experiments (8 experiments) and from the slower experiments (6 experiments) [38].

The first row contains the characteristics calculated from the separate evaluations of the samples. The assumption of common  $Ea_{02}$ ,  $Ea_{03}$ , and  $Ea_{04}$  and  $\sigma_2$ ,  $\sigma_3$ , and  $\sigma_4$  values for samples Scob and Pcob only slightly changed the performance of the modeling, as the rows DAEM<sub>1</sub> and DAEM<sub>2</sub> show in Table 5.5. In a further test, the preexponential factors of the cellulose decomposition ( $A_3$ ) and the wide, flat peak ( $A_4$ ) were also assumed to be common in the two samples [38]. Row DAEM<sub>3</sub> in Table 5.5 and Figure 5.5 show that this model variant still produced an acceptable performance. Table 5.5 Simultaneous evaluation of samples Scob and Pcob<sup>a</sup> [38].

Figure 5.5 displays the  $20^\circ\text{C}/\text{min}$  experiments. Plots (a) and (c) in the left-hand-side of Figure 5.5 belong to the regular least-squares evaluation of the eight experiments while plots (b) and (d) show the prediction from the six slower experiments.

The assumptions of evaluation DAEM<sub>3</sub> mean that the main difference between the pyrolysis kinetics of samples Scob and Pcob lies in the existence of the small low temperature peak in Pcob and the in different reactivity of the hemicellulose [38]. The rest of the decomposition (cellulose, lignin, and the slow carbonization

processes of the charcoal) can be described by identical kinetic parameters for both cobs.

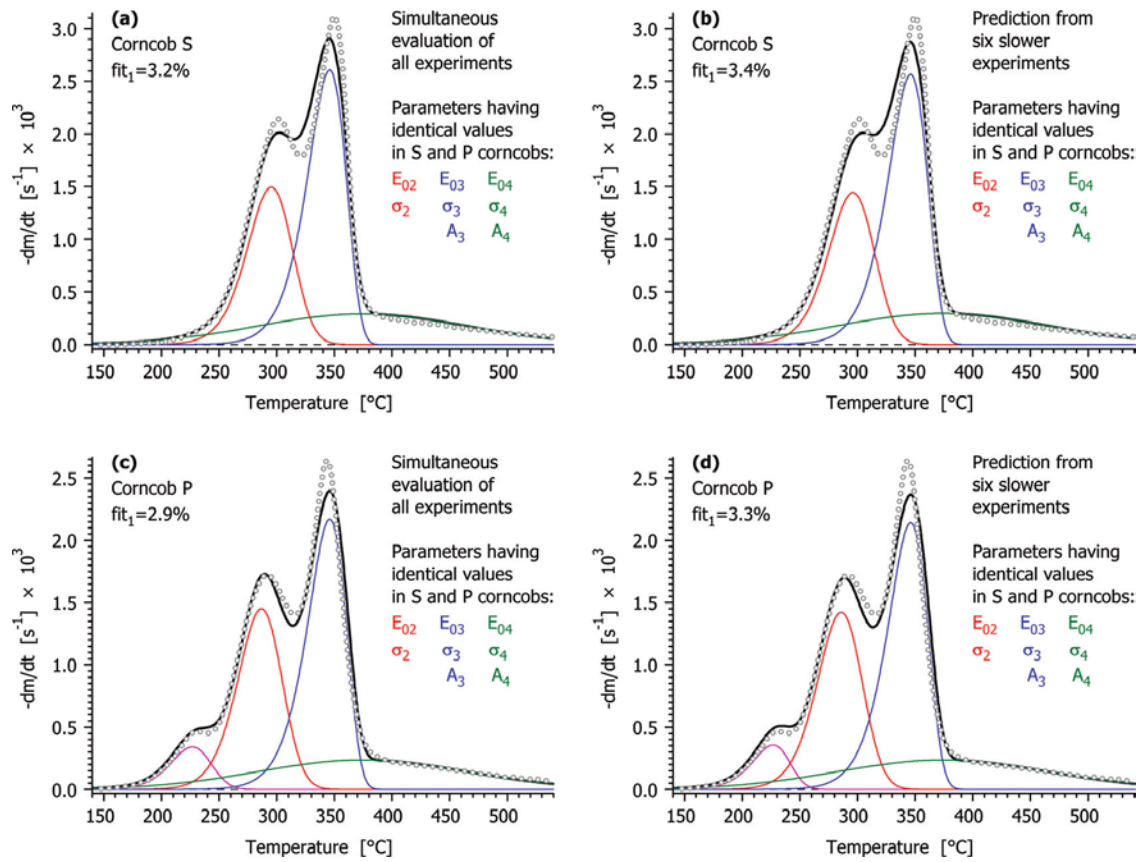


Figure 5.5 Evaluation by DAEM kinetics assuming eight common parameters for the two samples. The left-hand-side (plots a and c) belongs to the regular least squares evaluation of the eight available experiments while the right-hand-side (plots b and d) [38]

Table 5.5 Simultaneous evaluation of samples Scob and Pcob<sup>a</sup> [38]

Evaluation	same values in Scob and Pcob	$\frac{N_{param}}{N}$	$fit_8$ (%)	$fit_{20^\circ C/min}$ (%)	$fit_{20^\circ C/min}^{pred}$ (%)	$  \Delta E_0  $ (kJ/mol)	$  \Delta\sigma  $ (kJ/mol)	$  \Delta n  $	$  \Delta c  $
Scob <sub>1</sub> and Pcob <sub>1</sub>	-	3.5	1.8	2.0	2.4	7	0.5	-	0.002
DAEM <sub>1</sub>	$E_{02}, E_{03}, E_{04}$	3.1	1.9	2.2	2.6	1	0.4	-	0.004
DAEM <sub>2</sub>	$E_{02}, E_{03}, E_{04}, \sigma_2, \sigma_3, \sigma_4$	2.8	1.9	2.2	2.6	4	0.5	-	0.004
DAEM <sub>3</sub>	$E_{02}, E_{03}, E_{04}, \sigma_2, \sigma_3, \sigma_4, A_3, A_4$	2.5	2.4	3.0	3.3	4	0.7	-	0.003
n-order1	$E_{02}, E_{03}, E_{04}$	3.1	2.0	2.0	2.7	14	-	4.3	0.125
n-order2	$E_{02}, E_{03}, E_{04}, n_2, n_3, n_4$	2.8	2.0	2.3	2.7	2	-	0.5	0.07
n-order3	$E_{02}, E_{03}, E_{04}, n_2, n_3, n_4, A_3, A_4$	2.5	2.5	3.1	3.4	3	-	0.4	0.08

<sup>a</sup> Simultaneous evaluation of eight experiments assuming four partial reactions

### 5.3.3. MODELING WITH $n$ -ORDER KINETICS

The  $n$ -order kinetics has the same number of model parameters as the DAEM with Gaussian distribution, while its numerical solution is simpler and faster. To test this approach, evaluations similar to DAEM<sub>1</sub>, DAEM<sub>2</sub> and DAEM<sub>3</sub> were carried out with  $n$  - order kinetics [38]. The corresponding evaluations are denoted in Tables 5.3 and 5.4 by  $n\_order_1$ ,  $n\_order_2$ , and  $n\_order_3$ . The assumptions on common  $\sigma_2$ ,  $\sigma_3$ , and  $\sigma_4$  in evaluations DAEM<sub>2</sub> and DAEM<sub>3</sub> were replaced by assumptions on common  $n_2$ ,  $n_3$ , and  $n_4$  in evaluations  $n\_order_2$  and  $n\_order_3$ . The partial curves and  $fit$  qualities of the 20 °C/min experiments for evaluation  $n\_order_3$  and the results of the corresponding prediction tests are shown in Figure 5.6 in the same way as it was done in the case of evaluation DAEM<sub>3</sub> in Figure 5.3.

The data of Table 5.5 shows that similar fit qualities can be obtained by the  $n$ -order model. The prediction tests also gave similar results. The comparison of the kinetic parameters obtained from six and eight experiments revealed high  $\Delta c$  differences, especially for evaluation  $n\_order_1$ , accordingly the DAEM model has better-defined parameters during the evaluation [38]. Besides, the  $n$ -order kinetics describes the complexity of the biomass materials in a rather formal way while a DAEM gives a simplified, but clear picture on the different relativities of the different biomass species [38].

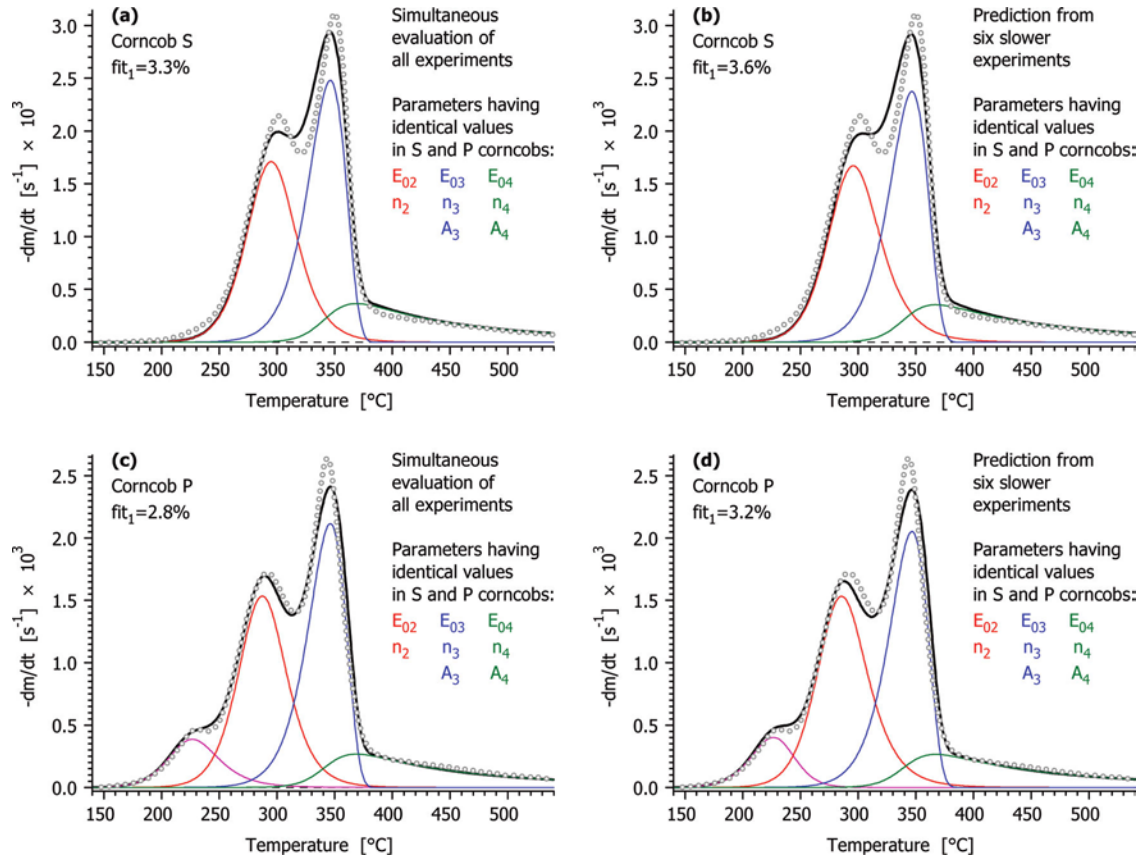


Figure 5.6 Evaluation by  $n$ -order kinetics assuming eight common parameters for the two samples. The left-hand-side (plots a and c) belongs to the regular least squares evaluation of the eight available experiments while the right-hand-side (plots b and [38]

*Notation:* The parameter values and other details are listed in Table 5.1 and 5.2 at evaluation  $n\_order3$

### 5.3.4. PREDICTION TESTS

Besides the quality of fit, an additional test was used to check the validity of the models. In this test, the experiments with the highest heating rate of the study were compared to predictions obtained from the evaluation of the slower experiments [38]. Such tests can be carried out for any type of kinetic modeling. The goodness of the model can be assessed by the fit quality and the prediction tests together. In the present work,  $fit\ 20^{\circ}C/min$  and  $fit\ 20^{\circ}C/min\ pred$  show the fit quality of the  $20^{\circ}C/min$  experiments in the regular evaluations and in the prediction tests, respectively [38]. The difference of the parameters obtained from a smaller and a larger set of the

experiments may be used to check the possibility of ill-definition problems in the evaluation.  $||\Delta E_{ao}||$ ,  $||\Delta\sigma||$ , and  $||\Delta c||$  are the rms differences between the results of the evaluations based on the slower experiments and on all available experiments [38]. The occurrence of a high value for  $||\Delta E_{ao}||$ ,  $||\Delta\sigma||$ , or  $||\Delta c||$  would indicate that the lower number of the experiments is not sufficient for the unique determination of the kinetic parameters. However, none of the calculations with the DAEM model indicated such a problem in the present study [38]. Table 5.1 lists these differences for the evaluations carried out on both 3 and 4 experiments. The evaluation of the Scob and Pcob samples without special restrictions on the parameters, as described in the previous section, are rows Scob1 and Pcob1 in this table. The highest  $||\Delta E_{ao}||$  in the table, 10 kJ/mol, belongs to evaluation Scob1 [38]. Note that similar uncertainties (standard deviations of 8–10 kJ/mol) were observed in a round-robin study on pure cellulose samples that were evaluated by simple first-order kinetics [38]. The  $||\Delta\sigma||$  and  $||\Delta c||$  values are negligible in Table 5.1. The differences between the *fit 20°C/min* and *fit 20°C/min* pred values are also low indicating that the prediction tests and the regular least-squares evaluations resulted in similar fit qualities for the 20 °C/min experiments [38]. However, these observations do not mean that three experiments are always enough for the unique determination of 12 – 16 kinetic parameters. Figure 4.26 indicates that the hemicellulose and cellulose peaks are well separated in the present samples; accordingly, the experiments contain ample information for the determination of the corresponding kinetic parameters. These peaks highly overlap each other in many agricultural residues and other materials of plant origin [38]. The merging of two peaks rises the possibility of more than one mathematical solution that describes the experiments equally well [38].

#### 5.4. CONCLUSIONS

The pyrolysis of corn cob samples was studied by a model of DAEM partial reactions at linear and stepwise heating programs. Four pseudocomponents were used, corresponding to the thermal decomposition of pectin (1); hemicelluloses (2); cellulose (3); and a wide, low reaction rate process that involved the lignin decomposition and the slow carbonization of the formed charcoals.

The pyrolysis of two different corn cob samples from different continents and climates were found similar except that the small pectin peak occurred only in one of the samples and some reactivity differences arose in the hemicellulose pyrolysis. When the experiments of the two samples were evaluated together, the following parameters required different values in the two samples: the weight factors of the partial peaks ( $c_j$ ) and the preexponential factor of the hemicellulose ( $A_2$ ). Note that the lack of the pectin peak corresponds to  $c_1 = 0$  in the model. Eight parameters ( $E_{a02}$ ,  $E_{a03}$ ,  $E_{a04}$ ,  $\sigma_2$ ,  $\sigma_3$ ,  $\sigma_4$ ,  $A_3$ , and  $A_4$ ) could be assumed identical in the two samples without a notable worsening of the fit quality.

The parameter values obtained at the joint evaluation of other biomass samples (corn stalk, rice husk, sorghum straw, and wheat straw) in work published by Várhegyi et al. [308] were similar to their counterparts of the present work. The values from the earlier work proved to be applicable for the corncob model, too. When the  $E_{a0}$  and  $\sigma$  values were employed as fixed parameters, high fit quality was observed. When the  $A$  values of the earlier work were also included as fixed parameters, a rougher, but still usable approximation was obtained. These observations suggest that it is possible to construct common models for wide ranges of biomass materials. If a rough approximation is enough, then only the parameters related to the sample compositions  $c_j$  should be varied from biomass to biomass.

When  $n$ -order kinetics was employed instead of the DAEM partial reaction, similar fit qualities were obtained. However, the  $n$ -order kinetics describes the complexity of the biomass materials in a rather formal way while a DAEM gives a simplified, but clear picture on the different reactivities of the different biomass species.

All the results in this work were checked by prediction tests. In these tests, 20°C/min experiments were simulated by the model parameters obtained from the evaluation of the experiments with stepwise  $T(t)$  and linear  $T(t)$  with slower heating rates.

An important aim of the kinetics is to produce submodels that can be coupled with transport phenomena to describe practical conversion systems. The coupling itself is obviously easier with models consisting of a few first-order reactions. A problem with the first-order kinetics, however, is that the activation energy is nearly inversely proportional to the peak width of the DTG curves at linear heating.

Accordingly, the flat, wide pyrolysis sections appearing at linear heating result in low formal activation energy values in the models based on first-order kinetics. This problem does not arise in the DAEMs because DAEMs can describe wide, flat peaks with realistic magnitudes of activation energies. There are possibilities, however, to obtain reasonable approximations with two or three first-order partial reactions. According to the present state of the literature, the first-order models need a considerable higher number of partial reactions than the DAEMs to describe a wide range of observations with a comparable precision in biomass pyrolysis



## CHAPTER 6

*“Experiment adds to knowledge, Credulity leads to error. “*

*Anonymous*

*“The man of science has learned to believe in justification, not by faith, but by verification.”*

*Thomas Henry Huxley*

## 6. FIXED CARBON YIELD OF CHARCOAL FROM CORN COB PYROLYSIS

Charcoal have been manufactured by man for more than 38,000 years [69, 343] and are among the most important renewable fuels in use today. The charcoal production technology remains fairly inefficient [41, 68, 69, 72, 344, 345]. According to Antal and Mok [72] and Várhegyi et al [73], traditional methods for charcoal production in developing countries realize yields of 20 wt % (even less), and modern industrial technology offers yields of only 25 - 37 wt % [68, 73]. This charcoals has a fixed - carbon content of about 70 - 80 wt % and offers a fixed - carbon yield of about 20 - 24 wt % [67]. The low efficiency is due to the fact that pyrolysis process hastily transforms biomass into a tarry vapour between 250 and 400 °C [69]. The tarry vapours, which consists of complex of organic compounds mixed with noncondensable gases, quickly escape the heated region of the reactor without establishing equilibrium and without forming charcoal [69]. Because of inherent inefficiency in the process there is a substantial loss of carbon and energy from the biomass feedstock (primarily as CO<sub>2</sub>) and, because of the chemical process as well, a significant production of portion of tarry vapours.

From a theoretical perspective, charcoal production should be efficient and quick. Thermochemical equilibrium calculations indicate that carbon is a preferred product of biomass pyrolysis at moderate temperatures, with byproducts of CO<sub>2</sub>, H<sub>2</sub>O, CH<sub>4</sub>, and traces of CO [69, 71]. Antal et al. [68, 72, 74, 75] based on thermochemical equilibrium calculations, pointed that, at 1MPa and 400°C, the maximum yield of carbon from cellulose is 27.7 wt % (i.e., 62.4 mol % of cellulose carbon is converted into biocarbon). More detailed calculations, based on the actual composition of the sample led Antal et al [68] to the conclusion that the theoretical yield of charcoal from most biomass feeds, at 1MPa and 400°C, should be in the approximate range 55% (corn cobs with a carbon content of 45%) to 71% (Macadamia nut shells with a carbon content of 58%).

The questions arises is it possible to produce higher charcoal and fixed carbon yield at atmospheric pressure? Could large particles provide high fixed-carbon yields of charcoal at atmospheric pressure? Or, Could the relatively low fixed carbon yield obtained at atmospheric pressure be a result of small particles and facile mass transfer of volatiles away from the hot, pyrolyzing solid?

The aim of this experimental work was to identify process conditions that improve the yield of charcoal from corncob and to elucidate the effects of particle size on fixed-carbon yields at atmospheric pressure.

Research were based on hypothesis:

1. Increasing particle size substantially improves fixed-carbon yields. This improvement in yield is a result of increasing heterogeneous interactions between the pyrolytic vapours and the solid charcoal together with its mineral matter, both of which may be catalytic for the formation of charcoal.
2. Elevated pressure enables the carbonization of liquid tar before it can vaporize and escape the solid matrix.

The validity of these hypotheses were examine using two different corn cob samples.

The effect of the influence of particle size, sample size, and vapour-phase residence time on experimental values of the fixed carbon yields of the charcoal products were analysed and compared with values of the calculated theoretical limiting values.

Also, the present study included three thermobalances: (TA Q5000, TA Q600 and a Mettler Toledo TGA/SDTA 851e). It is known that for studies using low sample masses, under atmospheric pressure, there is no conclusive evidence on the importance of the gas flow rate, as long as the product gases are swept out from its vicinity [268]. The actual gas velocities around the sample depend highly on the geometry of the furnace. Both the diameter of the furnace and the way that the sample is shelter (geometry and material of the crucibles) due to the sensitiveness of the instruments are key factors that influence on experiment results.

Most of the results and discussion in this chapter have been already published by in paper Wang, L., **Trninic M** et al. [41].

## **6.1. EXPERIMENTAL SECTION**

A round-robin study of corn cob charcoal and fixed-carbon yields involved three different thermogravimetric analyzers (TGAs) revealed the impact of sample size, mass and vapour phase reactions on the fixed-carbon yields of the charcoal products.

The experimental plan included:

1. Three atmospheric pressure, thermogravimetric analyzers (TGAs): models TA Q5000 and TA Q600 of TA Instruments and a Mettler Toledo model TGA/SDTA 851e
2. Two different corn cob samples
  - 2.1. Samples of corn cobs obtained from Surcin, Belgrade's municipality in Serbia (ZP Maize Hybrid, ZP 505), denoted here as sample Scob.
  - 2.2. Samples of corn cobs obtained from Oahu, Hawaii, USA (Pioneer HiBred International), denoted here as sample Pcob.
3. Two different ways of samples preparation.
  - 3.1. Samples in powder form (the corn cob was ground in a cutting mill mounted with a 1mm sieve),
  - 3.2. Single particle samples (using a sharp knife, a thin cross-section was sliced from a whole corn cob; cubic particles corresponding to cube sizes from 2 to 6 mm),
4. Four different mass of samples: 5, 10, 20, and 40 mg.
5. Two groups of experiments:
  - 5.1. Experiments with open crucibles - samples were placed into the open crucible (without lid),
  - 5.2. Experiments with closed crucibles - samples were placed into the crucibles covered with the lid. Every lid had a small pinhole.
6. Experiments in muffle furnace
7. The characterisation of charcoal (elemental and proximate analysis)

Experimental matrix is presented in Figure 6. 1.

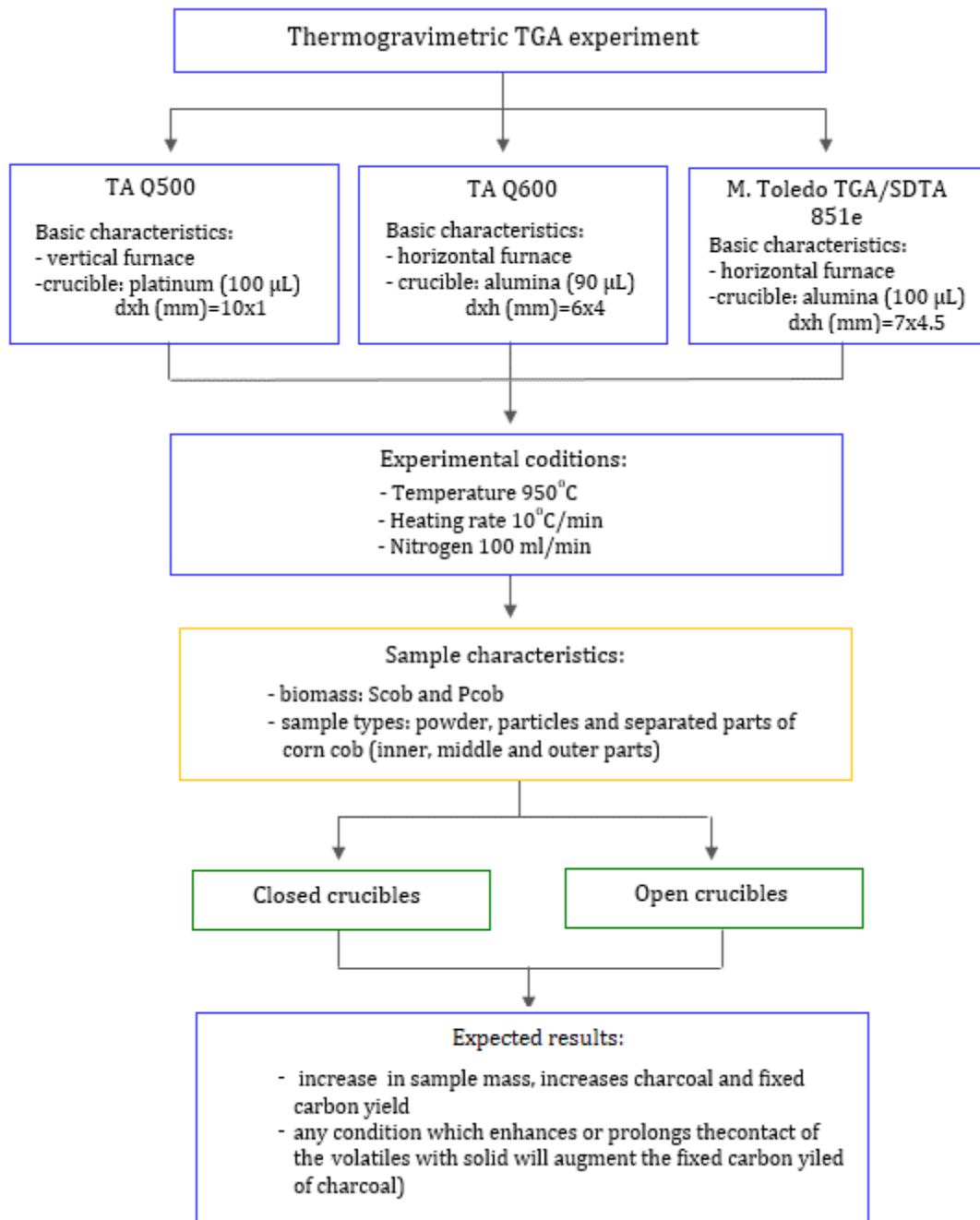


Figure 6.1 Experimental matrix with expected results

### 6.1.1. SAMPLES AND SAMPLES PREPARATION

#### **SAMPLE ORIGIN**

Grab samples of corn cobs were obtained from Serbia (ZP Maize Hybrid, ZP 505, denoted here as Scob) and Hawaii, USA (Pioneer HiBred International denoted here as Pcob).

#### **6.1.1.1. DRYING AND SAMPLE SIZE PREPARATION**

After receiving the corn cobs, they were put into a drying oven at 105 °C for about three days. Then the corn cobs were taken out of the drying chamber and prepared for the experimental procedure.

Each sample of corn cob was prepared for carbonization tests in two different ways

1. The corn cobs were grounded in a cutting mill mounted with a 1 mm sieve,
2. A thin cross-section was sliced from a whole cob. Photographs of this single particles are shown in Figure 6.2.

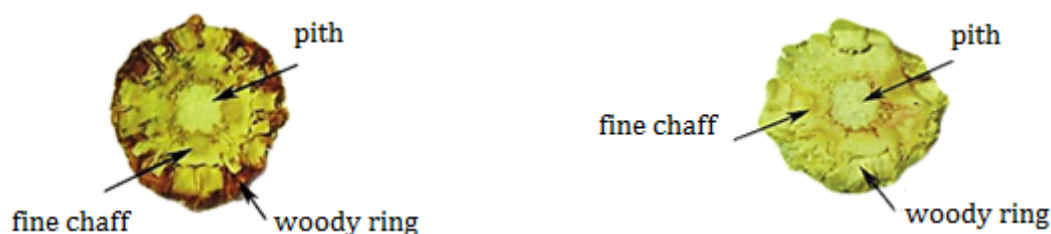


Figure 6.2 Cross-sectioned view of corn cob

After that, corn cob samples were stored in closed plastic bags. To guarantee that corn cob samples are without any moisture, a necessary amount was taken out of the bags or bottles and stored in glass crucibles in the drying oven (Termaks) at 105 °C for 24 hours before every experiment.

Characterisation of the corn cob samples (ultimate and proximate analysis) is already presented in Chapter 6.

### 6.1.2. EXPERIMENTAL APPARATUS AND EXPERIMENTAL PROCEDURE

Three atmospheric pressure, thermogravimetric analyzers (TGAs) were employed in this work: models TA Q5000 and TA Q600 of TA Instruments and a Mettler Toledo model TGA/SDTA 851e. Thermobalances are supported by a computer and software for control and data handling

A schematic diagram of the Thermal Instrument TA Q600 thermobalance is already shown in Figures 5.2. A schematic diagram of the Thermal Instrument TA Q5000 thermobalance is shown in Figures 6.3.

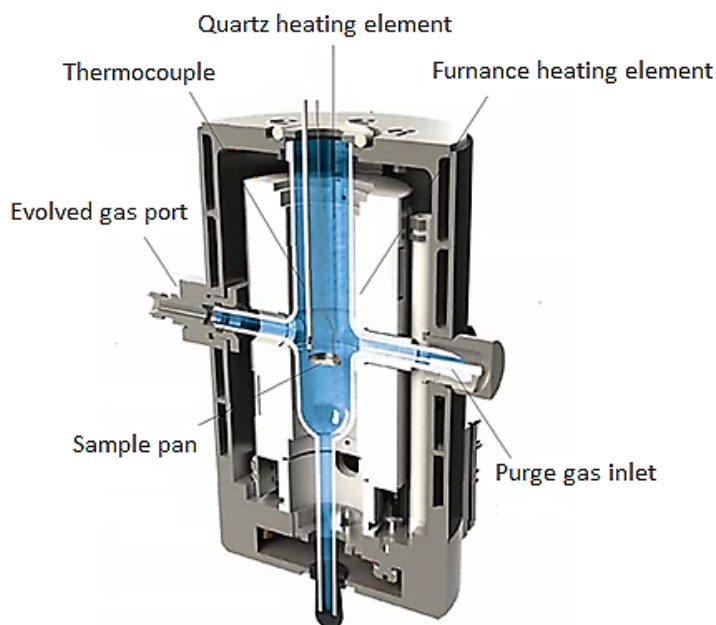


Figure 6.3 Schematic illustration of TA Q 5000 furnace part [39]

The Q5000 IR consists of a thermobalance, a furnace and an autosampler. The crucible hangs inside the furnace, which is radiantly heated by infrared lamps outside the furnace chamber. This allows very high heating rates compared to more traditional TGA's. Furthermore there are less temperature gradients present, which result in uniform heating of the sample, reduced weight error due to convection and more precise and reproducible temperatures. The furnace is insulated by multiple heat shields and a reflector to not influence the measuring equipment by the high temperatures in the furnace chamber [39]. The applicable range of linear heating 16 ranges from 0.1 °C/min up to 500 °C/min and with a ballistic heating rate the maximum is >2000 °C/min within the temperature range of ambient until 1200 °C [39]. The temperature is measured by a thermocouple with an isothermal temperature accuracy of +/- 1 °C [39].

A schematic diagram of Mettler Toledo model TGA/SDTA 851e is shown in Figures 6.4.

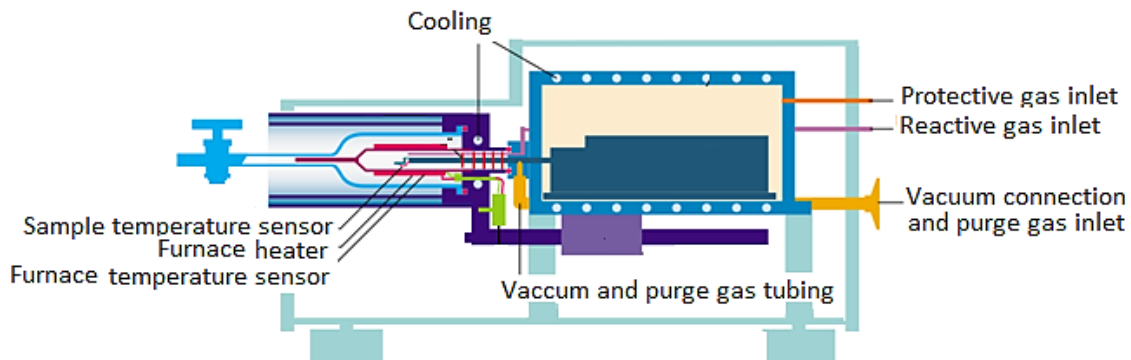


Figure 6.4 Schematic illustration of Mettler Toledo model TGA/SDTA 851e [40]

The system is based on a one beam horizontal design in which ceramic beam (balance arm) functions as part of a horizontal null-type balance. Balance arm accommodates the sample and measures its property changes. The horizontal furnace design helps minimize possible turbulence caused by thermal buoyancy and the purge gas. Model Mettler Toledo TGA/SDTA 851e that operates in the range 25 – 1100°C with a sensibility of 0.1 µg. In APPENDIX C technical specification of TGAs instruments are presented.

### ***CRUCIBLE/PAN CHARACTERISTICS***

Each thermogravimetric analyser (TGA) has different types of the sample holders (different geometry, material, depth, etc.). The type material and shape of the sample holder (crucible/pan) used for a measurement can have a large effect on the quality of the experimental results obtained. Considering the relevant factors before the measurement can often help to save time later on when interpreting the curve.

Deep crucibles may restrict gas flow more than flat. Also, reactions in the gas phase proceed more rapidly in completely open crucibles than in a so-called self-generated atmosphere. In a sealed crucible with a very small hole in the lid, or in a crucible with a lid without a hole placed loosely over the sample, the weight loss is shifted to a higher temperature [346].

In general, the material of which the crucible is made must not influence the reaction of the sample. However, platinum crucibles catalyse some reactions more than alumina (aluminium oxide) ones [347]. For example, platinum crucibles can promote combustion reactions. Sapphire crucibles are even more resistant and are especially suitable for the measurement of metals with high melting points, such as iron, which partially dissolve and penetrate ordinary alumina crucibles at high temperatures [347].

Regarding to mention Figure 6.5 and Table 6.1 summarize the geometry and depth of the crucibles and the pans used with each TGA.

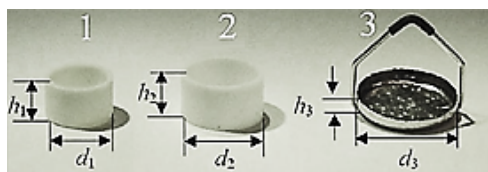


Figure 6.5 Crucibles/pans used in pyrolysis experiments [41]

Table 6.1 Specifications of Instruments and Their Crucibles/Pans [41]

Instruments	Crucible/ pan number.	Crucible/pan volume ( $\mu\text{l}$ )	Crucible geometry (d x h, mm)
TA Q600	1	90	6x4
Mettler Toledo TGA 851e	2	150	7x4,5
TA Q5000	3	100	10x1

### EXPERIMENT PROCEDURE

Before experiments, all samples of corn cob were dried in an oven at 105 °C for 24 h. All TGA runs employed nitrogen (99.99% pure) as purge gas with a flow rate of 100 ml/min. Prior to each experiment, a measured amount of corncob material (5, 10, 20, and 40 mg in single particle or powder form) was loaded into the appropriate crucible/sample pan. Each experiment was initiated with a 30 min purge at room temperature, followed by 30 min of drying at 105°C. Then, the sample was heated from 105 to 950 °C at a heating rate of 10 °C/min. This temperature program is summarized in Table 6.2.

Table 6.2 Temperature regime of Pyrolysis Experiment [41]

Step	Pyrolysis method				
	Dynamic	Isothermal	Time (min)	Heating rate (K/min)	Temperature (°C)
1		✓	30		25
2	✓			jump	25→105
3		✓	30		105
4	✓			10	105→950



## 6.2. EXPERIMENTAL RESULTS

### 6.2.1. PYROLYSIS BEHAVIOUR OF DIFFERENT CONSTITUENTS OF A CORN COB

Figures 6.6 and 6.7 are weight loss curves to 550 °C (not 950 °C) for the inner (pith), middle (woody ring), and outer (fine chaff) parts of Pcob and Scob compared to the relevant powder sample.

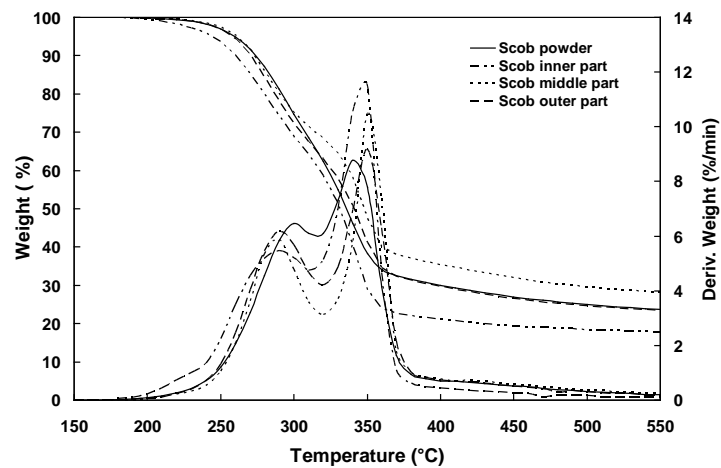


Figure 6.6 Pyrolysis and charcoal yield behaviour of different constituents of a corn cob (Scob) thin cross-section in an open crucible

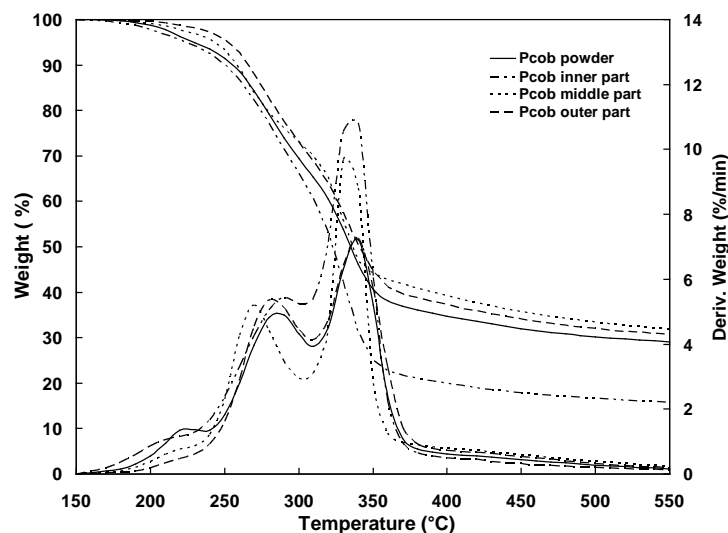


Figure 6.7 Pyrolysis and charcoal yield behaviour of different constituents of a corn cob (Pcob) thin cross-section in an open crucible

The Pcob and the Scob woody rings give the highest charcoal yields, whereas the powders give average yields between those of the woody rings and the inner piths that offer the lowest yields. Charcoal yields, at 550 °C are between 20 – 30%.

### 6.2.2. FIXED CARBON YIELDS

Here, the fixed – carbon yield values obtained under different experimental conditions are compared with the thermochemical equilibrium value of the fixed-carbon yield and values of the fixed-carbon yield obtained from proximate analysis of corn cobs.

#### ***THEORETICAL FIXED-CARBON YIELD***

The thermochemical equilibrium value of the fixed-carbon yield (the theoretical yield of carbon) represents the upper limit attainable by thermal processes [348]. The theoretical yield of carbon constitutes a benchmark against which the experimental values can be compared. The equilibrium yields of the products of biomass pyrolysis as a function of the reaction temperature and pressure is calculated by use of StanJan software [349]. When the (N), (S), and ash contents of the cobs are neglected, these elemental analyses can be used to calculate the yields of the pyrolysis products as a function of the pressure when thermochemical equilibrium is achieved at 400°C [41]. Figure 6.8 displays *theoretical equilibrium yields* of the products of corn cob as a function of the pressure at 400°C.

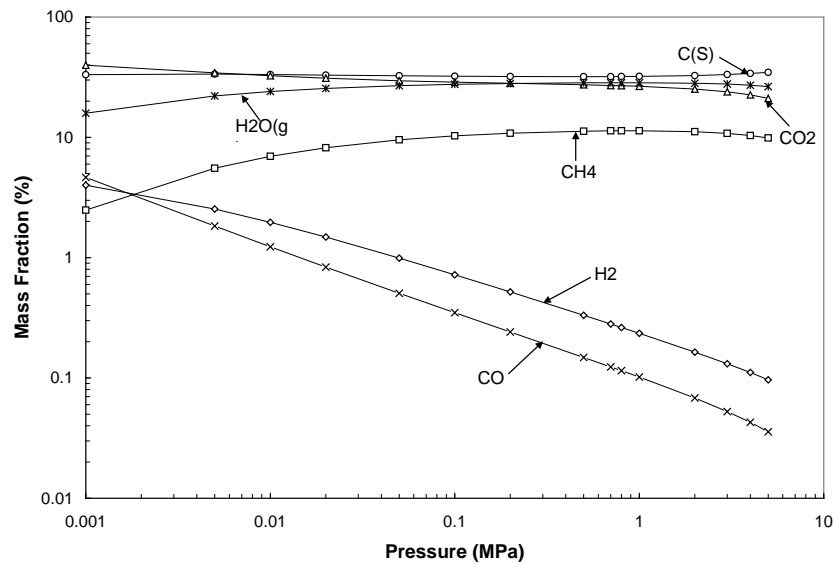


Figure 6.8 Effects of pressure on corn cob pyrolysis following the attainment of thermochemical equilibrium at 400 °C (results derived by StanJan software)

For  $S_{cob}$  and  $P_{cob}$ , theoretical fixed – carbon yield is:

$$y_{fc}^{th}(S\ cob) \approx 32.40 \% \quad (6.1)$$

$$y_{fC}^{th}(\text{P cob}) \approx 32.80 \% \quad (6.2)$$

It should be noted that in the StanJan calculations, the presence of nitrogen and sulphur are neglected. This is a consequence of the fact that these two elements compose only a small fraction of the mass of the biomass feed [67]. Moreover, StanJan makes no provision for their presence in solid chemical compounds that could be found in the product mixture [67]. Also, the ash content of the feed is also neglected. In general, StanJan predicts that solid C and the gases CO<sub>2</sub>, H<sub>2</sub>O, and CH<sub>4</sub> should be the only significant products present in equilibrium and that the distribution of these products is not strongly dependent upon either the assumed pyrolysis temperature or the assumed pressure [67, 69, 71].

Minerals in biomass, particularly the alkali metals, can have a catalytic effect on pyrolysis reactions leading to increased charcoal yields in some circumstances, in addition to the effect of ash contributing directly to charcoal yield. Philpot [69, 350], completed an extensive study of the influence of mineral matter on the pyrolysis of various plant materials. In general, higher charcoal yields were obtained from feedstocks with higher ash contents, but the effect was less strong above 5% ash content. Furneaux and Shafizadeh [69, 351], removed the mineral matter from ivory-nut meal by acid washings and observed a decrease in the char yield from 33 to 22%. Raveendran et al. [69, 352], also reported an increase in volatile yields as a result of de-ashing in some cases, but in the case of rice hulls and groundnut shells, the charcoal yield increased after deashing. The theoretical yield of the fixed-carbon (thermochemical equilibrium value) constitutes a benchmark against which the experimental values can be compared. According to Antal et al [67], the theoretical yield of carbon, which we hypothesize to be the upper limit attainable by thermal processes. The disparity between practice and theory indicates the improvements in yield that can potentially be realized by informed chemical reaction engineering of the carbonization process.

#### **THE FIXED-CARBON YIELDS OFFERED BY PROXIMATE ANALYSIS**

$$y_{fc} = \frac{fC}{(fC + VM)} \cdot 100, \% \quad (6.3)$$

Respectively, for Scob and Pcob:

$$y_{fC}^{Scob} = 17.73 \% \quad (6.4)$$

$$y_{fC}^{Pcob} = 18.23\% \quad (6.5)$$

## FIXED CARBON YIELDS OFFERED BY EXPERIMENTS WITH OPEN CURCIBLES

### EXPERIMENTS WITH CORN COB SINGLE PARTICLES

Figure 6.9 displays the effects of particle size on charcoal yields at 950°C as measured by the three TGA instruments.

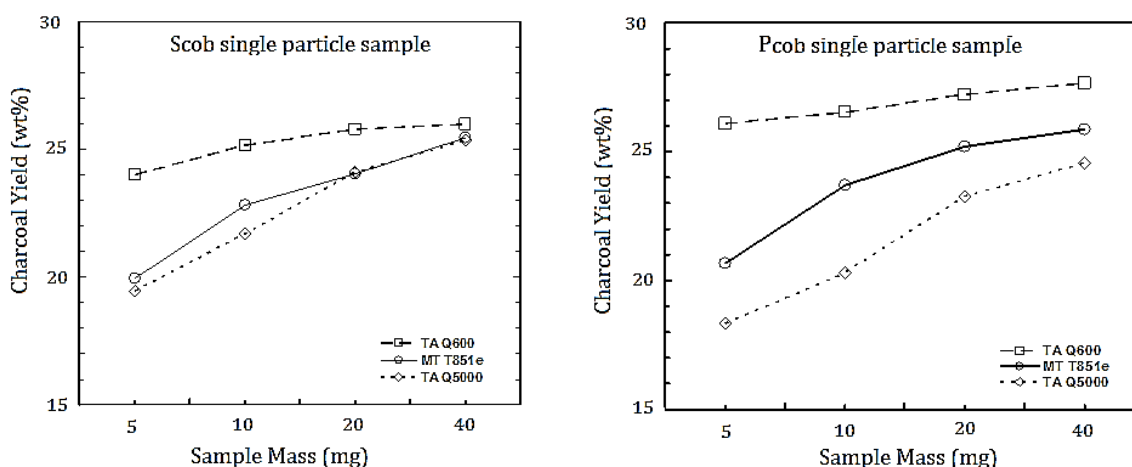


Figure 6.9 Influence of different instruments on one corn cob single particle sample charcoal yield in an open crucible

It should be noted that particle are cut from the woody ring of corn cobs. Since the woody ring is not representative of the composition of the whole cob, the charcoal and fixed-carbon yields cannot be directly compared to those of whole cobs. Upon heating particle samples decomposes by an unknown series of bond-breaking reactions. The species formed by this initial step may be sufficiently immobile to preclude rapid escape from the particle [353, 354]. Consequently they may undergo additional bond-breaking reactions to form volatiles or may experience condensation/polymerization reactions to form higher molecular weight products including charcoal [354]. During transport within the particle volatile species may undergo further reactions homogeneously in the gas phase or heterogeneously by reaction with the solid biomass or charcoal. The rate of volatiles mass transport within and away from the particle will influence the extent of these intraparticle secondary reactions [353, 354]. After escaping the particle, the tars and other volatiles may still undergo secondary reactions homogeneously in the vapor phase

or heterogeneously on the surface of other biomass or charcoal particles, [353, 355]. Depending on reaction conditions intra- and/or extra-particle secondary reactions can exert modest, to virtually controlling influence on product yields and distributions from wood pyrolysis [354].

For all of the cobs in all of the instruments, the charcoal yield increases with an increase in particle size. Furthermore, the TA Q600 instrument realizes a significantly higher charcoal yield than the other instruments (TA Q500 and MT T851e). The TA Q600 employs a narrow, deep crucible (Figures 6.6 and Table 6.2) that isolates the sample from the flow of purge gas and thereby enhances secondary reactions.

### EXPERIMENTS WITH CORN COB POWDER SAMPLES

Figure 6.10 display similar results representing the effects of sample size with two of the three cob powders on their respective charcoal yields. However, the charcoal yields from the powders are lower than the comparable yield from single cubes.

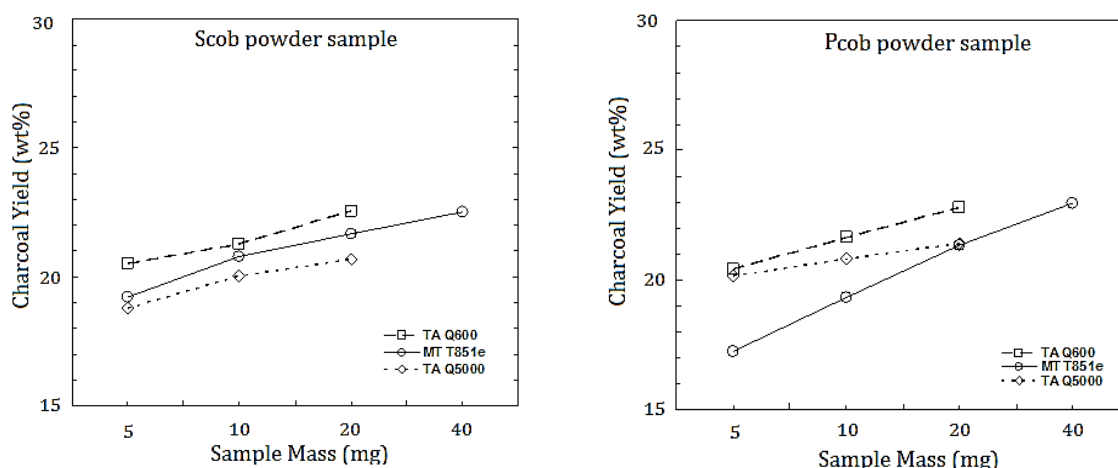


Figure 6.10 Influence of different instruments on corn cob powder sample charcoal yield in an open crucible

The lower yields may reflect compositional differences, as well as the reduced dimensions of the particles. According to Gavalas [356] and Janke [148] milled and sieved samples may have different composition due to different milling characteristics of minerals present in sample; fine particles contains more mineral than larger one. It is known that the generation of volatile gases inside the solid produces high pressures (up to 0.3 atm [357], depending on the biomass porosity), which force the volatiles toward both the hot charcoal layer and the interior of the solid [358, 359]. The intra-particle

contact between freshly formed pyrolysis oil vapours and charcoal/ash particles might lead to an increase in secondary repolymerization reactions. Tar trapped within the particles followed by polymerization/charring reactions could be an additional explanation for the higher charcoal yields.

### FIXED CARBON YIELDS OFFERED BY EXPERIMENTS WITH CLOSED CRUCIBLES

Figures 6.11 and 6.12 display the influence of closed crucibles with a small pinhole opening on charcoal yields for Pcob and Scob cubes and powder samples in the TA Q600 and MT T851e instruments.

In virtually all cases, the closure of the crucible substantially enhances the charcoal yield. Conditions that improve or prolong the contact of vapour-phase pyrolysis species with the solid serve to enhance the charcoal yield. The intermediates undergo further water-catalysed decomposition reactions giving charcoal, water and gases. These observations corroborate earlier work and reveal the importance of secondary reactions involving vapour-phase species in the formation of charcoal. Nevertheless, the yields remain significantly below the theoretical fixed-carbon yields.

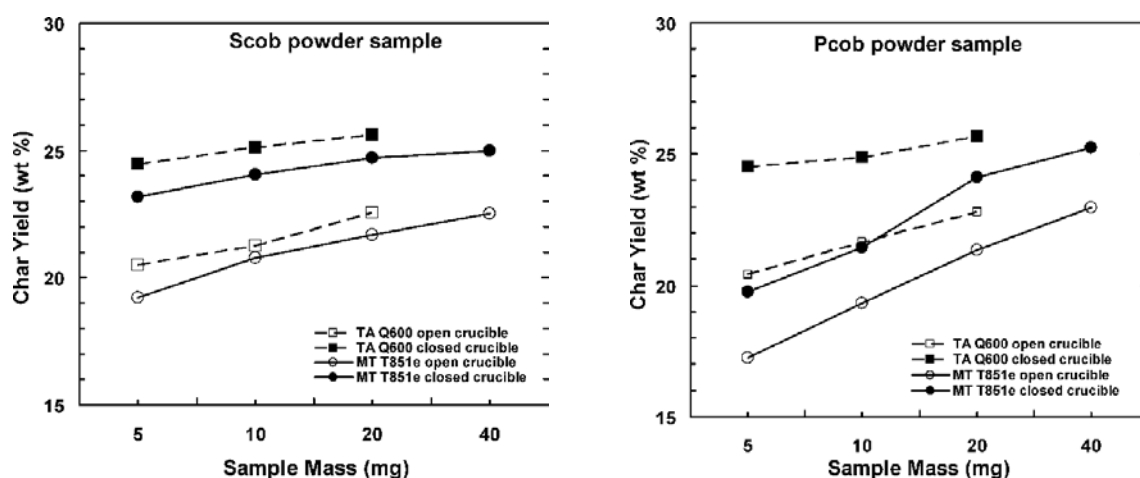


Figure 6.11 Effects of open versus closed crucible on Scob and Pcob powder sample charcoal yield

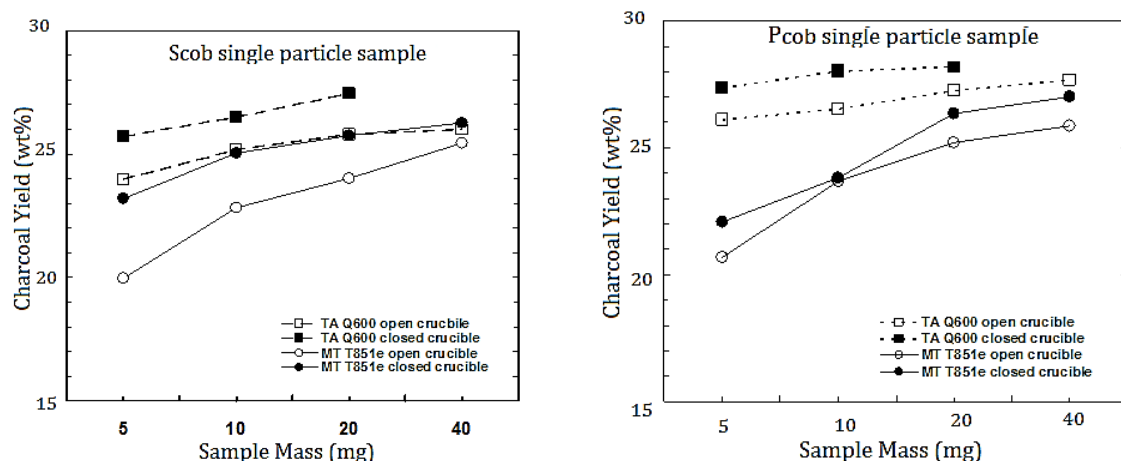


Figure 6.12 Effects of open versus closed crucible on Scob and Pcob particles sample charcoal yield

In Table 6.3 are listed values of the estimated fixed-carbon yields for the TA Q600 as a function of the sample size with open and closed crucibles.

Table 6.3 Charcoal and Fixed-Carbon Yields Realized in the TA Q600 [41]

Sample	Mass	Y <sub>char</sub> (%wt)		y <sub>fc</sub> * (%wt) <sup>a</sup>	
		Open crucibles	Closed crucibles	Open crucibles	Closed crucibles
Scob	(5 mg)	20.52	24.46	19.14	22.81
	(10 mg)	21.28	25.14	19.84	23.44
	(20 mg)	22.56	25.62	21.04	23.89
Pcob	(5 mg)	20.43	24.51	19.27	23.12
	(10 mg)	21.64	24.87	20.41	23.46
	(20 mg)		25.66	21.50	24.20

\* Y<sub>fc</sub> = Y<sub>char</sub> (100 - %VM - % char\_ash)/(100 - % A)

All estimated values exceed the comparable y<sub>fc</sub> obtained by the proximate analysis procedure. In all cases, larger sample sizes offered enhanced charcoal and estimated fixed carbon yields. In all cases, the closed crucible increased the estimated fixed-carbon yield by about 22 - 20%; nevertheless, even the closed crucible yields are much lower than the theoretical fixed-carbon yield.

### FIXED-CARBON YIELDS REALIZED AT ATMOSPHERIC PRESSURE IN A MUFFLE FURNACE

The charcoal sample remaining in the TGA from these runs was too small to ash. To obtain an estimate of the fixed-carbon yield, we employed the volatile matter and ash contents of charcoals heated to the same final temperature in the N<sub>2</sub>-purged muffle furnace. Corn

cob samples were placed in ceramic crucibles and thereafter covered with a lid. Then, the crucibles were placed in the retort (approximately 0.004 m<sup>3</sup>) that was covered with a metal lid prior to insertion into the muffle furnace (approximately 0.009 m<sup>3</sup>). The retort was purged with nitrogen for 30 min before heating as well as during the run to ensure carbonization in an inert atmosphere. The furnace was heated from room temperature to 950 °C with a heating rate of 5°C/min. The proximate analysis of charcoal are determined according to the ASTM standard (ASTM D 1762 – 84 (2007)).

In the muffle furnace heated to 950°C, covered crucibles with samples are placed. Samples are heated in three steps: with the furnace door open, for 2 min on the outer ledge of the furnace (300°C), then for 3 min on the edge of the furnace (500°C), then the samples are moved to the rear of the furnace for 6 min with the muffle door closed. After heating, samples are cooled down in a desiccator for 1 h and weighed. After volatile matter determination, samples are placed in in the muffle furnace at 750°C for 6 h, then cooled down in a desiccator for 1 h and weigh.

The percentage of fixed carbon in charcoal samples:

$$f_c^* = 100 - VM\% - ash\%, \text{ (wt \% db)} \quad (6.6)$$

Table 6.4 displays comparable charcoal yields obtained from whole cobs in closed crucibles under nitrogen in a muffle furnace at 950°C. Table 4.5 also displays proximate analyses of the muffle furnace charcoals that allow us to calculate the fixed carbon yields obtained from whole cobs at atmospheric pressure.

Table 6.4 Charcoal and fixed-carbon yields realized in a muffle furnace

sample	Proximate analyses (wt % db)				
	VM	fC	ash	y <sub>char</sub>	y <sub>fC</sub>
Scob	4.69	91.90	3.41	26.52	24.73
Pcob	4.61	91.85	3.54	26.77	25.25

The charcoal yield is higher than those given by TGA experiments.

Table 6.5 displays compared results of fixed carbon yield based on proximate, ultimate and experimental analysis. The lower fixed-carbon yields were realized from whole cobs in the muffle furnace under nitrogen, and these yields were nearly identical to the yields obtained from cob cross-sections under nitrogen in the microTGA. Still lower yields were obtained from powders in closed crucibles under nitrogen. Even lower yields were



obtained from powders in open crucibles under nitrogen. In all cases, the closed crucible increased the estimated fixed-carbon yield by about 15-20%. The lowest yields were delivered by the proximate analysis laboratory procedure; these were about 2/3 of those obtained at elevated pressure in practical equipment.

Table 6.5 Fixed-carbon yields realized by different approach (theoretical and experimental)

Sample	$y_{fc}$ (wt %)			
	$y_{fc}^1$	$y_{fc}^{th2}$	Open crucible	Closed crucible
Scob	17.73	32.40	19.14 – 21.04	21.81 – 23.89
Pcob	18.23	32.80	19.27 - 21.50	23.12 - 24.20

1 – Fixed carbon yield estimated by proximate analysis  
 2 – Theoretical carbon yield

The parity plot displayed in Figure 6. 13 summarizes findings.

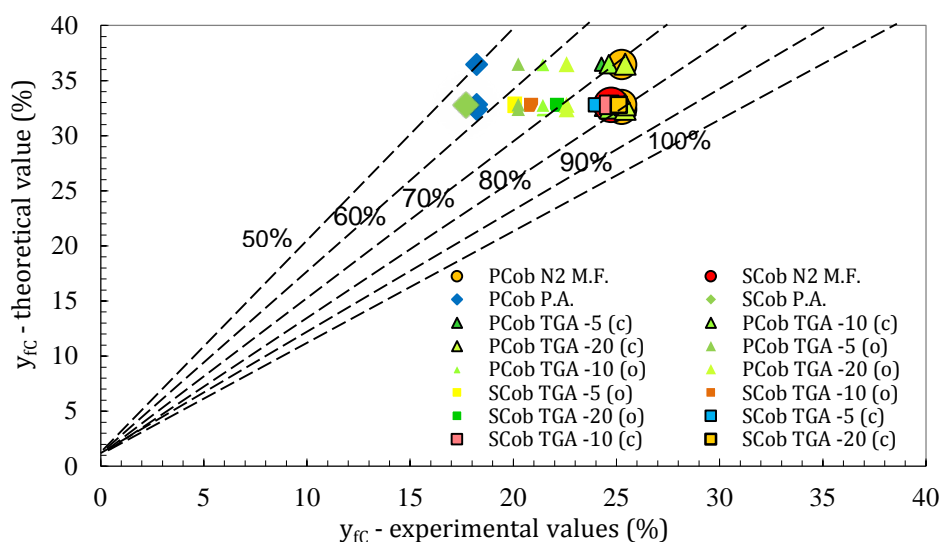


Figure 6.13 Parity plot displaying the experimental vs theoretical values  
 M.F. – results obtained from muffle furnace  
 TGA – results obtained from TGA  
 5(c), 10(c), 20(c) – with use of closed crucibles with 5,10 and 20mg samples  
 5(o), 10(o), 20(o) – with use of open crucibles with 5,10 and 20mg samples  
 P.A. – results calculated using the ultimate elemental analyses

Ordinate values of the parity plot represent the theoretical fixed-carbon yields, abscissa values represent experimental measurements of the fixed-carbon yields. The dashed diagonal lines indicate the percentage attainment of the theoretical yield. The highest yields obtained in this work were delivered by the muffle furnace process, realizing fixed-

carbon yields ranging 70-80% from of the theoretical limit. This values are closed to values given by experiments with closed crucibles ( $\approx 65 - 80\%$  of the theoretical limit).

To further explore the effects of the particle size on charcoal yield, it was sieved 10 g samples of the ground Pcob and Scob and measured the charcoal yield from each of the sieved samples (eight different particle sizes) using the MT T851e instrument.

Figure 6.14 displays the particle size distributions obtained from the two ground cob samples, while Figure 6.15 displays the charcoal yields. Both cobs provide evidence of nearly identical behaviour, with a steady increase in the charcoal yield from 15.2 to 23.5 wt % as the particle size increased from 0.063 - 0.125 to 2.5 - 3.0 mm. The particle size has a strong effect on the charcoal yield. This particle size effects on charcoal yields to mineral speciation. Bridgeman et al [360], showed that smaller particles are known to have higher concentrations of minerals than larger particles because of ash speciation by grinding, and the catalytic nature of the mineral matter caused the pyrolysis temperature of the smaller particles to decrease. However, minerals catalyse the formation of charcoal consequently, a putative increase in the mineral content of the smaller particles in our work would cause an increase in their charcoal yield and not a decrease [360].

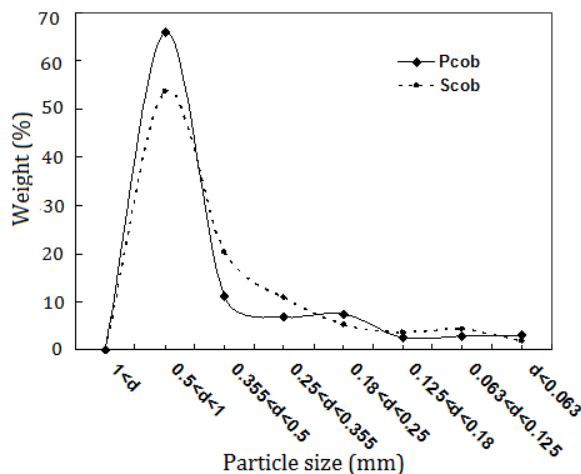


Figure 6.14 Particle size distributions of ground Pcob and Scob samples

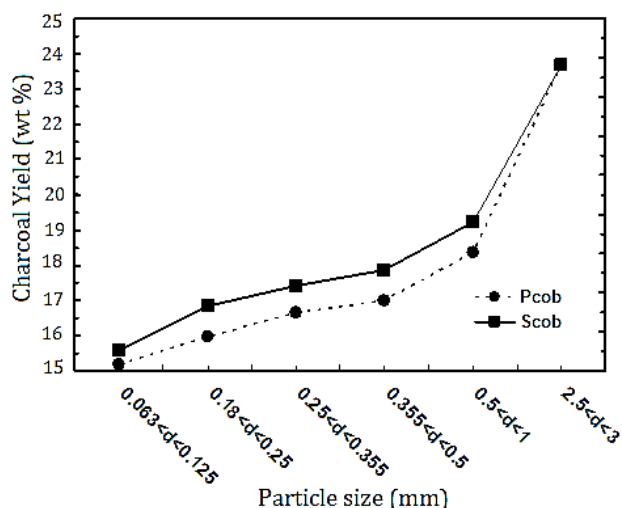


Figure 6.15 Influence of the particle size on Pcob and Scob charcoal yield (sample mass of 10 mg)

a - Representing charcoal yields from Pcob and Scob as single particle samples with a particle size of 2.5 – 3.0 mm

### INFLUENCE OF PRESSURE ON FIXED-CARBON YIELDS REALIZED

Influence of pressure on fixed-carbon yield is tested in a pressure vessel (the FC reactor) at the University of Hawaii (UH), College of Tropical Agriculture and Human Resources, Oahu, USA. Because of importation difficulties Scob was not tested in Hawaii. Instead of Scob similar type of corn cob (Wcob<sup>20</sup>) was tested (Table 6.6 nas 6.7). On the other hand, unlike any other biomass which UH have tested, Pcob ignites prematurely at elevated pressures in FC equipment.

Table 6.6 Ultimate Analyses of Wcorn cobs

Sample	Ultimate analysis (wt % db)						Sum
	C	H	O	N	S	ASH	
Wcob	47.79	6.37	43.19	0.52	0.09	2.04	100.00

Table 6.7 Proximate Analysis, Heating Value, and Fixed Carbon Yield of corn cobs

Sample	Proximate analysis (wt %)				
	MC*	VM	A	fC	HHV (MJ/kg)
Wcob	4.18	80.32	2.04	17.64	18.43

\*Moisture content on a wet mass basis

<sup>20</sup>Grab samples of Wcob were obtained from the Waimanalo farm of the UH College of Tropical Agriculture and Human Resources, Oahu, Hawaii

The Wcob feed was placed in a canister that was subsequently loaded into the top of the FC reactor that was then pressurized with air to 0.8 MPa. Electric heating coils at the bottom of the pressure vessel ignited the lower portion of the biomass. After the specified ignition time, compressed air was delivered to the top of the pressure vessel and flowed through the packed bed of feed to sustain the carbonization process. After sufficient air was delivered to carbonize the corncob, the airflow was halted and the reactor cooled overnight. The charcoal was removed from the reactor and proximate analysis (i.e., ASTM D 1762-84) was performed.

The Wcob was also pyrolysed in muffle furnace (at atmospheric pressure).

The atmospheric pressure value of 24.86 wt % is less than the FC fixed-carbon yields that range from 25.5 to 28.0 wt %, Table 6.8.

Table 6.8 Fixed-carbon yields realized by different approach (theoretical and experimental)

Sample	$y_{fc}^1$	$y_{fc}^{th2}$	$y_{fc}$ (wt %)		
			Open crucible	Muffle furnace	FC reactor
Wcob	18.01	33.1	24.73	24.86	26.74

1 - Fixed carbon yield estimated by proximate analysis

2 - Theoretical carbon yield

In agreement with work of Antal et al [67] pyrolysis at elevated pressure representing practical conditions offers a nominal 10% increase in the fixed-carbon yield above that which can be obtained under nitrogen at atmospheric pressure using an externally heated electrical furnace.

The highest yields obtained in this work were delivered by the FC process operating at elevated pressure, realizing fixed-carbon yields ranging from 70 - 90% of the theoretical limit.

### 6.2.3. THE ELEMENTAL ANALYSIS OF CHARCOAL

The energy dispersive X-ray spectroscopy (EDX) was used for the elemental analysis of a sample. EDX is a chemical microanalysis technique used in conjunction with scanning electron microscopy (SEM). All elements from boron through the periodic table can be detected with sensitivities of approximately a few tenths of one percent. When the sample is bombarded by the SEM's electron beam, electrons are ejected from the atoms

comprising the sample's surface. The resulting electron vacancies are filled by electrons from a higher state, and an X-ray is emitted to balance the energy difference between the two electrons' states [361]. The X-ray energy is characteristic of the element from which it was emitted. The EDS X-ray detector measures the relative abundance of emitted X-rays versus their energy. When an incident X-ray strikes the detector, it creates a charge pulse that is proportional to the energy of the X-ray [361]. The charge pulse is converted to a voltage pulse (which remains proportional to the X-ray energy) by a charge-sensitive preamplifier, then sent to a multichannel analyser where the pulses are sorted by voltage [361]. The energy, as determined from the voltage measurement, for each incident X-ray is sent to a computer for display and further data evaluation [361]. The spectrum of X-ray energy versus counts is evaluated to determine the elemental composition of the sampled volume [361].

The results of the EDX analyses are given in Table 6.9.

Table 6.9 SEM EDX Analyses of Scob charcoal, (wt %)

element	Open crucible					Closed crucible				
	sample					sample				
	1	2	3	4	5	1	2	3	4	5
C	82.17	85.85	74.51	82.71	68.26	80.89	86.70	88.66	85.96	86.12
O	11.34	12.71	13.83	14.28	5.37	13.84	10.40	9.16	10.81	10.92
K	5.10	1.20	8.76	1.94	19.02	2.74	2.62	2.06	2.86	2.65
Cl	0.07	0.01	0.11	0.01	0.39	0.10	0.04	0.01	0.04	0.02
Mg	0.60	0.11	1.06	0.39	1.58	0.67	0.05	0.01	0.13	0.05
Ca	0.28	0.08	0.43	0.09	1.00	0.17	0.13	0.09	0.15	0.13
Na	0.17	0.04	0.33	0.45	0.76	0.37	0.04	0.01	0.04	0.08
P	0.11	0.00	0.34	0.02	1.51	0.03	0.00	0.00	0.00	0.01
S	0.08	0.00	0.18	0.04	0.78	0.03	0.00	0.00	0.00	0.00
Si	0.08	0.00	0.45	0.07	1.34	1.18	0.00	0.00	0.00	0.00

The high carbon content of the closed crucible sample may result from carbonization of the tarry vapours that could coat the surface with carbon. Charcoal is rich with carbon and oxygen and poor with mineral matters.

Haykiri-Acma [362], described an increase in the particle size of hazelnut shells particles from 0.15 to 1.4 mm that caused an increase in the charcoal yield for 28.3 wt %.

The secondary reactions involving vapour-phase species are at least as influential as primary reactions in the formation of charcoal. Conditions that improve or prolong the

contact of vapour - phase pyrolysis species with the solid enhance the fixed-carbon yield of charcoal.

In a hot environment, vapour - phase pyrolysis species quickly decompose into carbon and gases, especially in the presence of catalytic mineral matter or solid carbon. Edye et al. [363] described that the alkali metal and calcium wood samples showed increased charcoal formation, low tar and high distillate yield compared to acid-washed wood. Nowakowski et al. [364], investigated cell-wall components (cellulose, hemicellulose (oat spelt xylan), lignin (Organosolv<sup>21</sup>), and model compounds (levoglucosan (an intermediate product of cellulose decomposition) and chlorogenic acid (structurally similar to lignin polymer units) to probe in detail the influence of potassium on their pyrolysis behaviours as well as their uncatalysed decomposition reaction. Cellulose and lignin were pretreated to remove salts and metals by hydrochloric acid (HCl), and this dematerialized sample was impregnated with 1% of potassium as potassium acetate (CH<sub>3</sub>COOK) [364].

Experimental results shown that potassium-catalysed pyrolysis has a huge influence on the charcoal formation stage and increases the charcoal yields considerably (from 7.7% for raw cellulose to 27.7% for potassium impregnated cellulose; from 5.7% for raw levoglucosan to 20.8% for levoglucosan with CH<sub>3</sub>COOK added) [364]. Major changes in the pyrolytic decomposition pathways were observed for cellulose, levoglucosan and chlorogenic acid [57]. The results for cellulose and levoglucosan are consistent with a base catalysed route in the presence of the potassium salt which promotes complete decomposition of glucosidic units by a heterolytic mechanism and favours its direct depolymerization and fragmentation to low molecular weight components (e.g. acetic acid, formic acid, glyoxal, hydroxyacetaldehyde and acetol) [57]. Base catalysed polymerization reactions increase the charcoal yield. Potassium-catalysed lignin pyrolysis is very significant: the temperature of maximum conversion in pyrolysis shifts to lower temperature by 70 K and catalysed polymerization reactions increase the charcoal yield from 37% to 51% [57]. The catalytic nature of the charcoal surface, inclusive of its carbon and its mineral matter content that leads to coke (i.e., secondary charcoal) formation from the tarry pyrolysis vapours [57]. To the best of this knowledge, charcoal was first used in the early 80s for catalytic cracking of wood tars [57].

---

<sup>21</sup>, Organosolv is extraction processes that can be used to separate lignin and other useful materials from biomass. Typical process conditions: Temperature - 160-200 °C, Time - 15-120 min, Pressure - 5-30 bar

The highest fixed-carbon yields are realized at experiments with closed crucibles. The closed crucible hinders the egress of volatiles and therefore pressure inside the crucible increases. [57]. Elevated pressure raises the saturation pressure and saturation temperature of tar, thereby delaying its transfer to the vapour phase and favouring the tar coking reactions that enhance the formation of charcoal [57]. Also, elevated pressure increases the partial pressure of the tarry vapours within the charcoal pores, thereby enhancing the coke forming, vapour-phase secondary reactions. In these ways, elevated pressure augments the fixed-carbon yields [57].

This insight was corroborated by Elyounssi et al. [57, 365], who enclosed thuja wood in spheres of clay wrapped with aluminum foil and thereafter heated the package at atmospheric pressure for long times at low temperatures to realize high fixed-carbon yields of charcoal. In this case, the clay enclosure wrapped in aluminum foil served the same role as pressure in restricting the escape of the pyrolytic vapours from the vicinity of hot pyrolyzing solid [365]. When the clay and aluminium wrapping was removed, the charcoal and fixed-carbon yields fell dramatically [365]

Similar results Liang et al. [57] described with experiments with red and white oak woods, laurel wood and sweetgum wood. The particle size strongly influences charcoal and fixed-carbon yields determined by the TGA [57]. For example, an increase in particle size from less than 0.125 mm to 7 mm increases the (open crucible at 0.1 MPa) charcoal yield at 950°C from 15% to 21% [57]. Also, the confinement of pyrolysis volatiles in closed crucibles enhances the charcoal and fixed-carbon yields measured by the TGA instruments [57]. For example, the measured charcoal yield from 40 mg of oak powder in an open crucible is 17% (see conclusion 3 above), whereas the value in a closed crucible is 21% [57]. The closed crucible value is about 63% of the theoretical fixed-carbon yield for oak [57]. In Table 6.10 compared results for red oak and sweet gum and Scob are presented.

The findings presented here suggest that the sample mass, particle size, and confinement of volatiles, any of which enhance the rates of secondary reactions, may be more important determinants of charcoal yield than heating rate [41, 57].

Table 6.10 Fixed-carbon yields realized by different approach (theoretical and experimental) of corn cob and some type of wood [41, 57]

	$y_{fc}^{th1}$	$y_{fc}^2$	$y_{fc}$		$y_{char}$	
			open crucible	closed crucible	open crucible	closed crucible
Read oak	32.7-34.9	16.87-14.15	15.46	19.20	16.87	21.28
Sweet gum	34.9-35.8	14.09-14.38	13.86	19.61	15.74	21.95
Corn cob	32.40	17.73	19.14-21.04	21.81-23.89	19.14-21.04	21.81-23.89

1 - theoretical yield of fixed carbon

2 - fixed carbon yield based on proximate analysis

### 6.3. DISCUSSION

Varhegyi et al. described an increase in the charcoal yield from 5 to 19 wt % when the pyrolysis of 1 mg samples of Avicel cellulose was conducted in covered (with pinhole) versus open crucibles. In particular, an important recent study by Shen et al. described an increase in the particle size of Australian Eucalyptus loxophleba wood particles from 0.18 to 1.5 mm that caused an increase in the charcoal yield from 14 to 20 wt %. This finding revealed the role of secondary reactions involving the interactions of pyrolytic volatile matter with the solid sample in the formation of charcoal and confirmed the speculation of Bradbury et al. that “the residence time of the volatiles in the cellulose during the pyrolysis reaction largely influences the extent of charcoal formation”.

Other evidence corroborating the importance of secondary reactions in charcoal formation includes:

1. The reduction in charcoal yield when pyrolysis is conducted in vacuum,
2. The reduction in charcoal yield when gas flow is increased, [184, 352, 353, 355] and
3. The increase in charcoal yield with increasing pressure [74, 185, 244, 355, 356, 360].

The following conclusion of Shen et al.: “Vapour-solid interactions (secondary reactions) are effectively the only source of charcoal formed during the pyrolysis of pure cellulose. These heterogeneous reactions alone can increase the charcoal yield from 0% to more than 40%.” However, in the case of whole biomass (not pure cellulose), it is likely that the primary, solid-phase pyrolysis reactions contribute to the formation of charcoal.



The foregoing observations concerning the effects of particle size and secondary reactions are in part a reflection of the catalytic nature of charcoal and its mineral matter content. It has been known that downdraft reactors deliver a tar - free gas because the tar - laden gas formatted by pyrolysis flows through the hot bed of charcoal at the bottom of the reactor that catalyses the decomposition of the tars to more gas and charcoal [366]. Gilbert et al. [367] showed that the main mode of tar conversion in the presence of charcoal at 800 °C is homogeneous vapour - phase cracking. In particular, competitive vapour - phase reactions play a key role in the formation at 800 °C of the heavy, refractory, condensable phase [367]. In any case, the temperature range for charcoal formation of 250-450 °C is much lower than that studied by Gilbert et al. [367] consequently, true, low-temperature primary tars are the reactants, and their sensitivity to the catalytic action of charcoal or mineral matter is not well-understood.

The catalytic action of the charcoal results (at least in part) from its mineral matter content. The metal ions K, Li, Ca, Fe, and Cu, typically present as mineral matter in biomass, greatly enhance the formation of charcoal from biomass. Yang et al. showed that in the case of corn straw, the removal of K<sup>+</sup> and Ca<sup>2+</sup> ions by water or acid washing lowers the yield of charcoal obtained from the straw [368]. Larger particles enhance the retention of alkali and alkaline earth metal species, thereby retaining catalytic species that enhance charcoal yields [369].

#### **6.4. PREDICTIVE MODEL OF CORN COB SLOW PYROLYSIS**

Pyrolysis is not only an independent thermochemical conversion technology but also part of the gasification and combustion process. Pyrolysis is a key conversion stage during gasification and combustion of biomass [112]. In order to model not only pyrolysis, but also gasification and combustion of volatiles in biomass combustion, it is necessary to express the complex mixture of the volatile matter and charcoal evolving from biomass pyrolysis and subsequently cracking of these products (during gasification and combustion), in terms of a few simple gaseous constituents [370]. Knowledge of yields and composition of volatiles is especially relevant for high volatile fuels such as biomass and waste.

For a certain biomass, the ratio between the yields of solid charcoal and volatile pyrolysis products depends on the particle size, temperature, pressure and heating rate [41, 57, 279, 355, 371]. Pyrolysis of biomass is a very complex process of interdependent

reactions; nevertheless, it can be reduced to the reaction illustrated in Figure 3.13, proposed by Di Blasi and Russo [8, 63]. In this model, biomass decomposes via three competing reactions into gas, charcoal and tar. The secondary reaction takes place in the gas/vapour-phase within the pores of the charcoal. Consecutively the tar is converted by two secondary reactions into secondary gasses and charcoal. The rate of the reaction is proportional with the concentration of the tar vapours.

In order to obtain the correlations for predicting the yields of charcoal, tar and volatiles produced during the pyrolysis and also to determine the composition of the light gas as a function of the pyrolysis temperature, the experimental data and experimental data published by several authors [19, 59, 186, 368] has been reviewed. As a result of this analysis, a steady mathematical model is developed which is able to determine the yield of charcoal, tar, gas and gas composition, based on ultimate analysis of biomass and that can be applicable to different types of biomass. This model is validated with published experimental data and used to evaluate the influence of several working parameters like temperature, biomass composition, etc.

#### **6.4.1. MODEL FORMULATION**

In order to determine empirical relation between the product yield and pyrolysis temperature, data from a set of investigation [19, 59, 166, 186, 193, 345, 372, 373], including agricultural biomass residues (Table 6.8), particles having a variety of sizes (100  $\mu\text{m}$  – 250mm) and pyrolysis reactor temperature (within 350 – 1000  $^{\circ}\text{C}$ ) were analysed. Following Neves et al. [374], the following information was recorded from each investigation: biomass type (corn cob, corn stover, corn stalks, rice husk, grape husk, rapeseed, tobacco and wheat straw), biomass characterisation (elemental and ultimate analysis), pyrolysis reactor type (fixed bed, fluidised bed), pyrolysis reactor scale (laboratory, pilot, etc.), heating rate, pyrolysis classification based on heating rate (slow, fast, flash, etc), the dependence of product yield on reactor peak temperature and general characteristics (catalyst, residence time, pyrolysis medium, etc.), Table 6.11.

Differences in product yields, in principle can be due to pyrolysis reactor configurations, operating conditions (volatile residence times and particle characteristics), and biomass type [86]. According to literature, it is believed that the first two factors are predominant, as variations in the biomass chemical composition cannot account for differences as large as those shown in Figures 6.13 – 6.16.

After reviewing different experimental data for biomass pyrolysis correlations between product yields and temperature are obtained. A function of temperature has been derived by applying the nonlinear least squares procedure to the experimental yields of each product.

Table 6.11 Characteristics of agricultural residues (literature data and results from present study

Raw material	Elemental analysis (wt daf %)						Proximate analysis (wt db %)				HHV MJ/kg	Ref.
	C	H	N	O	S	P	Moisture	Volatile	Fix- C	Ash		
Literature data for empirical model development												
corn cob	47.57	6.27	0.55	43.89	0.23		5.18	81.08	17.47	1.45		Liang et al [41]
maize	46.9	5.4	47.4	0.2	0.06			82.3	14.8	2.9	15.4	Encinar [59]
sunflower	44.2	5.4	0.7	50.4	0.1			76.2	13.3	10.5	11.5	Encinar [59]
grape	49.9	5.8	0.7	43.5	0.06			74	19.9	6.1	11.7	Encinar [59]
tobaco	47.8	5.9	0.6	45.6	0.1			74.4	19.2	6.4	15.6	Encinar [59]
corn cob	47.35	5.9	0.69	38.07	0.18					1.94	17.8	Mullen [349]
corn stover	46.6	4.99	0.79	40.05	0.22					4.88	18.3	Mullen [349]
corn cob	47.6	5	0	44.06				85.4		2.8	15.65	Raveendran [352]
wheat straw	47.5	5.4	0.1	35.8				83.9		11.2	17.99	Raveendran [352]
rice straw	36.9	5.0	0.4	37.9				80.2		19.8	16.78	Raveendran [352]
rice husk	38.9	5.1	0.6	32.0				81.6		23.5	15.29	Raveendran [352]
corn stover	50.1	5.01	0.93	33			9			11		Scott [375]
wheat straw	48.5	5.13	0.50		41.3		6.5			4.6		Scott [375]
straw	42.69	6.04	0.46	47.11						3.7	17.53	Fagbemi et al. [149]
grape residues	47.9	6.2	2.11		0.09		9			5.1	23.83	Di Blasi et al. [86]
rice husks	40.3	5.7	0.3		0.03		7			15.3	18.73	Di Blasi et al. [86]

Raw material	Elemental analysis (wt daf %)						Proximate analysis (wt db %)				HHV MJ/kg	Ref.	
	C	H	N	O	S	P	Moisture	Volatile	Fix- C	Ash			
wheat straw	43.6	6.2	0.3		0.08		7				5.5	22.66	Di Blasi et al. [86]
rapseed	62.1	9.1	3.9	24.9			4.9	81.7	7.9		5.5	26.7	Onay et al. [373]
rice husk								64.8	15.81		19.39		Iwasaki et al. [376]
wheat straw	46.5	6.3	0.9	46.3			7.1				3.2	18.51	Zanzi et al. [377]
Literature data for empirical model validation													
corn cob	47.57	6.27	0.55	43.89	0.23		5.18a	81.08	17.47		1.45		experiment (this study)
corn cob	43.77	6.23		50			7.57	84.37			8.06	18.25	Ioannidou [368]
corn stalk	43.8	6.42		49.78			6.44	91.26			2.3	18.17	Ioannidou [368]
corn cob	47.63	4.91	0.84	37.72	0.14	2.94	4.87	80.66			6.23		Cao et al [378]
corn cob	49	5.4	0.4	44.6			0	84.6	15.4		1		Demirbas [19]

Table 6.12. Experimental details used in this study

sample size	reactor type	pyrolysis process, heating rate	operation temperature	gas and gas flow	Ref.
Literature data for empirical model development					
	laboratory TGA	slow pyrolysis	350-950°C		Liang et al [41]
1<d<1.6	tube- stainless steel reactor		400-700 °C	N <sub>2</sub> , 200 cm <sup>3</sup> /min	Encinar [59]
2mm	bubbling fluidized bed	fast pyrolysis	500 °C		Mullen [349]
100 - 250mm	packed bed pyrolyser	50 K/min	773 K	N <sub>2</sub> ,	Raveendran [352]
	bench-scale fluidized bed	flash pyrolysis	400-650 °C	N <sub>2</sub>	Scott [375]

sample size	reactor type	pyrolysis process, heating rate	operation temperature	gas and gas flow	Ref.
105-250 $\mu\text{m}$					
10 cm	quartz tube reactor		500 -1000 °C	He	Fagbemi et al. [149]
1-3 mm	quartz tube reactor	slow (conventional) pyrolysis, 25 K/min	550-1200 K	N <sub>2</sub>	Di Blasi et al. [86]
0.2-1 mm	quartz tube reactor	slow (conventional) pyrolysis, 25 K/min	550-1200 K	N <sub>2</sub>	Di Blasi et al. [86]
0.5-1 mm	quartz tube reactor	slow (conventional) pyrolysis, 25 K/min	550-1200 K	N <sub>2</sub>	Di Blasi et al. [86]
0.224-1.8 mm	fixed-bed tubular reactor and tubular transport reactor	slow pyrolysis, 30 °C/min	400-550 °C	N <sub>2</sub> , 50,100, 200 or 400 cm <sup>3</sup> /min.	Onay et al. [373]
0.224-1.8 mm	fixed-bed tubular reactor and tubular transport reactor	fast pyrolysis, 300 °C/min	400-550 °C	N <sub>2</sub> , 100 cm <sup>3</sup> /min	Onay et al. [373]
0.224-1.8 mm	fixed-bed tubular reactor and tubular transport reactor	flash pyrolysis	400-550 °C	N <sub>2</sub> , 100 cm <sup>3</sup> /min	Onay et al. [373]
	fluidized bed reactor	slow pyrolysis, 10 °C/min	300-1200 °C	N <sub>2</sub>	Ioannidou [368]
	fluidized bed reactor	fast pyrolysis, $\lesssim$ 1000 °C/s	300-1200 °C	N <sub>2</sub>	Ioannidou [368]
	free fall reactor.	rapid pyrolysis, 500 °C/s	800-1000 °C	N <sub>2</sub> , 15 l/min	Zanzi et al. [377]
<1 mm	captive sample reactor	fast pyrolysis 52 °C/s	360-730 °C	He	Ioannidou [368]
<1 mm	captive sample reactor	fast pyrolysis 45 °C/s	380-680 °C	He	Ioannidou [368]

<b>sample size</b>	<b>reactor type</b>	<b>pyrolysis process, heating rate</b>	<b>operation temperature</b>	<b>gas and gas flow</b>	<b>Ref.</b>
Literature data for empirical model validation					
	laboratory TGA	slow pyrolysis	350-550°C		Present study the previous chapter)
<1 mm	fixed bed (non catalytic)	slow pyrolysis	500-700 °C	N <sub>2</sub> , 100 cm <sup>3</sup> /min	Ioannidou [368]
	tube- stainless steel reactor	slow pyrolysis, 30 K/min	550-1150 K	N <sub>2</sub> , 80 ml/min.	Cao et al [378]

### RELATION BETWEEN THE YIELDS OF CHARCOAL – PYROLYSIS TEMPERATURE

Figure 6.16 shows a compilation of literature data [19, 59, 86, 149, 349, 352, 368, 373, 375-378] concerning charcoal yields a function of pyrolysis temperature.

It was found that the thermal decomposition behaviour of biomass was consistent with the amount of volatile matter content. Biomass with a high volatile matter (as agricultural residues) can be easily decomposed by heating than that with lower volatile content. As the temperature increases, the final solid residual initially decreases, as a result of the competition between charring and devolatilisation reactions, which become successively more favoured [86]. The effect can be thought of as more volatile material being forced out of the charcoal at higher temperatures reducing yield but increasing the proportion of carbon in the charcoal (both total- and fixed-carbon) [216]. At a high pyrolysis temperature, the solid yields tended to become constant.

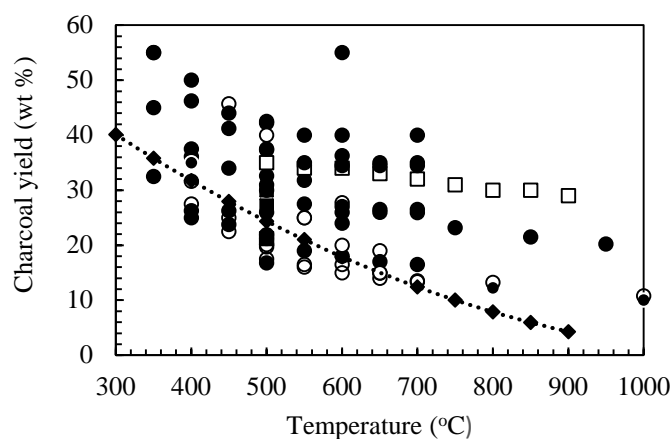


Figure 6.16 The charcoal yields (daf<sup>22</sup>) as functions of temperature

*(label: white dots – fast pyrolysis and small samples, black dots – slow pyrolysis and small samples, white square – fast pyrolysis and large samples, black square – slow pyrolysis and large samples)*

Note that the reaction conditions are not always the same. Flash pyrolysis leads to lower amount of charcoal compared to slow pyrolysis that is why there are lower values for Ioannidou's. Secondary reaction (tar cracking) in (this study) and carbonisation in (Demirbas [19]) lead to higher amount of charcoal.

A temperature depended charcoal is given by Equation 4.12 in the temperature range 300-950°C.

<sup>22</sup> daf – dry ash free



$$Y_{cc} = 7.97T^2 \cdot 10^{-5} - 0.125 \cdot T + 68.87, \text{ wt \% db} \quad R^2 = 0.82 \quad (6.7)$$

Where T is the pyrolysis temperature (bed temperature), °C

### RELATION BETWEEN THE YIELDS OF TAR - PYROLYSIS TEMPERATURE

Figure 6.17 shows a compilation of literature data [19, 59, 86, 149, 349, 352, 368, 373, 375-378] concerning tar yield a function of pyrolysis temperature.

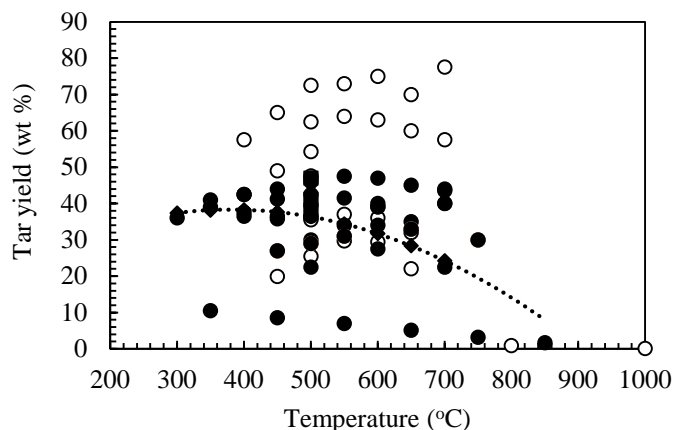


Figure 6.17 The tar yields as functions of temperature for corn cob  
*(label: white dots – fast pyrolysis and small samples, black dots – slow pyrolysis and small samples, white square – fast pyrolysis and large samples, black square – slow pyrolysis and large samples)*

The yield of liquid product was found to increase with pyrolysis temperature to give a maximum value at around 400-550°C [163] but dependent on equipment and other conditions. Above this temperature, secondary reactions causing vapour decomposition become more dominant and the condensed liquid yields are reduced. Peak liquid yields for slow pyrolysis are more variable. Demirbas [195] reports peak liquid yields of 28-41% at temperatures between 377°C and 577°C, depending on feedstock, when using a laboratory slow pyrolysis technique.

The decrease in tar yields and the corresponding increase in gas yields above the optimum temperature are probably due to secondary cracking of the pyrolysis vapour at relatively high temperatures [379]. Furthermore, the secondary decomposition of the charcoal at higher temperatures may as well give additional noncondensable gaseous product [379].

For laboratory packed-bed reactors, secondary reactions take place both across the bed (intraparticle activity may also be significant for large particle sizes) and in the heated extra-bed environment [160]. While for fluid-bed conversion the rates of tar increase and tar decrease are much larger because the distribution of volatile products is mainly dictated by extraparticle secondary reactions, which occur in a nearly isothermal environment [160].

Flash or fast pyrolysis maximize the yield of liquid products. This results from both primary volatile formation and secondary degradation of tar vapours becoming successively more favoured by higher temperatures [160].

A temperature depended tar is given by Equation 6.6 in the temperature range 300-950°C.

$$Y_{TAR} = -1.38T^2 \cdot 10^{-4} + 0.12 \cdot T + 12.64 \quad R^2 = 0.89 \quad (6.8)$$

Where T is pyrolysis temperature (bed temperature), °C

#### ***RELATION BETWEEN THE YIELDS OF GAS – PYROLYSIS TEMPERATURE***

Gas yields are generally low with irregular dependency on temperature below the peak temperature for liquid yield; above this gas yields are increased strongly by higher temperatures, as the main products of vapour decomposition are gases.

The decrease in liquid yield and the corresponding increase in gas yield above the optimum pyrolysis temperature are probably caused by the decomposition of some liquid vapours in the gas product.

Based on compilation of literature data [19, 59, 86, 149, 349, 352, 368, 373, 375-378], Figure 6.18 shows that higher pyrolysis temperature led to more volatilization resulting in higher yield of gaseous products.

The increase in gaseous products is believed to be predominantly due to secondary cracking of the pyrolysis vapours at higher temperatures [19]. At high pyrolysis temperature both the rate of primary pyrolysis and the rate of thermal cracking of tar to gaseous products are expectedly high. Further, a smaller particle is expected to produce higher gas yield because of the higher heat up rate and heat flux as compared to the larger particles. This observation agrees with the work of Wei et al. (2006) [20] who studied the effect of particle size on product distribution from pyrolysis of pine sawdust and apricot

stone in a free-fall reactor at 800°C. They reported that the decrease of biomass particle size contributed to an increase in the gas yields

A temperature depended tar is given by Equation 6.7 in the temperature range 300-1000°C.

$$Y_{GAS} = 1.12T^2 \cdot 10^{-4} - 0.058 \cdot T + 30.77, \% \text{ vol db} \quad R^2 = 0.9465 \quad (6.9)$$

Where T – pyrolysis temperature (bed temperature), °C

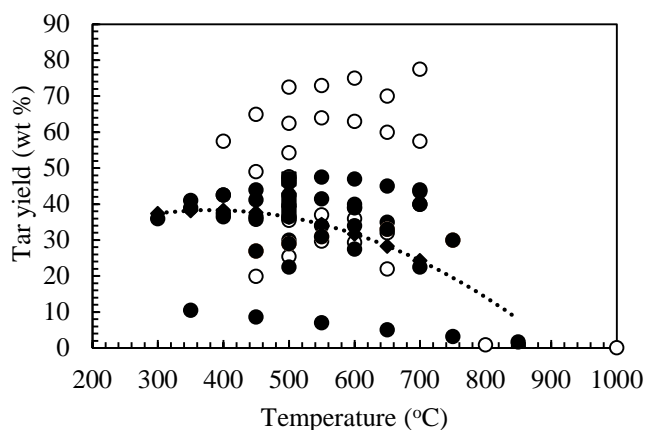


Figure 6.18 Gas yields as functions of temperature for corn cob (*label: white dots – fast pyrolysis and small samples, black dots – slow pyrolysis and small samples, white square – fast pyrolysis and large samples, black square – slow pyrolysis and large samples*)

### PRODUCT PROPERTIES

The pyrolysis gas consists (mf basis) mainly of CO<sub>2</sub> (the largest contribution), CO, CH<sub>4</sub>, and lower amounts of H<sub>2</sub> and C<sub>x</sub>H<sub>y</sub> (hydrocarbons) [86].

The yield of H<sub>2</sub>, CO, CO<sub>2</sub>, CH<sub>4</sub> is plotted against temperature in Figure 6.19, which is a compilation of some literature data [21, 22], using various agricultural residues, reactors and operating conditions (heating rate, particle size, etc.). Note that Figure 6.19 includes the activity of both the primary release of volatiles and secondary reactions.

As mentioned above increasing the temperature, gas yield increase due to the secondary reactions of pyrolysis vapours. Under fast heating and pyrolysis conditions, dehydration and pyrolysis processes could happen simultaneously [372]. This provides the opportunity for producing more hydrogen and carbon monoxide [59, 345, 372].

The pyrolysis gases consisted largely of CO and CO<sub>2</sub> with increased yield of CH<sub>4</sub> and H<sub>2</sub> at higher temperatures. The profile of gas evolution has two stages of gas evolution: the

abundance of CO and CO<sub>2</sub> at temperatures below 500 °C; and the release of H<sub>2</sub> and C<sub>x</sub>H<sub>y</sub> at higher temperatures. According to Di Blasi [86], this was attributed to the fact that CO<sub>2</sub> is a product of the primary pyrolysis of cellulose and hemicellulose by a pathway that becomes less favoured as the temperature increases [86]. The CO has the highest evolution rate for all biomass samples. The CO evolution mainly come from the decomposition of cellulose. Previous studies have shown that CO is formed during the primary decomposition of hemicellulose and cellulose with a smaller proportion of CO coming from lignin by the cracking of carbonyl (C-O-C) and carboxyl (C=O) in biomass [380, 381]. Above 600 °C, CO has a tendency to decrease. Other gases, including H<sub>2</sub>, CH<sub>4</sub>, and increases with temperature increase. H<sub>2</sub> is the main product of lignin. The increase in H<sub>2</sub> above 500 °C matched well with the decrease in hydrogen in the charcoal fraction and tar [86].

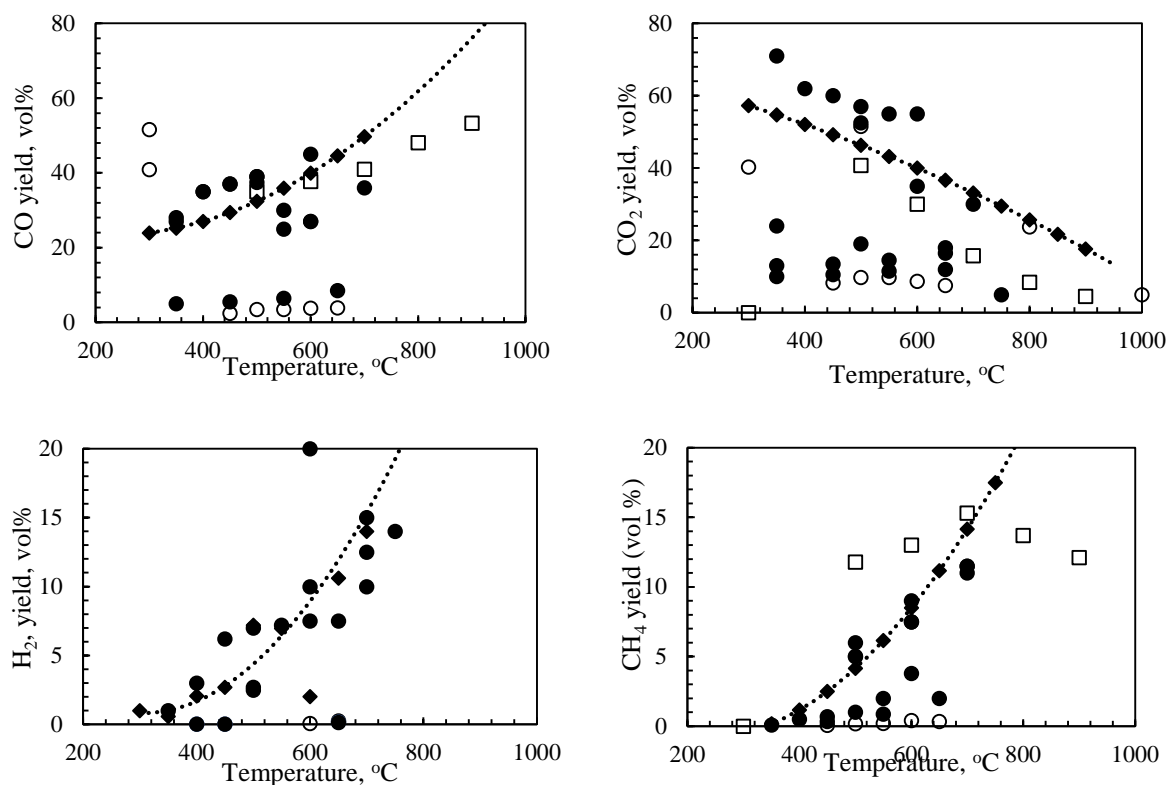


Figure 6.19 Gas yields for agricultural residues as functions of temperature: a) CO, b) CO<sub>2</sub>, c) H<sub>2</sub>, d) CH<sub>4</sub>

*(label: white dots – fast pyrolysis and small samples, black dots – slow pyrolysis and small samples, white square – fast pyrolysis and large samples, black square – slow pyrolysis and large samples)*

The yields of various gases were correlated against the pyrolysis temperature; particle size, and reactor type were found to be of limited influence on these empirical

relationships although it seems dependent on the heating rate and biomass being pyrolysed.

$$Y_{CO} = -2.65T^2 \cdot 10^{-4} + 0.27 \cdot T - 32.71, \% \text{ vol db} \quad R^2 = 0.64 \quad (6.10)$$

$$Y_{CO_2} = -2.85T^2 \cdot 10^{-5} - 0.029 \cdot T + 70.89, \% \text{ vol db} \quad R^2 = 0.78 \quad (6.11)$$

$$Y_{CH_4} = 6.69T^2 \cdot 10^{-5} - 0.037 \cdot T + 4.28, \% \text{ vol db} \quad R^2 = 0.98 \quad (6.12)$$

$$Y_{H_2} = -4.31T^2 \cdot 10^{-4} + 0.07 \cdot T + 17.67, \% \text{ vol db} \quad R^2 = 0.89 \quad (6.13)$$

The elemental composition of charcoal varies roughly from the one of biomass to the one of graphite (i.e. 100% carbon), being highly dependent on the pyrolysis conditions [42, 67-69]. The charcoal became highly carbon rich with higher temperatures. In other words, the higher pyrolysis temperatures volatilized less carbon containing compounds and acted to fix carbon in the charcoal rather than volatilize it. The carbon content of the charcoal usually increases with temperature being typically in the range of 85-95 wt% (daf) above 800 °C [42, 67-69]. According to Neves et al. [42] the enrichment in C is accompanied by a loss of O and H, the value of which decreases to 5 - 15% and < 2%, respectively. For corn cob, the maximum value of C content in charcoal is 87.71 wt% at 950 °C [41].

A temperature-dependent CHO composition of charcoals ( $Y_{j,ch}$ ) is here given by Equations 6.12 – 6.14, in the temperature range of 350-950 °C.

$$Y_{C,cc} = 7.77T^2 \cdot 10^{-5} - 0.08 \cdot T + 90.51, \text{wt \% db} \quad R^2 = 0.82 \quad (6.14)$$

$$Y_{H,cc} = -1.72T^2 \cdot 10^{-6} - 0.002 \cdot T + 5.47, \text{wt \% db} \quad R^2 = 0.86 \quad (6.15)$$

$$Y_{O,cc} = -9.11T^2 \cdot 10^{-5} + 0.10 \cdot T - 1.65, \text{wt \% db} \quad R^2 = 0.85 \quad (6.16)$$

The data on the elemental composition of tar was studied from literature [149, 186, 349, 367, 382]. The main components of tar are C, H and O. The oxygen content of tar decrease slightly with increasing temperature, whereas the carbon and hydrogen contents increase slightly [42, 369]. Data are more abundant between 400-600 °C since investigations usually are focused on the characterization of liquid products at operating conditions that maximize the yield of bio-oil (tar) [42]. The C/O ratios is higher in the tar than in the biomass feedstocks. According to Mullen et al. [349] this is because pyrolysis partitions O into the gas primarily as CO<sub>2</sub> and CO, along with the production of water.

The elemental composition composition of lumped tar seems relatively close to that of parent fuel, being highly oxygenated [42]. This indicates that biomass undergoes low

temperature decomposition (i.e. primary pyrolysis) into smaller tar molecules without significant change of the original chemical structure [42].

In addition to these correlations, the energy, mass, and molar balances for each element (C, H, O, and N) are set and used to calculate pyrolysis products. The energy balance was formulated to include an overall heat loss of the pyrolysis unit. This estimation of the heat losses can be fixed by the user as a percentage of the product of dry biomass mass flow entering the system (kg/h) and its lower heating value (LHV) (kJ/kg).

### OVERALL MASS BALANCE TO THE PYROLYSIS PROCESS

Following Neves et al. [374], overall mass balance to the biomass pyrolysis process is outline in Figure 6.20.

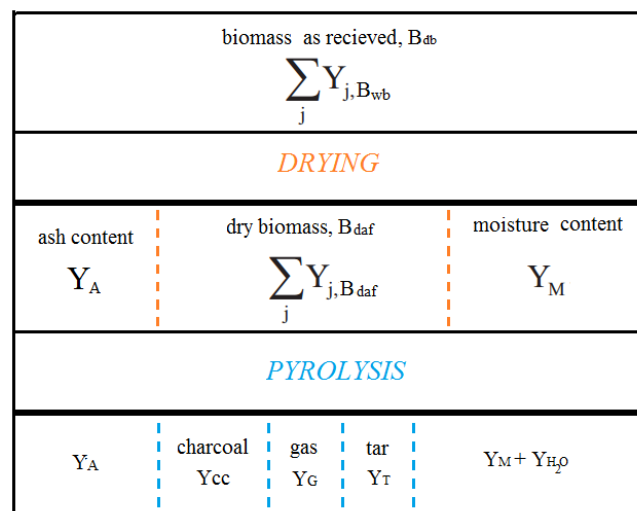


Figure 6.20 Overall mass balance to the biomass pyrolysis process. The presented quantities (Y) are mass ratios referred to the dry ash-free part of biomass (scheme based on Neves et al. [42] mass balance scheme)

The pyrolysis of raw biomass ( $B_{WB}$ ), include both drying and pyrolysis step, Equation 6.17

$$\frac{\sum_j Y_{j,B_{daf}} + Y_A}{(1 - Y_M)} = Y_{CC} + Y_T + Y_G + Y_{H_2O} + Y_M + Y_A \quad (6.17)$$

$$Y_G = Y_{CO_2} + Y_{CO} + Y_{CH_4} + Y_{H_2} \quad (6.18)$$

### The overall elemental mass balance

The overall elemental mass balances to the pyrolysis process is presented by equations.

Carbon balance:

$$Y_{C,Bdaf} = Y_{C,G} + Y_{C,CC} + Y_{C,T} \quad (6.19)$$

Hydrogen balance:

$$Y_{H,Bdaf} = Y_{H,G} + Y_{H,CC} + Y_{H,T} \quad (6.20)$$

Oxygen balance:

$$Y_{O,Bdaf} = Y_{O,G} + Y_{O,CC} + Y_{O,T} \quad (6.21)$$

Nitrogen balance:

$$Y_{N,Bdaf} = Y_{N,G} \quad (6.22)$$

### Overall energy balance to the pyrolysis process

The global energy balance equation is defined as follows:

$$Q_{bio,daf} = Q_{CC} + Q_T + Q_G + Q_{H_2O} \quad (6.23)$$

$$Q_{bio,daf} = Y_{Bdaf} \cdot LHV_{bio} \quad (6.24)$$

$$Q_{MCC} = Y_{CC} \cdot LHV_{CC} \quad (6.25)$$

$$Q_T = Y_T \cdot LHV_T \quad (6.26)$$

$$Q_G = Q_{G,stored} + Q_{G,sensible} = Y_T \cdot (LHV_G + \sum_j x_i \int_{T_o}^{T_p} c_{p,i} dT) \quad (6.27)$$

For the ideal gases used in this model, the specific heat capacities at constant pressure are calculated by the third-order polynomial equations taken from [186, 383]. Constant pressure specific heat ideal gas temperature relations are given in Table 6.12.

$$Q_{H_2O} = Y_{H_2O} \cdot (h_{H_2O} + \Delta h_{H_2O}) \quad (6.28)$$

$$\Delta h_{H_2O} = \int_{T_o}^{T_p} c_{p,H_2O} dT \quad (6.29)$$

Table 6.12 Constant pressure specific heat ideal gas temperature relations [186]

Gas	$c_p - kJ/kmol, \theta - T(Kelvin)/100$	Range K	Max. error %
N <sub>2</sub>	$c_p = 39.060 - 512.79\theta^{-1.5} + 1072.7\theta^{-2} - 820.40\theta^{-3}$	300-3500	0.43
O <sub>2</sub>	$c_p = 37.432 + 0.020102\theta^{1.5} - 178.57\theta^{-1.5} + 236.88\theta^{-2}$	300-3500	0.3
H <sub>2</sub>	$c_p = 56.505 - 702.74\theta^{-1} + 1165.0\theta^{-1} - 560.70\theta^{-1.5}$	300-3500	0.6
CO	$c_p = 69.145 - 0.70463\theta^{0.75} - 200.77\theta^{-0.5} + 176.76\theta^{-0.75}$	300-3500	0.42
H <sub>2</sub> O	$c_p = 143.05 - 183.54\theta^{0.25} + 82.751\theta^{0.5} - 3.6989\theta$	300-3500	0.43
CO <sub>2</sub>	$c_p = -3.7357 + 30.529\theta^{0.5} - 4.1034\theta + 0.024198\theta^2$	300-3500	0.19
CH <sub>4</sub>	$c_p = -672.87 + 439.74\theta^{0.25} - 24.875\theta^{0.75} + 323.88\theta^{-0.5}$	300-2000	0.15

### CALCULATION PROCEDURE

To solve the values of pyrolysis products, its components and energy values, an initial temperature was assumed and equations were solved using the “Engineering Equation Solver (EES)”. Equations were integrated in Equation 11.

EES has been found to be very suitable for modeling this kind of system, because it contains all of the necessary thermodynamic functions and it is possible for the model builder to make a user interface, which can make the model user-friendly [384].

### 6.4.2. VALIDATION OF THE MODEL

To our knowledge, there is limited data regarding gas, tar and char yields and its composition obtained using corn cob in a slow pyrolysis. So, it was decided to compare our developed model with experimental by other authors considering pyrolysis of corn residues.

This procedure was followed because of the limited experimental data to the simulated corn cob residues (i.e. gas and tar yield, gas composition, etc.). The developed model was compared with experimental data provided by Ionadiu et al. [368], Cao et al. [378], Demirbas [19], Mullan [349] and present experimental study.

The entire model is validated by comparison with the model calculation results with some experimental results published by other authors and experimental result from corn cob pyrolysis, Table 6.13.



The entire model are validated by comparing the calculation results with experimental results. The error in this comparison is estimated by the Root Mean Squared Error<sup>23</sup> (RMSE) defined as:

$$RMSE = \sqrt{\frac{\sum_{i=1}^n (X_{obs,i} - X_{model,i})^2}{n}} \quad (6.30)$$

Where  $X_{obs}$  is observed values,  $X_{model}$  is modeled values at place  $i$ ,  $n$  is number of data and  $X_{obs}$  is the value taken from other researchers and from experimental results of corn cob pyrolysis.

Figure 6.21 shows yield of the yield of charcoal, dry product gas and tar predicted by the model along with those found experimentally.

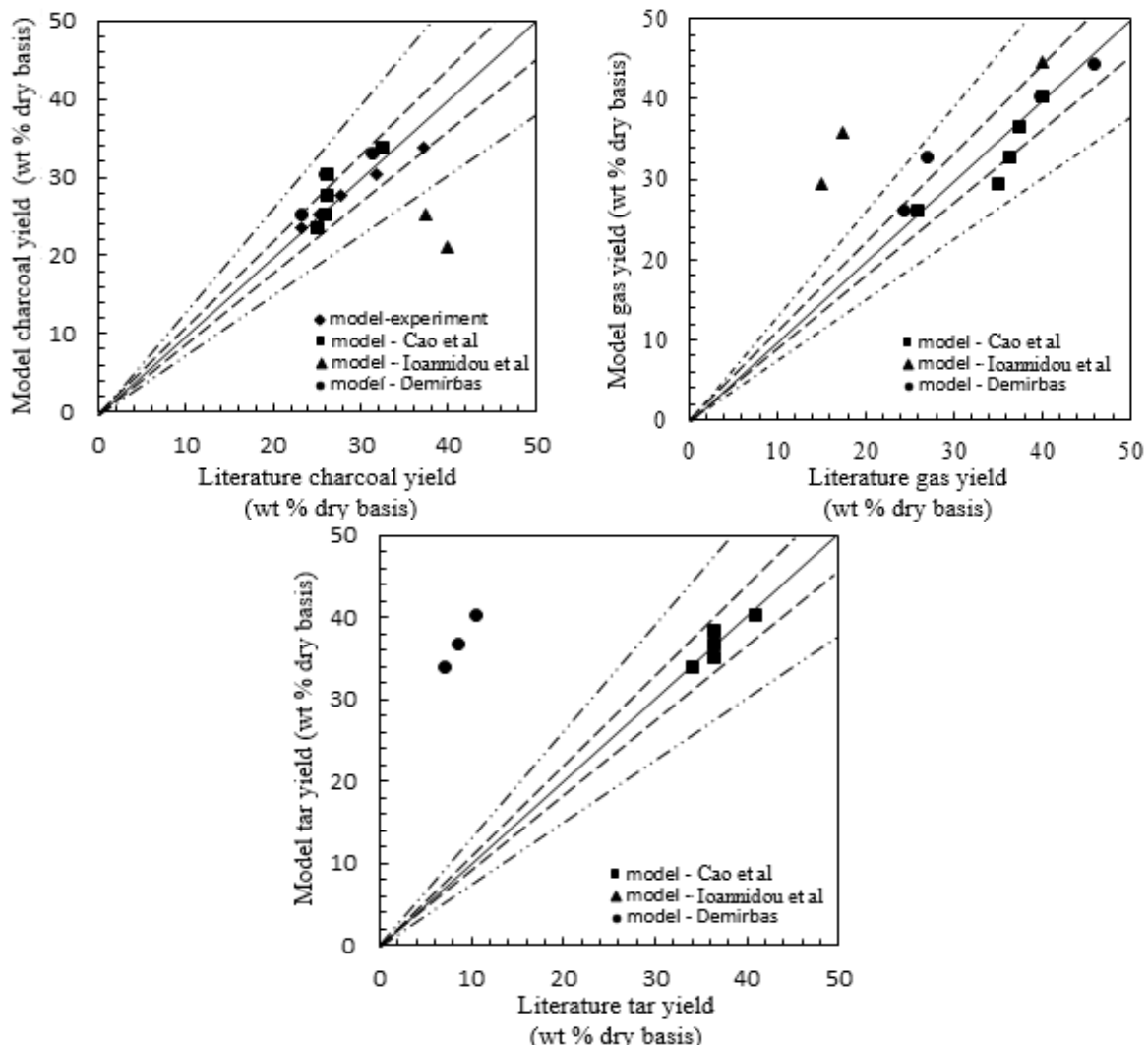


Figure 6.21 The yield of charcoal, gas and tar yield compared with literature data  
a) charcoal yield, b) gas yield and c) tar yield  
*(label: long dash line – 10% deviation; long dash dot dot - 25% deviation)*

<sup>23</sup> The Root Mean Square Error (RMSE) (also called the root mean square deviation, RMSD) is a frequently used measure of the difference between values predicted by a model and the values actually observed from the environment that is being modelled.

The model predicts most of measured yields within  $\pm 25\%$  accuracy and the prediction is often within the uncertainty of the measurements. In general, the model overestimates the measurement data with the predicted yields of tar significantly higher than the observed ones.

The comparison between literatures, experimental and predicted data for charcoal yield is shown in Figure 6.22. a). From this figure it can be concluded that the model predicts with good accuracy the charcoal yield although the differences for Ioannidou et al. [368] are higher than for other authors. The RMSE values obtained are 2.14, 22.99, 2.97 and 1.66 for input values of Cao et al. [378], Ionannidou et al. [368], Demirbas [19] and experiments respectively. The comparison between literatures, experimental and predicted data for gas yield is shown in Figure 4. b). Generally, model predicts with good accuracy the gas yield although the differences for Demirbas [19] are higher than for other authors. The RMSE values obtained are 8.48, 13.74, 10.9 for input values of Cao et al. [378], Ionannidou et al. [368] and Demirbas [19] respectively. The proposed model significantly overestimates the tar yield measured by Demirbas [19] (Figure 4. c)). For other two studies the model predicts with good accuracy the tar yield ( $\pm 25\%$  accuracy). The RMSE values obtained are 1.10, 9.09 and 28.31 for input values of Cao et al. [378], Ionannidou et al [368] and Demirbas [19] respectively.

Figure 6.22 shows the composition of the dry product gas predicted by the model along with those found experimentally.

The model predicts most of measured yields within  $\pm 25\%$  accuracy and the predictions are often within the uncertainty of the measurements. In general, the model overestimates the measurement data with the predicted yields of  $\text{CO}_2$  higher than the observed ones.

Comparison between model results and experimental measurements was done to show its predictive capability for specific biomass fuels.

In general, model generally agree with the experimental and literature data. Model overestimates the measurement data with the predicted yields of tar significantly higher than the observed ones. The differences in comparison with the experimental data are due to the simplifying assumptions used in defining the model.

This steady model is a practical model that predict the evolution of specific products of interest. Also, this empirical model is a way of compiling the collected experimental data in a structured tool that can be effectively used to analyse the biomass pyrolysis process

[374]. Additionally, it can be considered as a first step toward its extension to practical applications, where additional chemical and transport phenomena need to be incorporated.

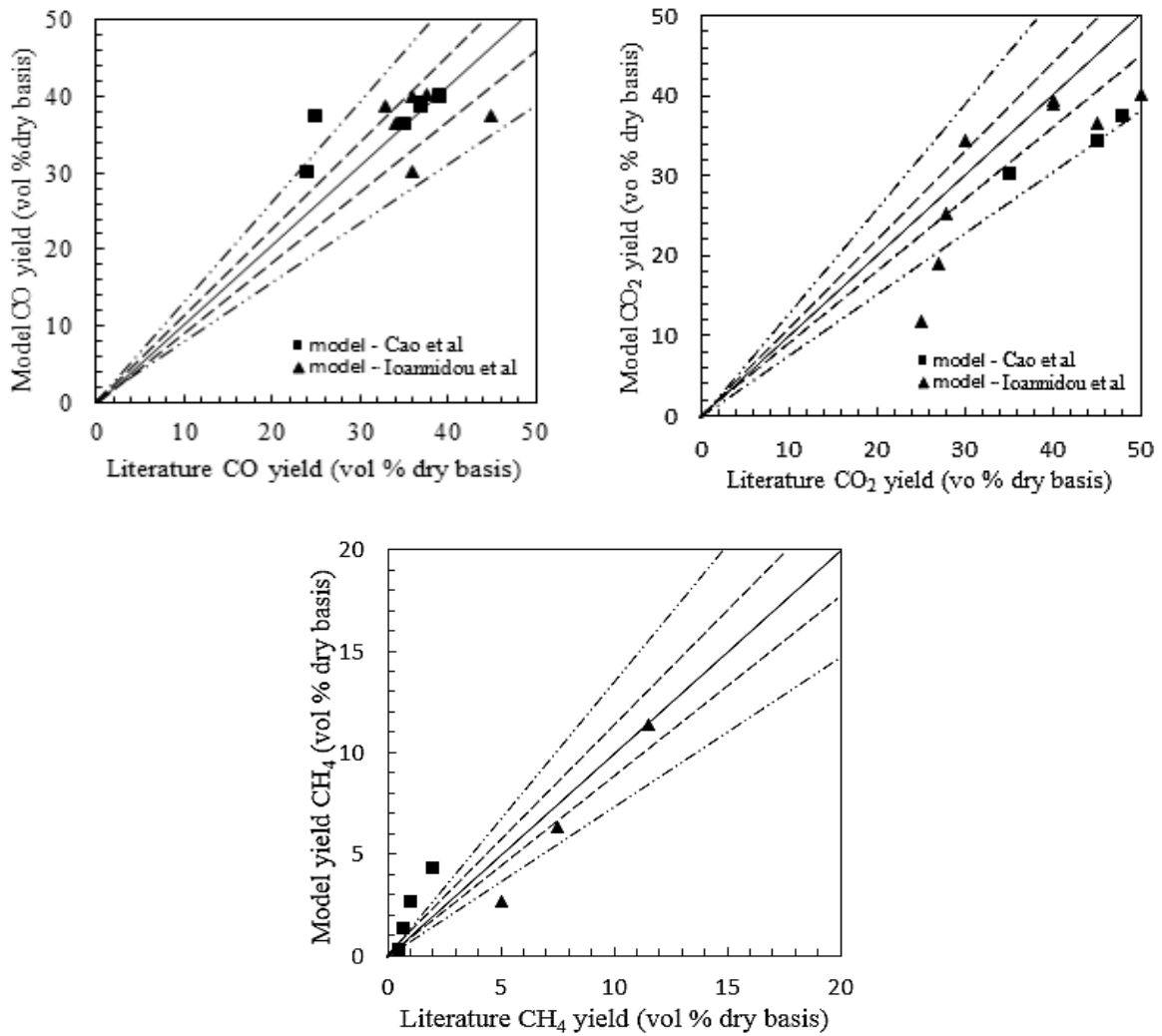


Figure 6.22 Yield of gas composition given by model and compared with literature data a) CO yield, b) CO<sub>2</sub> yield and c) CH<sub>4</sub> yield  
(**label:** long dash line – 10% deviation; long dash dot dot - 25% deviation)

Table 6.13 Comparison of present study results with literature data

	This study		Literature			
	Model	Experiment	Ioannidou et al. [368]	Ioannidou et al. [368]	Cao et al. [378]	Demirbas [19]
Reactor type			Captive sample	Fixed bed <sup>a</sup>		
Experimental results		corn cob	corn cob	corn cob	corn cob	corn cob
Operation temperature		350-550	360-730	500-700	600	950-1250
Product yields						
Gases	22.46-34.5		14-63 <sup>a</sup>	16-40 <sup>a</sup>	27-41 <sup>a</sup>	31.8-19.1
Liquid	34.98-44.96		15-30 <sup>a</sup>	22-40 <sup>a</sup>	34-44 <sup>a</sup>	11.3-1.7
Charcoal	39.4-27	38.7-22.5	17.6-48 <sup>a</sup>	37-55 <sup>a</sup>	24-32 <sup>a</sup>	31.8-19.1
Water and losses						36.7-6
Gas composition						
CO	33.17-11.7		41-51 <sup>c</sup>	37-44 <sup>c</sup>	28-40 <sup>e</sup>	
CO <sub>2</sub>	23.96-32.38		3.5-24 <sup>c</sup>	31-52 <sup>c</sup>	52-71 <sup>e</sup>	
H <sub>2</sub>	1.43-7.6		28-42.5 <sup>c</sup>	2-13 <sup>c</sup>	1-7 <sup>e</sup>	
CH <sub>4</sub>	0.3-4.3		7-9 <sup>c</sup>	4-13 <sup>c</sup>	0-3 <sup>e</sup>	
C <sub>2</sub> H <sub>6</sub> /C <sub>2</sub> H <sub>4</sub> or *C <sub>x</sub> H <sub>y</sub> (%)	1.004- 4.147*		0-1 <sup>c</sup>	1-4 <sup>c</sup>	0-1 <sup>e</sup>	
LHV of gas (MJm <sup>-3</sup> )		10-13	13-15			

## 6.6. CONCLUSION

1. The yield of charcoal ( $y_{char}$ ) from biomass is not a meaningful metric of the efficiency of a carbonization process. Instead, the fixed-carbon yield ( $y_{fc}$ ) should be used to characterize carbonization efficiency. When an elemental analysis of the feedstock is available, it can be used to calculate the yield of pure carbon that can be realized when thermochemical equilibrium ( $y_{fc}^{th}$ ) is reached in a carbonizer. This theoretical yield of pure carbon can be compared to the experimental value of the fixed-carbon yield and thereby used as a meaningful metric of the efficiency of the carbonization process.
2. The standard proximate analysis procedure offers a very low fixed-carbon yield of charcoal from corn cob. The fixed-carbon yields of charcoals produced by the proximate analysis procedure are about 1/2 of the theoretical value. The carbonization by TGA of small samples of small particles of corn cob in open crucibles deliver the lowest fixed-carbon yields (~65 % of the theoretical values for both samples). Standard proximate analysis procedures, which employ a closed crucible, realize somewhat improved yields (~75 % of the theoretical value for both samples).
3. Sample size strongly influences the charcoal and fixed carbon yields measured by TGA instruments. For example, in this work, an increase in corn cob powder sample size from 5 to 40 mg increases the (open crucible) measured charcoal yield at 550°C from 20.52% to 22.56% for Scob and from 20.43 to 22.80% for Pcob.
4. Also, the confinement of pyrolysis volatiles in closed crucibles enhances the charcoal and fixed-carbon yields measured by the TGA instruments. For example, the measured charcoal yield from 40 mg of Scob in an open crucible is 22.56% (22.80 for Pcob), whereas the value in a closed crucible is 25.62 % (25.66% Pcob). The closed crucible value is about 80% of the theoretical fixed-carbon yield for both corn cobs.
5. Relatively high fixed-carbon yields are obtained from whole corn cobs heated under N<sub>2</sub> in closed vessels in a muffle furnace (~77% of the theoretical value for Scob and ~78% of the theoretical value for Pcob). This is not a practical way to manufacture charcoal; electrical heat is too expensive to be used for carbonization.
6. Secondary pyrolysis reactions, which involve vapour-phase (or nascent vapour-phase) species, are at least as important as primary pyrolysis reactions in the formation of charcoal. Any condition (e.g., increasing pressure), which enhances or prolongs the contact of the vapour phase species with the solid, will augment the fixed carbon yield

of charcoal. Biomass pyrolysis is simply the fragmentation of the biopolymer into smaller organic compounds (e.g., levoglucosan, glycolaldehyde, various furans, etc.) at elevated temperature. Thermodynamic calculations indicate that these compounds are not stable at elevated temperature; the preferred products are carbon and light gases. Any condition that favours the attainment of thermodynamic equilibrium, by prolonging or enhancing the contact of the biopolymer fragments with the solid, necessarily augments the yield of carbon (i.e., biocarbon).

7. If bio-carbon (i.e., charcoal) is the desired product, carbonization equipment that does not require size reduction is best suited to maximize the biocarbon yield. Biomass is not easy to grind, shred, sliver, or chip. Size reduction demands considerable capital investment and wastefully consumes power. The fact that biocarbons are produced most efficiently without size reduction gives carbonization processes a considerable advantage over other technologies that convert biomass into higher value fuels.

8. A model for biomass pyrolysis has been developed in this chapter. It is a simple but rigorous model implemented in the equation solver program EES, with a user interface that makes the model user-friendly and facilitates the user obtaining an overview of the operating conditions in a certain computation. The model can be used to predict the final pyrolysis products and its composition and its main characteristics, such as the heating value, for a certain biomass with a defined ultimate composition and moisture. It has been validated with the data reported by experimental results and from various researchers and different biomasses and shows good agreement with the experimental data.

In addition, it has been used to evaluate the influence of different operating parameters on producer gas, presenting the following conclusions: (1) with increasing pyrolysis temperature, yield of liquid fraction increases until temperature reaches 500°C. At that temperature liquid yield is estimated to be 35 %wt. With further pyrolysis temperature, liquid yield decreases and gas yield increases. Increase in temperature favours the formation of hydrogen (H<sub>2</sub>), carbon-monoxide (CO), while carbon-dioxide (CO<sub>2</sub>) decreases. Formation of methane (CH<sub>4</sub>) reaches maximum at temperature between of 600°C and 700°C. The decomposition of biomass and its products at high temperatures is caused by secondary reactions; (2) it has been proven that the temperature has a significant influence on composition only up to a certain level, and it is limited by the

effectiveness of the heat-exchange equipment and the operating temperature constraints of the reactor.

The findings presented in this chapter suggest that the sample mass, particle size, and confinement of volatiles, any of which enhance the rates of secondary reactions, may be more important determinants of charcoal yield than heating rate.

The model helps to predict the behaviour of different biomass types, and is a useful tool for preliminary calculations, design, and operation of biomass pyrolysers. It is also a first step and can be used as an input to the gasification and combustion model of an internal combustion engine or another gas to energy engine to model a whole biomass co- or tri-generation plant.

*“A theory is a good theory if it satisfies two requirements: it must accurately describe a large class of observations on the basis of a model that contains only a few arbitrary elements, and it must make definite predictions about the results of future observations.”*  
*Stephen Hawking in A Brief History of Time*

## **7. PYROLYSIS EXTENSION TO PRACTICAL GASIFICATION**

### **MODELS**

#### **MODELING DOWNDRAFT GASIFICATION PROCESS WITH USE OF THE PREDICTIVE SLOW PYROLYSIS MODEL**

Although thermal decomposition of biomass has been experimentally and theoretically extensively studied and presented in this thesis, much remains to be learned about the fundamental chemical and physical processes governing the pyrolytic decomposition of biomass, on the one hand, and the applicability of the presented type of steady and kinetic description evaluated in this thesis for engineering purposes, on the other hand [80]. The analysis of conditions commonly applied in commercial pyrolysis processes, such as more severe heating conditions, larger particle and feed sizes, has been out of the scope of this thesis.

Also, in terms of engineering purposes, pyrolysis can be used not only as an independent process for the production of useful energy and chemical, but also as the first step in gasification or combustion process. The use of consistent data from pyrolysis, valid over wide temperature ranges and for different materials, is particularly important in gasification process because, contrary to coal gasification where the devolatilization stage contributes only for 20-40% of the total volatiles released, and biomass gasification this contribution increases up to 60-80% [80]. On the other hand, the pyrolysis characteristics influence the predictions of both the producer gas quality and activity of gasification reactions, through hydrogen, carbon dioxide, and steam concentrations [80, 319, 385].

In a first part of this chapter, the results of applying the present type of steady pyrolysis model over the downdraft gasification of corn cob is presented. Furthermore, it is



discussed some other important aspects for future work in the field of engineering applications.

### **7.1. MODELING OF CORN COB GASIFICATION – STEADY STATE MODEL**

The aim of this section is to provide a guide on the downdraft gasification characteristics of biomass, to determine the yields of gas, charcoal, tar, and particles produced during gasification, to determine the composition of the gas covering conditions typically found in gasification (300-950°C), to evaluate the influence of main input variables, such as moisture content and air/fuel ratio, temperature of the process, gasification medium, etc. Regarding to this, an empirical predictive model is developed to describe the general trends of product distribution as a function of temperature, which is made of elemental balances, energy balance and empirical relationships.

The gasification model is made of a series of modules each containing one process, Figure 6.1. An overall scheme is usually adopted by considering the different steps in which gasification process can be approximately subdivided: heating and drying, pyrolysis or devolatilisation, combustion or partial oxidation, and reduction (or charcoal gasification). A real gasification system differs from an ideal reactor at chemical equilibrium. For this reason, the pure equilibrium model [53, 54, 168, 169] has been modified to increase the results' accuracy.

For the model developed in this project, the following assumptions are made:

1. Adding a pyrolysis unit that, using correlations, predicts the formation of gas, charcoal and volatiles in this step of the gasification process,
2. Adding tar and charcoal leaving the gasifier as a percentage of tar and charcoal produced in the pyrolysis unit added [112]
3. Particles leaving the gasifier and set by the user as mg/Nm<sup>3</sup> in the producer gas. These particles are considered to consist only of carbon,
4. Producer gas consists of CO<sub>2</sub>, CO, H<sub>2</sub>, CH<sub>4</sub>, N<sub>2</sub>, and H<sub>2</sub>O.

#### ***FORMULATION OF THE MODEL***

After an extensive literature search, systematization of tar and particle content in gas were done. Reed и Das [366], reported that the raw producer gases of the investigated downdraft gasifiers exhibit a particle level in the range 50 mg/Nm<sup>3</sup> up to 500 mg/Nm<sup>3</sup>,

whereas the concentration of the high boiling tar components ranges from 50 mg/Nm<sup>3</sup> to 1000 mg/Nm<sup>3</sup>. . Rajvanshi [232], reported for downdraft gasification of many agricultural residues, range of tar content in producer gas for corn cob is estimated to be 1.43 - 7.24 g/ m<sup>3</sup>Ngas. As different tars are produced in a gasification reaction through complex set of reactions, predicting tar species in the product gas using any numerical technique is very difficult [386]. Due to that reason representative tar composition as reported in the literature was used as an input parameter in the model. The present study therefore considered the tar yield and composition as an input parameter in the model. According to Yamazaki et al. [387] the maximum tar yield was 4.5 wt %. The representative formula and composition of tar was taken from Da Silva's [388] Table 6.1.

Table 7.1 Tar Ultimate Analysis [13]

Gasifier	Ultimate analysis [wt %]					Cl	Tar formulae
	C	O	H	N	S		
Downdraft	62.59	27.0	6.54	2.56	0.40	0.54	C <sub>55.21</sub> H <sub>6.54</sub> O <sub>1.1,74</sub>

### The overall mass balance

Following procedure presented in Chapter 5, overall mas balance to the biomass pyrolysis process is outline in Figure 1.

The gasification of raw biomass (B<sub>WB</sub>), include both drying and pyrolysis step, Equation 7.1.

$$Y_{CC} + Y_T + Y_G + Y_{H_2O} + Y_M + Y_A + Y_{AIR} + Y_{STEAM} = Y_{CC} + Y_T + Y_G + Y_{H_2O} + Y_p + Y_A \quad (7.1)$$

$$Y_G = Y_{CO_2} + Y_{CO} + Y_{CH_4} + Y_{H_2} + Y_{N_2} \quad (7.2)$$

### The overall elemental mass balance

The overall elemental mass balances to the pyrolysis process is given by equations.

Carbon balance:

$$Y_{C,G} + Y_{C,CC} + Y_{C,T} = Y_{C,G} + Y_{C,CC} + Y_{C,T} + Y_{C,p} \quad (7.3)$$

Hydrogen balance:

$$Y_{H,G} + Y_{H,CC} + Y_{H,T} + Y_{H,steam} + Y_{H,H_2O} + Y_{H,M} = Y_{H,G} + Y_{H,CC} + Y_{H,T} \quad (7.4)$$

Oxygen balance:

$$Y_{O,G} + Y_{O,CC} + Y_{O,T} + Y_{O,H_2O} + Y_{O,M} + Y_{O,steam} + Y_{O,air} = Y_{O,G} + Y_{O,CC} + Y_{O,T} \quad (7.5)$$

Nitrogen balance:

$$Y_{N,G} + Y_{N,air} = Y_{N,G} \quad (7.6)$$

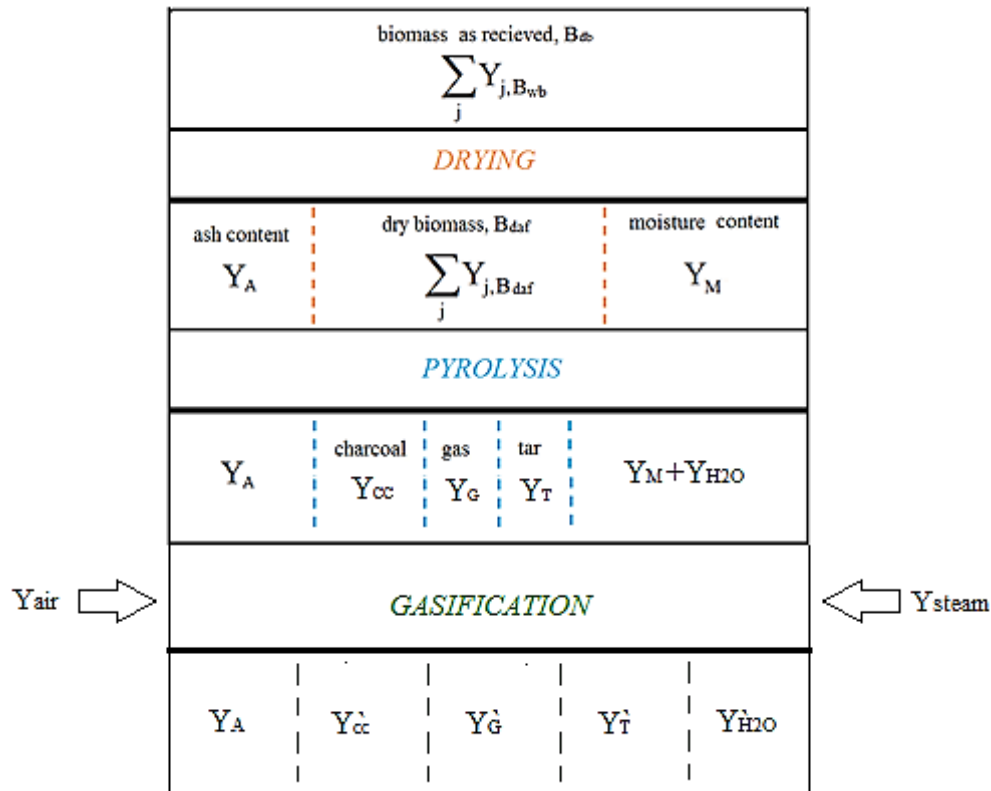


Figure 7. 1 Overall mass balance to the biomass gasification process. The presented quantities (Y) are mass ratios referred to the dry ash-free part of biomass

**Overall energy balance to the pyrolysis process**

The heat balance was then incorporated in the model which enabled prediction of the gasification temperature of the gasifier. The size of the gasifier was assumed to be small and the heat loss across the gasifier was neglected.

The global energy balance equation is defined as follows:

$$Q_{CC} + Q_T + Q_G + Q_{H_2O} + Q_M = Q_{CC} + Q_T + Q_G + Q_{H_2O} \quad (7.7)$$

$$Q_{CC} = Y_{CC} \cdot LHV_{CC} \quad (7.8)$$

$$Q_T = Y_T \cdot LHV_T \quad (7.9)$$

$$Q`_G = Q`_{G,stored} + Q`_{G,sensible} = Y`_T \cdot (LHV_G + \sum_j x_i \int_{T_o}^{T_p} c_{p,i} dT) \quad (7.10)$$

$$Q`_{H_2O} = Y`_{H_2O} \cdot (h_{H_2O} + \Delta h_{H_2O}) \quad (7.11)$$

$$\Delta h_{H_2O} = \int_{T_p}^{T_g} c_{p,H_2O} dT \quad (7.12)$$

Following Barman et al. [389], three more equations were obtained by considering the equilibrium of the water gas shift reaction, methane reaction and methane reforming reaction as follows:

**Water-gas shift reaction:**



$$K_1 = \frac{n_{CO_2} n_{H_2}}{n_{CO} n_{H_2O}} \quad (7.14)$$

The equilibrium constants  $K_1$  is evaluated from the following relation published by Pedroso et al. [390]:

$$K_1 = e^{\left\{\left(\frac{4276}{T}\right)^{-3.961}\right\}} \quad (7.15)$$

**Methane reaction:**



$$K_2 = \frac{n_{CH_4}}{n_C n_{H_2}^2} \quad (7.17)$$

The equilibrium constant  $K_2$  is evaluated from the relation proposed by Zainal et al. [391]:

$$\ln K_2 = \frac{7082.842}{T} - 6.567 \ln T + \frac{7.467}{2} T 10^{-3} - \frac{2.167}{6} T^2 10^{-6} + \frac{0.702}{2T^2} + 32.541 \quad (7.18)$$

**Methane Reforming Reaction**



$$K_3 = \frac{n_{CO} n_{H_2}^3}{n_{CH_4} n_{H_2O}} \quad (7.20)$$

Where  $n$  represents the corresponding mole fraction of the individual species.

The equilibrium constant  $K_3$  is evaluated from the relation proposed by Bottino et al.[392]:

$$K_3 = 1.198 (10^{13}) e^{\frac{-26830}{T}} \quad (7.21)$$

Solution of Equations 7.1 – 7.21 was done with the equation solver program, EES, to evaluate the composition. The initial gasification temperature was assumed.

Note: The composition of the pyrolysis products in the outgoing flows is based on equations presented in Chapter 6.

### VALUATION

To solve the values of  $n_{CO}$ ,  $n_{H_2}$ ,  $n_{CO_2}$ ,  $n_{H_2O}$ , and  $n_{CH_4}$ , initial temperature is assumed and substituted into Equations 67.14., 7.15 and 7.21 to initially calculate  $K_1$ ,  $K_2$  and  $K_3$ . Then, all three equilibrium constants are substituted into Equations 7.14, 7.17 and 7.20 respectively. Finally, all results are substituted into equations 7.1 – 7.12. For calculating the new value of temperature, equation (6.21) is used. The outlined procedure is repeated until temperature value is converged. The predicted results from the present modified equilibrium model is presented in Table 7.2. Results obtained in this analysis are in the good agreement with results obtained by literature review [393-397], Table 7.2. Comparing the predicted values with the experimental reported values from different authors, it can be said that the modified equilibrium model predicts with good accuracy the behaviour of downdraft gasifiers, especially for air biomass gasification conditions.

Table 7.2 Gas composition as a results of corn cob downdraft gasification modeling

	<b>N<sub>2</sub></b> (vol %)	<b>CO<sub>2</sub></b> (vol %)	<b>CO</b> (vol %)	<b>H<sub>2</sub></b> (vol %)	<b>CH<sub>4</sub><sup>1</sup></b> (vol %)	<b>H<sub>2</sub>O</b> (vol %)	<b>Hd</b> (MJ/m <sup>3</sup> )
wb	43.01	10.42	19.4	16.67	1.83	8.70	4.90
db	47.09	11.41	21.24	18.26	2.00		5.37

Fixed value of methane

Table 7.3 Gas composition after corn cob downdraft gasification, literature review

<b>N<sub>2</sub></b> (vol %)	<b>O<sub>2</sub></b> (vol %)	<b>CO<sub>2</sub></b> (vol %)	<b>CO</b> (vol %)	<b>H<sub>2</sub></b> (vol %)	<b>CH<sub>4</sub></b> (vol %)	<b>Hg</b> (MJ/m <sup>3</sup> )	<b>Hd</b> (MJ/m <sup>3</sup> )	<b>Ref.</b>
37.7	1.90	22.00	24.00	10.00	4.40		14.30	[393]
48.00		13.00	21.00	17.00	1.00	5.70		[394]
48.00		14.00	19.00	17.00	2.00	5.10		[395]
			18.60	16.50	6.40			[396]
50.32	0.87	10.76	17.79	15.80	3.73	5.56		[398]
50.00		10.00	20.00	20.00	in traces	5.60		[397]

## 7.2. GASIFICATION MODEL VALIDATION

The results obtained with the modified equilibrium model are validated with those obtained experimentally by different authors for different kinds of biomass. In order to predict the results and due to the lack of some information in the authors' paper, the model parameters are adjusted by minimising the sum of the differences between experimental and modelled results for producer gas composition.

The entire model is validated by comparison with the results of a steady state model for downdraft biomass gasifier Giltrap et al. [399] as well as with some experimental results from downdraft gasification published by Chee [372], Senelwa [400]. These results are shown in Figure 7.2.

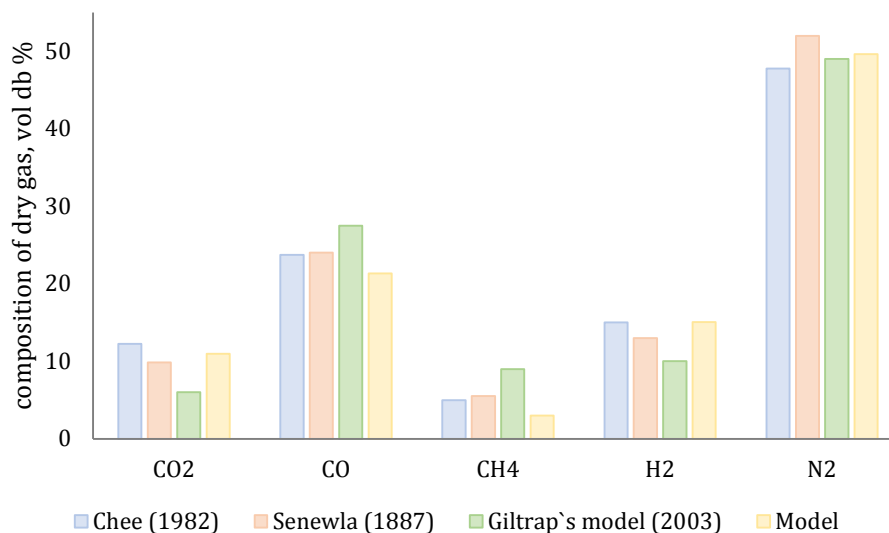


Figure 7.2 Composition of the dry product gas predicted by model compared with experimental results

The model produced reasonable agreement with the experimental results. The present model gives slightly smaller molar fractions of CH<sub>4</sub> and slightly smaller fractions of CO and CO<sub>2</sub> than the experimental results given by Chee et al. [372] and Senelwa [400]. Model gives results with higher accuracy than Giltrap's model.

The RMSE is calculated by Eq. (36) using the appropriate values of  $D_j$  and  $k$  ( $D = 6$ ,  $j = 0, 1$ , and  $k = \text{CO}, \text{CO}_2, \text{CH}_4, \text{H}_2, \text{N}_2$ ,  $m$  in Tables 4

The model is further validated by comparison of results given by variation of different parameters with the experimental results from Plis and Wilk [401], Mathieu and Dubuisson [402], Baratieri et al. [403].

### **EFFECT OF FEEDSTOCK PROPERTIES AND OPERATING PARAMETERS**

Because biomass is very variable in its composition and properties and also the gasifier conditions can be change; it is of great interest to have a model sensitive enough to predict the effect of the operational variables on the quality of producer gas. For this reason, the present developed model has been use to study the influence of:

1. moisture content in biomass,
2. equivalence ratio ( $\lambda$ ),
3. air-preheating,
4. steam injection
5. oxygen enrichment

on producer gas.

#### **Effect of equivalence ratio ( $\lambda$ ) on producer gas composition**

The variation of producer gas composition as function of the equivalence ratio ( $\lambda$ ) in an adiabatic gasifier of corn cob with a moisture content of 5% is shown in Figure 7.3. Considering an autothermal gasifier, the gasification temperature depends on the amount of air fed to the gasifier. As a result, varying ( $\lambda$ ) or gasification temperature will have the same effect on producer gas composition, heating value, and gasification efficiency. For this reason, only ER is plotted against producer gas composition and LHV.

Variation of the composition of producer gas and heating value in function of  $\lambda$  is presented in Figure 7.3 and Table 7.4.

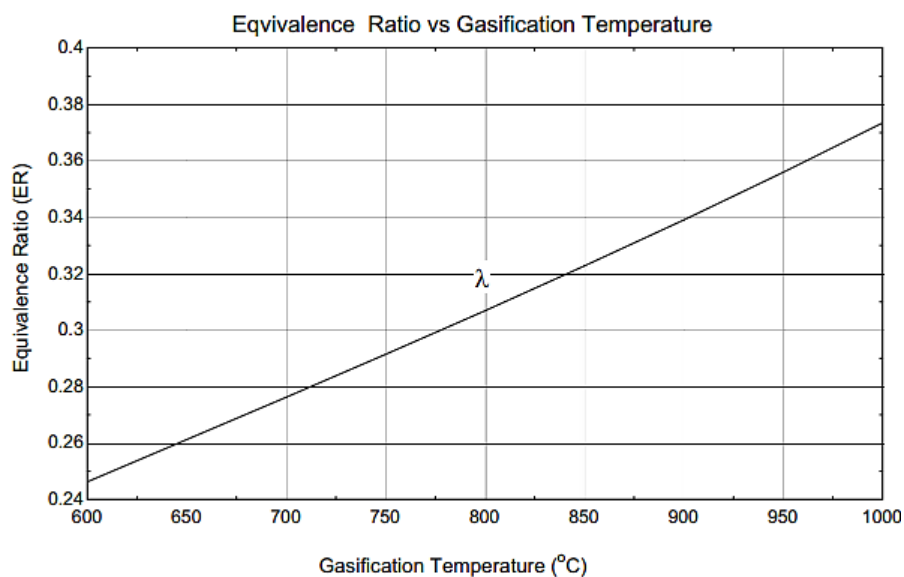


Figure 7.3 Influence of Equivalence Ratio on Gasification Temperature

These results were compared with the ones published by, Plis and Wilk [401], Mathieu and Dubuisson [402], Baratieri et al. [403] and Puig et al. [384]. The four models and resented model present the same qualitative and quantitative tendencies. H<sub>2</sub> percentage decreases when  $\lambda$  increases, the similar behaviour was observed by Plis and Wilk [401] and Puig et al. [384]. While H<sub>2</sub> decreases, CO<sub>2</sub> slightly increases and the CO percentage decreases, similar as in Puig et al. [384] model. Also, hetaing value of producer gas decrease with increase of  $\lambda$ , the same behaviour was observed by Plis and Wilk [401] and Puig et al. [384].

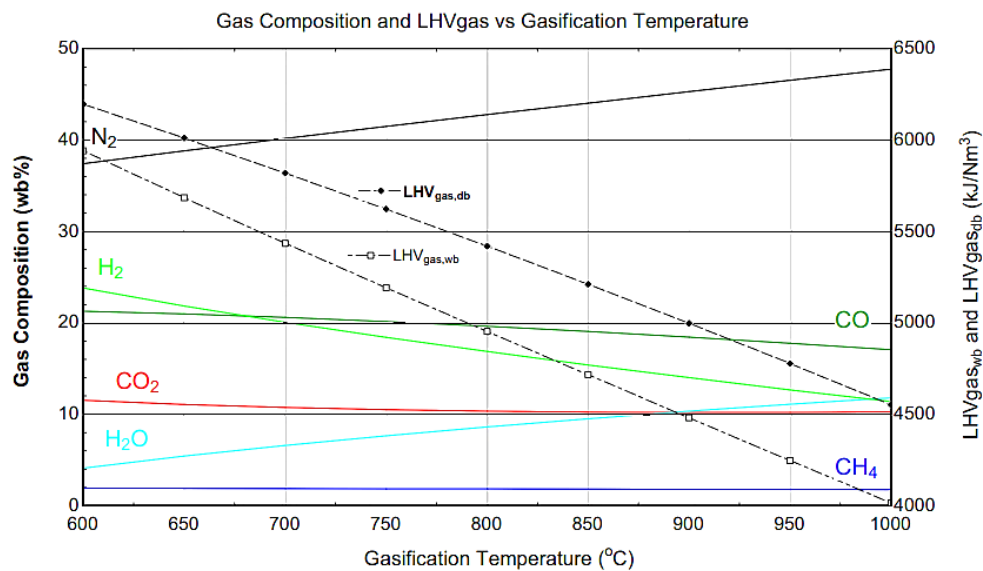


Figure 7.4 Influence of Equivalence Ratio on Gas Composition and LHV, for corn cob gasification with a moisture content of 5%



Table 7.4 Influence of Equivalence Ratio on Gas Composition and LHV

$\lambda$	<b>N<sub>2</sub></b> (vol% wb)	<b>CH<sub>4</sub></b> (vol% wb)	<b>CO<sub>2</sub></b> (vol% wb)	<b>CO</b> (vol% wb)	<b>H<sub>2</sub>O</b> (vol% wb)	<b>H<sub>2</sub></b> (vol% wb)	<b>Hd</b> (kJ/m <sup>3</sup> <sub>N</sub> )wb	<b>Hd</b> (kJ/m <sup>3</sup> <sub>N</sub> )db
0.25	37.40	1.92	11.51	21.26	4.11	23.80	5941	6195
0.26	38.81	1.89	11.06	20.97	5.43	21.84	5683	6010
0.28	40.16	1.87	10.73	20.59	6.60	20.06	5435	5819
0.29	41.47	1.85	10.49	20.13	7.65	18.41	5192	5622
0.31	42.76	1.83	10.33	19.62	8.61	16.86	4953	5419
0.32	44.02	1.81	10.23	19.05	9.50	15.39	4716	5211
0.34	45.27	1.79	10.19	18.43	10.32	13.99	4481	4997
0.36	46.51	1.78	10.20	17.76	11.09	12.65	4247	4777
0.37	47.74	1.76	10.26	17.06	11.80	11.38	4015	4552

### Effect of air preheating on producer gas composition

Air preheating is a means of increasing the conversion efficiency of the gasification process. The sensible heat in the air causes a rise in the gasification temperature, which in turn influences the product gas composition, causing an increase in the production of combustible gases, H<sub>2</sub> and CO, [384]. Air preheating offers an alternative and more economical approach than oxygen blown systems, [384]. The overall efficiency of the process on a thermal basis would be increased if the heat required for air preheating is recovered from the gas cooling section of the plant. Sugiyama et al. [404] suggested that the use of high temperature air as an oxidant achieves downsizing of the plant since a smaller volume of air is needed to bring the gasifier to the required operating temperature; which in turn reduces the size of the reactor and gas clean-up system needed, [384].

The influence of air preheating on the gasification is presented in Figure 7.5 and Table 7.5, for gasification of corn cob with moisture content of 5% and  $\lambda$  0.3. It was found that the gasification temperature increased almost linearly with air temperature. The rising temperature promotes the products of endothermic reactions and simultaneously the reactants of exothermic reactions, [384]. Another important consideration is that the air temperature has a high influence on the product gas. With air temperature increase, CO and H<sub>2</sub> increases while CO<sub>2</sub> decreases (the same as in Puig et al. [384]). Heating value of producer gas increases due to combustible gas increase.

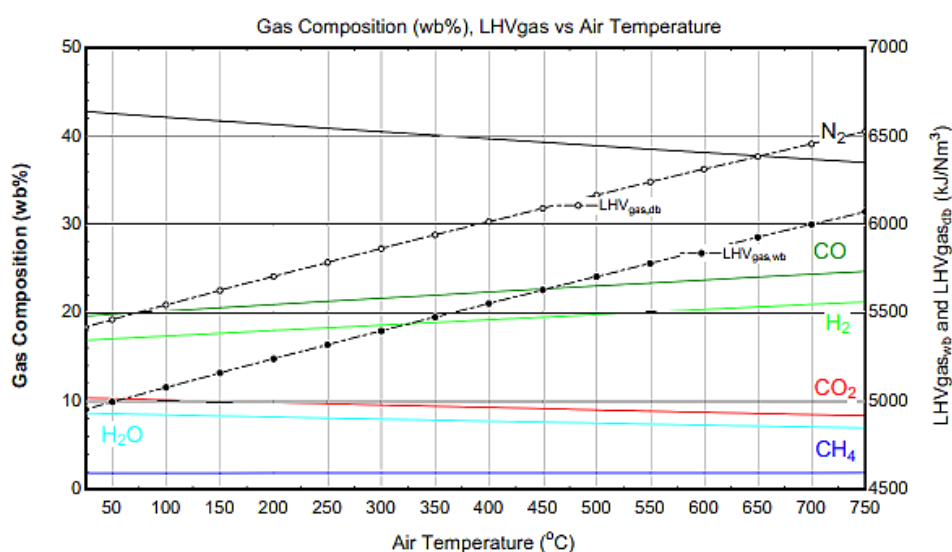


Figure 7.5 Influence of Air Temperature on Gas Composition and LHVgas, for gasification of corn cob with moisture content of 5% and  $\lambda= 0.3$

Table 7.5 Influence of Air Temperature on Gas Composition and LHV<sub>gas</sub>

<b>T<sub>air</sub></b>	<b>λ</b>	<b>V<sub>air</sub></b>	<b>N<sub>2</sub></b>	<b>CH<sub>4</sub></b>	<b>CO<sub>2</sub></b>	<b>CO</b>	<b>H<sub>2</sub>O</b>	<b>H<sub>2</sub></b>	<b>H<sub>d</sub></b>	<b>H<sub>d</sub></b>
°C		m <sup>3</sup> <sub>N</sub>	[vol% wb]	[vol% wb]	[vol% wb]	[vol% wb]	[vol% wb]	[vol% wb]	[k]/m <sup>3</sup> <sub>N</sub> ]wb	[k]/m <sup>3</sup> <sub>N</sub> ]db
25	0.31	137.70	42.76	1.83	10.33	19.62	8.61	16.86	4953	5419
50	0.30	136.60	42.54	1.83	10.26	19.80	8.55	17.02	4994	5461
100	0.30	134.30	42.11	1.83	10.11	20.18	8.42	17.34	5077	5544
150	0.29	132.10	41.70	1.83	9.96	20.55	8.30	17.66	5158	5625
200	0.29	129.90	41.28	1.84	9.82	20.91	8.18	17.97	5239	5706
250	0.28	127.80	40.87	1.84	9.68	21.27	8.06	18.28	5318	5785
300	0.28	125.70	40.47	1.84	9.54	21.62	7.95	18.58	5397	5863
350	0.28	123.70	40.07	1.84	9.40	21.97	7.83	18.89	5474	5940
400	0.27	121.70	39.67	1.85	9.26	22.32	7.72	19.19	5552	6016
450	0.27	119.80	39.28	1.85	9.12	22.67	7.60	19.48	5628	6091
500	0.26	117.90	38.89	1.85	8.99	23.01	7.49	19.78	5704	6166
550	0.26	116.00	38.50	1.85	8.85	23.35	7.38	20.07	5779	6239
600	0.25	114.20	38.12	1.86	8.72	23.68	7.27	20.36	5853	6312
650	0.25	112.40	37.74	1.86	8.59	24.01	7.16	20.64	5927	6384
700	0.25	110.70	37.37	1.86	8.46	24.34	7.05	20.92	5999	6454
750	0.24	109.00	37.00	1.86	8.33	24.67	6.94	21.20	6071	6524

### Effect of oxygen enrichment on producer gas composition

Figure 7.6 and Table 7.6 shows variation of producer gas with changes of oxygen fraction in the air for corn gasification.

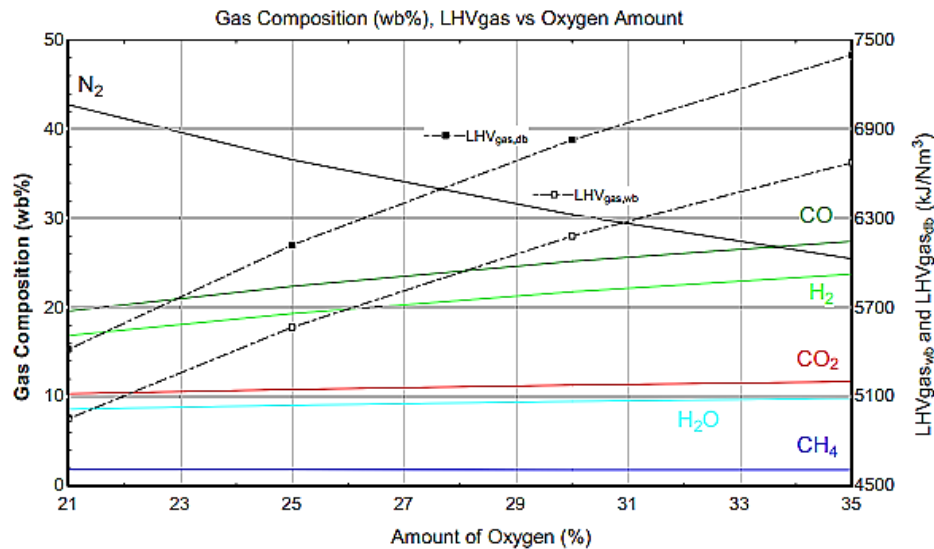


Figure 7.6 Influence of Oxygen Amount on Gas Composition and LHV<sub>gas</sub>, for gasification of corn cob with moisture content of 5% and  $\lambda$  0.3

The N<sub>2</sub> yield decreases with increasing oxygen fraction as expected. The percentage of H<sub>2</sub> in the producer gas increases continuously with oxygen fraction. A similar trend is also observed for CO, while CO<sub>2</sub> remains more or less constant. The same results were obtained by Puig et al. [384] and Babu and Sheth [405]. In Figure 5.7, shows the change in the volume of air required for the gasification according to the volumes of oxygen. Increasing the oxygen content enhances the conversion of carbon from biomass, increase heating, hence the efficiency of gasification. However, the use of oxygen is expensive.

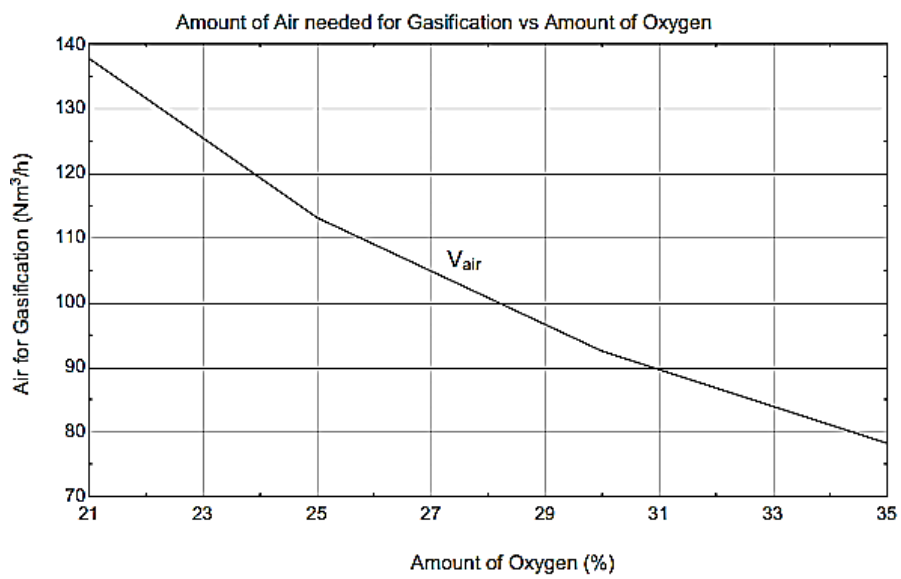


Figure 7.7 Influence of Oxygen on Gas Composition and LHV<sub>gas</sub>

Table 7.6 Influence of oxygen amount on gas composition and LHV<sub>gas</sub>

<b>O<sub>2</sub></b>	<b>Vair</b>	<b>N<sub>2</sub></b>	<b>CH<sub>4</sub></b>	<b>CO<sub>2</sub></b>	<b>CO</b>	<b>H<sub>2</sub>O</b>	<b>H<sub>2</sub></b>	<b>Hd</b>	<b>Hd</b>
	m <sup>3</sup> <sub>N</sub>	[vol% wb]	[vol% wb]	[vol% wb]	[vol% wb]	[vol% wb]	[vol% wb]	[kJ/m <sup>3</sup> N]wb	[kJ/m <sup>3</sup> N]db
21	137.7	42.76	1.828	10.33	19.62	8.609	16.86	4953	5419
25	113.1	36.59	1.819	10.82	22.4	9.046	19.32	5567	6120
30	92.47	30.42	1.81	11.31	25.19	9.482	21.79	6182	6829
35	78.19	25.48	1.803	11.7	27.42	9.83	23.76	6674	7402

### Effect of moisture content on producer gas composition

The effect of initial moisture content of corn cob on the producer gas composition at 800°C and  $\lambda$  0.31 presented in Figure 7.8 and Table 7.7.

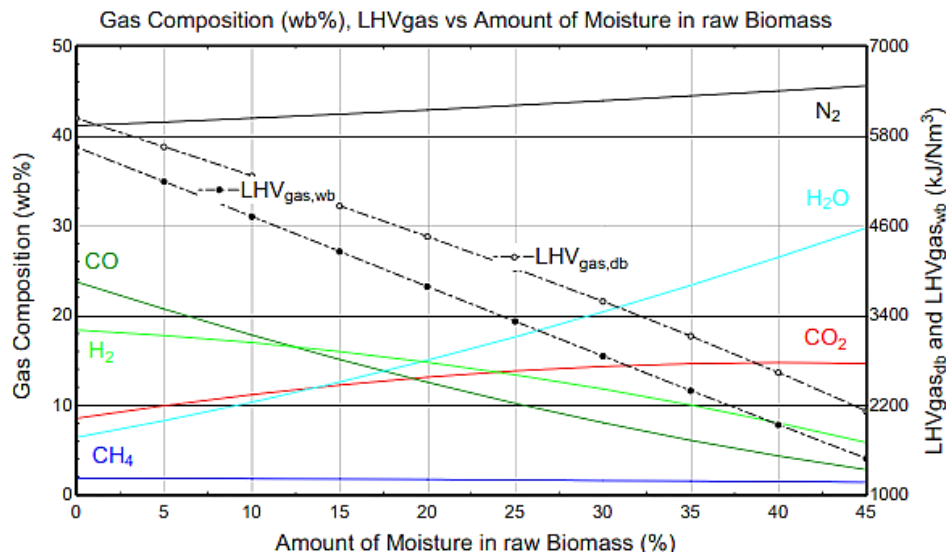


Figure 7.8 Influence of Biomass Moisture on Gas Composition and LHVgas

The percentage of CO<sub>2</sub> increases with the moisture content, while CO decreases. A similar trend is also observed for the H<sub>2</sub> in the fuel gas increases continuously with the moisture content. Heating value of producer gas decreases, due to additional air flow is required when increasing the moisture content in order to generate the heat required to keep the desired temperature at. The same tendencies were observed by Puig et al [384] and Pilsa and Wilk [401, 406].

In the literature, it is recommended to dry the biomass, if the moisture content in the biomass, exceeds 15-20% (by weight) [218, 407].

Table 7.7 Influence of Biomass Moisture on Gas Composition and LHVgas

<b>w</b>	<b>Vair</b>	<b>N<sub>2</sub></b>	<b>CH<sub>4</sub></b>	<b>CO<sub>2</sub></b>	<b>CO</b>	<b>H<sub>2</sub>O</b>	<b>H<sub>2</sub></b>	<b>Hd</b>	<b>Hd</b>
	m <sup>3</sup> <sub>N</sub>	[vol wb %]	[vol wb %]	[vol wb %]	[vol wb %]	[vol wb %]	[vol wb %]	[kJ/m <sup>3</sup> <sub>N</sub> ]wb	[kJ/m <sup>3</sup> <sub>N</sub> ]sb
0	130.2	41.13	1.872	8.52	23.73	6.389	18.36	5650	6036
5	131.4	41.53	1.835	9.931	20.69	8.263	17.75	5187	5654
10	132.8	41.96	1.794	11.17	17.8	10.32	16.96	4721	5265
15	134.4	42.41	1.749	12.24	15.08	12.56	15.96	4254	4865
20	136.2	42.89	1.7	13.12	12.53	14.99	14.77	3787	4454
25	138.1	43.39	1.648	13.81	10.18	17.6	13.38	3320	4029
30	140.2	43.91	1.592	14.31	8.019	20.38	11.78	2855	3586
35	142.6	44.45	1.533	14.62	6.064	23.34	9.989	2394	3122
40	145.1	45.01	1.471	14.73	4.319	26.47	8.006	1937	2634
45	147.7	45.57	1.405	14.64	2.787	29.75	5.841	1486	2116



### **7.3. CONCLUSION**

The gasification model is made up of a series of modules each containing one process. An overall scheme is usually adopted by considering the different steps in which gasification process can be approximately subdivided: heating and drying, pyrolysis or devolatilisation, combustion or partial oxidation, and reduction (or charcoal gasification). A real gasification system differs from an ideal reactor at chemical equilibrium. For this reason, the pure equilibrium model has been modified to increase the results' accuracy. For the model developed in this project, the following assumptions are made:

1. Adding a pyrolysis unit that, using correlations, predicts the formation of gas, charcoal and volatiles in this step of the gasification process [112]
2. Considering heat losses in pyrolysis and gasification units,
3. Adding tar and char leaving the gasifier as a percentage of tar and charcoal produced in the pyrolysis unit added [112]
4. Particles leaving the gasifier and set by the user as mg/Nm<sup>3</sup> in the producer gas. These particles are considered to consist only of carbon [112]
5. Producer gas consists of CO<sub>2</sub>, CO, H<sub>2</sub>, CH<sub>4</sub>, N<sub>2</sub>, and H<sub>2</sub>O (Setting the amount of CH<sub>4</sub> produced)

The fundamental equations in the model are conservation of mass and energy. In modelling the pyrolysis unit the energy demand for this unit is calculated as the difference in the energy contents of the incoming and outgoing flows. Determination of the gas composition from the gasification chamber is based on equations for element balances, the water gas shift equation and methanisation equation.

The model is sensitive enough to evaluate the influence of  $\lambda$ , air preheating, steam injection, oxygen enrichment and biomass moisture content in the quality of producer gas. The results predicted by the model are in good agreement with those predicted by other authors' models and can be summarised as follows:

1. Increasing the  $\lambda$  also means increasing the gasification temperature and decreasing the LHV of producer gas;
2. The use of high temperature air has a significant influence on producer gas composition. It was found that the gasification temperature increased almost linearly with air temperature. With air temperature increase, CO and H<sub>2</sub> increases while CO<sub>2</sub> decreases. Heating value of producer gas increases due to combustible gas increase.

3. Steam injection in biomass gasification raises the H<sub>2</sub> content of producer gas, similar trend is also observed for CO, while CO<sub>2</sub> remains more or less constant.
4. The LHV, CO and H<sub>2</sub> yields of producer gas increase when the oxygen fraction of air increases
5. Increasing the moisture content of biomass, percentage of CO<sub>2</sub> increases with the moisture content, while CO decreases. A similar trend is also observed for the H<sub>2</sub> in the fuel gas increases continuously with the moisture content. Heating value of producer gas decreases, due to additional air flow is required when increasing the moisture content in order to generate the heat required to keep the desired temperature.

This model has been validated with published experimental data. For downdraft gasifiers, the predicted values for air gasification are in very good agreement with the experimental ones for all cases.

These models will be able to predict phenomena in a wide range of experimental conditions and for different type of biomass material. Also, the model is accurate enough to predict the behaviour of downdraft fixed bed gasifiers for air and steam gasification. However, more experimental data is needed to evaluate the prediction capability of the model for air/steam biomass gasification in downdraft gasifiers.

*“As for the future, your task is not to foresee it, but to enable it.”  
Antoine de Saint-Exupery*

## 8. CONCLUSIONS AND FUTURE WORK

A comprehensive theoretical and experimental study of the pyrolysis of corn cob under regime controlled by chemical kinetics (Chapter 5), and theoretical and experimental study how to achieve high charcoal and the theoretical yield of carbon from corn cob (Chapter 6), have been presented. Since concluding remarks have been given separately in both these sections, the overall conclusions are outlined in this chapter.

### 8.1 ATTAINMENT OF THE THEORETICAL YIELD OF CARBON FROM CORN COB

The goal of this part of experimental work was to identify process conditions that improve the yield of charcoal from two different corn cob samples (Scob and Pcob). To realize this goal, first was calculated the theoretical fixed-carbon yield of charcoal by use of the elemental composition of the wood feedstock. Next, the effect of the influence of particle size, sample size, and vapour-phase residence time (influence of secondary pyrolysis) on experimental values of the fixed carbon yields of the charcoal products were analysed and compared with values of the calculated theoretical limiting values.

#### **It was learned that:**

1. The yield of charcoal ( $y_{\text{char}}$ ) from biomass is not a meaningful metric of the efficiency of a carbonization process. Instead, the fixed-carbon yield ( $y_{\text{fc}}$ ) should be used to characterize carbonization efficiency. When an elemental analysis of the feedstock is available, it can be used to calculate the yield of pure carbon that can be realized when thermochemical equilibrium ( $y_{\text{fc}}^{\text{th}}$ ) is reached in a carbonizer. This theoretical yield of pure carbon can be compared to the experimental value of the fixed-carbon yield and thereby used as a meaningful metric of the efficiency of the carbonization process.
2. Sample size strongly influences the charcoal and fixed carbon yields measured by TGA instruments. For example, in this work, an increase in corn cob powder sample size from 5 to 40 mg increases the (open crucible) measured charcoal yield at 550°C from

20.52% to 22.56% for Scob and from 20.43 to 22.80% for Pcob. Upon heating particle samples decomposes by an unknown series of bond-breaking reactions. The species formed by this initial step may be sufficiently immobile to preclude rapid escape from the particle. It is known that the generation of volatile gases inside the solid produces high pressures (up to 0.3 atm, depending on the biomass porosity), which force the volatiles toward both the hot charcoal layer and the interior of the solid. The intra-particle contact between freshly formed pyrolysis oil vapours and charcoal/ash particles might lead to an increase in secondary repolymerization reactions. Tar trapped within the particles followed by polymerization/charring reactions could be an additional explanation for the higher charcoal yields.

3. Secondary pyrolysis reactions, which involve vapour-phase species, are at least as important as primary pyrolysis reactions in the formation of charcoal. Any condition (e.g., increasing pressure), which enhances or prolongs the contact of the vapour phase species with the solid, will augment the fixed carbon yield of charcoal. Biomass pyrolysis is simply the fragmentation of the biopolymer into smaller organic compounds (e.g., levoglucosan, glycolaldehyde, various furans, etc.) at elevated temperature. Thermodynamic calculations indicate that these compounds are not stable at elevated temperature; the preferred products are carbon and light gases. Any condition that favours the attainment of thermodynamic equilibrium, by prolonging or enhancing the contact of the biopolymer fragments with the solid, necessarily augments the yield of carbon.

## **8.1 PREDICTIVE MODEL OF CORN COB PYROLYSIS**

Based on experimental and literature results an empirical steady model was developed. The aim of this developed model was to provide a guide on the pyrolysis characteristics of biomass, to determine the yields of pyrolysis, to determine the composition of the light gas covering conditions typically found in pyrolysis which can be used independently or in gasification and biomass combustion models.

This empirical model is a way of compiling the collected experimental data in a structured tool that can be effectively used to analyse the biomass pyrolysis process. Additionally, it can be considered as a first step toward its extension to practical applications, where additional chemical and transport phenomena need to be incorporated.

## 8.2 KINETICS OF CORN COB PYROLYSIS

The present thesis adds insight into the field of corn cob pyrolysis kinetics. The comprehensive thermal behavior of two different corncob samples were studied by thermogravimetry at linear and nonlinear heating programs in inert gas flow.

Various kinetic model approaches based on *first* and *n*th-order partial reactions in the summative model of pseudocomponents are employed in order to determine the best kinetic parameters that describe the experiments both at linear and stepwise heating programs. The TG and DTG curves associated with the pyrolysis of two corn cob (Scob and Pcob) samples was well described by the distributed activation energy model (DAEM) which assumes that the decomposition of complex components (pectine, hemicellulose, cellulose, and lignin) occurs through a series of reactions that have a range of activation energies. The resulting models described well the experimental data. When the evaluation was based on a smaller number of experiments, similar model parameters were obtained which were suitable for predicting experiments at higher heating rates. This test indicates that the available experimental information was sufficient for the determination of the model parameters. The checks on the prediction capabilities were considered to be an essential part of the model verification. In another test, the experiments of the two samples were evaluated together, assuming more or less common kinetic parameters for both corn cobs. This test revealed that the reactivity differences between the two samples are due to the differences in their hemicelluloses and extractives. The kinetic parameter values from a similar earlier work on other biomasses could also be used, indicating the possibilities of a common kinetic model for the pyrolysis of a wide range of agricultural byproduct.

### **It was learned that:**

1. Thermogravimetry is a useful tool to distinguish different biomass pseudocomponents (hemicellulose, cellulose, and lignin) from each other. That is, biomass pseudocomponents has its own thermal fingerprint which is dependent on the biomass chemical composition. Even the same chemical species may have differing reactivity if their pyrolysis is influenced by other species in their vicinity. For two different corn cob samples (Scob and Pcob) the main difference is the presence of a low temperature partial peak on the DTG curve of sample Pcob with peak top at 231 °C. This peak can be due to

pectin which is a regular constituent of corn cob; its typical abundance is about 3 wt%. The rest of the decomposition is similar for the two corn cobs, though the hemicellulose and cellulose peaks occur at somewhat lower temperatures for the Pcob cob. This can be due to the higher ash content of the Pcobs, because some inorganic impurities have strong catalytic effects and may lower the peak temperatures of the hemicellulose.

2. The obtained DEAM proved to be suitable for the prediction of the biomass pyrolysis behavior. The DAEM provides an easier, faster way for calculate the kinetic parametars as compared to the other traditional kinetic models. The traditional kinetic models utilizes a complex numerical integration technique requiring considerable amount of time and processing power. The DAEM was shown to work effectively to model the pyrolysis behaviour of biomass as the model requires only data from TGA experiments, and calculates the kinetics independent of sample composition. This provides an advantage of the DAEM as a means of providing a model-free approach to determining the activation energy for any sample undergoing pyrolysis.

3. It should be noted, kinetic models for the description of individual volatile evolutions from pyrolysis are unusually found in the literature [80]. These kinetic evaluations were performed in the attempt to better understande the pyrolytic process as a whole and to provide a kinetic approach that integrates the different chemical phenomena involved in biomass pyrolysis and could be useful for modeling the pyrolysis process as a unit or step in engineering applications. This development can be useful for the selection of the most appropriate configuration and operating conditions of chemical reactors on dependence of the desired composition and yields of the products [80].

### **8.3. FUTURE RESEARCH WORK**

1. The steady gasification model needs to be verified, either separate in TGA gasification experiments or in the gasifier reactor. Based on this analysis the proposed steady gasification model can be modified and improved.

2. It would be interesting to develop a kinetic model for biomass gasification incorporated with pyrolysis kinetic model. The development of model of whole biomass gasification could facilitatethe analysis of the optimal conditions to optimize and to minimize the current drawbacks of the gasification process.

It would be interested to couple pyrolysis kinetics model with transport equations, considering intra and extra-particle phenomena (e.g. shrinkage) and the operating conditions prevailing in practical pyrolysis reactors. The new developed model should be verified in pyrolysis experiments of corn cob (or different type of biomass). However, the pyrolysis reactor cannot be used in such experiments without some modifications, since shrinkage in both the axial and radial directions will be problematic to handle

## REFERENCES

1. Basu, P., *Biomass gasification and pyrolysis : practical design and theory*. 2010, Oxford, UK: Elsevier Inc. 365.
2. *Two-dimensional representation of a cellulose polymer, available at <http://www.chemistry.wustl.edu/>.*
3. Grønli, M.G., *A theoretical and experimental study of the thermal degradation of biomass*. 1996, Norwegian University of Science and Technology: Trondheim
4. *General structure of lignin. Inset of lignol monomers, available at <http://commons.wikimedia.org/wiki/File:Lignin.png>.*
5. Jones, J., et al., *Towards biomass classification for energy applications*, in *Science in Thermal and Chemical Biomass Conversion*, A.V. Bridgwater and D.G.B. Boocock, Editors. 2006. p. 956 (vol 1) 984 pp (vol 2).
6. Barrio, M., *Experimental investigation of small-scale gasification of woody biomass*, in *Norwegian University of Science and Technology, Faculty of Engineering Science and Technology*. 2002, Norwegian University of Science and Technology, Faculty of Engineering Science and Technology: Trondheim. p. 222.
7. *The European Commission, EU energy in Figures - Statistical Pocket book 2013*. 2013, Publications Office of the European Union: Luxembourg, Belgium.
8. Scowcroft, J., *Biomass 2020: Opportunities, Challenges and Solutions, part of the EURELECTRIC Renewables Action Plan (RESAP)*. 2011, The Union of the Electricity Industry–EURELECTRIC.
9. Uslu, A. and J.v. Stralen, *Sustainable biomass for electricity, heat and transport fuels in the EU27 - Policy summary (D5.4)*, in *Biomass role in achieving the Climate Change & Renewables EU policy targets. Demand and Supply dynamics under the perspective of stakeholders - Biomass Futures project (IEE 08 653 SI2. 529 241 )*, A. Uslu and J.v. Stralen, Editors. 2012.
10. Panoutsou, C. and A. Castillo, *Outlook on Market Segments for Biomass Uptake by 2020 (D2.3. )*, in *Biomass role in achieving the Climate Change & Renewables EU policy targets. Demand and Supply dynamics under the perspective of stakeholders . IEE 08 653 SI2. 529 241*. 2011
11. *Ministry of Energy, Development and Environmental Protection of Republic of Serbia, ENERGETSKI BILANS REPUBLIKE SRBIJE ZA 2014. GODINU*.
12. Khalil, R.A., *Thermal conversion of biomass with emphasis on product distribution, reaction kinetics and sulfur abatement*, in *Department of Energy and Process Engineering*. 2009, Norwegian University of Science and Technology: Trondheim.
13. Dong, L., H. Liu, and S. Riffat, *Development of small-scale and micro-scale biomass-fuelled CHP systems – A literature review*. *Applied Thermal Engineering*, 2009. **29**(11–12): p. 2119-2126.
14. Munajat, N.F.B., *Combustion of gasified biomass: Experimental investigation on laminar flame speed, lean blowoff limit and emission levels*. 2013, Department of Energy Technology, School of Industrial Technology and Management, Royal Institute of Technology: Stockholm, Sweden.
15. Venderbosch, R.H. and W. Prins, *Fast pyrolysis technology development*. *Biofuels, Bioproducts and Biorefining*, 2010. **4**(2): p. 178-208.
16. Bridgwater, A., *Thermal biomass conversion and utilization Biomass information system*. 1996, Brussels, Luxembourg: Office for Official Publications of the European Communities.
17. Graboski, M., *Kinetics of Char Gasification Reactions*, in *Biomass Gasification - Principles and Technology*, T.B. Reed, Editor. 1981, Park Ridge, N.Y. p. 154-182.



18. Oliver, M.P., *Secondary reactions of tar during thermochemical biomass conversion*. 2001, Swiss Federal Institute of Technology Zurich.
19. Demirbas, A., *Effects of temperature and particle size on bio-char yield from pyrolysis of agricultural residues*. Journal of Analytical and Applied Pyrolysis, 2004. **72**(2): p. 243-248.
20. Várhegyi, G. *Introduction to kinetic models for biomass pyrolysis. Part 1*. in *Nordic PhD course Analytical Techniques in Combustion*. 2010. NTNU \_ Trondheim, Norway.
21. Várhegyi, G., *Aims and methods in non-isothermal reaction kinetics*. Journal of Analytical and Applied Pyrolysis, 2007. **79**(1-2): p. 278-288.
22. Bradbury, A.G.W., Y. Sakai, and F. Shafizadeh, *A kinetic model for pyrolysis of cellulose*. Journal of Applied Polymer Science, 1979. **23**(11): p. 3271-3280.
23. Broido, A., *KINETICS OF SOLID-PHASE CELLULOSE PYROLYSIS*, in *Thermal Uses and Properties of Carbohydrates and Lignins*, F. Shafizadeh, K.V. Sarkanen, and D.A. Tillman, Editors. 1976, Academic Press. p. 19-36.
24. Broido, A. and M.A. Nelson, *Char yield on pyrolysis of cellulose*. Combust Flame, 1975. **24**: p. 263-268.
25. Di Blasi, C., *Modeling and simulation of combustion processes of charring and non-charring solid fuels*. Progress in Energy and Combustion Science, 1993. **19**(1): p. 71-104.
26. Петар, Г., *Моделирање процеса деволатализаације биомасе*. 2002, Машински факултет Универзитет у Београду: Београд.
27. Thurner, F. and U. Mann, *Kinetic investigation of wood pyrolysis*. Industrial & Engineering Chemistry Process Design and Development, 1981. **20**(3): p. 482-488.
28. Koufopoulos, C.A., A. Lucchesi, and G. Maschio, *Kinetic modelling of the pyrolysis of biomass and biomass components*. The Canadian Journal of Chemical Engineering, 1989. **67**(1): p. 75-84.
29. Antal, M.J., *Effects of reactor severity on the gas-phase pyrolysis of cellulose- and kraft lignin-derived volatile matter*. Industrial & Engineering Chemistry Product Research and Development, 1983. **22**(2): p. 366-375.
30. Antal, M., Jr., *A Review of the Vapor Phase Pyrolysis of Biomass Derived Volatile Matter*, in *Fundamentals of Thermochemical Biomass Conversion*, R.P. Overend, T.A. Milne, and L.K. Mudge, Editors. 1985, Springer Netherlands. p. 511-537.
31. Chan, W.-C.R., M. Kelbon, and B.B. Krieger, *Modelling and experimental verification of physical and chemical processes during pyrolysis of a large biomass particle*. Fuel, 1985. **64**(11): p. 1505-1513.
32. Gvero, P., *Modeliranje procesa devolatalizacije biomase, Doktorska disertacija*. 2002, Mašinski fakultet Univerziteta u Beogradu.
33. Srivastava, V.K., Sushil, and R.K. Jalan, *Prediction of concentration in the pyrolysis of biomass material—II*. Energy Conversion and Management, 1996. **37**(4): p. 473-483.
34. Di Blasi, C., *Heat, momentum and mass transport through a shrinking biomass particle exposed to thermal radiation*. Chemical Engineering Science, 1996. **51**(7): p. 1121-1132.
35. Miller, R.S. and J. Bellan, *A Generalized Biomass Pyrolysis Model Based on Superimposed Cellulose, Hemicellulose and Lignin Kinetics*. Combustion Science and Technology, 1997. **126**(1-6): p. 97-137.
36. Rath, J. and G. Staudinger, *Cracking reactions of tar from pyrolysis of spruce wood*. Fuel, 2001. **80**(10): p. 1379-1389.
37. Instruments, T., *TGA Q600 SPECIFICATIONS*.
38. Trninić, M., et al., *Kinetics of Corncob Pyrolysis*. Energy & Fuels, 2012. **26**(4): p. 2005-2013.
39. Instruments, T., *TGA Q500 SPECIFICATIONS*.
40. Mettler Toledo, T.S.S.-T.f.R.a.R., 2012.
41. Wang, L., et al., *Is Elevated Pressure Required To Achieve a High Fixed-Carbon Yield of Charcoal from Biomass? Part 1: Round-Robin Results for Three Different Corncob Materials*. Energy & Fuels, 2011. **25**(7): p. 3251-3265.

42. Neves, D., et al., *Characterization and prediction of biomass pyrolysis products*. Progress Energy Combustion Science, 2011. **37**: p. 611 - 630.
43. GmbH, E.A., *vario MACRO CHNS - Specifications*. 2004: Hanau, Germany
44. Sastry, A.B.a.R.C., *Biomass Gasification Processes in Downdraft Fixed Bed Reactors: A Review*. International Journal of Chemical Engineering and Applications, 2011. **2**(6).
45. Pavasović, V.I., Mladen, *Problem pri sagorevanju otpadne bio-mase vezanih za povećan sadržaj alkalnih metala u pepelu*, in *Sagorevanje bio-mase u energetske svrhe*, N. Ninić and S. Oka, Editors. 1992, Jugoslovensko društvo termičara, Naučna knjiga: Beograd.
46. Jenkins, B.M., et al., *Combustion properties of biomass*. Fuel Processing Technology, 1998. **54**(1-3): p. 17-46.
47. *Ministarstvo rudarstva i energetike Republike Srbije, Nacrt strategije razvoja energetike do 2025. godine, sa projekcijama do 2030. godine*, available at [http://www.parlament.gov.rs/upload/archive/files/lat/pdf/akta\\_procedura/2014/113-14Lat.pdf](http://www.parlament.gov.rs/upload/archive/files/lat/pdf/akta_procedura/2014/113-14Lat.pdf).
48. Lathrop, E.C. and J.H. Shollenberger, *Corn cobs : their composition, availability, farm and industrial uses* December 1947, Illinois, USA: Peoria, Ill. : U.S. Dept. of Agriculture, Agricultural Research Administration, Bureau of Agricultural and Industrial Chemistry, Northern Regional Research Laboratory.
49. Phillips, J., *Different Types of Gasifiers and Their Integration with Gas Turbines*.
50. Ciferno, J.P. and J.J. Marano, *Benchmarking Biomass Gasification Technologies for Fuels, Chemicals and Hydrogen Production - Prepared for U.S. Department of Energy National Energy Technology Laboratory*. 2002.
51. ANA, R., *Study of Lignocellulosic Biomass Pyrolysis: State of the Art and Modelling*, in *Department of Industrial Ecology*. 2007, KTH - Kungliga Tekniska Högskolan: Stockholm
52. Bridgwater, A., *Fast Pyrolysis of Biomass: A Handbook Volume 2*. 2002: CPL Pres.
53. Sharma, A.K., *Modeling and simulation of a downdraft biomass gasifier 1. Model development and validation*. Energy Conversion and Management, 2011. **52**(2).
54. Brown, D., T. Fuchino, and F. Maréchal, *Solid fuel decomposition modelling for the design of biomass gasification systems*. Computer Aided Chemical Engineering, 2006. **21**.
55. Peacocke, C. and S. Joseph. *Notes on Terminology and Technology in Thermal Conversion, International Biochar Initiative: [www.biochar-international.org](http://www.biochar-international.org)*.
56. Zajec, L., *SLOW PYROLYSIS IN A ROTARY KILN REACTOR: OPTIMIZATION AND EXPERIMENTS*. 2009, University of Iceland & the University of Akureyri: Akureyri, Iceland.
57. Wang, L., et al., *Is Elevated Pressure Required to Achieve a High Fixed-Carbon Yield of Charcoal from Biomass? Part 2: The Importance of Particle Size*. Energy & Fuels, 2013. **27**(4): p. 2146-2156.
58. Chaurasia, A. and B.V. Babu, *Modeling, Simulation, and Optimization of Pyrolysis of Biomass*. 2011: LAP LAMBERT Academic Publishing GmbH & Co. KG.
59. Encinar, J.M., et al., *Pyrolysis of maize, sunflower, grape and tobacco residues*. Journal of Chemical Technology & Biotechnology, 1997. **70**(4): p. 400-410.
60. *Chippewa Valley Ethanol Company, Corn Cobs as Sustainable Biomass for Renewable Energy, A Field-to-Facility Demonstration and Feasibility Study. Final Report to the Minnesota Department of Commerce Office of Energy Security*. 2009 Available at: <http://www.auri.org/>.
61. Bridgwater, A., *Thermal biomass conversion and utilization : biomass information system*. 1996: Luxembourg : Office for Official Publications of the European Communities.
62. Wang, L., J.E. Hustad, and M. Grønli, *Sintering Characteristics and Mineral Transformation Behaviors of Corn Cob Ashes*. Energy & Fuels, 2012. **26**(9): p. 5905-5916.
63. Antal Jr, M.J., *Mathematical modelling of biomass pyrolysis phenomena: Introduction*. Fuel, 1985. **64**(11): p. 1483-1486.

64. Antal, M., Jr., *Biomass Pyrolysis: A Review of the Literature Part 2—Lignocellulose Pyrolysis*, in *Advances in Solar Energy*, K. Böer and J. Duffie, Editors. 1985, Springer US. p. 175-255.
65. Antal, M.J., *Process for Charcoal Production from Woody and Herbaceous Plant Material*, U.S. Patent No. 5,435,983. 1995.
66. Antal, M.J., *Process for Charcoal Production from Woody and Herbaceous Plant Material*, U.S. Patent No. 5,551,958. 1996.
67. Antal, M.J., et al., *Attainment of the Theoretical Yield of Carbon from Biomass*. Industrial & Engineering Chemistry Research, 2000. **39**(11): p. 4024-4031.
68. Antal, M.J., et al., *High-Yield Biomass Charcoal†*. Energy & Fuels, 1996. **10**(3): p. 652-658.
69. Antal, M.J. and M. Grønli, *The Art, Science, and Technology of Charcoal Production†*. Industrial & Engineering Chemistry Research, 2003. **42**(8): p. 1619-1640.
70. Antal, M.J., et al., *Design and operation of a solar fired biomass flash pyrolysis reactor*. Solar Energy, 1983. **30**(4): p. 299-312.
71. Antal, M.J., K. Mochidzuki, and L.S. Paredes, *Flash Carbonization of Biomass*. Industrial & Engineering Chemistry Research, 2003. **42**(16): p. 3690-3699.
72. Antal, M.J. and W.S.L. Mok, *Review of methods for improving the yield of charcoal from biomass*. Energy & Fuels, 1990. **4**(3): p. 221-225.
73. Várhegyi, G., et al., *TG, TG-MS, and FTIR Characterization of High-Yield Biomass Charcoals*. Energy & Fuels, 1998. **12**(5): p. 969-974.
74. Mok, W.S.L. and M.J. Antal Jr, *Effects of pressure on biomass pyrolysis. I. Cellulose pyrolysis products*. Thermochemica Acta, 1983. **68**(2–3): p. 155-164.
75. Mok, W.S.L., et al., *Formation of charcoal from biomass in a sealed reactor*. Industrial & Engineering Chemistry Research, 1992. **31**(4): p. 1162-1166.
76. *British Standards Institution, Solid biofuels. Terminology, definitions and descriptions*. London:BSI. p. 34.
77. Stojiljkovic, D., *Potential of Biomass in Serbia*, in *European Union Sustainable Energy Week (EUSEW) 2011*: Brussels, Belgium.
78. *DIRECTIVE 2001/77/EC OF THE EUROPEAN PARLIAMENT AND OF THE COUNCIL OF THE EUROPEAN UNION - On the promotion of electricity produced from renewable energy sources in the internal electricity market*. 2007.
79. *DIRECTIVE 2009/28/EC OF THE EUROPEAN PARLIAMENT AND OF THE COUNCIL*. Official Journal of the European Union, 2009: p. L 140/16 - L 140/62.
80. Díaz, C.J.G., *Understanding Biomass Pyrolysis Kinetics: Improved Modeling -based on -comprehensive -thermokinetic Analysis*, in *Departament d'Enginyeria Química*. 2006, Escola Tècnica Superior d'Enginyeria Industrial de Barcelona Universitat Politècnica de Catalunya: Barcelona, Spain.
81. Predojević, Z.J., *Postupci pripreme lignocelulozne sirovine za dobijanje bioetanol* Hemijska industrija, 2010. **64**(4): p. 283-293.
82. Jäger-Waldau, A. and H. Ossenbrink, *Progress of electricity from biomass, wind and photovoltaics in the European Union*. Renewable and Sustainable Energy Reviews, 2004. **8**(2): p. 157-182.
83. Marković, J.P., et al., *Changes in the infrared attenuated total reflectance (ATR) spectra of lignins from alfalfa stem with growth and development*. Journal of Serbian Chemical Society, 2009. **74**(8–9): p. 885–892.
84. Yaman, S., *Pyrolysis of biomass to produce fuels and chemical feedstocks*. Energy Conversion and Management, 2004. **45**(5): p. 651-671.
85. Cui, Z., et al., *Enzymatic Digestibility of Corn Stover Fractions in Response to Fungal Pretreatment*. Industrial & Engineering Chemistry Research, 2012. **51**(21): p. 7153-7159.
86. Di Blasi, C., et al., *Product Distribution from Pyrolysis of Wood and Agricultural Residues*. Industrial & Engineering Chemistry Research, 1999. **38**(6): p. 2216-2224.

87. Wannapeera, J., N. Worasuwannarak, and S. Pipatmanomai, *Product yields and characteristics of rice husk, rice straw and corncob during fast pyrolysis in a drop-tube/fixed-bed reactor*. Songklanakarin Journal of Science and Technology, 2008. **30**(3): p. 393-404.
88. Sjöström, E., *Wood Chemistry Fundamentals and Applications*. 2nd ed. 1993, San Diego, California: Academic Press, Inc.
89. Obernberger, I., T. Brunner, and G. Bärnthaler, *Chemical properties of solid biofuels—significance and impact*. Biomass and Bioenergy, 2006. **30**(11): p. 973-982.
90. ECOTEC Research and Consulting Limited, *Renewable Energy Sector in the EU: its Employment and Export Potential - A Final Report to DG Environment*. January 2002.
91. EUROPEAN COMMISSION, *GREEN PAPER - A 2030 framework for climate and energy policies*. 2013.
92. Loo, S.v. and J. Koppejan, *The Handbook of Biomass Combustion and Co-firing*. 2008, London, UK: Earthscan.
93. Zhang, Y., A.E. Ghaly, and B. Li, *Physical Properties of Corn Residues*. American Journal of Biochemistry and Biotechnology, 2012. **8**(2): p. 44-53.
94. Lee, D., et al., *Composition of Herbaceous Biomass Feedstocks*. 2007, Brookings, USA: North Central Sun Grant Center South Dakota State University.
95. Shaojun, X., et al., *Corn Stalk Ash Composition and Its Melting (Slagging) Behavior during Combustion*. Energy & Fuels, 2010. **24**(9): p. 4866-4871.
96. Pan, X. and Y. Sano, *Fractionation of wheat straw by atmospheric acetic acid process*. Bioresource Technology, 2005. **96**(11): p. 1256-1263.
97. Demirbas, A., *Fuel characteristics of olive husk and walnut, hazelnut, sunflower, and almond shells*. Energy Sources, 2002. **24**(3): p. 215-221.
98. Obernberger, I., et al., *Concentrations of inorganic elements in biomass fuels and recovery in the different ash fractions*. Biomass and Bioenergy, 1997. **12**(3): p. 211-224.
99. Maniatis, K., G. Guiu, and J. Riesgo, *The european commission perspective in biomass and waste thermochemical conversion, in Pyrolysis and Gasification of Biomass and Waste, Proceedings of an Expert Meeting*. October 2002, CPL Press, Newbury. p. 1 – 18.
100. Eurostat. *Total production of primary energy (annualy)*. Available from: <http://epp.eurostat.ec.europa.eu/>.
101. [www.iea.org](http://www.iea.org). International Energy Agency
102. *Energy for the Future: Renewable Sources of Energy. White Paper for a Community Strategy and Action Plan. COM (97) 599 final, 26 November 1997 [follow-up to the Green Paper]*. 1997. p. 54.
103. Ruska, M. and J. Kiviluoma, *Renewable electricity in Europe, Current state, drivers, and scenarios for 2020*. 2011, VTT Technical Research Centre of Finland: JULKAISIJA – UTGIVARE – PUBLISHER.
104. Марковић, Д., et al., *Бела књига Електропривреде Србије*. ЈП „Електропривреда Србије“: Београд.
105. Capros, P., et al., *Analysis of the EU policy package on climate change and renewables*. Energy Policy, 2011. **39**(3): p. 1476-1485.
106. Michalena, E. and J.M. Hills, *Renewable energy issues and implementation of European energy policy: The missing generation?* Energy Policy, 2012. **45**(0): p. 201-216.
107. *WHITE PAPER Roadmap to a Single European Transport Area – Towards a competitive and resource efficient transport system*, EUROPEAN COMMISSION, Brussels, 28.3.2011.
108. Kampman, B., A. van-Grinsven, and H. Croezen, *Sustainable alternatives for land-based biofuels in the European Union - Assessment of options and development of a policy strategy 2012*, CE Delft, Delft
109. Svetlana Ladanai, J.V., *Global Potential of Sustainable Biomass for Energy*. 2009, SLU, Swedish University of Agricultural Sciences, Department of Energy and Technology.

110. Beurskens, L.W.M. and M. Hekkenberg, *Renewable Energy Projections as Published in the National Renewable Energy Action Plans of the European Member States*. 2011, European Environment Agency (EEA).
111. Flamos, A., et al., *Using Biomass to Achieve European Union Energy Targets—A Review of Biomass Status, Potential, and Supporting Policies*. International Journal of Green Energy, 2011. **8**(4): p. 411-428.
112. Arnavat, M.P., *Performance Modelling and Validation of Biomass Gasifiers for Trigenation Plants*. 2011, Universitat Rovira i Virgili: Tarragona. p. 227.
113. Ministry of Energy, Development and Environmental Protection of Republic of Serbia, *ENERGETSKI BILANS REPUBLIKE SRBIJE ZA 2013. GODINU*.
114. Ministry of Energy, Development and Environmental Protection, *NATIONAL RENEWABLE ENERGY ACTION PLAN OF THE REPUBLIC OF SERBIA IN ACCORDANCE WITH THE TEMPLATE AS PER DIRECTIVE 2008/29/EC (DECISION 2009/548/EC)*. 2013.
115. Vasiljević, A. and M. Jokić, *Regional Profile of the Biomass Sector in Serbia Timok Forest Area 2013*.
116. van-Berkum, S. and N. Bogdanov, *Serbia on the road to EU accession : consequences for agricultural policy and the agri-food chain*. 2012: Wallingford, Oxfordshire [u.a.] : CABI.
117. Glavonjić Branko, L.P., *Biomass energy resource in Serbia*, in *Regional Conference: Harmonization of methodologies for estimation and sustainable incorporation of biomass and other RES in municipal and national strategies for energy development*. 2010: Skopje, Macedonia.
118. Brkić, M.J., T.V. Janić, and S.M. Igić, *Assessmen tof speciesand quantity of biomass in Serbia and guidelines of usage*. Thermal Science, 2012. **16**(1): p. S79-S86.
119. Vasiljević, A.L., *Potentials for forest woody biomass production in Serbia*. Thermal Science, 2014.
120. Glavonjic, B. *Wood energy: definition, objectives and challenges in South East Europe*. in *Workshop on "Policy options for wood energy"*. 2009. Dubrovnik, Croatia.
121. Einhorn-Stoll, U., H. Kunzek, and G. Dongowski, *Thermal analysis of chemically and mechanically modified pectins*. Food Hydrocolloids, 2007. **21**(7): p. 1101-1112.
122. Грубор, Б., et al., *Пројекат Министарства за рударство и енергетику: Обновљиви извори енергије – техничко и тржишно економски инструменти и механизми подстицаја коришћења (ЕЕ-273019Б)*. 2007, Институт Нуклеарне Науке - Винча (Лабораторија за термотехнику и енергетику).
123. Ilić, M., B. Grubor, and M. Tešić, *THE STATE OF BIOMASS ENERGY IN SERBIA*. THERMAL SCIENCE, 2004. **8**(2): p. pp 5-19.
124. Dodić, S.N., et al., *Situation and perspectives of waste biomass application as energy source in Serbia*. Renewable and Sustainable Energy Reviews, 2010. **14**(9): p. 3171-3177.
125. Jovanović, B.M., Parović, *Stanje i razvoj biomase u Srbiji*. Alternativna Energija Srbije, 2009.
126. Powlson, D., *Cereals straw for bioenergy: Environmental and agronomic constraints* in *Expert consultation: Cereals straw resources for bioenergy in the European Union*. 2006: Pamplona, Spain. p. 45-59
127. Rosentrater, K.A., D. Todey, and R. Persyn, *Quantifying Total and Sustainable Agricultural Biomass Resources in South Dakota – A Preliminary Assessment*. Agricultural Engineering International: the CIGR Journal of Scientific Research and Development, 2009. **9**: p. 1059-1058-1.
128. M.Ilić, et al., *ENERGETSKI POTENCIJAL I KARAKTERISTIKE OSTATAKA BIOMASE I TEHNOLOGIJE ZA NJENU PRIPREMU I ENERGETSKO ISKORIŠĆENJE U SRBIJI - Studija je urađena u okviru projekta ev. broj NP EE611-113A finansiranog od strane Ministarstva za nauku, tehnologije i razvoj Republike Srbije*. 2003: Beograd

129. Stojiljković, D. *RENEWABLE ENERGY SOURCES - hydro, solar and biomass*, available at [http://www.confindustria.it/Conf2004/DbDoc2004.nsf/0/c69582e2287c06bdc1257b2b0030c882/\\$FILE/UNIVERSITY%20OF%20BELGRADE.pptx](http://www.confindustria.it/Conf2004/DbDoc2004.nsf/0/c69582e2287c06bdc1257b2b0030c882/$FILE/UNIVERSITY%20OF%20BELGRADE.pptx). 2013.
130. Balat, M., et al., *Main routes for the thermo-conversion of biomass into fuels and chemicals. Part 2: Gasification systems*. Energy Conversion and Management, 2009. **50**(12): p. 3158-3168.
131. Nussbaumer, T., *Combustion and Co-combustion of Biomass: Fundamentals, Technologies, and Primary Measures for Emission Reduction†*. Energy & Fuels, 2003. **17**(6): p. 1510-1521.
132. Milligan, J.B., *Downdraft gasification of biomass*. 1994, Aston University, Birmingham, UK.
133. Knoef, H., *Handbook Biomass Gasification*. 2005, Enschede, Netherlands: BTG Biomass Technology Group.
134. !!! INVALID CITATION !!!
135. Kaupp, A. and J.R. Goss, *State of the Art for Small Scale (to 50 kW) Gas Producer-Engine System, Final Report, US Department of Agriculture, NO. 53-319R-0-141*. 1984: Tipi Workshop, Colorado, USA.
136. Bridgwater, A., *Review of Thermochemical Biomass Conversion*. 1991: Contractor Report, ETSU B 1202, Department of Energy.
137. McKendry, P., *Energy production from biomass (part 3): gasification technologies*. Bioresource Technology, 2002. **83**(1): p. 55-63.
138. Demirbas, A., *Biofuels : securing the planet's future energy needs*. 2009: New York ; London : Springer.
139. Demirbas, A., *Biorefineries: For Biomass Upgrading Facilities*. 2010: Springer London New York.
140. Demirbaş, A., *Biomass resource facilities and biomass conversion processing for fuels and chemicals*. Energy Conversion and Management, 2001. **42**(11): p. 1357-1378.
141. Emrich, W., *Handbook of Charcoal Making: The Traditional and Industrial Methods*. 1985: Springer.
142. Tiilikkala, K., L. Fagernäs, and J. Tiilikkala, *History and Use of Wood Pyrolysis Liquids as Biocide and Plant Protection Product*. The Open Agriculture Journal, 2010. **4**: p. pp 111-118.
143. Antal, M., Jr., *Biomass Pyrolysis: A Review of the Literature Part 1—Carbohydrate Pyrolysis*, in *Advances in Solar Energy*, K. Böer and J. Duffie, Editors. 1985, Springer New York. p. 61-111.
144. Karamarković, V., *Sagorevanje i gasifikacija biomase, Naučna monografija*.
145. Sadaka, S., *Pyrolysis: Sun Grant BioWeb and the University of Tennessee*.
146. Curtis, L.J. and D.J. Miller, *Transport model with radiative heat transfer for rapid cellulose pyrolysis*. Industrial & Engineering Chemistry Research, 1988. **27**(10): p. 1775-1783.
147. Anthony, D.B. and J.B. Howard, *Coal devolatilization and hydrogasification*. AIChE Journal, 1976. **22**: p. 625-656.
148. Goran, J., *Прилог проучавању гасификације југословенских лигнита* Универзитет у Београду: Београд.
149. Fagbemi, L., L. Khezami, and R. Capart, *Pyrolysis products from different biomasses: application to the thermal cracking of tar*. Applied Energy, 2001. **69**(4): p. 293-306.
150. Gustafsson, C. and T. Richards, *Pyrolysis Kinetics of Washed Precipitated Lignin*. BioResources, 2009. **4**(1): p. 26-37.
151. Vreugdenhil, B.J. and R.W.R. Zwart, *Tar formation in pyrolysis and gasification*. 2009, ECN (Energy research Centre of the Netherlands).
152. Grønli, M.G., L.H. Sørensen, and J.E. Hustad, *Thermogravimetric analysis of four Scandinavian wood species under nonisothermal conditions*, in *Nordic seminar on biomass combustion - NTH*. 1992: Trondheim, Norway.
153. V., H., A. T., and R. R., *ON THERMAL PROPERTIES OF A PYROLYSING WOOD PARTICLE*.

154. Yang, Y.B., et al., *Combustion of a Single Particle of Biomass*. Energy & Fuels, 2008. **22**(1): p. 306-316.
155. Solomon, P.R., M.A. Serio, and E.M. Suuberg, *Coal pyrolysis: Experiments, kinetic rates and mechanisms*. Progress in Energy and Combustion Science, 1992. **18**(2): p. 133-220.
156. Gauthier, G., et al., *Pyrolysis of Thick Biomass Particles: Experimental and Kinetic Modelling*. CHEMICAL ENGINEERING TRANSACTIONS, 2013. **32**.
157. B.V., B. and C. A.S., *MODELING & SIMULATION OF PYROLYSIS: INFLUENCE OF PARTICLE SIZE AND TEMPERATURE*.
158. Overend, R.P., *THERMOCHEMICAL CONVERSION OF BIOMASS*, in *RENEWABLE ENERGY SOURCES CHARGED WITH ENERGY FROM THE SUN AND ORIGINATED FROM EARTH - MOON INTERACTION*, E.E. Shpilrain, Editor. 2009, Encyclopedia of Life Support Systems (EOLSS) p. 270.
159. Babu, B.V. and A.S. Chaurasia, *Modeling for pyrolysis of solid particle: kinetics and heat transfer effects*. Energy Conversion and Management, 2003. **44**(14): p. 2251-2275.
160. Di Blasi, C., *Modeling chemical and physical processes of wood and biomass pyrolysis*. Progress in Energy and Combustion Science, 2008. **34**(1): p. 47-90.
161. Laurendeau, N.M., *Heterogeneous kinetics of coal char gasification and combustion*. Progress in Energy and Combustion Science, 1978. **4**(4): p. 221-270.
162. Park, W.C., A. Atreya, and H.R. Baum, *Experimental and theoretical investigation of heat and mass transfer processes during wood pyrolysis*. Combustion and Flame, 2010. **157**(3): p. 481-494.
163. Bridgwater, A.V., *Principles and practice of biomass fast pyrolysis processes for liquids*. Journal of Analytical and Applied Physics, 1999. **51** ((1-2)): p. 3-22.
164. Basu, P., *Biomass Gasification, Pyrolysis and Torrefaction (Second Edition) Practical Design and Theory*. 2013, London NW1 7BY, UK, San Diego, CA 92101-4495, USA: Elsevier.
165. Tumuluru, J.S., et al., *Review on Biomass Torrefaction Process and Product Properties and Design of Moving Bed Torrefaction System Model Development*, in *2011 ASABE Annual International Meeting*. 2011: Louisville, Kentucky, USA.
166. Zanzi, R., et al., *Biomass torrefaction*, in **The 6th Asia-Pacific International Symposium on Combustion and Energy Utilization**. 2002: Kuala Lumpur.
167. Doat, J.P.B.J., *Volume III Biomass Conversion*, in *Bioenergy 84*, E.H.A. Ellegaard, Editor. 1985, Elsevier Applied Science: London
168. Silva, V.B. and A. Rouboa, *Using a two-stage equilibrium model to simulate oxygen air enriched gasification of pine biomass residues*. Fuel Processing Technology, 2013. **109**.
169. Gautam, G., *Parametric Study of a Commercial-Scale Biomass Downdraft Gasifier: Experiments and Equilibrium Modeling*. 2010, Auburn University Graduate School: Auburn, Alabama.
170. Rabe, R.C., *A Model for the Vacuum Pyrolysis of Biomass*, in *Department of Process Engineering at the University of Stellenbosch*. 2005, University of Stellenbosch: Stellenbosch.
171. Sharma, P.K., D. Rapp, and N.K. Rahotgi, *Methane Pyrolysis and Disposing Off Resulting Carbon*, in *In Situ Resource Utilization (ISRU 3) Technical Interchange Meeting*. 1999: Denver, CO, USA.
172. Patwardhan, P.R., *Understanding the product distribution from biomass fast pyrolysis*. 2010, Iowa State University: Ames, Iowa, USA.
173. Varma, A. and B. Behera, *Green Energy : Biomass Processing and Technology*. 2003, New Delhi, India: Capital Publishing Company.
174. Diebold, J.P. and A. Power, *Engineering aspects of the vortex pyrolysis reactor to produce primary pyrolysis oil vapors for use in resins and adhesives*, in *Research in Thermochemical Biomass Conversion* A.V. Bridgwater and J.L. Kuester, Editors. 1988 Springer. p. 1194 (609-628).

175. Becidan, M., Ø. Skreiberg, and J.E. Hustad, *NO<sub>x</sub> and N<sub>2</sub>O Precursors (NH<sub>3</sub> and HCN) in Pyrolysis of Biomass Residues*. Energy & Fuels, 2007. **21**(2): p. 1173-1180.
176. McElligott, K.M., *BIOCHAR AMENDMENTS TO FOREST SOILS: EFFECTS ON SOIL PROPERTIES AND TREE GROWTH*. 2011, University of Idaho: Moscow, Idaho, USA.
177. Karve, P., et al., *Biochar for Carbon Reduction Sustainable Agricultural and Soil Management (BiocharM), A Report for the APN (Asia Pacific Network for Climate Change Research)*. 2011.
178. Coutinho, A.R., J.D. Rocha, and C.A. Luengo, *Preparing and characterizing biocarbon electrodes*. Fuel Processing Technology, 2000. **67**(2): p. 93-102.
179. Coutinho, A.R. and C.A. Luengo, *Preparing and Characterizing Electrode Grade Carbons from Eucalyptus Pyrolysis Products*, in *Advances in Thermochemical Biomass Conversion*, A.V. Bridgwater, Editor. 1993, Springer Netherlands. p. 1230-1241.
180. Ibrahim, N.B., *Bio-oil from Flash Pyrolysis of Agricultural Residues*, in *Department of Chemical and Biochemical Engineering*. 2012, Technical University of Denmark.
181. Bridgwater, A.V. and M.L. Cottam, *Opportunities for biomass pyrolysis liquids production and upgrading*. Energy & Fuels, 1992. **6**(2): p. 113-120.
182. French, R.J., J. Hrdlicka, and R. Baldwin, *Mild hydrotreating of biomass pyrolysis oils to produce a suitable refinery feedstock*. Environmental Progress & Sustainable Energy, 2010. **29**(2): p. 142-150.
183. Kovács, V.B. and A. Meggyes, *Energetic Utilisation of Pyrolysis Gases in IC Engine*. Acta Polytechnica Hungarica 2009. **6**(4).
184. Smets, K., et al., *Flash pyrolysis of rapeseed cake: Influence of temperature on the yield and the characteristics of the pyrolysis liquid*. Journal of Analytical and Applied Pyrolysis, 2011. **90**(2): p. 118-125.
185. Sun, S., et al., *Experimental and numerical study of biomass flash pyrolysis in an entrained flow reactor*. Bioresource Technology, 2010. **101**(10): p. 3678-3684.
186. Mullen, C.A., et al., *Analysis and Comparison of Bio-Oil Produced by Fast Pyrolysis from Three Barley Biomass/Byproduct Streams*. Energy & Fuels, 2009. **24**(1): p. 699-706.
187. Şensöz, S. and D. Angın, *Pyrolysis of safflower (Charthamus tinctorius L.) seed press cake: Part 1. The effects of pyrolysis parameters on the product yields*. Bioresource Technology, 2008. **99**(13): p. 5492-5497.
188. Lee, K.-H., et al., *Influence of Reaction Temperature, Pretreatment, and a Char Removal System on the Production of Bio-oil from Rice Straw by Fast Pyrolysis, Using a Fluidized Bed*. Energy & Fuels, 2005. **19**(5): p. 2179-2184.
189. Tsai, W.T., M.K. Lee, and Y.M. Chang, *Fast pyrolysis of rice straw, sugarcane bagasse and coconut shell in an induction-heating reactor*. Journal of Analytical and Applied Pyrolysis, 2006. **76**(1-2): p. 230-237.
190. Horne, P.A. and P.T. Williams, *Influence of temperature on the products from the flash pyrolysis of biomass*. Fuel, 1996. **75**(9): p. 1051-1059.
191. Pyle, O., *Process for producing solid industrial fuel*. 1976, Google Patents.
192. Emrich, W., *Handbook of Charcoal Making - The Traditional and Industrial Methods*. 1985: Springer Netherlands.
193. Scott, D.S., et al., *The role of temperature in the fast pyrolysis of cellulose and wood*. Industrial & Engineering Chemistry Research, 1988. **27**(1): p. 8-15.
194. PA, B., *Biomass Pyrolysis Processes: Review of Scope, Control and Variability*. UKBRC Working Paper 5, 2009.
195. Demirbaş, A., *Carbonization ranking of selected biomass for charcoal, liquid and gaseous products*. Energy Conversion and Management, 2001. **42**(10): p. 1229-1238.
196. F., A., C. Beenackers, and V. Swaaij, *Wood pyrolysis and carbon dioxide char gasification kinetics in a fluidized bed*, in *Fundamentals of Thermochemical Biomass Conversion*, R.P. Overend, T.A. Milne, and L.K. Mudge, Editors. 1985, Elsevier Applied Science Publishers: London. p. 691-715.



197. Sadaka, S., *Pyrolysis*. Sun Grant BioWeb and the University of Tennessee.
198. Gómez, C.J. and L. Puigjaner, *Slow Pyrolysis of Woody Residues and an Herbaceous Biomass Crop: A Kinetic Study*. *Industrial & Engineering Chemistry Research*, 2005. **44**(17): p. 6650-6660.
199. Debdoubi, A., et al., *The effect of heating rate on yields and compositions of oil products from esparto pyrolysis*. *International Journal of Energy Research*, 2006. **30**(15): p. 1243-1250.
200. Yu, J., J.A. Lucas, and T.F. Wall, *Chapter 1. The Formation of Char's Structure During the Devolatilization of Pulverized Coal*, in *Focus on Combustion Research*, S.Z. Jiang, Editor. 2006.
201. Mackay, D.M. and P.V. Roberts, *The influence of pyrolysis conditions on yield and microporosity of lignocellulosic chars*. *Carbon*, 1982. **20**(2): p. 95-104.
202. Varhegyi, G., et al., *Simultaneous thermogravimetric-mass spectrometric studies of the thermal decomposition of biopolymers. 1. Avicel cellulose in the presence and absence of catalysts*. *Energy & Fuels*, 1988. **2**(3): p. 267-272.
203. Varhegyi, G., et al., *Simultaneous thermogravimetric-mass spectrometric studies of the thermal decomposition of biopolymers. 2. Sugarcane bagasse in the presence and absence of catalysts*. *Energy & Fuels*, 1988. **2**(3): p. 273-277.
204. Mok, W.S.L. and M.J. Antal Jr, *Effects of pressure on biomass pyrolysis. II. Heats of reaction of cellulose pyrolysis*. *Thermochemica Acta*, 1983. **68**(2-3): p. 165-186.
205. Branca, C. and C. Di Blasi, *Multistep Mechanism for the Devolatilization of Biomass Fast Pyrolysis Oils*. *Industrial & Engineering Chemistry Research*, 2006. **45**(17): p. 5891-5899.
206. Branca, C., C. Di Blasi, and R. Elefante, *Devolatilization of Conventional Pyrolysis Oils Generated from Biomass and Cellulose*. *Energy & Fuels*, 2006. **20**(5): p. 2253-2261.
207. Palmer, R.C., *Effect of Pressure on Yields of Products in the Destructive Distillation of Hardwood*. *Journal of Industrial & Engineering Chemistry*, 1914. **6**(11): p. 890-893.
208. Ward, S.M. and J. Braslaw, *Experimental weight loss kinetics of wood pyrolysis under vacuum*. *Combustion and Flame*, 1985. **61**(3): p. 261-269.
209. Rensfelt, B.W.E., *A pressurized thermo-balance for pyrolysis and gasification studies of biomass, wood and peat*, in *Fundamentals of Thermochemical Biomass Conversion*, R.P. Overend, T.A. Milne, and L.K. Mydger, Editors. 1985, Elsevier Applied Science Publishers: London. p. 747-759.
210. Blackadder, W. and E. Rensfelt., *A pressurized thermo-balance for pyrolysis and gasification studies of biomass, wood and peat*, in *Fundamentals of Thermochemical Biomass Conversion*, R.P. Overend, T.A. Milne, and L.K. Mudge, Editors. 1985, Elsevier Applied Science Publishers: London. p. 747-759.
211. M.Shrestha, S.C.B.R., *State of the Art for Biocoal Technology, AIT - GTZ Biocoal Project*. 1988, AIT, Bangkok.
212. Bhattacharya S. C., Shrestha R. M., and S. S., *State of the Art for Biocoal Technology*, in *AIT - GTZ Biocoal Project*. 1988: Asian Institute of Technology, Bangkok, Thailand.
213. Richard, J.-R. and M. Antal, Jr., *Thermogravimetric Studies of Charcoal Formation from Cellulose at Elevated Pressures*, in *Advances in Thermochemical Biomass Conversion*, A.V. Bridgwater, Editor. 1993, Springer Netherlands. p. 784-792.
214. Blackadder, W. and E. Rensfelt, *A Pressurized Thermo Balance for Pyrolysis and Gasification Studies of Biomass, Wood and Peat*, in *Fundamentals of Thermochemical Biomass Conversion*, R.P. Overend, T.A. Milne, and L.K. Mudge, Editors. 1985, Springer Netherlands. p. 747-759.
215. Xu, X., et al., *Carbon-Catalyzed Gasification of Organic Feedstocks in Supercritical Water†*. *Industrial & Engineering Chemistry Research*, 1996. **35**(8): p. 2522-2530.
216. Brandt, P., E. Larsen, and U. Henriksen, *High Tar Reduction in a Two-Stage Gasifier*. *Energy & Fuels*, 2000. **14**(4): p. 816-819.

217. Várhegyi, G., et al., *Kinetics of the thermal decomposition of cellulose in sealed vessels at elevated pressures. Effects of the presence of water on the reaction mechanism*. Journal of Analytical and Applied Pyrolysis, 1993. **26**(3): p. 159-174.
218. Huynh, C.V., *Performance characterization of a pilot-scale oxygen enriched-air and steam blown gasification and combustion system*. 2011, Iowa State University.
219. Shafizadeh, F. and P.P.S. Chin, *Pyrolytic production and decomposition of 1,6-anhydro- 3,4-dideoxy-β-d-glycero-hex-3-enopyranos-2-ulose*. Carbohydrate Research, 1976. **46**(1): p. 149-154.
220. Bilbao, R., J. Arauzo, and A. Millera, *Kinetics of thermal decomposition of cellulose: Part I. Influence of experimental conditions*. Thermochimica Acta, 1987. **120**(0): p. 121-131.
221. Bilbao, R., J. Arauzo, and A. Millera, *Kinetics of thermal decomposition of cellulose: Part II. Temperature differences between gas and solid at high heating rates*. Thermochimica Acta, 1987. **120**(0): p. 133-141.
222. Bilbao, R., A. Millera, and J. Arauzo, *Kinetics of weight loss by thermal decomposition of xylan and lignin. Influence of experimental conditions*. Thermochimica Acta, 1989. **143**(0): p. 137-148.
223. Bilbao, R., A. Millera, and J. Arauzo, *Thermal decomposition of lignocellulosic materials: influence of the chemical composition*. Thermochimica Acta, 1989. **143**(0): p. 149-159.
224. Babu, B.V. and A.S. Chaurasia, *Parametric study of thermal and thermodynamic properties on pyrolysis of biomass in thermally thick regime*. Energy Conversion and Management, 2004. **45**(1): p. 53-72.
225. Di Blasi, C., et al., *Pyrolytic behavior and products of some wood varieties*. Combustion and Flame, 2001. **124**(1-2): p. 165-177.
226. Bellais, M., *Modelling of the pyrolysis of large wood particles*. 2007, KTH - Royal Institute of Technology Sweden.
227. Luo, S., et al., *Influence of particle size on pyrolysis and gasification performance of municipal solid waste in a fixed bed reactor*. Bioresource Technology, 2010. **101**(16): p. 6517-6520.
228. Beenackers, F.A.C. and V. Swaaij, *Wood pyrolysis and carbon dioxide char gasification kinetics in a fluidized bed*, in *Fundamentals of Thermochemical Biomass Conversion*, R.P. Overend, T.A. Milne, and L.K. Mudge, Editors. 1985, Elsevier Applied Science London p. 691-715.
229. Di Blasi, C., *Kinetic and Heat Transfer Control in the Slow and Flash Pyrolysis of Solids*. Industrial & Engineering Chemistry Research, 1996. **35**(1): p. 37-46.
230. Demirbas, A., *Effect of initial moisture content on the yields of oily products from pyrolysis of biomass*. Journal of Analytical and Applied Pyrolysis, 2004. **71**(2): p. 803-815.
231. Gray, M.R., W.H. Corcoran, and G.R. Gavalas, *Pyrolysis of a wood-derived material. Effects of moisture and ash content*. Industrial & Engineering Chemistry Process Design and Development, 1985. **24**(3): p. 646-651.
232. Rajvanshi, A.K., *Biomass Gasification*, in *Alternative Energy in Agriculture*, D.Y. Goswami, Editor. 1986, CRC Press. p. 83 - 102.
233. Zolin, A., et al., *The Influence of Inorganic Materials on the Thermal Deactivation of Fuel Chars*. Energy & Fuels, 2001. **15**(5): p. 1110-1122.
234. Tsuchiya, Y. and K. Sumi, *Thermal decomposition products of cellulose*. Journal of Applied Polymer Science, 1970. **14**(8): p. 2003-2013.
235. Nassar, M.M., A. Bilgesu, and G.D.M. MacKay, *Effect of Inorganic Salts on Product Composition During Pyrolysis of Black Spruce*. Wood and Fiber Science, 1986. **18**(1): p. 3-10.
236. Nassar, M.M. and G.D.M. Mackay, *Studies on the mechanism of flame retarding*. Thermochimica Acta, 1984. **81**(0): p. 9-14.
237. Utioh, A.C., N.N. Bakhshi, and D.G. Macdonald, *Pyrolysis of grain screenings in a batch reactor*. The Canadian Journal of Chemical Engineering, 1989. **67**(3): p. 439-446.

238. Hagge, M.J. and K.M. Bryden, *Modeling the impact of shrinkage on the pyrolysis of dry biomass*. Chemical Engineering Science, 2002. **57**(14): p. 2811-2823.
239. Kansa, E.J., H.E. Perlee, and R.F. Chaiken, *Mathematical model of wood pyrolysis including internal forced convection*. Combustion and Flame, 1977. **29**(0): p. 311-324.
240. Soltes, E.J. and T.J. Elder, *Pyrolysis*, in *Organic Chemicals from Biomass*, I.S. Goldstein, Editor. 1981: CRC Press.
241. Raveendran, K., A. Ganesh, and K.C. Khilar, *Pyrolysis characteristics of biomass and biomass components*. Fuel, 1996. **75**(8): p. 987-998.
242. Yang, H., et al., *Characteristics of hemicellulose, cellulose and lignin pyrolysis*. Fuel, 2007. **86**(12-13): p. 1781-1788.
243. Jensen, A., et al., *TG-FTIR Study of the Influence of Potassium Chloride on Wheat Straw Pyrolysis*. Energy & Fuels, 1998. **12**(5): p. 929-938.
244. Shen, J., et al., *Effects of particle size on the fast pyrolysis of oil mallee woody biomass*. Fuel, 2009. **88**(10): p. 1810-1817.
245. Lédé, J., *Cellulose pyrolysis kinetics: An historical review on the existence and role of intermediate active cellulose*. Journal of Analytical and Applied Pyrolysis, 2012. **94**(0): p. 17-32.
246. Antal, M.J., G. Várhegyi, and E. Jakab, *Cellulose Pyrolysis Kinetics: Revisited*. Industrial & Engineering Chemistry Research, 1998. **37**(4): p. 1267-1275.
247. BREBU, M. and C. VASILE, *THERMAL DEGRADATION OF LIGNIN – A REVIEW*. CELLULOSE CHEMISTRY AND TECHNOLOGY, 2009.
248. Wenzl, H.F.J., *The Chemical Technology of Wood*. 1970: Academic Press.
249. Brebu, M. and C. Vasile, *Thermal degradation of lignin - A review*. CELLULOSE CHEMISTRY AND TECHNOLOGY, 2010. **44**(9): p. 353-363.
250. Várhegyi, G., et al., *Kinetic modeling of biomass pyrolysis*. Journal of Analytical and Applied Pyrolysis, 1997. **42**(1): p. 73-87.
251. Berkowitz, N., *On the differential thermal analysis of coal*. Fuel, 1957. **36**(3): p. 355-373.
252. Mohan, D., C.U. Pittman, and P.H. Steele, *Pyrolysis of Wood/Biomass for Bio-oil: A Critical Review*. Energy & Fuels, 2006. **20**(3): p. 848-889.
253. Elder, T. and EJSoltes, *Pyrolysis*, in *Organic Chemicals From Biomass* I.S. Goldstein, Editor. 1981, CRC Press: Boca Raton, Florida. p. 63-99.
254. Antal, M.J., Jr. and G. Varhegyi, *Cellulose Pyrolysis Kinetics: The Current State of Knowledge*. Industrial & Engineering Chemistry Research, 1995. **34**(3): p. 703-717.
255. Богомолов, Б.Д., *Химия древесины и основы химии высокомолекулярных соединений* 1973, Москва: Лесная промышленность.
256. Caballero, J.A., et al., *Pyrolysis kinetics of almond shells and olive stones considering their organic fractions*. Journal of Analytical and Applied Pyrolysis, 1997. **42**(2): p. 159-175.
257. Varhegyi, G., et al., *Thermogravimetric-mass spectrometric characterization of the thermal decomposition of sunflower stem*. Energy & Fuels, 1989. **3**(6): p. 755-760.
258. Pokol, G., G. Várhegyi, and D. Dollimore, *Kinetic Aspects of Thermal Analysis*. C R C Critical Reviews in Analytical Chemistry, 1988. **19**(1): p. 65-93.
259. Prakash, N. and T. Karunanithi, *Kinetic Modeling in Biomass Pyrolysis – A Review*. Journal of Applied Sciences Research, 2008. **4**(12): p. 1627-1636.
260. Várhegyi, G., P. Szabó, and M.J. Antal, *Kinetics of Charcoal Devolatilization*. Energy & Fuels, 2002. **16**(3): p. 724-731.
261. Broido, A. and M. Weinstein, *Thermogravimetric Analysis of Ammonia-Swelled Cellulose*. Combustion Science and Technology, 1970. **1**(4): p. 279-285.
262. Grønli, M.G. and M.C. Melaaen, *Mathematical Model for Wood Pyrolysis Comparison of Experimental Measurements with Model Predictions*. Energy & Fuels, 2000. **14**(4): p. 791-800.

263. Várhegyi, G., M.G.G. Grønli, and C. Di Blasi, *Effects of Sample Origin, Extraction, and Hot-Water Washing on the Devolatilization Kinetics of Chestnut Wood*. Industrial & Engineering Chemistry Research, 2004. **43**(10): p. 2356-2367.
264. TANG, W.K. and HERBERT W. EICKNER, *Effect of Inorganic Salts on Pyrolysis of Wood, Cellulose, and Lignin Determined by Differential Thermal Analysis*. U.S. FOREST SERVICE RESEARCH FPL 82, JANUARY 1968.
265. Shafizadeh, F. and G.D. McGinnis, *Chemical composition and thermal analysis of cottonwood*. Carbohydrate Research, 1971. **16**(2): p. 273-277.
266. Havens, J.A., et al., *A Mathematical Model of the Thermal Decomposition of Wood*. Combustion Science and Technology, 1972. **5**(1): p. 91-98.
267. Mészáros, E., et al., *Thermogravimetric and Reaction Kinetic Analysis of Biomass Samples from an Energy Plantation*. Energy & Fuels, 2004. **18**(2): p. 497-507.
268. Grønli, M., M.J. Antal, and G. Várhegyi, *A Round-Robin Study of Cellulose Pyrolysis Kinetics by Thermogravimetry*. Industrial & Engineering Chemistry Research, 1999. **38**(6): p. 2238-2244.
269. Várhegyi, G., E. Jakab, and M.J. Antal, *Is the Broido-Shafizadeh Model for Cellulose Pyrolysis True?* Energy & Fuels, 1994. **8**(6): p. 1345-1352.
270. Várhegyi, G., et al., *Tobacco pyrolysis. Kinetic evaluation of thermogravimetric–mass spectrometric experiments*. Journal of Analytical and Applied Pyrolysis, 2009. **86**(2): p. 310-322.
271. Becidan, M., et al., *Thermal Decomposition of Biomass Wastes. A Kinetic Study*. Industrial & Engineering Chemistry Research, 2007. **46**(8): p. 2428-2437.
272. Akita, K. and M. Kase, *Determination of kinetic parameters for pyrolysis of cellulose and cellulose treated with ammonium phosphate by differential thermal analysis and thermal gravimetric analysis*. Journal of Polymer Science Part A-1: Polymer Chemistry, 1967. **5**(4): p. 833-848.
273. Babu, B.V., *Biomass pyrolysis: a state-of-the-art review*. Biofuels, Bioproducts and Biorefining, 2008. **2**(5): p. 393-414.
274. LEE, T.V., *KINETIC ANALYSIS AND MODELING OF WOOD PYROLYSIS UNDER NONISOTHERMAL CONDITIONS*. 1982, Graduate Faculty of Texas Tech University.
275. Broido, A. and M. Weinstein. *Low temperature isothermal pyrolysis of cellulose*. in *3rd Int. Conf. on Thermal Analysis*. 1971. Basel, Switzerland.
276. Shafizadeh, F., *Pyrolysis and Combustion of Cellulosic Materials*, in *Advances in Carbohydrate Chemistry*, L.W. Melville and R.S. Tipson, Editors. 1968, Academic Press. p. 419-474.
277. Di Blasi, C., *Comparison of semi-global mechanisms for primary pyrolysis of lignocellulosic fuels*. Journal of Analytical and Applied Pyrolysis, 1998. **47**(1): p. 43-64.
278. White, J.E., W.J. Catallo, and B.L. Legendre, *Biomass pyrolysis kinetics: A comparative critical review with relevant agricultural residue case studies*. Journal of Analytical and Applied Pyrolysis, 2011. **91**(1): p. 1-33.
279. Nunn, T.R., et al., *Product compositions and kinetics in the rapid pyrolysis of sweet gum hardwood*. Industrial & Engineering Chemistry Process Design and Development, 1985. **24**(3): p. 836-844.
280. Belderok, H.J.M., *Experimental investigation and modeling of the pyrolysis of biomass*, in *Department of Mechanical Engineering*. 2007, Eindhoven University of Technology.
281. Hanna, S.K., *Diffusion of solid fuel on a vibrating grate*, in *Department of Energy Technology Fluid Mechanics and Combustion*. 2007, Aalborg University: Aalborg. p. 132.
282. Shafizadeh, F., *ALTERNATIVE PATHWAYS FOR PYROLYSIS OF CELLULOSE*, in *ACS Energy and Fuels Symposia - SYMPOSIUM ON MATHEMATICAL MODELING OF BIOMASS PYROLYSIS PHENOMENA*, WASHINGTON DC. 1983
283. Dekui, S., et al., *The Overview of Thermal Decomposition of Cellulose in Lignocellulosic Biomass*. 2013.

284. Antal, M.J., et al. *Recent Progress in Kinetics Models for Coal Pyrolysis*, available at <https://web.anl.gov>.
285. Antal, M.J., H.L. Friedman, and F.E. Rogers, *Kinetics of Cellulose Pyrolysis in Nitrogen and Steam*. Combustion Science and Technology, 1980. **21**(3-4): p. 141-152.
286. Villermaux, J., et al., *A new model for thermal volatilization of solid particles undergoing fast pyrolysis*. Chemical Engineering Science, 1986. **41**(1): p. 151-157.
287. Cordero, T., F. García, and J.J. Rodríguez, *A kinetic study of holm oak wood pyrolysis from dynamic and isothermal TG experiments*. Thermochimica Acta, 1989. **149**(0): p. 225-237.
288. Flynn, J.H., *Thermal analysis kinetics-problems, pitfalls and how to deal with them*. Journal of thermal analysis, 1988. **34**(1): p. 367-381.
289. Capart, R., L. Khezami, and A.K. Burnham, *Assessment of various kinetic models for the pyrolysis of a microgranular cellulose*. Thermochimica Acta, 2004. **417**(1): p. 79-89.
290. Laidler, K.J., *Unconventional applications of the Arrhenius law*. Journal of Chemical Education, 1972. **49**(5): p. 343.
291. Manyà, J.J., E. Velo, and L. Puigjaner, *Kinetics of Biomass Pyrolysis: a Reformulated Three-Parallel-Reactions Model*. Industrial & Engineering Chemistry Research, 2002. **42**(3): p. 434-441.
292. Burnham, A.K. and R.L. Braun, *Global Kinetic Analysis of Complex Materials*. Energy & Fuels, 1998. **13**(1): p. 1-22.
293. Shafizadeh, F. and S. Chin Peter P, *Thermal Deterioration of Wood*, in *Wood Technology: Chemical Aspects*. 1977, AMERICAN CHEMICAL SOCIETY. p. 57-81.
294. Varhegyi, G., et al., *Kinetics of the thermal decomposition of cellulose, hemicellulose, and sugarcane bagasse*. Energy & Fuels, 1989. **3**(3): p. 329-335.
295. Orfão, J.J.M., F.J.A. Antunes, and J.L. Figueiredo, *Pyrolysis kinetics of lignocellulosic materials—three independent reactions model*. Fuel, 1999. **78**(3): p. 349-358.
296. Milosavljevic, I. and E.M. Suuberg, *Cellulose Thermal Decomposition Kinetics: Global Mass Loss Kinetics*. Industrial & Engineering Chemistry Research, 1995. **34**(4): p. 1081-1091.
297. Evans, R.J. and T.A. Milne, *Molecular characterization of the pyrolysis of biomass. 1. Fundamentals*. Energy Fuels, 1987. **1**: p. 311-9.
298. Boroson, M.L., et al., *Product yields and kinetics from the vapor phase cracking of wood pyrolysis tars*. AIChE Journal, 1989. **35**(1): p. 120-128.
299. Morf, P.O., *Secondary reactions of tar during thermochemical biomass conversion*. 2001, Technische Wissenschaften ETH Zürich, Nr. 14341, 2001: Zürich.
300. Morf, P., P. Hasler, and T. Nussbaumer, *Mechanisms and kinetics of homogeneous secondary reactions of tar from continuous pyrolysis of wood chips*. Fuel, 2002. **81**(7): p. 843-853.
301. Acton, Q.A., *Advances in Carbon Research and Application*. 2013: ScholarlyEditions™, Atlanta, Georgia, USA.
302. Avni, E., et al., *Mathematical modelling of lignin pyrolysis*. Fuel, 1985. **64**(11): p. 1495-1501.
303. Vand, V., *A theory of the irreversible electrical resistance changes of metallic films evaporated in vacuum*. Proceedings of the Physical Society 1943. **55** (3).
304. Pitt, G.J., *The Kinetics of the Evolution of Volatile Products from Coal*. Fuel, 1962. **41**: p. 264-274.
305. Anthony, D.B. and J.B. Howard, *Coal Devolatilization and Hydrogasification*. A.I.Ch.E. Journal of Analytical and Applied Physics, 1976: p. 625-655.
306. Braun, R.L. and A.K. Burnham, *Analysis of Chemical Reaction Kinetics Using a Distribution of Activation Energies and Simpler Models*. Energy and Fuels, 1987. **1** p. 153-161.
307. Saidi, M.S., M.R. Hajaligol, and F. Rasouli, *Numerical simulation of a burning cigarette during puffing*. Journal of Analytical and Applied Pyrolysis, 2004. **72**(1): p. 141-152.
308. Várhegyi, G.b., et al., *Thermogravimetric Study of Biomass Pyrolysis Kinetics. A Distributed Activation Energy Model with Prediction Tests*. Energy & Fuels, 2010. **25**(1): p. 24-32.
309. Hornung, A., *Transformation of Biomass*. 2014: John Wiley & Sons.

310. Teukolsky, H.W.P.S.A. and W.T. Vetterling, *Numerical Recipes The Art of Scientific Computing, 3rd Edition*. 2007.
311. Numerics, V., Inc., and IMSL, *Fortran 90 Mathematical Programming Library, Version 3.0; IMSL Software*. Visual Numerics Inc.: Houston, TX, 1996.
312. Donskoi, E. and D.L.S. McElwain, *Optimization of coal pyrolysis modeling*. Combustion and Flame, 2000. **122**(3): p. 359-367.
313. Beall, F.E., H., *THERMAL DEGRADATION OF WOOD COMPONENTS: A REVIEW OF THE LITERATURE*. FPL Research paper no 130. USAD Forest Products Laboratory, 1970.
314. Várhegyi, G., *Kinetic evaluation of non-isothermal thermoanalytical curves in the case of independent thermal reactions*. Thermochimica Acta, 1979. **28**(2): p. 367-376.
315. Várhegyi, G., et al., *Thermogravimetric Study of Biomass Pyrolysis Kinetics. A Distributed Activation Energy Model with Prediction Tests*. Energy & Fuels, 2010. **25**(1): p. 24-32.
316. Várhegyi, G.b., H. Chen, and S. Godoy, *Thermal Decomposition of Wheat, Oat, Barley, and Brassica carinata Straws. A Kinetic Study*. Energy & Fuels, 2009. **23**(2): p. 646-652.
317. Várhegyi, G.b., et al., *Thermogravimetric Analysis of Tobacco Combustion Assuming DAEM Devolatilization and Empirical Char-Burnoff Kinetics*. Industrial & Engineering Chemistry Research, 2009. **49**(4): p. 1591-1599.
318. Koufopoulos, C.A., et al., *Modelling of the pyrolysis of biomass particles. Studies on kinetics, thermal and heat transfer effects*. The Canadian Journal of Chemical Engineering, 1991. **69**(4): p. 907-915.
319. Blasi, C.D., G. Signorelli, and G. Portoricco, *Countercurrent Fixed-Bed Gasification of Biomass at Laboratory Scale*. Industrial & Engineering Chemistry Research, 1999. **38**(7): p. 2571-2581.
320. Di Blasi, C., *The state of the art of transport models for charring solid degradation*. Polymer International, 2000. **49**(10): p. 1133-1146.
321. Branca, C., C.D. Blasi, and R. Elefante, *Devolatilization and Heterogeneous Combustion of Wood Fast Pyrolysis Oils*. Industrial & Engineering Chemistry Research, 2005. **44**(4): p. 799-810.
322. Branca, C., et al., *H2SO4-Catalyzed Pyrolysis of Corncobs*. Energy & Fuels, 2010. **25**(1): p. 359-369.
323. Cooley, S. and M.J. Antal Jr, *Kinetics of cellulose pyrolysis in the presence of nitric oxide*. Journal of Analytical and Applied Pyrolysis, 1988. **14**(2-3): p. 149-161.
324. Font, R., et al., *Thermogravimetric kinetic study of the pyrolysis of almond shells and almond shells impregnated with CoCl2*. Journal of Analytical and Applied Pyrolysis, 1991. **21**(3): p. 249-264.
325. Cozzani, V., et al., *A new method to determine the composition of biomass by thermogravimetric analysis*. The Canadian Journal of Chemical Engineering, 1997. **75**(1): p. 127-133.
326. Reynolds, J.G., A.K. Burnham, and P.H. Wallman, *Reactivity of Paper Residues Produced by a Hydrothermal Pretreatment Process for Municipal Solid Wastes*. Energy & Fuels, 1997. **11**(1): p. 98-106.
327. de Jong, W., A. Pirone, and M.A. Wójtowicz, *Pyrolysis of Miscanthus Giganteus and wood pellets: TG-FTIR analysis and reaction kinetics* ☆. Fuel, 2003. **82**(9): p. 1139-1147.
328. Wójtowicz, M.A., et al., *Modeling the evolution of volatile species during tobacco pyrolysis*. Journal of Analytical and Applied Pyrolysis, 2003. **66**(1-2): p. 235-261.
329. Yi, S.-C. and M.R. Hajaligol, *Product distribution from the pyrolysis modeling of tobacco particles*. Journal of Analytical and Applied Pyrolysis, 2003. **66**(1-2): p. 217-234.
330. de Jong, W., et al., *TG-FTIR pyrolysis of coal and secondary biomass fuels: Determination of pyrolysis kinetic parameters for main species and NOx precursors*. Fuel, 2007. **86**(15): p. 2367-2376.
331. Sonobe, T. and N. Worasuwannarak, *Kinetic analyses of biomass pyrolysis using the distributed activation energy model*. Fuel, 2008. **87**(3): p. 414-421.

332. Chen, Y., J. Duan, and Y.-h. Luo, *Investigation of agricultural residues pyrolysis behavior under inert and oxidative conditions*. Journal of Analytical and Applied Pyrolysis, 2008. **83**(2): p. 165-174.
333. Yu, F., R. Ruan, and P. Steele, *Consecutive reaction model for the pyrolysis of corn cob*. Transactions of the ASABE, 2008. **51**(3 1023-1028 CODEN: TARSBB): p. 1023–1028.
334. Aboyade, A.O., et al., *Non-isothermal kinetic analysis of the devolatilization of corn cobs and sugar cane bagasse in an inert atmosphere*. Thermochemica Acta, 2011. **517**(1–2): p. 81-89.
335. *ASTM E871-82(2013), Standard Test Method for Moisture Analysis of Particulate Wood Fuels*, ASTM International, West Conshohocken, PA, 2013, [www.astm.org](http://www.astm.org).
336. *ASTM E872-82(2013), Standard Test Method for Volatile Matter in the Analysis of Particulate Wood Fuels*, ASTM International, West Conshohocken, PA, 2013, [www.astm.org](http://www.astm.org).
337. *ASTM D1102-84(2013), Standard Test Method for Ash in Wood*, ASTM International, West Conshohocken, PA, 2013, [www.astm.org](http://www.astm.org).
338. Fisher, T., et al., *Pyrolysis behavior and kinetics of biomass derived materials*. Journal of Analytical and Applied Pyrolysis, 2002. **62**(2): p. 331-349.
339. Várhegyi, G., G. Groma, and M. Lengyel, *DSC examination of alloys*. Thermochemica Acta, 1979. **30**(1–2): p. 311-317.
340. Conesa, J.A., et al., *Kinetic model for the combustion of tyre wastes*. Fuel, 1998. **77**(13): p. 1469-1475.
341. Shampine, L. and M. Reichelt, *The MATLAB ODE Suite*. 18, 1997. **1**: p. 1-22.
342. Lagarias, J., et al., *Convergence Properties of the Nelder–Mead Simplex Method in Low Dimensions*. SIAM Journal on Optimization, 1998. **9**(1): p. 112-147.
343. Bard, E., *Extending the Calibrated Radiocarbon Record*. Science, 2001. **292**(5526): p. 2443-2444.
344. Muylaert, M.S., J. Sala, and M.A.V. de Freitas, *The charcoal's production in Brazil — process efficiency and environmental effects*. Renewable Energy, 1999. **16**(1–4): p. 1037-1040.
345. Lin, J.-C.M., *Development of a high yield and low cycle time biomass char production system*. Fuel Processing Technology, 2006. **87**(6): p. 487-495.
346. Gabbott, P., *Principles and Applications of Thermal Analysis*. 2008, Oxford, UK: Blackwell Publishing Ltd.
347. Haines, P.J., *Introduction - The need for proper practice*, in *Principles of Thermal Analysis and Calorimetry*, P.J. Haines, Editor. 2002, The Royal Society of Chemistry: Cambridge, UK.
348. Antal, M.J., et al., *New Prospects for Biocarbons*, in *Progress in Thermochemical Biomass Conversion*. 2008, Blackwell Science Ltd. p. 1179-1185.
349. Mullen, C.A., et al., *Bio-oil and bio-char production from corn cobs and stover by fast pyrolysis*. Biomass and Bioenergy, 2010. **34**(1): p. 67-74.
350. Philpot, C.W., *Influence of Mineral Content on the Pyrolysis of Plant Materials*. Forest Science, 1970. **16**(4): p. 461-471.
351. Furneaux, R.H. and F. Shafizadeh, *Pyrolytic production of 1,6-anhydro-β-d-mannopyranose*. Carbohydrate Research, 1979. **74**(1): p. 354-360.
352. Raveendran, K., A. Ganesh, and K.C. Khilar, *Influence of mineral matter on biomass pyrolysis characteristics*. Fuel, 1995. **74**(12): p. 1812-1822.
353. Gvero, P.M., *Istraživanje kinetike oslobađanja gorivih isparljivih materija drveta*. 1997, Mašinski fakultete Univerziteta u Beogradu Beograd.
354. Boroson, M.L., et al., *Effects of extra-particle secondary reactions of fresh tars on liquids yields in hardwood pyrolysis*. 1987. Medium: X; Size: Pages: 51-58.
355. Hancox, R.N., G.D. Lamb, and R.S. Lehrle, *Sample size dependence in pyrolysis: An embarrassment, or a utility?* Journal of Analytical and Applied Pyrolysis, 1991. **19**(0): p. 333-347.
356. Gavalas, G.R., *Coal Pyrolysis*. 1982, Elsevier. p. 177.

357. Wichman, I.S. and M.C. Melaaen, *A Simplified Model for the Pyrolysis of Charring Materials* in *COMBUSTION AND FLAME* A.V. Bridgwater, Editor. 1994, Blackie Academic and Professional: London. p. 887-906.
358. K., L.C., C.R. F., and J.M. Singer. *CHARRING PYROLYSIS OF WOOD IN FIRES BY LASER SIMULATION*. in *16th Symp (Int) on Combustion*. 1976. MIT, Cambridge, MA, USA.
359. Olivier Dufaud, et al., *Highlighting the Importance of the Pyrolysis Step on Dust Explosions*. *CHEMICAL ENGINEERING TRANSACTIONS*, 2012. **26**.
360. Bridgeman, T.G., et al., *Influence of particle size on the analytical and chemical properties of two energy crops*. *Fuel*, 2007. **86**(1–2): p. 60-72.
361. *Handbook Of Analytical Methods For Materials*. Materials Evaluation and Engineering, Inc.
362. Haykiri-Acma, H., *The role of particle size in the non-isothermal pyrolysis of hazelnut shell*. *Journal of Analytical and Applied Pyrolysis*, 2006. **75**(2): p. 211-216.
363. Edey, L.A., G.N. Richards, and G. Zheng, *Transition Metals as Catalysts for Pyrolysis and Gasification of Biomass*, in *Clean Energy from Waste and Coal*. 1992, American Chemical Society. p. 90-101.
364. Nowakowski, D.J. and J.M. Jones, *Uncatalysed and potassium-catalysed pyrolysis of the cell-wall constituents of biomass and their model compounds*. *Journal of Analytical and Applied Pyrolysis*, 2008. **83**(1): p. 12-25.
365. Elyounssi, K., J. Blin, and M. Halim, *High-yield charcoal production by two-step pyrolysis*. *Journal of Analytical and Applied Pyrolysis*, 2010. **87**(1): p. 138-143.
366. Reed, T.B. and A. Das, *Handbook of Biomass Downdraft Gasifier Engine Systems*. 1988, U.S. Department of Energy Colorado, USA: Solar Technical Information Program
367. Agblevor, F.A., S. Besler, and A.E. Wiseloge, *Fast Pyrolysis of Stored Biomass Feedstocks*. *Energy & Fuels*, 1995. **9**(4): p. 635-640.
368. Ioannidou, O., et al., *Investigating the potential for energy, fuel, materials and chemicals production from corn residues (cobs and stalks) by non-catalytic and catalytic pyrolysis in two reactor configurations*. *Renewable and Sustainable Energy Reviews*, 2009. **13**(4): p. 750-762.
369. Choi, J.W. *Features of fast pyrolysis of woody biomass and evaluation of biooil upgrading process with noble metal catalysts*. in *2nd FOREBIOM Workshop - Potentials of Biochar to Mitigate Climate Change*. 2014. Busian, Korea.
370. Ptasiński, K.J., M.J. Prins, and A. Pierik, *Exergetic evaluation of biomass gasification*. *Energy*, 2007. **32**(4): p. 568-574.
371. Thunman, H., et al., *Composition of Volatile Gases and Thermochemical Properties of Wood for Modeling of Fixed or Fluidized Beds*. *Energy & Fuels*, 2001. **15**(6): p. 1488-1497.
372. Chee, C.S., *The air gasification of wood chips in a downdraft gasifier*. 1987, Kansas State University.
373. Onay, O. and O. Kockar, *Technical note: slow, fast and flash pyrolysis of rape seed*. *Renew Energy*, 2003. **28**: p. 2417 - 2433.
374. Neves, D., et al., *Characterization and prediction of biomass pyrolysis products*. *Progress in Energy and Combustion Science*, 2011. **37**(5): p. 611-630.
375. Scott, D.S., J. Piskorz, and D. Radlein, *Liquid products from the continuous flash pyrolysis of biomass*. *Industrial & Engineering Chemistry Process Design and Development*, 1985. **24**(3): p. 581-588.
376. Toshiyuki Iwasaki, Seiichi Suzuki, and T. Kojima, *Influence of Biomass Pyrolysis Temperature, Heating Rate and Type of Biomass on Produced Char in a Fluidized Bed Reactor*. *Energy and Environment Research*, 2014. **4**(2).
377. Zanzi, R., K. Sjöström, and E. Björnbom, *Rapid pyrolysis of agricultural residues at high temperature*. *Biomass and Bioenergy*, 2002. **23**(5): p. 357-366.
378. Cao, Q., et al., *Pyrolytic behavior of waste corn cob*. *Bioresource Technology*, 2004. **94**(1): p. 83-89.



379. Punsuwan, N. and C. Tangsathitkulchai, *Product Characterization and Kinetics of Biomass Pyrolysis in a Three-Zone Free-Fall Reactor*. International Journal of Chemical Engineering and Applications, 2014: p. 10.
380. Fitzer, E., *Book Review: Chemistry and Physics of Carbon, Vol. 1 and 2. Edited by P. L. Walker jr.* Angewandte Chemie International Edition in English, 1967. **6**(12): p. 1092-1093.
381. Yang, H., et al., *Characteristics of hemicellulose, cellulose and lignin pyrolysis*. Fuel, 2007. **86**(12-13).
382. Agblevor, F. 2011: WO International Patent Application 2011/103313 A2.
383. Karamarkovic, R. and V. Karamarkovic, *Energy and exergy analysis of biomass gasification at different temperatures*. Energy, 2010. **35**(2): p. 537-549.
384. Puig-Arnabat, M., J.C. Bruno, and A. Coronas, *Modified Thermodynamic Equilibrium Model for Biomass Gasification: A Study of the Influence of Operating Conditions*. Energy & Fuels, 2012. **26**(2): p. 1385-1394.
385. Radmanesh, R., J. Chaouki, and C. Guy, *Biomass gasification in a bubbling fluidized bed reactor: Experiments and modeling*. AIChE Journal, 2006. **52**(12): p. 4258-4272.
386. Barman, N.S., S. Ghosh, and S. De, *Gasification of biomass in a fixed bed downdraft gasifier – A realistic model including tar*. Bioresource Technology, 2012. **107**.
387. Yamazaki, T., et al., *Effect of Superficial Velocity on Tar from Downdraft Gasification of Biomass*. Energy & Fuels, 2005. **19**(3): p. 1186-1191.
388. Silva, J.N.d., *Tar Formation in Corncob Gasification*. 1984, Purdue University: Purdue University, West Lafayette, Indiana, USA.
389. Barman, N. and S. Ghosh, *Gasification of biomass in a fixed bed downdraft gasifier: a realistic model including tar*. Bioresour Technol, 2012. **107**: p. 505 - 511.
390. D.T., P., et al., *Biomass gasification on a new really tar free downdraft gasifier*. Revista Ciencias Exatas, 2005. **11**(1).
391. Zainal, Z.A., et al., *Prediction of performance of a downdraft gasifier using equilibrium modeling for different biomass materials*. Energy Conversion and Management, 2001. **42**(12): p. 1499-1515.
392. Bottino, A., et al., *Steam reforming of methane in equilibrium membrane reactors for integration in power cycles*. Catalysis Today, 2006. **118**(1–2): p. 214-222.
393. Goran, J. and M. Nebojš, *BIOMASS GASIFICATION IN SMALL-SCALE UNITS FOR THE USE IN AGRICULTURE AND FORESTRY IN FR YUGOSLAVIA*. Thermal Science, 2001. **5**(2).
394. Reed, T.B. and A. Das, *Handbook of Biomass Downdraft Gasifier Engine Systems* 1988: Biomass Energy Foundation. 140.
395. Bridgwater, A.V., *The technical and economic feasibility of biomass gasification for power generation*. Fuel, 1995. **74**(5): p. 631-653.
396. Rajvanshi, A.K., *Biomass gasification*, in *Alternative Energy in Agriculture*, D.Y. Goswami, Editor. 1986, CRC Press. p. 83-102.
397. Doering, O.C., T.J. O'Hare, and R.M. Peart, *Small scale gasification of biomass: The case of corn cob gasifiers*. Energy, 1979. **4**(2): p. 235-248.
398. Silva, J.N.d., *TAR FORMATION IN CORNCOB GASIFICATION*. 1984, Purdue University, United States - Indiana.
399. Giltrap, D.L., R. McKibbin, and G.R.G. Barnes, *A steady state model of gas-char reactions in a downdraft biomass gasifier*. Solar Energy, 2003. **74**(1): p. 85-91.
400. Senelwa, K., *The air gasification of woody biomass from short rotation forests short rotation forests*. 1997, Massey University, New Zealand.
401. Plis, P. and R.K. Wilk, *Theoretical and experimental investigation of biomass gasification process in a fixed bed gasifier*. Energy, 2011. **36**(6): p. 3838-3845.
402. Mathieu, P. and R. Dubuisson, *Performance analysis of a biomass gasifier*. Energy Conversion and Management, 2002. **43**(9–12): p. 1291-1299.

403. Baratieri, M., et al., *Biomass as an energy source: Thermodynamic constraints on the performance of the conversion process*. Bioresource Technology, 2008. **99**(15): p. 7063-7073.
404. Sugiyama, S., et al., *Gasification performance of coals using high temperature air*. Energy, 2005. **30**(2-4): p. 399-413.
405. Babu, B.V. and P.N. Sheth, *Modeling and simulation of reduction zone of downdraft biomass gasifier: Effect of char reactivity factor*. Energy Conversion and Management, 2006. **47**(15-16): p. 2602-2611.
406. Sadaka, S., *Gasification*.
407. Carlos, L., *High temperature air/steam gasification of biomass in an updraft fixed bed batch type gasifier*, in KTH, School of Industrial Engineering and Management (ITM), Materials Science and Engineering, Energy and Furnace Technology. 2005, KTH, School of Industrial Engineering and Management (ITM): Stockholm.
408. Sheng, C. and J.L.T. Azevedo, *Estimating the higher heating value of biomass fuels from basic analysis data*. Biomass and Bioenergy, 2005. **28**(5): p. 499-507.
409. *ANSI/ASABE S593.1, Terminology and Definitions for Biomass Production, Harvesting and Collection, Storage, Processing Conversion and Utilization*. JAN 2011, American National Standards Institute (ANSI) and American Society of Agricultural and Biological Engineers (ASABE).
410. KG, I.-W.G.C., *IKA Calorimeter System C 5000 control*. 2007: Staufen, German.
411. Niessen, W.R., *Combustion and Incineration Processes Applications in Environmental Engineering*. Third Edition ed. 2002: CRC Press.
412. Parikh, J., S.A. Channiwala, and G.K. Ghosal, *A correlation for calculating HHV from proximate analysis of solid fuels*. Fuel, 2005. **84**(5): p. 487-494.

## **APPENDIX A. PERFORMANCE INDICATORS**

Summarised overview of influential process parameters.

Table A.1 The influence of pyrolysis process parameters on the pyrolysis products

Process parameter		Influence
Heating Rate	Low	<ul style="list-style-type: none"> <li>→ Slow pyrolysis</li> <li>→ Secondary reactions occurs, (resistance to mass or heat transfer inside the biomass particles occurs)</li> </ul>
	High	<ul style="list-style-type: none"> <li>→ Flash pyrolysis</li> <li>→ Reduces secondary reactions and the further degradation of the earlier formed products</li> <li>→ Favours a decrease of the charcoal yield.</li> <li>→ Formed charcoal is more reactive than those produced at low heating rate</li> <li>→ Maximize either gas or liquid products (according to the temperature employed)</li> </ul>
Temperature	High	<ul style="list-style-type: none"> <li>→ Lead to lower charcoal and tar yield</li> <li>→ Increases the proportion of carbon in the charcoal (hydrogen and oxygen decreases).</li> <li>→ Increases liquid yield up to a maximum value, usually at 450 to 600°C (depending on equipment and other conditions)</li> <li>→ Increases gas yields</li> <li>→ Favours the formation of H<sub>2</sub> at the expense of heavy hydrocarbons that are dehydrogenated from cracking, concentration of CH<sub>4</sub> is the highest between 600°C and 700°C, concentrations of CO and H<sub>2</sub> are rising while CO<sub>2</sub> decreases uniformly with the temperature</li> </ul>
Residence Time	Short	<ul style="list-style-type: none"> <li>→ Fast pyrolysis</li> <li>→ Increase liquid yield</li> </ul>
	Long	<ul style="list-style-type: none"> <li>→ Slow pyrolysis</li> <li>→ Favours the secondary pyrolysis.</li> <li>→ Increase charcoal yield</li> <li>→ In rapid pyrolysis increases the time for contact between tar and charcoal.</li> <li>→ In rapid pyrolysis makes the charcoal less reactive.</li> <li>→ In fast pyrolysis increase the time for contact between tar and charcoal which makes the charcoal less reactive.</li> <li>→ The secondary reactions occurs in the gaseous phase</li> </ul>
Pressure	Low	<ul style="list-style-type: none"> <li>→ Tar yield increases.</li> </ul>
	Elevated	<ul style="list-style-type: none"> <li>→ Secondary reaction occurs,</li> <li>→ Charcoal yield increases and tar decreases,</li> </ul>

<b>Process parameter</b>	<b>Influence</b>
<b>Ambient Atmosphere and Medium flow</b>	<ul style="list-style-type: none"><li>→ In a vacuum, primary products are rapidly removed or thinned out in the gas phase, and thus -are not available for further decomposition and reaction,</li><li>→ Presence of water or steam is known to speed up the breakdown and degradation of molecules by way of hydrolysis of the biomass and rearrangement of the intermediate products.</li><li>→ Low flows favour charcoal yield and are preferred for slow pyrolysis;</li><li>→ High gas flows are used in fast pyrolysis, effectively stripping off the vapours as soon as they are formed.</li></ul>

---

## **APENDIX B ULTIMATE AND PROXIMATE ANALYSIS**

## PROXIMATE ANALYSIS

A proximate analysis includes measurement of moisture level, volatile matter and ash content.

The used equipment were glass containers (different size), porcelain crucibles (45 x 30 mm) with lids, crucible rack, drying oven (Termaks), muffle furnace (Nabertherm LV 15/11), desiccators and precision balance (Mettler Toledo XP204S Precision Balance). Each group of experiments was performed several times if there were any suspicion that the numbers might be wrong.

## MOISTURE CONTENT

Moisture Content analysis is performed according to the standard ASTM E871 [335].

The corn cob samples were placed in the glass crucibles with a diameter of 6 cm. The bowl was first dried for 30 minutes in the oven at 103 °C. Samples of about 50 g were put in the bowls, weighed and placed in the oven at 103 °C for 16 hours. After removal they were put into the desiccator and cooled down to room temperature. After that, corn cob samples were weighed and reinserted in the oven for two more hours. This procedure was repeated until the weight difference was less than 0.2 percent for two consecutive measurements.

The moisture content was calculated according to equation:

$$M = \left(1 - \frac{m_3 - m_1}{m_2 - m_1}\right) \cdot 100, \% \quad (\text{B.1})$$

where:

M – Moisture content in the corn cob sample, (wt %)

m<sub>1</sub> – Crucible weight, (g)

m<sub>2</sub> – Initial weight of the sample and crucible, (g)

m<sub>3</sub> – Dry weight of the sample and crucible, (g)

## VOLATILE MATTER

The volatile matter is determined by establishing the loss in weight resulting from heating the fuels under rigidly controlled conditions according to the ASTM E872 [336]. During each volatile matter determination three small crucibles of 35 mm with lids and a

sample holder. This was done to avoid accidentally errors, e.g. air contact in the muffle furnace, which leads to combustion of the corn cob sample. Before every usage the crucibles were burned at 950 °C for 10 min and blown out with pressurized air to clean them. The crucibles were weighed to the nearest 0.1 mg and recorded as crucible weight,  $m_c$ . Then approximately 1 g of the corn cob sample was filled into the crucible, covered with a lid and weighed. The weight was recorded as initial weight,  $m_i$ . Then up to three different corn cob samples was placed on the crucible rack and put into the muffle furnace at 950 °C for exactly 7 min. Then they had to be removed without disturbing the lid and cooled down to room temperature. The covered crucible was weighed to the nearest 0.1 mg and recorded as final weight,  $m_f$ .

The volatile matter was calculated according to equation:

$$VM = \left( \frac{m_i - m_f}{m_i - m_c} \right) \cdot 100, \% \quad (B.2)$$

where:

VM -volatile matter, (% oven dry weight basis)

$m_i$  - initial weight of the sample and crucible, (g)

$m_f$ - weight of the sample's ash and crucible, (g)

$m_c$  - crucible weight, (g)

## ASH CONTENT

The ash content of the corn cob is determined according to ASTM D1102 [337]. During each ash content determination three covered crucibles filled with the same corn cob sample were used. Before every usage the crucibles were burned at 950 °C for 10 min and blown out with pressurized air to clean them. The crucibles were weighed to the nearest 0.1 mg and recorded as crucible weight,  $m_c$ . Then approximately 2 g of the corn cob sample was filled into the crucible, covered with a lid and weighed. The weight was recorded as initial weight,  $m_i$ . Then up to three different corn cob samples was placed on the crucible rack and put into the muffle furnace at 600 °C for 1 h. This is necessary to pyrolyze the fuels first and protect them against explosive combustion. After that, the lid is removed and the crucibles put back in the muffle furnace at 600 °C for another 4 h. Then the crucibles with the ash was removed from the furnace and cooled down to room temperature before weighing.



The ash content was calculated according to equation:

$$A = \left( \frac{m_i - m_f}{m_i - m_c} \right) \cdot 100, \% \quad (\text{B.3})$$

Where:

A – Ash content in sample, (% oven dry weight basis)

$m_i$  – Initial weight of the sample and crucible, (g)

$m_f$  – Weight of the sample and crucible after analysis, (g)

$m_c$  – Crucible weight, (g)

### **FIXED CARBON**

Fixed carbon (fC) in a corn cob is determined from the following equation:

$$fC = 100 - A - VM, \% \quad (\text{B.4})$$

Where:

fC – Fixed carbon, (% oven dry weight basis)

A – Ash content in sample, (% oven dry weight basis)

VM – Volatile matter in sample, (% oven dry weight basis)

### **ULTIMATE ANALYSIS**

During ultimate analysis the chemical composition and the heating value of a sample are determined. In the chemical composition usually the weight percentages of carbon, hydrogen, oxygen, nitrogen, sulphur and ash are given. From this composition the heating value, a measure for the amount of energy that can be obtained from a sample, can be determined experimentally or calculated via an empirical relation.

The ultimate analysis of the fuels is performed with the elemental analyser vario MACRO CHNS. The elemental analyser it can be run in CHN or CHNS mode for a quantitative determination of the elements C, H, N or C, H, N, S. In this work it is only used in CHNS mode.

### **GENERAL MEASURING PRINCIPLE**

The basic principle of elemental analyser operation is high temperature catalytic tube combustion of the sample at 800°C to 1200°C. During combustion gas mixture of (CO<sub>2</sub>),

(N<sub>2</sub>), (H<sub>2</sub>O) and (SO<sub>2</sub>) is formed. All other volatile gases (e.g. oxygen, halogens, etc.) are removed from the gas stream by condensation and absorption. The analysed gases are separated from each other by means of compound specific adsorption/desorption columns and determined in succession with a thermal conductivity detector (TCD). (N<sub>2</sub>) passes through all columns and enters the TCD. After the detection of the (N<sub>2</sub>), the (CO<sub>2</sub>) column is quickly heated and (CO<sub>2</sub>) is released to the TCD and detected. The (H<sub>2</sub>O) column is then heated and the desorbed gas is diverted directly to the TCD. Finally, the (SO<sub>2</sub>) column is heated and (SO<sub>2</sub>) is quantified by the TCD. Furthermore, percent contents of the elements are calculated from the detector signal in connection with the sample weight and the stored calibration curve. Functional diagram of elemental analyser is presented in Figure B.1

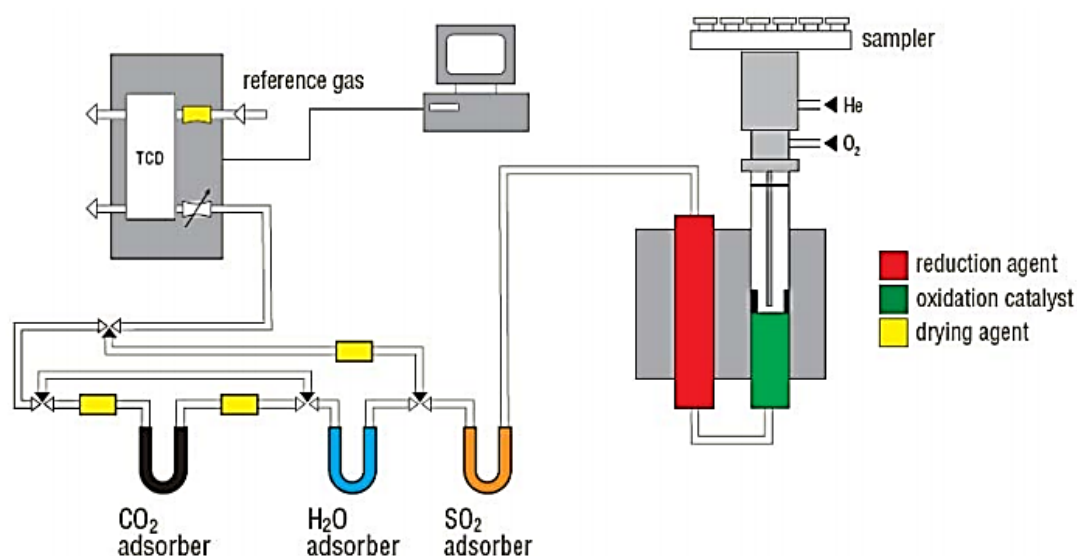


Figure B.1 Functional diagram vario MACRO CHNS [43]

## SAMPLE PREPARATION

For the analyses of the corn cob it is necessary to prepare samples with a weight of approximately 50 mg by packing them into tin foils. With a tweezers the tin foil is tightly closed above the material, and then it's put into a moulding plug and placed into a hand pressing tool, where it is formed to a pallet. After palletisation, pallet samples are placed in the carousel of the automatic sample feeder on the top of the elemental analyser.

## PERFORMING MEASUREMENT

Before performing measurements with real fuels a standard procedure consisting of several runs with a standard material have to be done to calibrate the system. The sample drops into the ash finger of the combustion tube (filled with tungsten ( $WO_3$ ) granulate). Parallel to the sample feeding procedure, the oxygen dosing in the ash finger begins through the oxygen inlet and the oxygen lance, so that the sample drops into a highly oxygenated atmosphere and combusts explosively. During combustion the elements (C), (H), (N), and (S) produced in addition to the molecular nitrogen ( $N_2$ ) and the oxidation products ( $O_2$ ), ( $H_2O$ ), ( $NO_x$ ), ( $SO_2$ ) and ( $SO_3$ ) [43]. If the sample contains halogens, volatile halogen compounds will be produced. In the following reduction tube (filled with copper, corundum, silver wool) ( $NO_x$ ) and ( $SO_3$ ) oxides reducing to ( $N_2$ ) and ( $SO_2$ ). The excess oxygen will be bound, and halogens will be bound on silver wool, [43]. The gas flow, that now only consists of the carrier gas helium (He), ( $N_2$ ), ( $CO_2$ ), ( $H_2O$ ) and ( $SO_2$ ), flows through the adsorption column for  $SO_2$ , ( $H_2O$ ) and ( $CO_2$ ). ( $O_2$ ), ( $H_2O$ ) and ( $SO_2$ ) are sequentially adsorbed on specific columns. ( $N_2$ ) passes through all three columns and enters the TCD. After the detection of the ( $N_2$ ), ( $CO_2$ ), ( $H_2O$ ) and ( $SO_2$ ) are detected by TCD as it is explained in section above.

The oxygen content of the corn cob which is also included in the analysis results, is calculated by difference between 100 % and the sum of ash content (AC), (N) content, (C) content, (S) content and (H) content, (Equation B.5).

$$O = 100 - (A + N + C + S + H), \% \quad (B.5)$$

Where:

O – Oxygen content, (wt % db)

A – Ash content, (wt % db)

N – Nitrogen content, (wt % db)

C – Carbon content, (wt % db)

S – Sulphur content, (wt % db)

H – Hydrogen content, (wt % db)

## HEATING VALUE

The heating value is one of the most important properties of biomass fuels for design calculations or numerical simulations of thermal conversion systems for biomass. The heating value of a biomass fuel can be determined experimentally by employing an adiabatic bomb calorimeter, which measures the enthalpy change between reactants and products. However, the measurement is a complicated and time-consuming process that requires the set-up, measurement and calculation procedures [408]. In contrast, the conventional analysis, i.e. proximate and ultimate analyses, is a basic fuel characterisation and can be carried out more easily, quickly, and cheaply by using common or modern laboratory equipments [408].

Here, heating value of corn cobs are determined experimentally and with empirical equations.

The heating value of any fuel is the energy released per unit mass or per unit volume of the fuel when the fuel is completely burned:

$$H = \frac{Q}{m_f} \quad (\text{B.6})$$

Where:

H – Heating value of a fuel, (kJ/kg)

Q – Heat released by combustion, (kJ)

$m_f$  – Mass of a fuel, (kg)

The heating value is a measure of the energy available from the fuel, and it is a characteristic for each substance. The heating value of a fuel depends on the assumption made on the condition of water molecules in the final combustion products. Therefore, the heating value for fuels is expressed as the high heating value (HHV) and as the low heating value (LHV).

**Higher Heating Value (HHV)** - The full energy content of a fuel. It is the amount of heat produced when a fuel is fully combusted, all of the products of combustion are cooled to 25°C and the water vapour formed during combustion is condensed into liquid water, [409].

The higher heating value takes into account the latent heat of vaporization of water in the combustion products, and is useful in calculating heating values for fuels where condensation of the reaction products is practical (e.g., in a gas-fired boiler used for space

heat). In other words, (HHV) assumes all the water component is in liquid state at the end of combustion (in product of combustion) and that heat above 150°C can be put to use.

**Lower Heating Value (LHV)** - The amount of heat produced when a fuel is fully combusted, all of the products of combustion are cooled to 25°C and the water vapour formed during combustion is still in vapour form. It can be obtained by subtracting the latent heat of vaporization of water from the higher heating value [409].

Relation between heating values:

$$\text{HHV} = \text{LHV} + 25(9\text{H} + \text{W}) \quad (\text{B.7})$$

Where:

HHV – High heating value, (kJ/kg)

LHV – Low heating value, (kJ/kg)

W – Moisture content in fuel, (wt %)

H – Hydrogen content in fuel, (wt %)

9H - Water vapour (H<sub>2</sub>O) created by the combustion of the (H) in the fuel

25 – a hundredth of the latent heat of vaporization ( $r=2450$  kJ/kg), (kJ/kg).

The heating value of a biomass fuel can be determined experimentally by employing an adiabatic bomb calorimeter, which measures the enthalpy change between reactants and products.

The heating value of the corn cobs were determined by combustion of the samples in a calorimeter (IKA Labor Technik C5000).

## **PERFORMING MEASUREMENT**

Approximately 1 g of corn cobs were weighed in a glass crucible with the precision balance. Then the crucible was placed in the crucible holder. A cotton filament was fixed on the ignition wire and placed into the sample. Then the crucible holder was placed into the steel bomb and those were closed carefully. The steel bomb is placed on the closure head of the calorimeter. After all necessary settings the measurement started. The closure head closed automatically and the steel bomb dives into the inner vessel. Through the oxygen inlet pure oxygen is filled into the steel bomb with a pressure of 30 bar [410]. A pump fills the inner vessel with water. A magnetic stirrer keeps the water moving for a constant heat distribution [410]. The fuel sample is electrically ignited. After the combustion and measurement of the temperature difference the water is cooled down by

the cooling system and the over pressure is released from the steel bomb. The closure head opens and the steel bomb can be removed.

The HHV is calculated with equation:

$$\text{HHV} = \frac{C\Delta t_w - Q}{m_f} \quad (\text{B.8})$$

where:

HHV – High heating value, (kJ/kg)

C – Heat capacity of the calorimeter system (9500J/°C)

tw – Increase in temperature of the calorimeter system during a combustion experiment, °C,

Q = 50J – Extraneous energy from electrical ignition and from combustion of the cotton thread

mg – mass of a fuel, (g)

## HEATING VALUE

The heating value of a biomass fuel can be determined experimentally by employing an adiabatic bomb calorimeter, which measures the enthalpy change between reactants and products.

Results of corn cob heating value determined experimentally and empirically are presented in Table C.3. There are a number of formulae proposed in the literature to estimate the higher heating value (HHV) of biomass fuels from the basic analysis data, Dulong's [411] and Parikh's [412]:

$$\text{HHV} = 33.86C + 144.4 \left( H - \frac{O}{8} \right) + 9.428S \quad (\text{B.9})$$

$$\text{HHV} = 0.3536fC + 0.1559VM - 0.0078A \quad (\text{B.10})$$

Table B.1 High heating value of corn cob (measured and calculated value)

sample	HHV (measured) (MJ/kg)	HHV (equ. C.9) (MJ/kg)	HHV (equ. C.10) (MJ/kg)
Scob	18.63	17.33	18.81
Pcob	18.87	17.24	18.67

The results of the formulae based on the ultimate analysis (Dulong's equation) for corn cobs differ strongly from the measured results. The correlations based on the proximate

data have low accuracy because the proximate analysis provides only an empirical composition of the biomass. The correlations based on ultimate analysis (Parikh's equation) are the most accurate.

The formulae based on the ultimate analysis are generally more accurate than those based on proximate analysis (with more than 90% predictions in the range of  $\approx 5\%$  error).

## **APPENDIX C TGA SPECIFICATIONS**



The three thermo-gravimetric analysers were used for this work were a models TA Q5000 and TA Q600 of TA Instruments and a Mettler Toledo model TGA/SDTA 851e. Each of these was linked to a personal computer loaded with Thermal Analysis and Star software respectively. The equipment specifications are given in Table C.1, C.2 and C3.

Table C.1 Technical specifications of TA Q 5000

Temperature Controlled Thermobalance	Included
Dynamic Range	100 mg
Weighing Accuracy	+/- 0.01
Weighing Precision	+/- 0.01 %
Sensitivity	< 0.1 µg
Baseline Dynamic Drift*	< 10 µg
Signal Resolution	0.01 µg
Furnace Heating	Infrared
Temperature Range	Ambient to 1200 °C
Isothermal Temp Accuracy	0.1 °C
Ballistic Heating	> 2000 °C/min
Linear Heating Rate	0.1 to 500 °C/min
Furnace Cooling (Forced air / N <sub>2</sub> )	1200 to 35 °C < 10 min
Vacuum	10 <sup>2</sup> torr
Temperature Calibration	Electromagnetic Coil / Curie Point Stds
Autosampler - 25 sample	Included
Hi-Res TGA	Included
Auto Stepwise TGA	Included
Modulated TGA	Included
TGA/MS Operation	Option
TGA/FTIR Operation	Option
Platinum™ Software	Included /sample thermocouple positioned immediately adjacent to the sample. A second thermocouple is located slightly above in the same sleeve 50, 100 µl
Sample Pans	Platinum-HT, 100 µl Ceramic 100, 250 µl Aluminum 80 µl Aluminum Sealed Pan 20 µl

Table C.2 Technical specifications of TA Q600

System Design	Horizontal Balance & Furnace
Balance Design	Dual Beam (growth compensated)
Sample Capacity	200 mg (350 mg including sample holder)
Balance Sensitivity	0.1 µg
Furnace Type	Bililar Wound
Temperature Range	Ambient to 1500 °C
Heating Rate - Ambientto 1000 °C	0.1 to 1000 °C/min
Heating Rate - Ambient to 1500 °C	0.1 to 25 °C/min
Furnace Cooling	Forced Air (1500 to 50 °C in < 30 min, 1000 °C in 50 °C in < 20 min)
Thermocouples	Platinum/Platinum-Rhodium (Type R)
Temperalure Calibration	Curie Point or Metal Standards (1 to 5 Points)
DTA Sensitivity	0.001 °c
Calorimetric Accuracy/Precision	± 2 % (based on metal standards)
Mass Flow Controller with Automatic Gas Switching	Included
Vacuum	to 7 Pa (0.05 torr)
Reactive Gas Capability	Included - separate gas tube
Dual Sample TGA	Included
AutoStepwise TGA	Included
Sample Pans	Platinum: 40 µl, 110 µl Alumina: 40 µl, 90 µl

Table C.3 Technical specifications of Mettler Toledo TGA/SDT 851e

Temperature	
Range	RT ... 1100°C
Accuracy	± 0.25
Reproducibility	± 0.15
Heating Time	
RT ... 1000°C	5 min
RT...1600 °C	-
Cooling Time not regulated from 1000°C to 100 °C	20 min
Cooling agent	water with protection
Mettler Toledo balance	
Balance type	MT1
Measuring range	1 g
Resolution (without changing weighing range)	1 µg
Noise (RMS)	≤ 1 µg
SDTA (Single Differential Thermal Analysis)	
Resolution	0.005 °C
Noise (RMS)	0.01°C
Sensor Type	R - Thermoelement (Pt - Pt/Rh 13%)
Signal Time Constant	15 s (without crucible)
Sampling Rate	max 10 measuring points per seconds
Dimensions	
Width Depth Height	452x278x646 mm
Weight	38kg

**APENDIX D PUBLISHED SCI PAPERS RELATED TO DOCTORAL  
THESIS**

# Is Elevated Pressure Required To Achieve a High Fixed-Carbon Yield of Charcoal from Biomass? Part 1: Round-Robin Results for Three Different Corncob Materials

Liang Wang,<sup>†</sup> Marta Trninic,<sup>‡</sup> Øyvind Skreiberg,<sup>§</sup> Morten Gronli,<sup>†</sup> Roland Considine,<sup>||</sup> and Michael Jerry Antal, Jr.\*<sup>||</sup>

<sup>†</sup>Department of Energy and Process Engineering, Norwegian University of Science and Technology (NTNU), Kolbjørn Hejes vei 1B, NO-7491 Trondheim, Norway

<sup>‡</sup>Department of Process Engineering, Faculty of Mechanical Engineering, University of Belgrade, Kraljice Marije 16, 11000 Belgrade, Serbia

<sup>§</sup>SINTEF Energy Research, Sem Saelands vei 11, NO-7465 Trondheim, Norway

<sup>||</sup>Hawaii Natural Energy Institute, School of Ocean and Earth Science and Technology, University of Hawaii at Manoa, Honolulu, Hawaii 96822, United States

**ABSTRACT:** Elevated pressure secures the highest fixed-carbon yields of charcoal from corncob. Operating at a pressure of 0.8 MPa, a flash-carbonization reactor realizes fixed-carbon yields that range from 70 to 85% of the theoretical thermochemical equilibrium value from Waimanalo corncob. The fixed-carbon yield is reduced to a range from 68 to 75% of the theoretical value when whole Waimanalo corncobs are carbonized under nitrogen at atmospheric pressure in an electrically heated muffle furnace. The lowest fixed-carbon yields are obtained by the standard proximate analysis procedure for biomass feedstocks; this yield falls in a range from 49 to 54% of the theoretical value. A round-robin study of corncob charcoal and fixed-carbon yields involving three different thermogravimetric analyzers (TGAs) revealed the impact of vapor-phase reactions on the formation of charcoal. Deep crucibles that limit the egress of volatiles from the pyrolyzing solid greatly enhance charcoal and fixed-carbon yields. Likewise, capped crucibles with pinholes increase the charcoal and fixed-carbon yields compared to values obtained from open crucibles. Large corncob particles offer much higher yields than small particles. These findings show that secondary reactions involving vapor-phase species (or nascent vapor-phase species) are at least as influential as primary reactions in the formation of charcoal. Our results offer considerable guidance to industry for its development of efficient biomass carbonization technologies. Size reduction handling of biomass (e.g., tub grinders and chippers), which can be a necessity in the field, significantly reduces the fixed-carbon yield of charcoal. Fluidized-bed and transport reactors, which require small particles and minimize the interaction of pyrolytic volatiles with solid charcoal, cannot realize high yields of charcoal from biomass. When a high yield of corncob charcoal is desired, whole corncobs should be carbonized at elevated pressure. Under these circumstances, carbonization is both efficient and quick.

## INTRODUCTION

Coal combustion is the largest source of carbon dioxide emissions in the U.S.A.<sup>1</sup> Alternatives to coal-fired powerplants (e.g., wind, photovoltaics, solar thermal, natural gas, etc.) are now being deployed, but cost-competitive substitutes for coal as a reductant (i.e., coke) are lacking. CO<sub>2</sub> emissions from the iron and steel industries represented 16% of energy-related CO<sub>2</sub> emissions in 2000.<sup>2</sup> During that year, coal use was responsible for 8.7 Gt or 37% of global CO<sub>2</sub> emissions from fossil fuels. In 2008, CO<sub>2</sub> emissions because of coal grew to 12.6 Gt (i.e., 42% of global CO<sub>2</sub> emissions).<sup>3</sup> This growth of emissions was (in part) due to world crude steel production that increased from 848 Mt in 2000 to 1.3 Gt in 2008.<sup>4</sup> Most of the CO<sub>2</sub> emissions associated with conventional crude steelmaking result from the reduction process in a blast furnace,<sup>5</sup> whereby coke made from hard coal and/or pulverized coal made from steam coal are used to convert iron ore into iron.

The substitution of biocarbon (i.e., charcoal) for coal in the iron and steel industry can reduce CO<sub>2</sub> emissions<sup>6</sup> if the biocarbon is manufactured efficiently from sustainably grown

biomass. This use of biocarbon is not novel; before the dawn of recorded history, mankind employed charcoal to smelt tin for the manufacture of bronze tools,<sup>7</sup> and today in Brazil, blast furnaces use charcoal produced from *Eucalyptus* wood that is cultivated nearby.<sup>8</sup> Likewise, the Norwegian ferroalloy industry makes heavy use of charcoal imports from the Pacific.<sup>9</sup> Unfortunately, biocarbon is not produced efficiently by conventional technology,<sup>10–12</sup> consequently, greenhouse gas emissions associated with biocarbon production are unnecessarily large and worrisome.<sup>13–15</sup> The goal of this work is to learn what reaction conditions offer the highest yields of biocarbon from biomass.

Anxiety about the efficient production of charcoal and its resultant properties motivated one of the earliest publications concerned with industrial chemistry research. In 1851, Violette, who was Commissioner of Gunpowder Production in France, the same post that was held earlier by Lavoisier, released the

Received: March 23, 2011

Revised: June 2, 2011

Published: June 02, 2011

































# Kinetics of Corncob Pyrolysis

Marta Trninić,<sup>†</sup> Liang Wang,<sup>‡</sup> Gábor Várhegyi,<sup>\*,§</sup> Morten Grønli,<sup>‡</sup> and Øyvind Skreiberg<sup>||</sup>

<sup>†</sup>Department of Process Engineering, Faculty of Mechanical Engineering, University of Belgrade, Kraljice Marije 16, 11000 Belgrade, Serbia

<sup>‡</sup>Norwegian University of Science and Technology, Department of Energy and Process Engineering, Kolbjørn Hejes vei 1A, 7491 Trondheim, Norway

<sup>§</sup>Institute of Materials and Environmental Chemistry, Research Centre for Natural Sciences, Hungarian Academy of Sciences, PO Box 17, Budapest, Hungary 1525

<sup>||</sup>SINTEF Energy Research, Sem Saelands vei 11, 7465 Trondheim, Norway

**ABSTRACT:** Two different corn cob samples from different continents and climates were studied by thermogravimetry at linear and nonlinear heating programs in inert gas flow. A distributed activation energy model (DAEM) with three and four pools of reactants (pseudocomponents) was used due to the complexity of the biomass samples of agricultural origin. The resulting models described well the experimental data. When the evaluation was based on a smaller number of experiments, similar model parameters were obtained which were suitable for predicting experiments at higher heating rates. This test indicates that the available experimental information was sufficient for the determination of the model parameters. The checks on the prediction capabilities were considered to be an essential part of the model verification. In another test, the experiments of the two samples were evaluated together, assuming more or less common kinetic parameters for both cobs. This test revealed that the reactivity differences between the two samples are due to the differences in their hemicelluloses and extractives. The kinetic parameter values from a similar earlier work on other biomasses (Várhegyi, G.; Bobály, B.; Jakab, E.; Chen, H. *Energy Fuels*, 2011, 25, 24–32) could also be used, indicating the possibilities of a common kinetic model for the pyrolysis of a wide range of agricultural byproduct.

## 1. INTRODUCTION

There is a growing interest in biomass fuels and raw materials due to climatic change problems. The thermal decomposition reactions play a crucial role during several of the biomass utilization processes. Thermogravimetric analysis (TGA) is a high-precision method for the study of the pyrolysis at low heating rates, under well-defined conditions in the kinetic regime. It can provide information on the partial processes and reaction kinetics. On the other hand, TGA can be employed only at relatively low heating rates because the true temperature of the samples may become unknown at high heating rates. TGA has frequently been employed in the kinetic modeling of the thermal degradation of biomass materials. Due to the complex composition of biomass materials, the conventional linearization techniques of the nonisothermal kinetics are not suitable for the evaluation of the TGA experiments. Therefore, the TGA experiments of biomass materials are usually evaluated by the nonlinear method of least-squares (LSQ), assuming more than one reaction.<sup>1–5</sup>

Biomass fuels and residues contain a wide variety of pyrolyzing species. Even the same chemical species may have differing reactivity if their pyrolysis is influenced by other species in their vicinity. The assumption of a distribution in the reactivity of the decomposing species frequently helps the kinetic evaluation of the pyrolysis of complex organic samples.<sup>6</sup> The distributed activation energy models (DAEM) have been used for biomass pyrolysis kinetics since 1985, when Avni et al. applied a DAEM for the formation of volatiles from lignin.<sup>7</sup> The use of DAEM in pyrolysis research was subsequently

extended to a wider range of biomasses and materials derived from plants.<sup>8–18</sup>

Due to the complexity of the investigated materials, the model was expanded to simultaneous parallel reactions (pseudocomponents) that were described by separate DAEMs.<sup>9–15,17,18</sup> The increased number of unknown model parameters required least-squares evaluation on larger series of experiments with linear and nonlinear temperature programs.<sup>9,15,17,18</sup> The model parameters obtained in this way allowed accurate prediction outside of the domain of the experimental conditions of the given kinetic evaluations.<sup>9,15,18</sup> The prediction tests helped to confirm the reliability of the model.

The present work aims at testing the applicability of this approach on a biomass of high applicability potential. Corn cob is a highly important agricultural byproduct. The worldwide yearly corn production is around 800 million ton. The cob/grain ratio is estimated to be 12–20% on a dry basis.<sup>19</sup> The final report of a recent feasibility study<sup>20</sup> lists the advantages of corn cob utilization as: “Cobs represent a small, 12% portion of corn stover remaining on the field and cob removal has negligible impact on organic carbon depletion from the soil; Cobs have limited nutrient value to the soil; ...Cobs are collected at the combine discharge which avoids the inclusion of rocks and dirt in the biomass supply;... Whole and ground

Received: February 14, 2012

Revised: March 16, 2012

Published: March 20, 2012





















## **BIOGRAPHY OF THE AUTHOR**

Marta R. Trninć was born on 1st of September 1977 in Belgrade, Serbia (former SR Serbia, SFR Yugoslavia).

She attended the Primary school “Moše Pijade” and Primary Music School “Vladimir Đorđević” in parallel. After completing Primary school she attended and finished the 14<sup>th</sup> Belgrade Gymnasium in Belgrade.

Desiring more education, she entered the Belgrade University, Faculty of Mechanical Engineering. After graduation (five years of studies), in 2007 she entered the Ph.D. program at the Department of Process Engineering, Faculty of Mechanical Engineering, financed by Norwegian University of Technology and Science, as a part of collaboration Project “Sustainable Energy and Environmental” between Faculty of Mechanical engineering, Belgrade University and Norwegian University of Technology and Science (NTNU), Trondheim.

During Ph.D studies she worked as a research assistant in several national research projects financed by the Ministry of Education, Science and Technological Development of the Republic of Serbia and as a teacher assistant at the Department of Process Engineering, Faculty of Mechanical Engineering.

Her research work was focused on mathematical modeling and operational optimization of pyrolysis processes, kinetic modeling of pyrolysis processes, mathematical modeling and operational optimization of biomass gasification processes, biomass for combined heat and power generation etc.

She attended several international training course in field of analytical techniques in combustion, kinetic modeling of biomass pyrolysis, energy efficiency and energy management in industrial enterprises etc.

From September 2009 until June 2010 she stayed at Norwegian University of Technology and Science (NTNU), Trondheim where she joined the Thermal engineering laboratory (Varmeteknisk\*Lab) to assist in laboratory research in corn cob pyrolysis. During her stay at NTNU she had opportunity to work as laboratory assistant for laboratory classes for Master students.

She published more than fifteen scientific and conference papers.

Прилог 1.

## Изјава о ауторству

Потписана Марта Трнинић

број индекса ДЗ/07

### Изјављујем

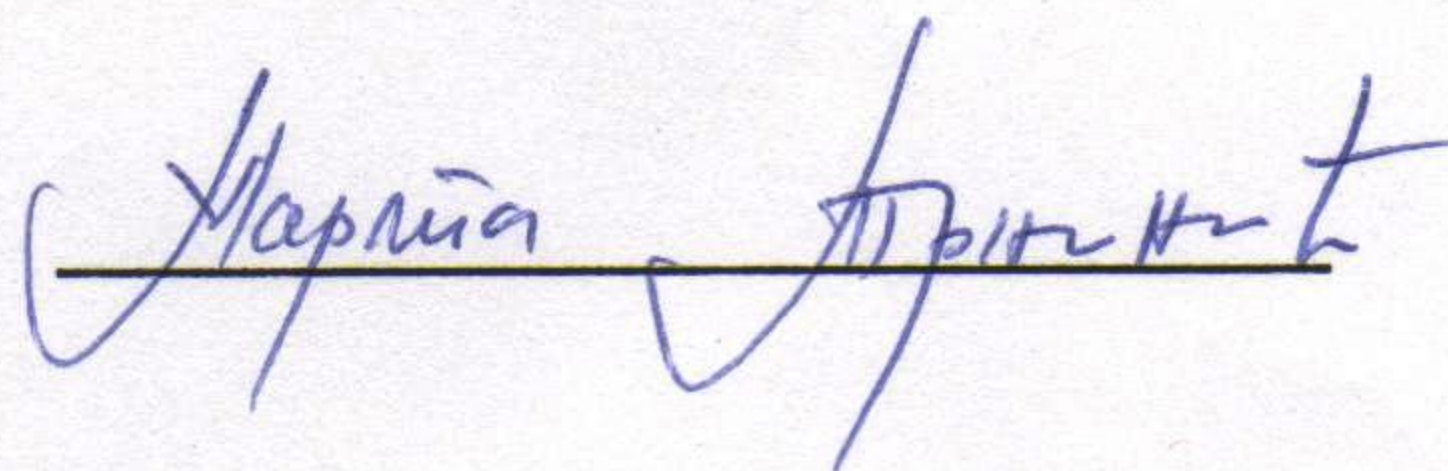
да је докторска дисертација под насловом

MODELING AND OPTIMISATION OF CORN COB PYROLYSIS  
(МОДЕЛИРАЊЕ И ОПТИМИЗАЦИЈА ПРОЦЕСА ПИРОЛИЗЕ КУКУРУЗНОГ  
ОКЛАСКА)

- резултат сопственог истраживачког рада,
- да предложена дисертација у целини ни у деловима није била предложена за добијање било које дипломе према студијским програмима других високошколских установа,
- да су резултати коректно наведени и
- да нисам кршио/ла ауторска права и користио интелектуалну својину других лица.

Потпис докторанда

У Београду, 19.3.2015.

  
\_\_\_\_\_

Прилог 2.

## Изјава о истоветности штампане и електронске верзије докторског рада

Име и презиме аутора Марта Р. Трнинић

Број индекса Д 3/07

Студијски програм Докторске академске студије

Наслов рада MODELING AND OPTIMISATION OF CORN COB PYROLYSIS  
(МОДЕЛИРАЊЕ И ОПТИМИЗАЦИЈА ПРОЦЕСА ПИРОЛИЗЕ КУКУРУЗНОГ  
ОКЛАСКА)

Ментор Проф Др Александар Јововић

Потписана Марта Трнинић \_\_\_\_\_

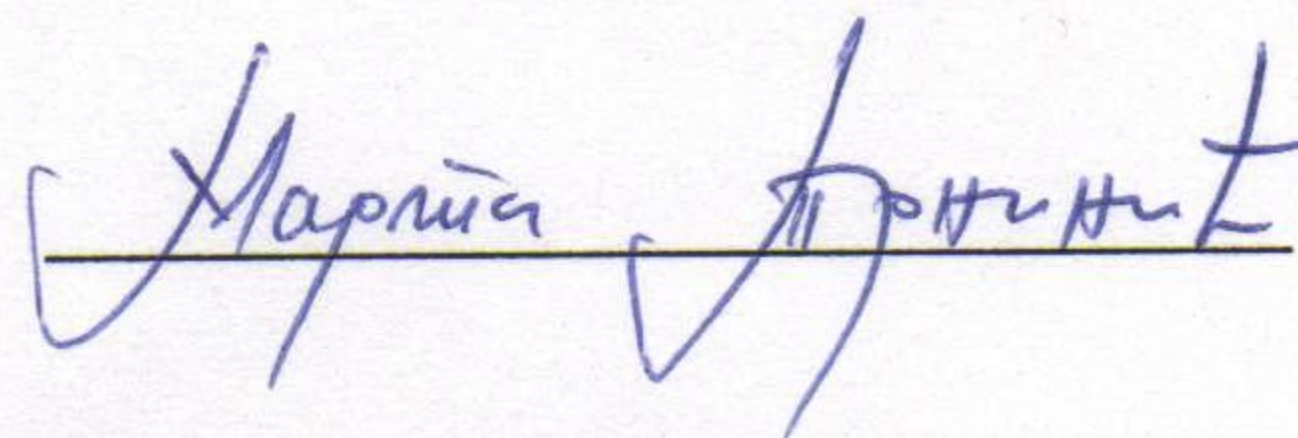
Изјављујем да је штампана верзија мог докторског рада истоветна електронској верзији коју сам предао/ла за објављивање на порталу **Дигиталног репозиторијума Универзитета у Београду**.

Дозвољавам да се објаве моји лични подаци везани за добијање академског звања доктора наука, као што су име и презиме, година и место рођења и датум одбране рада.

Ови лични подаци могу се објавити на мрежним страницама дигиталне библиотеке, у електронском каталогу и у публикацијама Универзитета у Београду.

Потпис докторанда

У Београду, 19. 3. 2015.



Прилог 3.

## Изјава о коришћењу

Овлашћујем Универзитетску библиотеку „Светозар Марковић“ да у Дигитални репозиторијум Универзитета у Београду унесе моју докторску дисертацију под насловом:

MODELING AND OPTIMISATION OF CORN COB PYROLYSIS  
(МОДЕЛИРАЊЕ И ОПТИМИЗАЦИЈА ПРОЦЕСА ПИРОЛИЗЕ КУКУРУЗНОГ  
ОКЛАСКА)

која је моје ауторско дело.

Дисертацију са свим прилозима предао/ла сам у електронском формату погодном за трајно архивирање.

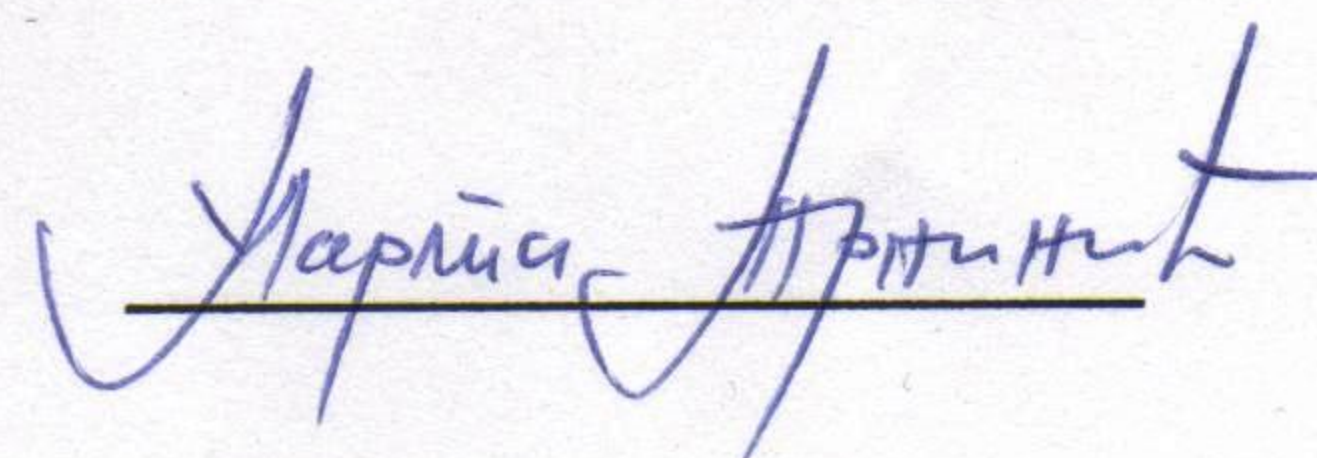
Моју докторску дисертацију похрањену у Дигитални репозиторијум Универзитета у Београду могу да користе сви који поштују одредбе садржане у одабраном типу лиценце Креативне заједнице (Creative Commons) за коју сам се одлучио/ла.

1. Ауторство
2. Ауторство - некомерцијално
3. Ауторство – некомерцијално – без прераде
4. Ауторство – некомерцијално – делити под истим условима
5. Ауторство – без прераде
6. Ауторство – делити под истим условима

(Молимо да заокружите само једну од шест понуђених лиценци, кратак опис лиценци дат је на полеђини листа).

Потпис докторанда

У Београду, 19.3.2015.

  
\_\_\_\_\_



1. Ауторство - Дозвољаваате умножавање, дистрибуцију и јавно саопштавање дела, и прераде, ако се наведе име аутора на начин одређен од стране аутора или даваоца лиценце, чак и у комерцијалне сврхе. Ово је најслободнија од свих лиценци.

2. Ауторство – некомерцијално. Дозвољаваате умножавање, дистрибуцију и јавно саопштавање дела, и прераде, ако се наведе име аутора на начин одређен од стране аутора или даваоца лиценце. Ова лиценца не дозвољава комерцијалну употребу дела.

3. Ауторство - некомерцијално – без прераде. Дозвољаваате умножавање, дистрибуцију и јавно саопштавање дела, без промена, преобликовања или употребе дела у свом делу, ако се наведе име аутора на начин одређен од стране аутора или даваоца лиценце. Ова лиценца не дозвољава комерцијалну употребу дела. У односу на све остале лиценце, овом лиценцом се ограничава највећи обим права коришћења дела.

4. Ауторство - некомерцијално – делити под истим условима. Дозвољаваате умножавање, дистрибуцију и јавно саопштавање дела, и прераде, ако се наведе име аутора на начин одређен од стране аутора или даваоца лиценце и ако се прерада дистрибуира под истом или сличном лиценцом. Ова лиценца не дозвољава комерцијалну употребу дела и прерада.

5. Ауторство – без прераде. Дозвољаваате умножавање, дистрибуцију и јавно саопштавање дела, без промена, преобликовања или употребе дела у свом делу, ако се наведе име аутора на начин одређен од стране аутора или даваоца лиценце. Ова лиценца дозвољава комерцијалну употребу дела.

6. Ауторство - делити под истим условима. Дозвољаваате умножавање, дистрибуцију и јавно саопштавање дела, и прераде, ако се наведе име аутора на начин одређен од стране аутора или даваоца лиценце и ако се прерада дистрибуира под истом или сличном лиценцом. Ова лиценца дозвољава комерцијалну употребу дела и прерада. Слична је софтверским лиценцама, односно лиценцама отвореног кода.